*Technical Report*

# Heat Transfer Analysis and Modeling of a Parabolic Trough Solar Receiver Implemented in Engineering Equation Solver

R. Forristall

**NREL**

**National Renewable Energy Laboratory**

# Heat Transfer Analysis and Modeling of a Parabolic Trough Solar Receiver Implemented in Engineering Equation Solver

R. Forristall

## NREL

**National Renewable Energy Laboratory**

**NOTICE**

This report was prepared as an account of work sponsored by an agency of the United States government. Neither the United States government nor any agency thereof, nor any of their employees, makes any warranty, express or implied, or assumes any legal liability or responsibility for the accuracy, completeness, or usefulness of any information, apparatus, product, or process disclosed, or represents that its use would not infringe privately owned rights. Reference herein to any specific commercial product, process, or service by trade name, trademark, manufacturer, or otherwise does not necessarily constitute or imply its endorsement, recommendation, or favoring by the United States government or any agency thereof. The views and opinions of authors expressed herein do not necessarily state or reflect those of the United States government or any agency thereof.

# HEAT TRANSFER ANALYSIS AND MODELING OF A PARABOLIC TROUGH SOLAR RECEIVER IMPLEMENTED IN ENGINEERING EQUATION SOLVER

## ABSTRACT

This report describes the development, validation, and use of a heat transfer model implemented in Engineering Equation Solver (EES). The model determines the performance of a parabolic trough solar collector's linear receiver, also called a heat collector element (HCE). All heat transfer and thermodynamic equations, optical properties, and parameters used in the model are discussed. The modeling assumptions and limitations are also discussed, along with recommendations for model improvement.

The model was implemented in EES in four different versions. Two versions were developed for conducting HCE design and parameter studies, and two versions were developed for verifying the model and evaluating field test data. One- and two-dimensional energy balances were used in the codes, where appropriate. Each version of the codes is discussed briefly, which includes discussing the relevant EES diagram windows, parameter tables, and lookup tables. Detailed EES software instructions are not included; however, references are provided.

Model verification and a design and parameter study to demonstrate the model versatility are also presented. The model was verified by comparing the field test versions of the EES codes with HCE experimental results. The design and parameter study includes numerous charts showing HCE performance trends based on different design and parameter inputs. Based on the design and parameter study, suggestions for HCE and trough improvements and further studies are given.

The HCE performance software model compared well with experimental results and provided numerous HCE design insights from the design and parameter study. The two design versions of the EES codes of the HCE performance model are provided in the appendix.

## ACKNOWLEDGMENTS

# CONTENTS

# FIGURES

# TABLES

# SYMBOLS

$a$ = accommodation coefficient of annulus gas

$A_{cs}$ = absorber pipe cross-sectional flow area $[m^2]$

$A_{cs,b}$ = minimum cross-section of receiver support bracket $[m^2]$

$A_i$ = circumferential area of receiver segment "i" $[m^2]$

$b$ = interaction coefficient of annulus gas

$C, m, n$ = constants

$c_{ave,i}$ = HTF specific heat at average temperature of receiver segment "i" $[^oC]$

$D_2$ = inside diameter of absorber pipe $[m]$

$D_3$ = outside diameter of absorber pipe $[m]$

$D_4$ = inside diameter of glass envelope $[m]$

$D_5$ = outside diameter of glass enveope $[m]$

$D_h$ = hydraulic diameter of absorber pipe $[m]$

$D_p$ = outside diameter of absorber pipe flow restriction insert pipe (or cylinder) $[m]$

$f$ = Darcy friction factor

$f_2$ = friction factor for the inner surface of the absorber pipe

$g$ = gravitational constant, $9.81$ m/s$^2$

$h_1$ = convection heat transfer coefficient for the HTF at $T_1$ $[W/m^2$-K$]$

$h_{34}$ = convection heat transfer coefficient of annulus gas at $T_{34}$ $[W/m^2$-K$]$

$h_{56}$ = convection heat transfer coefficient of air at $T_{56}$ $[W/m^2$-K$]$

$\overline{h}_{b,i}$ = convection heat transfer coefficient of air evaluated at the average receiver support bracket film temperature for receiver segment "i" $[W/m^2$-K$]$

$h_{i,in}$ = enthalpy at inlet of receiver segment "i" $[J/kg]$

$h_{i,out}$ = enthalpy at outlet of receiver segment "i" $[J/kg]$

$K$ = incident angle modifier

$k_1$ = thermal conductance of HTF at $T_1$ $[W/m$-K$]$

$k_{23}$ = thermal conductance of absorber wall at $T_{23}$ $[W/m$-K$]$

$k_{34}$ = thermal conductance of annulus gas at $T_{34}$ $[W/m$-K$]$

$k_{56}$ = thermal conductance of air at $T_{56}$ $[W/m$-K$]$

$k_b$ = conduction heat transfer coefficient of air evaluated at the average receiver support bracket film temperature for receiver segment "i" $[W/m$-K$]$

$k_{std}$ = thermal conductance of annulus gas at standard temperature and pressure $[W/m$-K$]$

$\dot{m}$ = mass flow rate $[kg/s]$

$n_i$ = number of receiver support brackets on receiver segment "i"

$Nu_{D2}$ = Nusselt number of HTF based on $D_2$

$Nu_{D5}$ = Nusselt number of air based on $D_5$

$P_a$ = annulus gas pressure $[mmHg]$

$P_b$ = exterior perimeter of receiver support bracket $[m]$

$P_{inlet,i}$ = HTF pressure at inlet of receiver segment "i" $[^oC]$

$P_{outlet,i}$ = HTF pressure at outlet of receiver segment "i" $[^oC]$

$Pr_1$ = Prandtl number of HTF evaluated at $T_1$

$Pr_2$ = Prandtl number of HTF evaluated at $T_2$

$Pr_{34}$ = Prandtl number of annulus gas at $T_{34}$

| | | |
|---|---|---|
| $\text{Pr}_5$ | = | Prandtl number of air at $T_5$ |
| $\text{Pr}_{56}$ | = | Prandtl number for air at $T_{56}$ |
| $\text{Pr}_6$ | = | Prandtl number of air at $T_6$ |
| $P_w$ | = | absorber pipe inner wetted surface perimeter [m] |
| $\dot{q}'_{12conv}$ | = | convection heat transfer rate between the heat transfer fluid and inside wall of the absorber pipe per unit receiver length [W/m] |
| $\dot{q}'_{23cond}$ | = | conduction heat transfer rate through the absorber pipe wall per unit receiver length [W/m] |
| $\dot{q}'_{3SolAbs}$ | = | solar irradiation absorption rate into the absorber pipe per unit receiver length [W/m] |
| $\dot{q}'_{3SolAbs,i}$ | = | incident solar irradiation absorption rate into the absorber pipe of receiver segment "i" per unit segment length [W/m] |
| $\dot{q}'_{34conv}$ | = | convection heat transfer rate between the outer surface of the absorber pipe to the inner surface of the glass envelope per unit receiver length [W/m] |
| $\dot{q}'_{34conv,i}$ | = | convection heat transfer rate for receiver segment "i" between the outer surface of the absorber pipe to the inner surface of the glass envelope per receiver segment length [W/m] |
| $\dot{q}'_{34rad}$ | = | radiation heat transfer rate between the outer surface of the absorber pipe to the inner surface of the glass envelope per unit receiver length [W/m] |
| $\dot{q}'_{34rad,i}$ | = | radiation heat transfer rate for receiver segment "i" between the outer surface of the absorber pipe to the inner surface of the glass envelope per receiver segment length [W/m] |
| $\dot{q}'_{36conv}$ | = | convection heat transfer rate between the outer surface of the absorber pipe to the atmosphere per unit receiver length [W/m] |
| $\dot{q}'_{36conv,i}$ | = | convection heat transfer rate between the outer surface of the absorber pipe to the atmosphere per unit receiver segment length for receiver segment "i" [W/m] |
| $\dot{q}'_{57rad}$ | = | radiation heat transfer rate between the outer surface of the glass envelope to the sky per unit receiver length [W/m] |
| $\dot{q}'_{37rad,i}$ | = | radiation heat transfer rate between the outer surface of the absorber pipe to the sky per unit receiver segment length for receiver segment "i" [W/m] |
| $\dot{q}'_{45cond}$ | = | conduction heat transfer rate through the glass envelope per unit receiver length [W/m] |
| $\dot{q}'_{5SolAbs}$ | = | solar irradiation absorption rate into the absorber pipe per unit receiver length per unit receiver length [W/m] |
| $\dot{q}'_{5SolAbs,i}$ | = | incident solar irradiation absorption rate into the glass envelope of receiver segment "i" per unit segment length [W/m] |
| $\dot{q}'_{56conv}$ | = | convection heat transfer rate between the outer surface of the glass envelope to the atmosphere per unit receiver length [W/m] |
| $\dot{q}'_{37rad}$ | = | radiation heat transfer rate between the outer surface of the absorber pipe to the sky per unit receiver length [W/m] |
| $\dot{q}_{cond,bracket,i}$ | = | conductive heat loss through each receiver support bracket on receiver segment "i" [W] |
| $\dot{q}_{cond,bracket,total,i}$ | = | total conductive heat losses through all receiver support brackets on receiver segment "i" [W] |
| $\dot{q}'_{HeatLoss}$ | = | total heat loss rate from the heat collecting element to the surroundings [W/m] |
| $\dot{q}''_{HeatLoss,i}$ | = | heat loss rate per unit circumferential area to the atmosphere from receiver segment "i" (excluding bracket losses) [W/m$^2$] |

$\dot{q}''_{HeatLoss,total,i}$ = total heat loss rate per unit circumferential area from receiver segment "i" [W/m$^2$]

$\dot{q}''_i$ = net heat flux per unit circumferential area of receiver segment "i" [W/m$^2$]

$\dot{q}'_{si}$ = solar irradiance per receiver unit length [W/m]

$\dot{q}''_{SolarAbs,i}$ = incident solar irradiation absorption rate per unit circumferential area of receiver segment "i" [W/m$^2$]

$Ra_{D3}$ = Rayleigh number of annulus gas based on D$_3$

$Ra_{D5}$ = Rayleigh number of air based on D$_5$

$Re_{D2}$ = Reynolds number of HTF based on D$_2$

$Re_{D2,ave,i}$ = Reynolds number based on D$_2$ and evaluated at the average HTF bulk temperature of receiver segment "i"

$Re_{D5}$ = Reynolds number of air based on D$_5$

$T_1$ = mean (bulk) temperature of the HTF [$^{\circ}$C]

$T_2$ = absorber pipe inner surface temperature [$^{\circ}$C]

$T_{23}$ = average absorber wall temperature, $(T_2 + T_3)/2$ [$^{\circ}$C]

$T_3$ = absorber pipe outer surface temperature [$^{\circ}$C]

$T_{34}$ = average temperature of annulus gas, $(T_3+T_4)/2$ [$^{\circ}$C]

$T_4$ = glass envelope inner surface temperature [$^{\circ}$C]

$T_5$ = glass envelope outer surface temperature [$^{\circ}$C]

$T_{56}$ = average temperature of air, $(T_5 + T_6)/2$ [$^{\circ}$C]

$T_6$ = atmosphere temperature [$^{\circ}$C]

$T_7$ = estimated effective sky temperature [$^{\circ}$C]

$T_{base,i}$ = temperature at base of receiver support bracket for receiver segment "i" [$^{\circ}$C]

$T_{inlet,i}$ = HTF temperature at inlet of receiver segment "i" [$^{\circ}$C]

$T_{outlet,i}$ = HTF temperature at outlet of receiver segment "i" [$^{\circ}$C]

$v_{56}$ = kinematic viscosity of air at T$_{56}$ [m$^2$/s]

$v_{i,in}$ = bulk fluid velocity at inlet of receiver segment "i" [J/kg]

$v_{i,out}$ = bulk fluid velocity at outlet of receiver segment "i" [J/kg]

$\Delta h_i$ = change in enthalpy through receiver segment "i" ($h_{inlet,i} - h_{outlet,i}$) [J/kg]

$\Delta L_{aperture}$ = receiver segment length [m]

$\Delta P_i$ = change in HTF pressure through receiver segment "i" ($P_{inlet,i} - P_{outlet,i}$) [Pa]

$\Delta T_i$ = change in HTF temperature through receiver segment "i" ($T_{inlet,i} - T_{outlet,i}$) [K]

$\rho_{ave,i}$ = HTF density at average temperature of receiver segment "i" [kg/m$^3$]


Greek Letters

$\alpha$ = thermal diffusivity of air at T$_{56}$ [m$^2$/s]

$\alpha_{abs}$ = absorptance of the absorber selective coating

$\alpha_{env}$ = absorptance of the glass envelope

$\beta$ = volumetric thermal expansion coefficient of annulus gas or air [1/K]

$\delta$ = molecular diameter of annulus gas [cm]

$\varepsilon$ = equivalent surface roughness [m]

$\varepsilon'_{\#}$ = optical efficiency terms

$\varepsilon_3$ = emissivity of absorber selective coating

$\varepsilon_4$ = emissivity of inner surface of glass envelope

$\varepsilon_5$ = emissivity of outer surface of glass envelope

$\mu_{ave,i}$ = dynamic fluid viscosity of HTF at the average temperature of receiver segment "i" [N-s/m$^2$]

$\gamma$ = ratio of specific heats of annulus gas

$\eta_{abs}$ = effective optical efficiency at the absorber

$\eta_{env}$ = effective optical efficiency at the glass envelope

$\lambda$ = mean-free-path between collisions of a molecule of annulus gas [cm]

$\pi$ = ratio of the circumference to diameter of a circle, 3.14159

$\sigma$ = Stefan-Boltzmann constant [W/m$^2$-K$^4$]

$\tau_{env}$ = transmittance of the glass envelope


EES Lookup and Parametric Tables


Design Study Version:

$c$ = specific heat [J/kg-K]

$\eta_{Col}$ = collector efficiency [%]

$k$ = thermal conductance [W/m-K]

$\mu$ = dynamic viscosity [kg/m-s]

$P_v$ = vapor pressure [kPa]

$q_{HeatGain}$ = HTF heat gain per unit receiver length [W/m]

$q_{HeatLoss}$ = heat loss per unit receiver length [W/m]

$\rho$ = density [kg/m$^3$]

$T$ = temperature [$^o$C]

$T_{1ave}$ = average bulk HTF temperature between the receiver inlet and outlet [$^o$C]

AZTRAK Test Data Version:

$\eta_{Col}$ = collector efficiency [%]

$I_b$ = direct normal incident solar irradiation per unit area [W/m$^2$]

$q_{HeatGain}$ = heat gain per unit receiver length [W/m]

$q_{heat,loss,col,area}$ = heat loss per projected collector area [W/m$^2$]

$T_6$ = ambient temperature [$^o$C]

$T_{diffAir}$ = temperature difference between the average HTF temperature and ambient temperature [$^o$C]

$T_{in}$ = HTF inlet bulk temperature [$^o$C]

$T_{out}$ = HTF outlet bulk temperature [$^o$C]

$v_1$ = HTF inlet volumetric flow rate [L/min]

$V_6$ = wind speed [m/s]

KJC Test-loop Data Version:

$\Delta P$ = HTF pressure drop through receiver [Pa]

$\eta_{Col}$ = collector efficiency [%]

$I_b$ = direct normal incident solar irradiation per unit area [W/m$^2$]

$\Theta$ = solar incident angle from the normal to the projected collector area [degrees]

$q_{cond,bracket}$ = total conductive losses through receiver support brackets [W]

$q_{HeatGain}$ = HTF heat gain per receiver length [W/m]

$q_{HeatLoss}$ = heat loss per receiver length [W/m]

$q_{heat,loss,HCE,length}$ = heat loss per receiver length [W/m]

$q_{OptLoss}$ = total optical loss per receiver length [W/m]

$q_{opt,loss}$ = total optical loss per receiver length [W/m]

| $q_{opt,loss,K}$ | = | optical losses due to solar incident angle per receiver length [W/m] |
| $T_{1inlet}$ | = | HTF bulk inlet temperature [$^{o}$C] |
| $T_{1outlet}$ | = | HTF bulk outlet temperature [$^{o}$C] |
| $T_{6F}$ | = | ambient temperature [$^{o}$F] |
| Time | = | local time |
| $T_{inF}$ | = | HTF bulk inlet temperature [$^{o}$F] |
| $T_{outF}$ | = | HTF bulk outlet temperature [$^{o}$F] |
| $T_{outletF}$ | = | HTF bulk outlet temperature [$^{o}$F] |
| $v_{1inlet}$ | = | HTF bulk inlet velocity [m/s] |
| $v_{1outlet}$ | = | HTF bulk outlet velocity [m/s] |
| $V_{1Volg}$ | = | HTF volumetric inlet flow rate [gpm] |
| $V_{1volg,outlet}$ | = | HTF volumetric outlet flow rate [gpm] |
| $V_{6mph}$ | = | wind speed [mph] |

# 1. Introduction

This report describes the development, validation, and use of a heat transfer model implemented in Engineering Equation Solver (EES). The model determines the performance of a parabolic trough solar collector's linear receiver, also called a heat collector element (HCE). All heat transfer and thermodynamic equations, optical properties, and parameters used in the model are discussed, as are all model inputs and outputs. Inputs include collector and HCE geometry, optical properties, heat transfer fluid (HTF) properties, HTF inlet temperature and flow rate, solar insolation, wind speed, and ambient temperature. Outputs include collector efficiency, outlet HTF temperature, heat gain, and heat and optical losses. Modeling assumptions and limitations are also discussed, along with recommendations for model improvement.

The model was implemented in EES in four versions: One-Dimensional Design Study, Two-Dimensional Design Study, AZTRAK Test Data, and KJC Test-Loop Data. The two design study versions were developed for conducting HCE design and parameter studies. The two test data versions were developed for verifying the model and evaluating field test data. One- and two-dimensional energy balances were used in the codes. When evaluating long receivers, the two-dimensional model becomes necessary. The one-dimensional model is valid for short receivers and for conducting design and parameter comparisons. The one-dimensional version offers faster convergence times. The discussion of each version of the codes includes the EES diagram windows, parameter tables, and lookup tables. Detailed EES software instructions are not included; however, references are provided.

Model verification and a design and parameter study to demonstrate the model versatility are also presented. The model was verified by comparing the field test versions of the EES codes with experimental results. The field tests included data from a collector test platform at Sandia National Laboratories (SNL) in Albuquerque, New Mexico, and data from a test-loop of collectors in an operating solar plant in Kramer Junction, California. The design and parameter study section includes numerous charts showing HCE performance trends based on different design and parameter inputs. Based on the design and parameter study, suggestions for further studies and trough improvements are discussed.

Additional model development analysis is provided in the appendices, along with a copy of the two design study versions of the EES codes, and numerous analysis and parameter references. The AZTRAK and KJC Test-Loop Data versions of the code are not included; however, they are very similar to the design study versions. They differ slightly because of the required inputs and output comparisons.

The HCE performance software model compared well with the receiver field test results and provided numerous HCE design insights from the design and parameter study.

## 1.1 Background

Concentrating solar power (CSP) has been used for more than 100 years. Initially, CSP was used for small-scale solar thermal-mechanical applications, with outputs to 100 kW, mainly for water pumping [Duffie and Beckman 1991]. Only after the energy crises of 1973 did the idea of large-scale solar power plants take hold [Thomas and Guven 1993]. Starting in the late 1980s, nine solar electric generating systems (SEGSs) have been built and operated in the Mojave Desert of southern California. These SEGS plants range in size from 30 MW to 80 MW and total 354 MW of peak generating power for the Southern California Edison utility company. They supply enough electricity for more than 300,000 residents and displace more than 2 million barrels of oil per year [Solel 2002].

Five SEGSs located in Kramer Junction, California are shown in an aerial view (Figure 1.1). The SEGSs shown are operated by the Kramer Junction Corporation Operating Company (KJCOC). The plants are

natural gas-supplemented steam Rankine turbine/generator systems. The natural gas supplements the required energy input during times of low solar insolation and allows the plants to operate 24 h/d at peak output. The buildings shown in the middle of the collector fields contain the heat exchangers, natural gas boilers, and pumping and generating equipment. Some SEGS plant designs are solar only; others have thermal storage capability.



**Figure 1.1  Aerial view of five, 30-MW SEGS solar plants (source: Price et al. 2002)**

A schematic of a SEGS power plant is shown in Figure 1.2. The plant consists of rows of solar troughs (also called solar collector assemblies [SCAs]), a storage system that stores the thermal energy (optional), heat exchangers that generate superheated steam, and a standard power cycle that converts the thermal energy to electrical. There may also be a supplemental boiler system (a gas boiler in this case). The solar energy is captured by an HTF – which could be synthetic oil or molten salt – and transferred to heat exchangers for thermal storage or steam generation. The thermal storage collects the solar energy during periods of high solar insolation, and supplements the heat input during periods of low insolation. The natural gas boiler would be used to further modulate the heat input and allow for 24-h plant operation. Typically, the trough field is designed to provide enough heat input to raise the temperature of an HTF to around 400$^\circ$C – high enough to generate superheated steam for a standard Rankine steam generating plant. The outlet temperature is maintained by the HTF flow rate, the thermal storage (if applicable), and the natural gas heater (if applicable).

Figure 1.3 shows a row of SCAs from an experimental solar test facility in Spain. The figure illustrates the major components of a solar trough. It consists of the parabolic trough reflector, steel support structure, absorber pipe (HCE), and a single-axis drive mechanism. The trough reflector provides an aperture about 5 m wide that can extend for several thousand meters depending on the number of SCAs in a particular plant. The HCE is about 115 mm in diameter and 4 m long between the support braces that support it at the focal line. Each SCA system can move independently from the rest of the collector field. This allows for maintenance and a mechanism for controlling the HTF temperature, since one or a number of SCAs can be taken off sun during operation, which effectively controls the solar input.
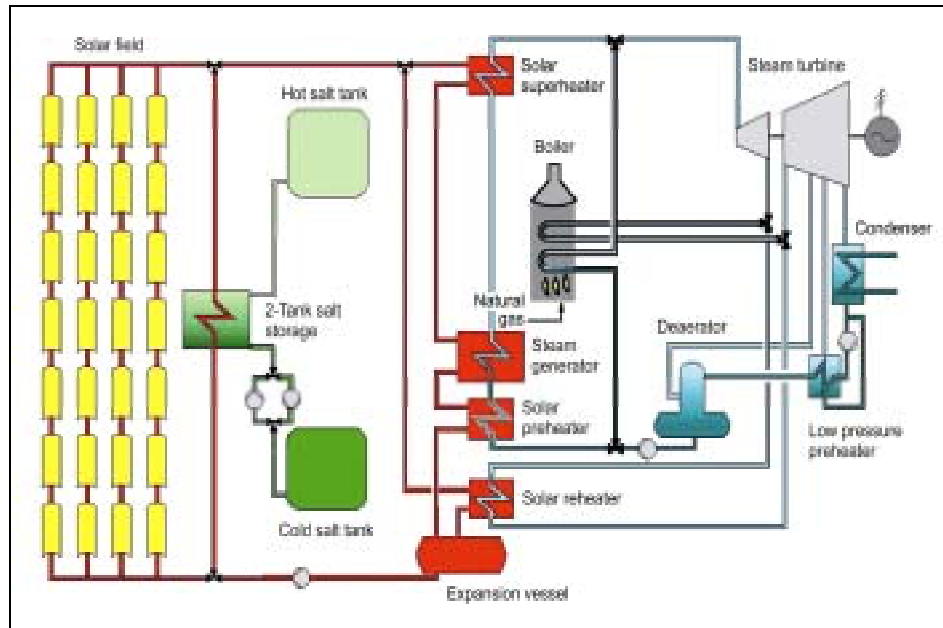
**Figure 1.2  Process flow schematic of a large-scale parabolic trough solar power plant with thermal storage capability (source: Flabeg Solar International)**
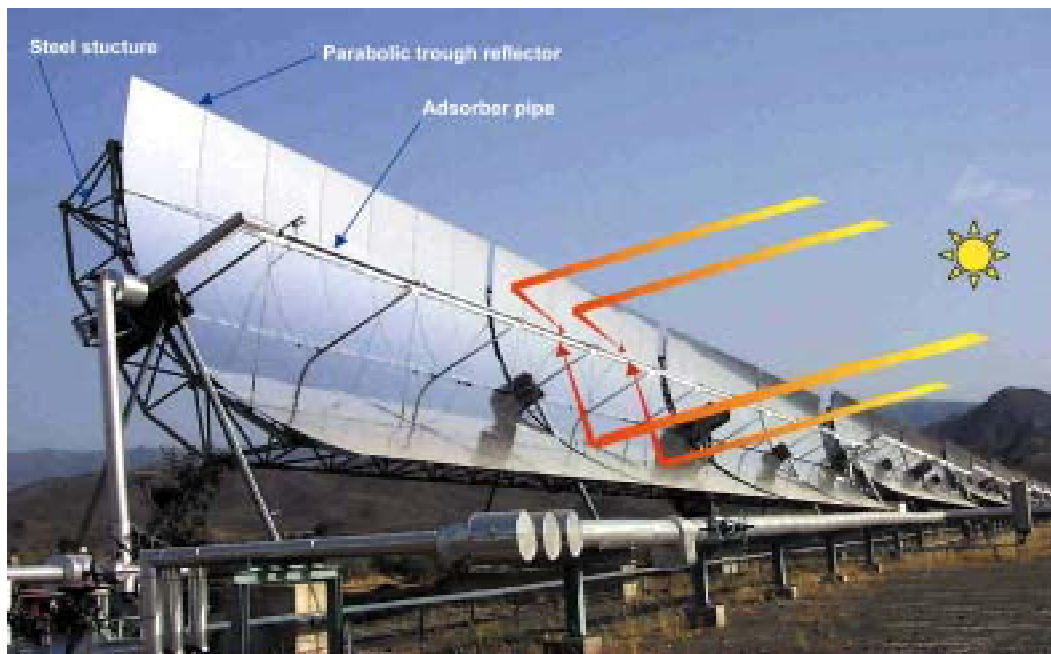


**Figure 1.3  Parabolic trough SCA located at a solar research test facility in Spain
(source: Plataforma Solar de Almeria)**

A diagram of an HCE is shown in Figure 1.4. The HCE consist of an absorber inside a glass envelope with bellows at either end. The absorber is typically a stainless steel tube about 70 mm in diameter with a special coating (selective coating) on the outside surface to provide the required optical properties. The selective coating has a high absorptance for radiation in the solar energy spectrum, and low emittance in

3

the long wave energy spectrum to reduce thermal radiation losses [Duffie and Beckman 1991]. Section 6.2 includes a discussion of the selective coating type, which has a strong influence on HCE performance.



1. Bellow
2. Glass Tube (Envelope)
3. Absorber Tube (Pipe)
4. Getter
5. Getter Bridge
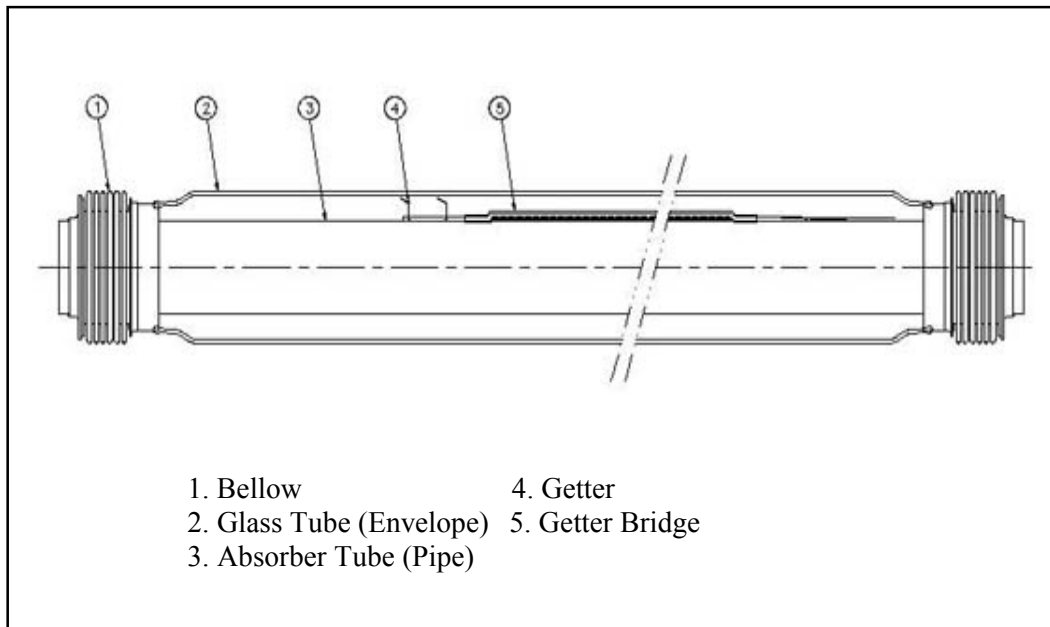
**Figure 1.4  Schematic of an HCE (source: Solel Solar Systems Ltd.)**

The glass envelope protects the absorber from degradation and reduces heat losses. It is typically made from Pyrex,® which maintains good strength and transmittance under high temperatures. To reduce reflective losses, the glass envelope goes through an anti-reflective treatment – basically a slight chemical etching. The annulus space between the absorber and the glass envelope is under vacuum to reduce thermal losses and protect the selective coating [Price et al. 2002]. The getter bridge installed in the annulus consists of metallic compounds designed to absorb hydrogen – which naturally permeates from the HTF and if left in the annulus would decrease the HCE performance (see Sections 6.3 and 6.5). The getter is a vacuum loss indicator consisting of barium, which turns white when exposed to oxygen.

The bellows provide a glass-to-metal seal and allow thermal expansion between the metal absorber and glass envelope. The bellows also allow the absorber to protrude beyond the glass envelope so that HCEs can be butt welded together to form a continuous receiver. Furthermore, the space between bellows provides a place to attach the HCE support brackets (see Figure 2.6 in Section 2.2).

For years, a combination of operating problems, collector cost, and low oil prices has restricted the growth of CSP [Duffie and Beckman 1991]. With recent improvements in materials, optics, structures, and controls – along with a renewed awareness of the importance of cleaner energy sources – CSP has become a more viable option for large-scale electricity generation. Leading the technology has been parabolic trough solar technology, which is the most proven and lowest cost large-scale CSP technology available [Price, et al. 2002].

## 1.2    Motivation

Early in the parabolic trough technology development, inefficient HCEs were a principal cause of poor SEGS performance [Price et al. 2002], so improving the HCE became a priority. A useful tool for improving the HCE was a heat transfer software model that could be used to evaluate new and current

HCE designs. The first software model was designed in the early 1990s, and upgraded several years later. The software played a useful part in HCE improvements, which have proven to be the primary reason for increases to the SEGS plants' performance [Price et al. 2002]. However, the HCE performance software tended to be problematic and in need of another upgrade.

The first version of the software model was developed by Virtus Energy Research Associates in 1992 and written in Microsoft QuickBasic [Cohen et al. 1999]. It (along with the later version and this current version) was based on a methodology proposed by SNL [1993]. Because QuickBasic had become obsolete, SNL developed a second version in 1999 written in Microsoft Excel Visual Basic. The second version improved algorithms and the user interface. However, it used a numerical solution technique that often could not converge on a solution and, because of simplifications in the heat transfer model, could not model many receiver configurations.

In conjunction with an expanded R&D effort to develop higher performance parabolic trough receivers, the National Renewable Energy Laboratory (NREL) funded by the U.S. Department of Energy (DOE) decided an improved HCE performance model was needed to meet the analysis needs of the program. This work, sponsored by NREL, consists of developing and documenting this model.

The new HCE performance model implemented in EES improves the heat transfer analysis, versatility, and speed of computation; provides additional model detail (two-dimensional energy balance model, HCE support bracket losses, pressure losses, etc.); improves the model robustness (valid for larger ranges of HTF flow properties, imbedded warning messages if correlations or HTF properties are used out of range of validity); and improves the modeling input and output capabilities. It was developed independently from the previous two models so it validates the heat transfer methodology originally proposed by SNL and all the changes to the original methodology (more detailed Nusselt number correlations, HCE support bracket losses, two-dimensional model etc.). Finally, it was developed in a more powerful programming environment that is more amenable to model changes and improvements. The model is described in Section 2.

## 2. HCE Performance Model

The HCE performance model is based on an energy balance about the collector and the HCE. The energy balance includes the direct normal solar irradiation incident on the collector, optical losses from both the collector and HCE, thermal losses from the HCE, and the heat gain into the HTF. For short receivers (< 100 m) a one-dimensional energy balance gives reasonable results; for longer receivers a two-dimensional energy balance becomes necessary. All the equations and relationships used in both the one- and two-dimensional HCE performance models are described in the following sections.

### 2.1 One-Dimensional Energy Balance Model

The HCE performance model uses an energy balance between the HTF and the atmosphere, and includes all equations and correlations necessary to predict the terms in the energy balance, which depend on the collector type, HCE condition, optical properties, and ambient conditions.

Figure 2.1a shows the one-dimensional steady-state energy balance for a cross-section of an HCE, with and without the glass envelope intact, and Figure 2.1b shows the thermal resistance model and subscript definitions. For clarity, the incoming solar energy and optical losses have been omitted from the resistance model. The optical losses are due to imperfections in the collector mirrors, tracking errors, shading, and mirror and HCE cleanliness (see Section 2.1.6.1). The effective incoming solar energy (solar energy minus optical losses) is absorbed by the glass envelope ($\dot{q}'_{5SolAbs}$) and absorber selective coating

($\dot{q}'_{3SolAbs}$). Some energy that is absorbed into the selective coating is conducted through the absorber ($\dot{q}'_{23cond}$) and transferred to the HTF by convection ($\dot{q}'_{12conv}$); remaining energy is transmitted back to the glass envelope by convection ($\dot{q}'_{34conv}$) and radiation ($\dot{q}'_{34rad}$) and lost through the HCE support bracket through conduction ($\dot{q}'_{cond,bracket}$). The energy from the radiation and convection then passes through the glass envelope by conduction ($\dot{q}'_{45cond}$) and along with the energy absorbed by the glass envelope ($\dot{q}'_{5SolAbs}$) is lost to the environment by convection ($\dot{q}'_{56conv}$) and radiation ($\dot{q}'_{57rad}$). If the glass envelope is missing, the heat loss from the absorber is lost directly to the environment. The model assumes all temperatures, heat fluxes, and thermodynamic properties are uniform around the circumference of the HCE. Also, all flux directions shown in Figure 2.1a are positive.

With the help of Figure 2.1, the energy balance equations are determined by conserving energy at each surface of the HCE cross-section, both with and without the glass envelope intact.

with the glass envelope:

$$\dot{q}'_{12conv} = \dot{q}'_{23cond} \tag{2.1a}$$
$$\dot{q}'_{3SolAbs} = \dot{q}'_{34conv} + \dot{q}'_{34rad} + \dot{q}'_{23cond} + \dot{q}'_{cond,bracket} \tag{2.1b}$$
$$\dot{q}'_{34conv} + \dot{q}'_{34rad} = \dot{q}'_{45cond} \tag{2.1c}$$
$$\dot{q}'_{45cond} + \dot{q}'_{5SolAbs} = \dot{q}'_{56conv} + \dot{q}'_{57rad} \tag{2.1d}$$
$$\dot{q}'_{HeatLoss} = \dot{q}'_{56conv} + \dot{q}'_{57rad} + \dot{q}'_{cond,bracket} \tag{2.1e}$$

without the glass envelope:

$$\dot{q}'_{12conv} = \dot{q}'_{23cond} \tag{2.2a}$$
$$\dot{q}'_{3SolAbs} = \dot{q}'_{36conv} + \dot{q}'_{37rad} + \dot{q}'_{23cond} + \dot{q}'_{cond,bracket} \tag{2.2b}$$
$$\dot{q}'_{HeatLoss} = \dot{q}'_{36conv} + \dot{q}'_{37rad} + \dot{q}'_{cond,bracket} \tag{2.2c}$$

In the case without the glass envelope, Equations 2.1c and 2.1d drop out, and the 4 subscript for the convection and radiation from the absorber change to 6 and 7, respectively, since the heat loss from the absorber outer surface escapes directly to the environment instead of through the glass envelope.

Note that the solar absorptance $\dot{q}'_{3SolAbs}$ and $\dot{q}'_{5SolAbs}$ are treated as heat flux terms. This simplifies the solar absorption terms and makes the heat conduction through the absorber pipe and glass envelope linear. In reality, the solar absorption in the absorber (opaque metal material) and glass envelope (semitransparent material) are volumetric phenomena. However, most of the absorption in the absorber occurs very close to the surface (about 6 angstroms) [Ozisik 1973], and although solar absorption occurs throughout the thickness of the glass envelope, the absorptance is relatively small ($\alpha = 0.02$). Therefore, any error in treating solar absorption as a surface phenomenon should be relatively small.

All the terms in Equations 2.1 and 2.2 are defined in Table 2.1. Dotted variables indicate rates and the prime indicates per unit length of receiver. A double prime will indicate per unit normal aperture area.

a) One-dimensional energy balance

$\dot{q}'_{5SolAbs}$  $\dot{q}'_{34conv}$  $\dot{q}'_{34rad}$  $\dot{q}'_{45cond}$  $\dot{q}'_{56conv}$  $\dot{q}'_{23cond}$  $\dot{q}'_{57rad}$  $\dot{q}'_{3SolAbs}$  $\dot{q}'_{12conv}$  $\dot{q}'_{cond,bracket}$

$\dot{q}'_{36conv}$  $\dot{q}'_{37rad}$  $\dot{q}'_{23cond}$  $\dot{q}'_{3SolAbs}$  $\dot{q}'_{12conv}$  $\dot{q}'_{cond,bracket}$

absorber pipe
selective coating
heat transfer fluid
glass envelope

With Glass Envelope

Without Glass Envelope

b) Thermal resistance model

conduction
(HCE support bracket)

radiation

radiation

(1) convection (2) conduction (3) radiation convection (4) conduction (5) radiation convection (7) (6)

(1) heat transfer fluid
(2) absorber inner surface
(3) absorber outer surface
(4) glass envelope inner surface
(5) glass envelope outer surface
(6) surrounding air
(7) sky

**Figure 2.1  a) One-dimensional steady-state energy balance and b) thermal resistance model for a cross-section of an HCE**

**Table 2.1 Heat Flux Definitions**

| Heat Flux (W/m)* | Heat Transfer Mode | Heat Transfer Path | |
|---|---|---|---|
| | | **From** | **To** |
| $\dot{q}'_{12conv}$ | convection | inner absorber pipe surface | heat transfer fluid |
| $\dot{q}'_{23cond}$ | conduction | outer absorber pipe surface | inner absorber pipe surface |
| $\dot{q}'_{3SolAbs}$ | solar irradiation absorption | incident solar irradiation | outer absorber pipe surface |
| $\dot{q}'_{34conv}$ | convection | outer absorber pipe surface | inner glass envelope surface |
| $\dot{q}'_{34rad}$ | radiation | outer absorber pipe surface | inner glass envelope surface |
| $\dot{q}'_{45cond}$ | conduction | inner glass envelope surface | outer glass envelope surface |
| $\dot{q}'_{5SolAbs}$ | solar irradiation absorption | incident solar irradiation | outer glass envelope surface |
| $\dot{q}'_{56conv}$ | convection | outer glass envelope surface | ambient |
| $\dot{q}'_{57rad}$ | radiation | outer glass envelope surface | sky |
| $\dot{q}'_{36conv}$ | convection | outer absorber pipe surface | ambient |
| $\dot{q}'_{37rad}$ | radiation | outer absorber pipe surface | sky |
| $\dot{q}'_{cond,bracket}$ | conduction | outer absorber pipe surface | HCE support bracket |
| $\dot{q}'_{HeatLoss}$ | convection and radiation | heat collecting element | ambient and sky |
| * Per unit aperture length. | | | |

### 2.1.1 Convection Heat Transfer between the HTF and the Absorber

From Newton's law of cooling, the convection heat transfer from the inside surface of the absorber pipe to the HTF is

$$\dot{q}'_{12conv} = h_1 D_2 \pi (T_2 - T_1) \tag{2.3}$$

with

$$h_1 = Nu_{D2} \frac{k_1}{D_2} \tag{2.4}$$

where

$\quad h_1 \quad = \quad$ HTF convection heat transfer coefficient at $T_1$ (W/m$^2$-K)
$\quad D_2 \quad = \quad$ inside diameter of the absorber pipe (m)
$\quad T_1 \quad = \quad$ mean (bulk) temperature of the HTF ($^{\circ}$C)
$\quad T_2 \quad = \quad$ inside surface temperature of absorber pipe ($^{\circ}$C)
$\quad Nu_{D2} \quad = \quad$ Nusselt number based on $D_2$
$\quad k_1 \quad = \quad$ thermal conductance of the HTF at $T_1$ (W/m-K)

In these equations, both $T_1$ and $T_2$ are independent of angular and longitudinal HCE directions, as will be all temperatures and properties in the one-dimensional energy balance model.

The Nusselt number depends on the type of flow through the HCE. At typical operating conditions, the flow in an HCE is well within the turbulent flow region. However, during off-solar hours or when evaluating the HCE heat losses on a test platform, the flow in the HCE may become transitional or laminar because of the viscosity of the HTF at lower temperatures. Therefore, to model the heat losses under all conditions, the model includes conditional statements to determine type of flow. The Nusselt number used for each flow condition is outlined in Section 2.1.1.1.

### 2.1.1.1    Turbulent and Transitional Flow Cases

To model the convective heat transfer from the absorber to the HTF for turbulent and transitional cases (Reynolds number > 2300) the following Nusselt number correlation developed by Gnielinski [1976] is used.

$$Nu_{D2} = \frac{f_2/8(\mathrm{Re}_{D2}-1000)\mathrm{Pr}_1}{1+12.7\sqrt{f_2/8}\left(\mathrm{Pr}_1^{2/3}-1\right)}\left(\frac{\mathrm{Pr}_1}{\mathrm{Pr}_2}\right)^{0.11} \tag{2.5}$$

with

$$f_2 = \left(1.82\log_{10}(\mathrm{Re}_{D2})-1.64\right)^{-2} \tag{2.6}$$

where

    $f_2$   =   friction factor for the inner surface of the absorber pipe
    $\mathrm{Pr}_1$   =   Prandtl number evaluated at the HTF temperature, $T_1$
    $\mathrm{Pr}_2$   =   Prandtl number evaluated at the absorber inner surface
                 temperature, $T_2$

Along with being valid for turbulent pipe flow, this Nusselt number correlation accounts for transitional flow states for Reynolds numbers between 2300 and 4000. Furthermore, the correlation adjusts for fluid property variations between the absorber wall temperature and bulk fluid temperature. The correlation is valid for $0.5 < \mathrm{Pr}_1 < 2000$ and $2300 < \mathrm{Re}_{D2} < 5E6$. If used out of this range of validity, the code will display a warning message. Except for $\mathrm{Pr}_2$, all fluid properties are evaluated at the mean HTF temperature, $T_1$. The correlation assumes uniform heat flux and temperature, and assumes the absorber has a smooth inner surface.

### 2.1.1.2    Laminar Flow Case

An option to model the flow as laminar is included in all the one-dimensional versions of the HCE heat transfer codes. When the laminar option is chosen and the Reynolds number is lower than 2300, the Nusselt number will be constant. For pipe flow, the value will be 4.36 [Incropera and DeWitt 1990]. For annulus flow, the value will depend on the ratio between the pipe insert diameter and absorber inside diameter, $D_p/D_2$ (see Section 2.1.1.3). Pipe and annulus flow values were derived assuming constant heat flux. If the laminar option is not chosen and the Reynolds number is less than 2300, the code will use the turbulent flow model described in Section 2.1.1.1, but will display the following warning message: "The result may not be accurate, since $2300 < \mathrm{Re}_{D2} < (5E6)$ does not hold. See Function fq_12conv. $\mathrm{Re}_{D2} =$ (value)."

### 2.1.1.3    Annulus Flow Case

One possible use of the HCE performance model will be to evaluate HCE testing conducted on an AZTRAK testing platform located at SNL (see Section 3.1.2). The test platform is essentially a scaled-down version of a trough plant. Unfortunately, the test platform does not have the same volumetric pumping capability and collector lengths as a trough plant. Therefore, to simulate field heat transfer

characteristics, a pipe is inserted in the center of the HCE [Dudley et al. 1994]. This decreases the cross-sectional flow area of the HTF, increasing the flow velocities, and thus increasing the Reynolds number. To apply to this type of HCE testing, the code is set up to model the HTF flow as annulus flow when prompted.

The turbulent pipe flow correlations described in Section 2.1.1.2 can be used for annulus flow by substituting the inside pipe diameter, $D_2$, with the following hydraulic diameter [Incropera and DeWitt 1990].

$$D_h = \frac{4A_{cs}}{P_w} = D_2 - D_p \tag{2.7}$$

where

$$
\begin{aligned}
A_{cs} &= \text{flow cross-sectional area (m}^2\text{)} \\
P_w &= \text{wetted perimeter (m)} \\
D_p &= \text{outside diameter of pipe insert (m)} \\
D_2 &= \text{inner diameter of absorber pipe (m)}
\end{aligned}
$$

For laminar flow through an annulus, the Nusselt number depends on the ratio $D_p/D_2$. Table 2.2 lists Nusselt numbers for various diameter ratios. The table is a modified version of a table for uniform heat flux occurring at both the inner and outer surfaces of the annulus [Incropera and DeWitt 1990].

**Table 2.2  Nusselt Number for Laminar Annulus Flow with Uniform Heat Flux**

| $D_p/D_2$ | $Nu_{Dh}$ |
|-----------|-----------|
| 0 | 4.364 |
| 0.05 | 4.792 |
| 0.10 | 4.834 |
| 0.20 | 4.833 |
| 0.40 | 4.979 |
| 0.60 | 5.099 |
| 0.80 | 5.24 |
| 1.00 | 5.385 |

### 2.1.2  Conduction Heat Transfer through the Absorber Wall

Fourier's law of conduction through a hollow cylinder describes the conduction heat transfer through the absorber wall [Incropera and DeWitt 1990].

$$\dot{q}'_{23cond} = 2\pi k_{23}\left(T_2 - T_3\right)/\ln\left(D_3/D_2\right) \tag{2.8}$$

where

$$
\begin{aligned}
k_{23} &= \text{absorber thermal conductance at the average absorber} \\
&\quad \text{temperature } (T_2+T_3)/2 \text{ (W/m-K)} \\
T_2 &= \text{absorber inside surface temperature (K)} \\
T_3 &= \text{absorber outside surface temperature (K)} \\
D_2 &= \text{absorber inside diameter (m)} \\
D_3 &= \text{absorber outside diameter (m)}
\end{aligned}
$$

10

In this equation the conduction heat transfer coefficient is constant, and is evaluated at the average temperature between the inner and outer surfaces.

The conduction coefficient depends on the absorber material type. The HCE performance model includes three stainless steels: 304L, 316L, and 321H, and one copper: B42. If 304L or 316L is chosen, the conduction coefficient is calculated with the following equation.

$$k_{23} = (0.013)T_{23} + 15.2 \qquad\qquad (2.9a)$$

If 321H is chosen,

$$k_{23} = (0.0153)T_{23} + 14.775 \qquad\qquad (2.9b)$$

Both equations were determined by linearly fitting data from Davis [2000]. If copper is chosen, the conduction coefficient is a constant of 400 W/m-K [ASM Handbook Committee 1978]. Conductive resistance through the selective coating has been neglected.

### 2.1.3 Heat Transfer from the Absorber to the Glass Envelope

Convection and radiation heat transfer occur between the absorber and the glass envelope. The convection heat transfer mechanism depends on the annulus pressure [KJCOC 1993]. At low pressures ($< \sim 1$ torr), the heat transfer mechanism is molecular conduction. At higher pressures ($> \sim 1$ torr), the mechanism is free convection. The radiation heat transfer occurs because of the difference in temperatures between the outer absorber surface and the inner glass envelope surface. The radiation heat transfer calculation is simplified by assuming the glass envelope is opaque to infrared radiation and assuming gray ($\rho = \alpha$) surfaces.

#### 2.1.3.1  Convection Heat Transfer

Two heat transfer mechanisms are evaluated to determine the convection heat transfer between the absorber and glass envelope ($\dot{q}'_{34conv}$), free-molecular and natural convection [KJCOC 1993]. In the HCE performance model, the larger of the two values is chosen. This results in a smooth transition between the two heat transfer modes, as shown in Figure 2.2.

**Heat Loss Vs. Annulus Pressure**

Heat Loss (W/m)

Annulus Pressure (torr)

0.0001    0.001    0.01    0.1    1    10    100    1000
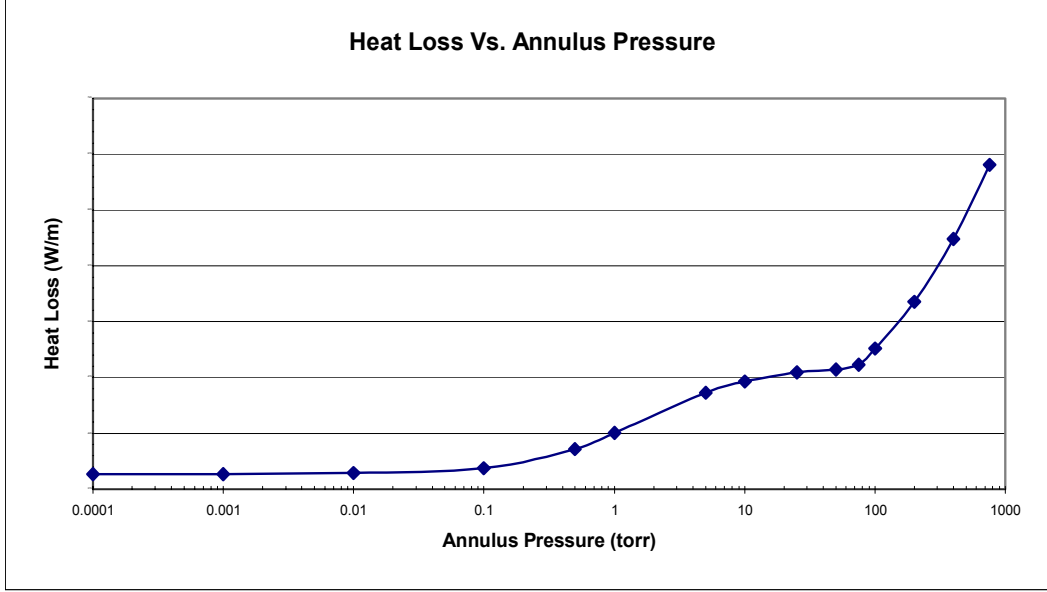
**Figure 2.2  Chart of heat loss per unit length of receiver as a function of annulus pressure**

### 2.1.3.1.1    Vacuum in Annulus

When the HCE annulus is under vacuum (pressure $<$ ~1 torr), the convection heat transfer between the absorber and glass envelope occurs by free-molecular convection [Ratzel et al.1979].

$$\dot{q}'_{34conv} = \pi D_3 h_{34} (T_3 - T_4) \tag{2.10}$$

with

$$h_{34} = \frac{k_{std}}{(D_3/2\ln(D_4/D_3) + b\lambda(D_3/D_4 + 1))} \tag{2.11}$$

$$b = \frac{(2-a)(9\gamma - 5)}{2a(\gamma + 1)} \tag{2.12}$$

$$\lambda = \frac{2.331E(-20)(T_{34} + 273.15)}{(P_a\delta^2)} \tag{2.13}$$

where

$D_3$  =  outer absorber surface diameter (m)
$D_4$  =  inner glass envelope surface diameter (m)
$h_{34}$  =  convection heat transfer coefficient for the annulus gas at $T_{34}$ (W/m²-K)
$T_3$  =  outer absorber surface temperature (°C)
$T_4$  =  inner glass envelope surface temperature (°C)
$k_{std}$  =  thermal conductance of the annulus gas at standard temperature and pressure (W/m-K)
b  =  interaction coefficient

$$\lambda = \text{mean-free-path between collisions of a molecule (cm)}$$

$$a = \text{accommodation coefficient}$$

$$\gamma = \text{ratio of specific heats for the annulus gas}$$

$$T_{34} = \text{average temperature } (T_3 + T_4)/2 \ (^oC)$$

$$P_a = \text{annulus gas pressure (mmHg)}$$

$$\delta = \text{molecular diameter of annulus gas (cm)}$$

This correlation is valid for $Ra_{D4} < (D_4 / (D_4 - D_3))^4$, but slightly overestimates the heat transfer for very small pressures ($\sim< 0.0001$ torr). The molecular diameters of the gases, $\delta$, were obtained from Marshal [1976] and are shown in Table 2.3. The table also compares the convection heat transfer coefficients ($h_{34}$) and other parameters that are used in the calculation for each of the three gases included in the HCE performance model.

**Table 2.3  Heat Transfer Coefficients and Constants for Each Annulus Gas**

| Annulus Gas | $k_{std}$ [W/m-K] | b | $\lambda$ [cm] | $\gamma$ | $\delta$ [cm] | $h_{34}$ [W/m²-K] |
|---|---|---|---|---|---|---|
| Air | 0.02551 | 1.571 | 88.67 | 1.39 | 3.53E-8 | 0.0001115 |
| Hydrogen | 0.1769 | 1.581 | 191.8 | 1.398 | 2.4E-8 | 0.0003551 |
| Argon | 0.01777 | 1.886 | 76.51 | 1.677 | 3.8E-8 | 0.00007499 |
| $T_{1avg}$ = 300 $^oC$, Insolation = 940 W/m² | | | | | | |

### 2.1.3.1.2   Pressure in Annulus

When the HCE annulus loses vacuum (pressure > ~1 torr), the convection heat transfer mechanism between the absorber and glass envelope occurs by natural convection. Raithby and Holland's correlation for natural convection in an annular space between horizontal cylinders is used for this case [Bejan 1995].

$$q'_{34conv} = \frac{2.425 k_{34}(T_3 - T_4)\left(\Pr Ra_{D3}/(0.861 + \Pr_{34})\right)^{1/4}}{\left(1 + (D_3/D_4)^{3/5}\right)^{5/4}} \quad (2.14)$$

$$Ra_{D3} = \frac{g\beta(T_3 - T_4)D_3^3}{\alpha\nu} \quad (2.15)$$

For an ideal gas

$$\beta = \frac{1}{T_{avg}} \quad (2.16)$$

$$k_{34} = \text{thermal conductance of annulus gas at } T_{34} \text{ (W/m-K)}$$

$$T_3 = \text{outer absorber surface temperature } (^oC)$$

$$T_4 = \text{inner glass envelope surface temperature } (^oC)$$

$$D_3 = \text{outer absorber diameter (m)}$$

$$D_4 = \text{inner glass envelope diameter (m)}$$

$$\Pr_{34} = \text{Prandtl number}$$

$$Ra_{D3} = \text{Rayleigh number evaluated at } D_3$$

$$\beta = \text{volumetric thermal expansion coefficient (1/K)}$$

$$T_{34} = \text{average temperature, } (T_3 + T_4)/2 \ (^oC)$$

This correlation assumes long, horizontal, concentric cylinders at uniform temperatures, and is valid for $Ra_{D4} > (D_4 / (D_4 - D_3))^4$. All physical properties are evaluated at the average temperature $(T_3 + T_4)/2$.

### 2.1.3.2    Radiation Heat Transfer

The radiation heat transfer between the absorber and glass envelope ($\dot{q}'_{34rad}$) is estimated with the following equation [Incropera and DeWitt 1990].

$$\dot{q}'_{34rad} = \frac{\sigma \pi D_3 \left(T_3^{\,4} - T_4^{\,4}\right)}{\left(1/\varepsilon_3 + (1 - \varepsilon_4)D_3/(\varepsilon_4 D_4)\right)} \tag{2.17}$$

where

| | | |
|---|---|---|
| $\sigma$ | = | Stefan-Boltzmann constant (W/m$^2$-K$^4$) |
| $D_3$ | = | outer absorber diameter (m) |
| $D_4$ | = | inner glass envelope diameter (m) |
| $T_3$ | = | outer absorber surface temperature (K) |
| $T_4$ | = | inner glass envelope surface temperature (K) |
| $\varepsilon_3$ | = | Absorber selective coating emissivity |
| $\varepsilon_4$ | = | glass envelope emissivity |

Several assumptions were made in deriving this equation: nonparticipating gas in the annulus, gray surfaces, diffuse reflections and irradiation, and long concentric isothermal cylinders. Also, the glass envelope is assumed to be opaque to infrared radiation. Not all these assumptions are completely accurate. For instance, neither the glass envelope nor the selective coatings are gray, and the glass envelope is not completely opaque for the entire thermal radiation spectrum [Touloukian and DeWitt 1972]. However, any errors associated with the assumptions should be relatively small.

### 2.1.4  Conduction Heat Transfer through the Glass Envelope

The conduction heat transfer through the glass envelope uses the same equation as the conduction through the absorber wall described in Section 2.1.2. The anti-reflective treatment on the inside and outside surfaces of the glass envelope is assumed to introduce no thermal resistance and to have no effect on the glass emissivity. This should be fairly accurate since the treatment is a chemical etching and does not add additional elements to the glass surface [Mahoney 2002]. As in the absorber case, the temperature distribution is assumed to be linear. Furthermore, the thermal conductance is assumed constant – as explained in Section 2.1 – with a value of 1.04 (Pyrex® glass) [Touloukian and DeWitt 1972].

### 2.1.5  Heat Transfer from the Glass Envelope to the Atmosphere

The heat will transfer from the glass envelope to the atmosphere by convection and radiation. The convection will either be forced or natural, depending on whether there is wind. Radiation heat loss occurs due to the temperature difference between the glass envelope and sky.

### 2.1.5.1 Convection Heat Transfer

The convection heat transfer from the glass envelope to the atmosphere ($\dot{q}'_{56conv}$) is the largest source of heat loss, especially if there is a wind. From Newton's law of cooling

$$\dot{q}'_{56conv} = h_{56}\pi D_5 \left(T_5 - T_6\right) \tag{2.18}$$

$$h_{56} = \frac{k_{56}}{D_5} Nu_{D5} \tag{2.19}$$

where

| | | |
|---|---|---|
| $T_5$ | = | glass envelope outer surface temperature ($^{\circ}$C) |
| $T_6$ | = | ambient temperature ($^{\circ}$C) |
| $h_{56}$ | = | convection heat transfer coefficient for air at $(T_5 - T_6)/2$ (W/m$^2$-K) |
| $k_{56}$ | = | thermal conductance of air at $(T_5 - T_6)/2$ (W/m-K) |
| $D_5$ | = | glass envelope outer diameter (m) |
| $Nu_{D5}$ | = | average Nusselt number based on the glass envelope outer diameter |

The Nusselt number depends on whether the convection heat transfer is natural (no wind) or forced (with wind).

### 2.1.5.1.1 No Wind Case

If there is no wind, the convection heat transfer from the glass envelope to the environment will be by natural convection. For this case, the correlation developed by Churchill and Chu will be used to estimate the Nusselt number [Incropera and DeWitt 1990].

$$\overline{Nu}_{D5} = \left\{0.60 + \frac{0.387 Ra_{D5}^{1/6}}{\left[1 + \left(0.559/Pr_{56}\right)^{9/16}\right]^{8/27}}\right\}^2 \tag{2.20}$$

$$Ra_{D5} = \frac{g\beta\left(T_5 - T_6\right)D_5^{3}}{\left(\alpha_{56}\nu_{56}\right)} \tag{2.21}$$

$$\beta = \frac{1}{T_{56}} \tag{2.22}$$

$$Pr_{56} = \frac{\nu_{56}}{\alpha_{56}} \tag{2.23}$$

where

| | | |
|---|---|---|
| $Ra_{D5}$ | = | Rayleigh number for air based on the glass envelope outer diameter, $D_5$ |
| g | = | gravitational constant (9.81) (m/s$^2$) |

$\alpha_{56}$ = thermal diffusivity for air at $T_{56}$ (m²/s)
$\beta$ = volumetric thermal expansion coefficient (ideal gas) (1/K)
$Pr_{56}$ = Prandtl number for air at $T_{56}$
$\nu_{56}$ = kinematic viscosity for air at $T_{56}$ (m²/s)
$T_{56}$ = film temperature $(T_5 + T_6)/2$ (K)

This correlation is valid for $10^5 < Ra_{D_o} < 10^{12}$, and assumes a long isothermal horizontal cylinder. Also, all the fluid properties are determined at the film temperature, $(T_5 + T_6)/2$.

### 2.1.5.1.2 Wind Case

If there is wind, the convection heat transfer from the glass envelope to the environment will be forced convection. The Nusselt number in this case is estimated with Zhukauskas' correlation for external forced convection flow normal to an isothermal cylinder [Incropera and DeWitt 1990].

$$\overline{Nu}_{D5} = C \, Re_{D5}{}^m \, Pr_6{}^n \left( \frac{Pr_6}{Pr_5} \right)^{1/4} \tag{2.24}$$

with

| Re$_D$ | C | m |
|---|---|---|
| 1-40 | 0.75 | 0.4 |
| 40-1000 | 0.51 | 0.5 |
| 1000-200000 | 0.26 | 0.6 |
| 200000-1000000 | 0.076 | 0.7 |

and

$$n = 0.37, \text{ for } Pr <= 10$$
$$n = 0.36, \text{ for } Pr > 10$$

This correlation is valid for $0.7 < Pr_6 < 500$, and $1 < Re_{D5} < 10^6$. All fluid properties are evaluated at the atmospheric temperature, $T_6$, except $Pr_5$, which is evaluated at the glass envelope outer surface temperature.

### 2.1.5.2 Radiation Heat Transfer

As will be discussed in Section 2.1.6, the useful incoming solar irradiation is included in the solar absorption terms. Therefore, the radiation transfer between the glass envelope and sky, discussed here, is caused by the temperature difference between the glass envelope and sky. To approximate this, the envelope is assumed to be a small convex gray object in a large blackbody cavity (sky). The net radiation transfer between the glass envelope and sky becomes [Incropera and DeWitt 1990]

$$\dot{q}'_{57rad} = \sigma D_5 \pi \varepsilon_5 \left( T_5{}^4 - T_7{}^4 \right) \tag{2.25}$$

where

$\sigma$ = Stefan-Boltzmann constant (5.670E-8) (W/m²-K⁴)
$D_5$ = glass envelope outer diameter (m)
$\varepsilon_5$ = emissivity of the glass envelope outer surface

$$T_5 = \text{glass envelope outer surface temperature (K)}$$
$$T_7 = \text{effective sky temperature (K)}$$

The sky, especially during less than clear conditions, does not act like a blackbody; however, it is common practice to model it as such and to use an effective to compensate for the difference as stated by Duffie and Beckman [1991]. As they stated, "the effective sky temperature accounts for the fact that the atmosphere is not at a uniform temperature and that the atmosphere radiates only in certain wavelength bands." Furthermore, "the atmosphere is essentially transparent in the wavelength region from 8 to 14 μm, but outside of this 'window' the atmosphere has absorbing bands covering much of the infrared spectrum." Several relations have been proposed to relate the effective sky temperature for clear skies to measured meteorological data; however, to simplify the model, the effective sky temperature is approximated as being $8^{\circ}$C below the ambient temperature – as determined in the original HCE heat loss model for an ambient temperature of $22^{\circ}$C [KJC Operating Company 1993].

### 2.1.6  Solar Irradiation Absorption

The optical losses and solar absorption – given the direct normal solar irradiation, solar angle, and optical properties of the trough mirrors and HCE components – is very difficult to model accurately with a set of equations that can be solved with a software program like EES. Because of this, optical efficiency terms are estimated and combined to form an effective optical efficiency, which in turn is used to determine the optical loss and solar absorption terms.

### 2.1.6.1    Optical Properties

The optical properties used in the HCE performance model were obtained from a combination of sources. Some were determined by SEGS plant performance modeling completed by NREL. Some were determined by tests conducted by SNL, and Solel Solar Systems Ltd. of Israel – the prime HCE manufacturer. Some were evaluated and revised with ray tracing software developed by NREL.

Table 2.4 lists terms used to estimate the effective optical efficiencies. The table was generated from data published in a report by NREL [Price et al. 2002], which in turn was based on field tests [Dudley et al. 1994], and software performance modeling . The first three terms, $\varepsilon'_1$, $\varepsilon'_2$, and $\varepsilon'_3$, and the last term, $\varepsilon'_6$, are strictly estimates. The clean mirror reflectance $\rho_{cl}$ is a known value, and the two dirt effect approximations $\varepsilon'_4$ and $\varepsilon'_5$ are recommendations by Duffie and Beckman [1991]. The data in the table are valid only for solar incidence irradiation normal to the collector aperture. An incident angle modifier term is added to account for incident angle losses, which includes trough end shading, changes in reflection and refraction, and selective coating incident angle effects.

**Table 2.4  Estimates of Effective Optical Efficiency Terms [Price 2001]**

| | |
|---|---|
| $\varepsilon'_1$ = HCE Shadowing (bellows, shielding, supports) | 0.974 |
| $\varepsilon'_2$ = Tracking Error | 0.994 |
| $\varepsilon'_3$ = Geometry Error (mirror alignment) | 0.98 |
| $\rho_{cl}$ = Clean Mirror Reflectance | 0.935 |
| $\varepsilon'_4$ = Dirt on Mirrors* | reflectivity/$\rho_{cl}$ |
| $\varepsilon'_5$ = Dirt on HCE | $(1 + \varepsilon'_4)/2$ |
| $\varepsilon'_6$ = Unaccounted | 0.96 |
| * reflectivity is a user input (typically between 0.88 and 0.93) | |

In Table 2.4, there are terms for collector geometric effects (shadowing, tracking, alignment), mirror and glass envelope transmittance effects (mirror reflectance, and dirt), and a term for unexplained differences between field test data and modeled data. Testing continues to refine all these values and to better understand the optics of the HCEs. In the EES codes for the HCE performance model, the optical efficiency terms can also be manually entered (see Section 3).

Another term, *incident angle modifier*, is needed for cases when the solar irradiation is not normal to the collector aperture. It is a function of the solar incidence angle to the normal of the collector aperture. The equation was determined from HCE testing conducted at SNL [Dudley et al. 1994].

$$K = \cos(\theta) + 0.000884\theta - 0.00005369\theta^2 \tag{2.26}$$

Other optical properties include the glass envelope absorptance, emittance, and transmittance; and the selective coating absorptance and emittance. The glass envelope absorptance and emissivity are constants (independent of temperature) and are constant for all selective coating types ($\alpha = 0.02$, $\varepsilon = 0.86$). The transmittance and the selective coating properties (see Table 2.5) coincide with the selective coating types. Both the envelope transmittance and the coating absorptance are constants; the coating emittance is a function of temperature. All the selective coating types listed are included in the EES codes. The "Solel UVAC Cermet avg" selective coating is the reference value used in all the design study and comparison charts shown in this report, unless stated otherwise.

**Table 2.5  Optical Properties for Each Selective Coating**

| Selective Coating | Envelope Transmittance | Coating Absorptance | Coating Emittance | |
|---|---|---|---|---|
| | | | @ 100$^\circ$C | @ 400$^\circ$C |
| Luz Black Chrome | 0.935 | 0.94 | 0.11 | 0.27 |
| Luz Cermet | 0.935 | 0.92 | 0.06 | 0.15 |
| Solel UVAC Cermet a | 0.965 | 0.96 | 0.07 | 0.13 |
| Solel UVAC Cermet b | 0.965 | 0.95 | 0.08 | 0.15 |
| Solel UVAC Cermet avg | 0.965 | 0.955 | 0.076 | 0.14 |
| Solel UVAC Cermet Proposed a | 0.97 | 0.98 | 0.04 | 0.10 |
| Solel UVAC Cermet Proposed b | 0.97 | 0.97 | 0.02 | 0.07 |

The emittance equations used in the codes are shown in Table 2.6, and coincide with the emittance values in Table 2.5. For all the coating types, the emittance values between the two reference points, 400$^\circ$C and 100$^\circ$C, are nearly linear. However, more test data were available for the UVAC (Universal Vacuum Air Collector) Cermets, and thus this emittance is described with a second-order polynomial fit; the other coating emittance values use linear fits. Also, the two proposed selective coatings (Solel UVAC Cermet Proposed a and Solel UVAC Cermet Proposed b) were specified by the manufacturer for a single temperature of 400$^\circ$C; therefore, the temperature dependency had to be approximated. This was done with a slope and intercept to resemble the trends of the results for the Cermet tested by SNL.

**Table 2.6 Temperature-Dependent Emittance Equations**

| Coating Type | Coating Emittance* |
|---|---|
| Luz Black Chrome | 0.0005333 (T + 273.15) - 0.0856 |
| Luz Cermet | 0.000327 (T + 273.15) - 0.065971 |
| Solel UVAC Cermet a | $(2.249E\text{-}7)T^2 + (1.039E\text{-}4)T + 5.599E\text{-}2$ |
| Solel UVAC Cermet b | $(1.565E\text{-}7)T^2 + (1.376E\text{-}4)T + 6.966E\text{-}2$ |
| Solel UVAC Cermet avg | $(1.907E\text{-}7)T^2 + (1.208E\text{-}4)T + 6.282E\text{-}2$ |
| Solel UVAC Cermet Proposed a | $(2.084E\text{-}4)T + 1.663E\text{-}2$ |
| Solel UVAC Cermet Proposed b | $(1.666E\text{-}4)T + 3.375E\text{-}3$ |
| * All temperatures are in degrees Celsius. | |

### 2.1.6.2 Solar Irradiation Absorption in the Glass Envelope

As stated in Section 2.1, the solar absorption into the glass envelope is treated as a heat flux to simplify the model. Physically this is not true. The solar absorption in the glass envelope is a heat generation phenomenon and is a function of the glass thickness. However, this assumption introduces minimal error since the solar absorptance coefficient is small for glass, 0.02 [Touloukian and DeWitt 1972], and the glass envelope is relatively thin, 6 mm. Also, an optical efficiency is estimated to calculate the solar absorption. With this stated, the equation for the solar absorption in the glass envelope becomes

$$\dot{q}'_{5SolAbs} = \dot{q}'_{si}\eta_{env}\alpha_{env} \tag{2.27}$$

with

$$\eta_{env} = \varepsilon'_1\varepsilon'_2\varepsilon'_3\varepsilon'_4\varepsilon'_5\varepsilon'_6\rho_{cl}K \tag{2.28}$$

where

$\dot{q}'_{si}$ = solar irradiation per receiver length (W/m)

$\eta_{env}$ = effective optical efficiency at the glass envelope

$\alpha_{env}$ = absorptance of the glass envelope (Pyrex® glass)

K = incident angle modifier (as defined by Equation 2.26)

All terms in Equation 2.28, except for K, are from Table 2.4. The solar irradiation term ($\dot{q}'_{si}$) in Equation 2.27 is determined by multiplying the direct normal solar irradiation by the projected normal reflective surface area of the collector (aperture area) and dividing by the receiver length. All terms in both equations are assumed to be independent of temperature.

### 2.1.6.3 Solar Irradiation Absorption in the Absorber

The solar energy absorbed by the absorber occurs very close to the surface; therefore, it is treated as a heat flux (see Section 2.1). The equation for the solar absorption in the absorber becomes

$$\dot{q}'_{3SolAbs} = \dot{q}'_{si}\eta_{abs}\alpha_{abs} \tag{2.29}$$

with

$$\eta_{abs} = \eta_{env}\tau_{env} \tag{2.30}$$

where

$\eta_{abs}$ = effective optical efficiency at absorber
$\alpha_{abs}$ = absorptance of absorber
$\tau_{env}$ = transmittance of the glass envelope

In Equation 2.30, $\eta_{env}$ is the same value shown in Section 2.1.6.2. Again, all terms are assumed to be independent of temperature.

### 2.1.7 Heat Loss through HCE Support Bracket

The HCEs are supported at the collector focal line by support brackets that run from the collector structure to the absorber pipe (see Figures 2.3 and 2.4). There is a support bracket at each end of every HCE (about every 4 m of receiver length). The bracket losses are approximated by treating the support bracket as an infinite fin with base temperature 10 degrees less than the outer absorber surface temperature $T_3$ at the point where the bracket is attached. This estimated base temperature accounts for heat losses along the short distance from the bracket attachment to the minimum cross-sectional area, which is assumed to be the base of the fin (~ 5 cm with ~ 4 cm insulated).



**Figure 2.3  Examples of solar trough receiver support brackets**



**Figure 2.4  Close-up of receiver support bracket attachment to absorber tube**

The bracket heat loss is estimated with the following equation [Incropera and DeWitt 1990].

$$\dot{q}'_{cond,bracket} = \sqrt{\bar{h}_b P_b k_b A_{cs,b}} \left( T_{base} - T_6 \right) \Big/ L_{HCE} \qquad (2.31)$$

where

$$
\begin{array}{rcl}
\bar{h}_b & = & \text{average convection coefficient of bracket (W/m}^2\text{-K)} \\
P_b & = & \text{perimeter of bracket (m)} \\
k_b & = & \text{conduction coefficient (W/m-K)} \\
A_{cs,b} & = & \text{minimum cross-sectional area of bracket (m}^2\text{)} \\
T_{base} & = & \text{temperature at base of bracket (}^o\text{C)} \\
T_6 & = & \text{ambient temperature (}^o\text{C)} \\
L_{HCE} & = & \text{HCE length (m)}
\end{array}
$$

The perimeter of the bracket $P_b$ in Equation 2.31 is the perimeter around the two 1-in.x 1-in. square tubes (0.2032 m) that run from the absorber attachment bracket to the collector structure (see Figure 2.4). The cross-sectional area $A_{cs,b}$ is the cross-sectional area of the two connection tabs, 1 in. x 1/8 in. (1.613E-4 m$^2$), connecting the square tubes to the absorber attachment bracket. These dimensions were chosen because the square tubes are the parts of the support brackets that are exposed to convection heat transfer to the environment, and the two connection tabs form the smallest cross-section area near the base of the support bracket (fin) where conduction heat transfer occurs from the absorber pipe. The conduction coefficient ($k_b$) for the HCE support bracket is a constant equal to 48.0 W/m-K (plain carbon steel at 600 K).

The film coefficient $\bar{h}_b$ in Equation 2.31 depends on the wind speed. If there is no wind (<= 0.1 m/s), the film coefficient is estimated with the same Churchill and Chu correlation described in Section 2.1.5.1.1 for natural convection from a long isothermal horizontal cylinder. If there is wind (> 0.1 m/s), the film coefficient is estimated with Zhukauskas' correlation described in Section 2.1.5.1.2. For both cases, "2 inches" is used as the effective diameter of the HCE support brackets and the average isothermal bracket temperature is estimated as ($T_{base}$ + $T_6$) / 3 – the bracket base temperature plus the ambient temperature, divided by three. This estimate is based on intuition; however, the calculations gave reasonable results (see Section 5.2). Also, during the comparison with experimental data, the film coefficient was within expected values, 2-25 W/m$^2$-K for free convection and 25–250 W/m$^2$-K for forced convection [Incropera and DeWitt 1990].

### 2.1.8  No Glass Envelope Case

As mentioned in Section 2.1, the HCE is modeled with and without the glass envelope. Most of the equations discussed so far are for the glass envelope intact case. When the glass envelope is missing, the five energy balance equations, Equation 2.1, collapse down to three (as shown in Section 2.1). The equations for $\dot{q}'_{12conv}$ and $\dot{q}'_{23cond}$ remain unchanged for the two cases. Without the glass envelope, the convection and radiation heat transfer equations for the absorber are calculated with the same equations given in Section 2.1.5. Also, the solar absorption term for the absorber is adjusted to account for the solar flux that is no longer lost with the glass envelope. In this case $\eta_{abs}$ equals $\eta_{env}$ as defined in Section 2.1.6.2, without the $\varepsilon_5$ term, which accounted for particulate matter on the HCE.

## 2.2 Two-Dimensional Energy Balance Model

This model was constructed by dividing the length of the receiver into "N" segments of equal length, with temperature continuity at the bounding surfaces (Figure 2.5). The radial heat fluxes are assumed uniform and normal to the surfaces for each segment and are evaluated at the average temperature between the left and right side of the segment (($T_{right,i}$+$T_{left,i}$)/2). The longitudinal temperature is assumed to be nearly linear (see Section 6.12) and the conduction coefficient constant. Therefore, the right and left side longitudinal conduction terms cancel out, and only the HTF will transfer energy in the longitudinal direction. With these assumptions, the radial heat transfer terms can be modeled with the one-dimensional energy balance (see Section 2.1). The steady-state energy balance for the receiver can be estimated with the following equation.

$$0 \approx \sum_{1}^{N} \dot{q}_i'' A_i + \dot{m}\left[\left(h + \frac{1}{2}v^2\right)_{1,in} - \left(h + \frac{1}{2}v^2\right)_{N,out}\right] \tag{2.32}$$

where

$$
\begin{aligned}
\dot{q}_i'' &= \text{net heat flux per unit area } (W/m^2) \\
A_i &= \text{circumferential area of segment "i" } (m^2) \\
\dot{m} &= \text{mass flow rate (kg/s)} \\
h &= \text{enthalpy (J/kg)} \\
v &= \text{bulk fluid velocity (m/s)}
\end{aligned}
$$

In this equation, potential energy is neglected, and mass flow is constant. The kinetic energy is retained because the HTF expands thermally, especially for long receivers (>700 m). The velocity will be needed for the pressure drop and local Reynolds number calculations, which are used to determine the flow energy and radial HTF heat convection terms, respectively (see Section 2.1).

For a receiver segment "i" of length $\Delta L_{aperture}$, the energy balance becomes

$$0 = \dot{q}_i'' A_i + \dot{m}\left[\left(h + \frac{1}{2}v^2\right)_{i,in} - \left(h + \frac{1}{2}v^2\right)_{i,out}\right] \tag{2.33}$$

The net heat flux $\left(\dot{q}_i''\right)$ in Equations 2.32 and 2.33 includes solar absorption and heat loss.

$$\dot{q}_i'' A_i = \dot{q}_{SolarAbs,i}'' A_i - \dot{q}_{HeatLoss,i}'' A_i \tag{2.34}$$

The solar absorption term includes both the absorber $\left(\dot{q}_{3SolAbs,i}'\right)$ and the glass envelope $\left(\dot{q}_{5SolAbs,i}'\right)$.

$$\dot{q}_{SolarAbs,i}'' A_i = \dot{q}_{3SolAbs,i}' \Delta L_{aperture} + \dot{q}_{5SolAbs,i}' \Delta L_{aperture} \tag{2.35}$$

These are the same solar absorption terms as described in Sections 2.1.6.2 and 2.1.6.3.

The heat loss in Equation 2.34 includes the radiation and convection heat losses from the glass envelope and the conductive losses through the support brackets.

$$\dot{q}''_{HeatLoss,i} A_i = \dot{q}'_{57rad,i} \Delta L_{aperture} + \dot{q}'_{56conv,i} \Delta L_{aperture} + \dot{q}_{cond,bracket,total,i} \qquad (2.36)$$

where

$$\dot{q}_{cond,bracket,total,i} = n_i \dot{q}_{cond,bracket,i} \qquad (2.37)$$

Again, the radiation and convection terms are evaluated with the average longitudinal temperatures for each receiver segment (see Sections 2.1.5.1 and 2.1.5.2). The conductive heat loss through the bracket is described in Section 2.1.7. It is evaluated with the average longitudinal temperature for each segment. The parameter $n_i$ is the number of brackets attached to the HCE segment "i" and is a function of the segment length $\Delta L_{aperture}$. The code includes logic to determine the base temperature and number of brackets as determined by the segment length and location along the receiver. The code also normalizes the bracket conduction term when required.

Assuming the HTF density is only a function of temperature (incompressible with pressure), the change in enthalpy in Equation 2.33 can be approximated with the following equation.

$$\Delta h_i \approx c_{ave,i} \Delta T_i \qquad (2.38)$$

where

$$\Delta T_i = \left( T_{inlet,i} - T_{outlet,i} \right)$$

The specific heat in Equation 2.38 ($C_{ave,i}$) and the density ($\rho_{ave,i}$) are evaluated at the average HTF temperature along the length of the receiver segment. A complete derivation of Equation 2.38 is provided in Appendix C.

Substituting all the above results into Equation 2.33 gives

$$0 = \left( \dot{q}'_{3solAbs,i} + \dot{q}'_{5solAbs,i} - \dot{q}'_{34rad,i} - \dot{q}'_{34conv,i} \right) \Delta L_{aperture}$$
$$+ \dot{m} \left[ c_{ave,i} \left( T_{in,i} - T_{out,i} \right) + \frac{1}{2} \left( v_{in,i}^2 - v_{out,i}^2 \right) \right] - \dot{q}_{cond,bracket,total,i} \qquad (2.39)$$

And, solving for the outlet temperature gives

$$T_{out,i} = \frac{\left( \left( \dot{q}'_{3solAbs,i} + \dot{q}'_{5solAbs,i} - \dot{q}'_{34rad,i} - \dot{q}'_{34conv,i} \right) \Delta L_{aperture,i} - \dot{q}_{cond,bracket,total,i} \right)}{\left( \dot{m} c_{ave,i} \right)}$$
$$+ \frac{\frac{1}{2} \left( v_{in,i}^2 - v_{out,i}^2 \right)}{c_{ave,i}} + T_{in,i} \qquad (2.40)$$
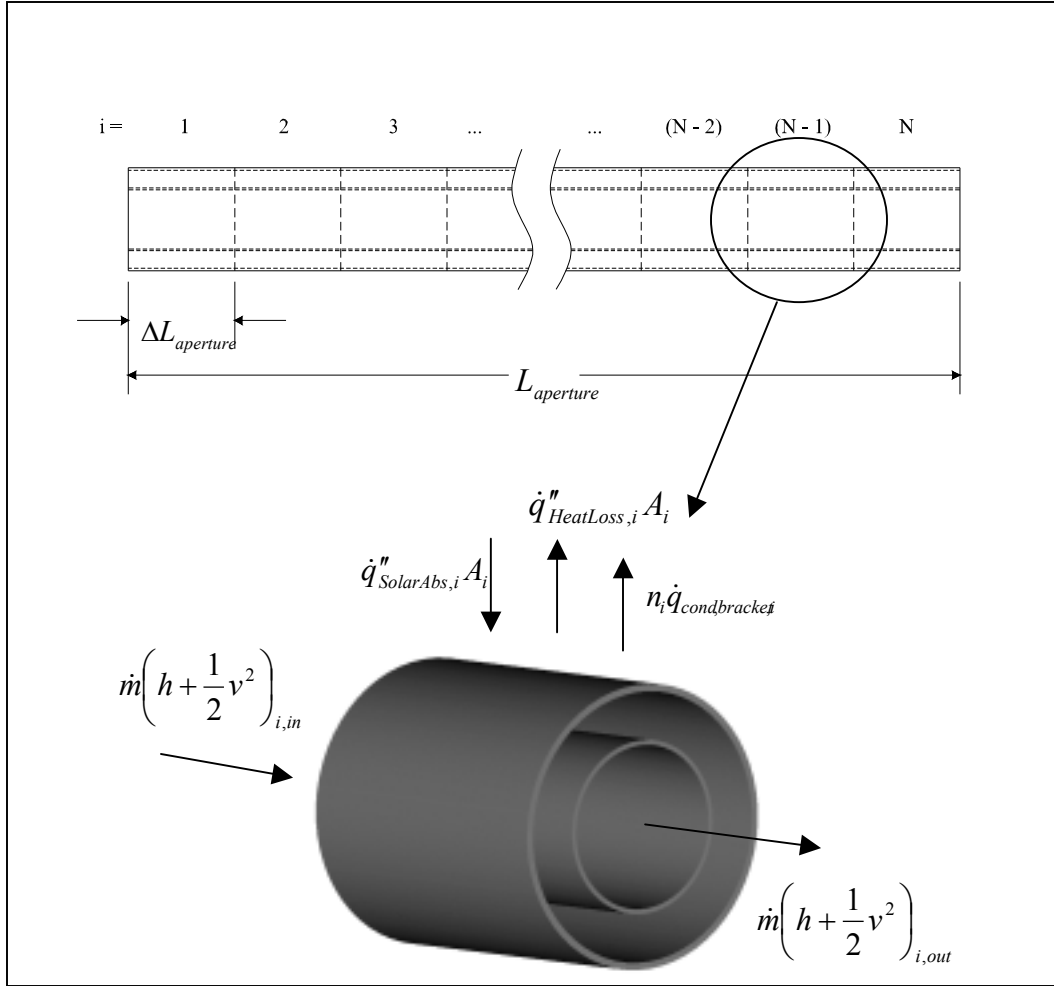
**Figure 2.5  Schematic of the two-dimensional heat transfer model**

In this equation, the inlet velocity ($v_{in,i}$) is determined from the absorber cross-sectional area and volumetric flow rate, both of which are inputs. The remaining velocities are calculated from conservation of mass and continuity at the segment boundaries.

$$v_{out,i} = \frac{\dot{m}}{\rho_{out,i} A_{cs}}$$
(2.41)

$$v_{in,(i+1)} = v_{out,i}$$
(2.42)

The change in pressure $(\Delta P_i)$ in Equation 2.40 is estimated with an equation to calculate pressure loss in a horizontal pipe with fully developed turbulent flow [Munson et al. 1990].

$$\Delta P_i = \frac{f \Delta L_{aperture} \left( \dot{m}/A_{cs} \right)^2}{2 D_2 \rho_{ave,i}}$$
(2.43)

Where f is the Darcy friction factor, and can be estimated for turbulent pipe flow with the following Colebrook equation [Munson et al. 1990].

$$\frac{1}{\sqrt{f}} = -2Log\left(\frac{\varepsilon/D_2}{3.7} + \frac{2.51}{\mathrm{Re}_{D2,ave,i}\sqrt{f}}\right) \qquad (2.44)$$

Here, $\varepsilon$ is the equivalent roughness (~1.5E-6 m for drawn pipe), and $\mathrm{Re}_{D2,ave,i}$ is the Reynolds number calculated at the average axial HTF bulk temperature for each receiver segment.

$$\mathrm{Re}_{D2,ave,i} = \frac{\rho_{ave,i} v_{ave,i} D_2}{\mu_{ave,i}} \qquad (2.45)$$

with

$$\mu_{ave,i} = \text{dynamic fluid viscosity (N-s/m}^2)$$

The outlet temperature, outlet velocity, pressure drop, heat gain, and heat loss can be determined with these equations. If the calculations are done without the glass envelope, the following substitutions are made.

$$\dot{q}'_{5solAbs,i} \to 0$$
$$\dot{q}'_{57rad,i} \to \dot{q}'_{37rad,i}$$
$$\dot{q}'_{56conv,i} \to \dot{q}'_{36conv,i}$$

## 2.3    Assumptions and Simplifications

Numerous assumptions and simplifications made in the modeling of the HCE performance model are listed in Table 2.7. Many have already been discussed, but are included for completeness. Some items in Table 2.7 warrant further discussion.

The heat transfer model assumes $\dot{q}'_{si}$ is uniform both around the circumference (see Section 2.1) and along the length of the HCE. The actual solar flux pattern on the HCE will depend on the collector geometry, alignment errors, tracking errors, and any optical aberrations in the mirrors. The true solar flux profile around the circumference will be similar to an asymmetric normal distribution with the maximum at the point closest to the collector and the minimum located on the HCE side opposite the collector.[1] The profile along the length of the HCE will include hot points where the flux overlaps because of mirror misalignments and aberrations. The influence of the "true" solar flux profile still requires more study to better understand the loss in performance.

The model assumes that the flow is uniform; however, because of the nonuniform solar flux around the circumference of the HCE, the flow will be heated asymmetrically and thus will be nonuniform. To

---

[1] Thomas and Guven [1994] provide good examples of the flux distribution around the circumference of the absorber based on collector mirror optical errors.

accurately predict the convective heat transfer rate for this type of flow, a computational fluid dynamics model would need to be used. The extent of the flow nonuniformity and how much that affects the heat transfer will require further study. For now, this is assumed to be a negligible effect, and besides, as stated earlier, the model assumes a uniform flux.

Another effect of the nonuniform solar flux would be nonuniform temperature profiles around the circumference. The profiles would be nonlinear with the maximum temperatures closest to the collector and the minimum temperatures on the opposite side of the HCE, which would receive no concentrated solar. The error associated with assuming uniform circumferential temperatures requires further study; however, assuming uniformity in the flow and temperature profiles should cause the heat fluxes to be overestimated and not underestimated, if there is much difference.

The model neglects the radiation heat transfer influence from the collector, ground, and surrounding troughs. A simple radiation zonal analysis was conducted to determine a first approximation to this error (see Appendix D). The results showed that neglecting these influences could add an error of 5%–10% to the radiation heat transfer from the glass envelope. However, since the error results in the radiation heat transfer being overpredicted, it was decided to leave the simplification in place. This was justified because the radiation loss is relatively small compared to the convective loss, and since the model typically underpredicts losses (see Section 5).

Many correlations in the model are based on a uniform temperature in the longitudinal direction. However, because the heat gain per unit length decreases as the HTF temperature increases, and because the radiation heat loss is nonlinear, the true temperature profile will be nonlinear (see Section 6.12). Assuming a uniform temperature – or using a linear averaged temperature – may overpredict the heat gain and underpredict the heat loss; however, assuming uniform temperature profiles allows all the heat fluxes to be treated as one-dimensional and thus significantly simplifies the model.

The film coefficients used to estimate forced convection from the HCE and HCE support brackets are based on a correlation that assumes the wind acts normal to the axis. In practice, the wind will be very turbulent and nonuniform in both magnitude and direction throughout a SEGS plant. Therefore, modeling the wind as normal to axis of the HCE and support bracket should result in the worst-case scenario for forced convection heat loss, and would still answer some questions a designer may have about the effect of heat loss caused by wind on an HCE. As shown in Section 6.4, when the annulus between the absorber and glass envelope is under vacuum, the heat losses are fairly insensitive to wind speed.

As mentioned in Section 2.1.6.1, the optical properties are estimates based on experimental data and software models. Unfortunately, the testing has been limited, and the variation of the optical properties is not very well known. Tests have shown that there is some variation, even over a single HCE. Therefore, the assumption in the HCE performance model that the optical properties are uniform may not be valid. Furthermore, in the model, the absorptance terms and glass envelope transmittance and emittance are assumed to be independent of temperature. This is also known not to be true; however, dependence on temperature is assumed to be weak.

**Table 2.7  Assumptions and Simplifications Made in the HCE Performance Models**

| Model Component | Assumptions and Simplifications |
|---|---|
| $\dot{q}'_{12conv}$, convection heat transfer between the HTF and absorber (Section 2.1.1) | • $T_1$ is the bulk temperature.<br>• Uniform flow.<br>• For laminar flow in an annulus, uniform flux was assumed. |
| $\dot{q}'_{23cond}$ and $\dot{q}'_{45cond}$, conduction heat transfers through the absorber wall and glass envelope (Sections 2.1.2 and 2.1.3.3) | • Linear in radial direction.<br>• Negligible conduction in circumferential and longitudinal HCE directions.<br>• Negligible thermal resistance from absorber coating and glass envelope anti-reflection treatment.<br>• Constant thermal conductance. |
| $\dot{q}'_{34conv}$, convection heat transfer between the absorber and glass envelope (Section 2.1.3.1) | • Constant convection heat coefficient.<br>• At low pressures ($\sim< 0.0001$), the heat transfer may be slightly overestimated.<br>• Long, horizontal, concentric cylinders at uniform temperatures. |
| $\dot{q}'_{34rad}$, radiation heat transfer between the absorber and glass envelope (Section 2.1.3.2) | • Annulus gas is nonparticipating.<br>• Both surfaces are gray.<br>• Diffuse irradiation and reflections.<br>• Surfaces are formed from long concentric isothermal cylinders.<br>• Glass envelope is opaque to radiation in the infrared range. |
| $\dot{q}'_{56conv}$, convection heat transfer between the glass envelope and atmosphere (Section 2.1.4.1) | • Wind direction is normal to the axis of the HCE.<br>• Long isothermal horizontal cylinders. |
| $\dot{q}'_{56rad}$, radiation heat transfer between the glass envelope and sky (Section 2.1.4.2) | • Effective sky temperature is 8° below the ambient temperature.<br>• Small convex gray object in a large blackbody cavity.<br>• Collector has a 5% effect on radiation leaving glass envelope outer surface. |
| optical properties (Section 2.1.6.1) | • Uniform properties.<br>• Negligible degradation with time.<br>• Anti-reflection treatment has negligible affect on glass envelope emittance.<br>• Incident angle modifier is the same for each HCE and each collector type.<br>• Optical properties don't vary from HCE to HCE.<br>• Optical properties are independent of temperature, except for the selective coating emissivity. |
| $\dot{q}'_{3SolAbs}$ and $\dot{q}'_{5SolAbs}$ (Sections 2.1.6.2 and 2.1.6.3) | • Can be treated as heat fluxes. |
| $\dot{q}'_{si}$ (Section 2.1.5.2) | • Uniform along HCE circumference and length.<br>• Neglected HCE and bracket shadowing. |

Table 2.7  (con't)

| Model Component | Assumptions and Simplifications |
|---|---|
| $\dot{q}'_{cond,bracket}$  (Section 2.1.5) | • Estimated as an infinite fin.<br>• Wind is normal to the bracket axis.<br>• Convection and conduction coefficients are constant.<br>• Conduction cross-sectional area is at the two 1-in. x 1/8-in. connection tabs from the square   tubes to the absorber connection bracket.<br>• Convection perimeter is the perimeter of the two 1-in. x 1=in. square tubes.<br>• Convection coefficient is estimated by treating the bracket as a long horizontal isothermal cylinder with a 2-in. diameter.<br>• Base temperature is estimated as ($T_3$ - 10) and average temperature is estimated as ($T_{base}$ + $T_6$)/3. |
| thermal-physical property data | • Minimal interpolation and extrapolation errors.<br>• HTF data are based on average test data at saturation pressures.<br>• The HTF thermal-physical properties could change over time. |
| $\dot{q}'_{cond,bracket}$  (Section 2.1.5) | • Estimated as an infinite fin.<br>• Wind is normal to the bracket axis.<br>• Convection and conduction coefficients are constant.<br>• Conduction cross-sectional area is at the two 1-in. x 1/8-in. connection tabs from the square tubes to the absorber connection bracket.<br>• Convection perimeter is the perimeter of the two 1-in. x 1=in. square tubes.<br>• Convection coefficient is estimated by treating the bracket as a long horizontal isothermal cylinder with a 2-in. diameter.<br>• Base temperature is estimated as ($T_3$ - 10) and average temperature is estimated as ($T_{base}$ + $T_6$)/3. |
| thermal-physical property data | • Minimal interpolation and extrapolation errors.<br>• HTF data are based on average test data at saturation pressures.<br>• The HTF thermal-physical properties could change over time. |
| two-dimensional model (Section 2.2 and Appendix) | • Temperature continuity between receiver segment lengths.<br>• Heat transfer analysis for each receiver segment assumes a one-dimensional model evaluated at the average temperatures along the length of the segment.<br>• HTF density is only a function of temperature.<br>• Constant specific heat for each segment.<br>• Absorber pipe inner surface is smooth.<br>• Conduction in the longitudinal direction is negligible.<br>• All heat fluxes are normal to the surfaces.<br>• Constant mass flow. |
| General | • Heat losses through cross piping are not included.<br>• HCE end-losses from shielding and solar incident angle are not included.<br>• Shadowing from adjacent troughs is neglected.<br>• All heat fluxes, optical properties, thermodynamic properties, and temperatures are uniform around circumference and length of HCE segments. |

Other optical property assumptions made in the model include: (1) the incident angle modifier term (K) is the same for each HCE and collector type, and (2) the selective coating emissivities follow the experimentally determined temperature functions. As mentioned earlier, the modifier is based on one set of test data conducted on a UVAC HCE on a LS-2 type collector, and most likely is different for different HCE and collector types. The selective coating emittance functions were determined from experimental measurements on HCEs at temperatures lower than normal HCE SEGS operating temperatures [Dudley et al. 1994]. Therefore, the emissivity functions may not be accurate at elevated temperatures. (The error, if any, associated with this is not completely known. Additional optical testing is planned to answer this question.)

As one can see by the number of assumptions associated with $\dot{q}'_{cond,bracket}$, the calculation of the conduction losses through the HCE support brackets is a rough approximation. For instance, both the bracket base temperature and the bracket average temperature are based on calculated guesses. However, the estimated bracket film coefficient and resulting losses are within expected values – 2 to 25 W/m$^2$-K for free convection and 25 to 250 W/m$^2$-K for forced convection [Incropera and DeWitt 1990], and the comparisons with the KJC test-loop data revealed the bracket losses to contribute 1% to 4% of the total HCE thermal losses, depending on the ambient conditions and HTF temperature (see Section 5.2).

Thermal-physical property data are based on tables in brochures provided by the manufacturer (see Lookup Table References in Appendix A). However, the manufacturer has warned that there could be variations in properties from batch to batch, and that properties change over time, especially after numerous thermal cycles and mechanical agitation. Furthermore, the thermal-physical property data are based on experiments conducted at saturation pressure. The actual pressures will be higher, depending on the pumping requirements of a particular SEGS plant on a particular day. Furthermore, the EES program interpolates and extrapolates the thermal-physical data from lookup tables. Nonetheless, errors associated with all these HTF property factors should have only a small influence on the data (see Section 6.10), and only when using the HCE performance model to compare with actual field data, whose HTF properties could differ slightly from the data in the code.

A few general assumptions warrant further explanation. The model does not include losses through crossover piping. In an actual SEGS plant (see Figure 1.1), the solar field can consist of numerous rows of collectors, and can cover many acres of land. The actual crossover piping segments can become very long, and the quality of its insulation will vary; therefore, crossover piping can result in fairly significant heat loss from the HTF. The model accounts for none of these losses. In addition, in a SEGS plant one row of troughs can partially shade another during morning and late afternoon operations. Also, during the mornings and afternoons, the troughs at the ends of rows will experience some end shadowing. These factors are also not accounted for in the model. However, the crossover piping losses, trough to trough shading, and end losses become significant only when the model is used to evaluate actual SEGS data.

## 2.4    Model Limitations and Suggested Improvements

The HCE performance model has numerous limitations. For instance, because the model neglects the nonuniformity in the solar insolation around the circumference and length of the HCE, these effects cannot be evaluated. This also means that asymmetric design changes cannot be evaluated – such as adding a reflective coating to part of the inside surface of the glass envelope to reflect back to the absorber some of the concentrated solar flux that misses the absorber and to reduce some of the absorber thermal radiation loss.[2]

---

[2] See Duke Solar Energy [2001] for an example of such a study.

The HCE performance model simplifies other analysis, which limits the amount of information that can be gained. For instance, the model simplifies the heat transfer analysis between the absorber and HTF. This means the model cannot be used to evaluate HTF enhancement devices such as helical coil and twisted tape inserts, or machined longitudinal fins and helical ribs on the inside surface of the absorber pipe.[3] Also, as mentioned in Section 2.1.5.1, the wind effects are simplified. The wind is modeled as blowing normal to the receiver axis with no obstructions, so the model is not much help in evaluating actual wind losses that may occur as the wind blows from all directions and around adjacent SCAs. Furthermore, the model neglects the receiver radiation heat loss effects from the collector (see Appendix D), ground, and surrounding SCAs, and assumes an effective sky temperature for the radiation heat transfer loss (see Section 2.1.5.2), so studies of these effects also cannot be conducted with this model.

The HCE performance model does not calculate location- or time-dependent parameters, or initial guesses or parameter bounds, so these values have to be manually changed when needed. One time- and location-dependent parameter is the solar incident angle. To evaluate the KJC test-loop data, the solar incident angle was calculated with a separate program and manually input into the parameter table (see Sections 2.1.6.1, 3.2.2, and 5.2). Having to manually input the solar incident angle makes conducting studies on changing the tilt of the CSAs or changing the outer surface properties of the absorber difficult. Also, since the model does not calculate initial guesses or parameter bounds, these values have to be manually input into the EES variable information window. And for some design changes, this window may have to be updated for the model to converge. Changing the guesses and bounds can become tedious, especially when dealing with a long receiver that has a relatively small segment step size (resulting in large parameter arrays).

The HCE performance model does not do optimization or exergy analysis, both of which would help identify HCE performance limitations. However, an incremental optimization parameter study, similar to Section 6.11 for the glass envelope outer diameter, can be conducted. As shown in Section 2, the HCE performance model is based on first law analysis, which provides values for collector efficiency, heat gain, and heat losses. However, it does not provide information on the limitations for improving these values or help identify specific components that have high irreversibility. Exergy analysis could not only provide second law efficiencies to identify improvement limitations, but could also help identify collector and HCE components that have the most room for improvement. As stated by Bejan, "With exergy analysis a designer can better focus effort so that losses are effectively pinpointed and reduced" [1988].

The HCE performance model can be improved, if necessary, to eliminate or reduce some of these limitations. For instance, the circumferential direction of the HCE cross-section could be modeled in discrete segments, similar to the two-dimensional model described in Section 2.2. The solar flux for each segment could be approximated with a weighted average of the expected profile[4] at the segment location. This would allow some analysis of the influence of the nonuniformity of the solar insolation around the HCE circumference. It would be best, however, to make this modification to the current one-dimensional version of the HCE performance model and not the two-dimensional, since a three-dimensional model may have convergence problems and require long iteration times.

---

[3] See samples on pages 504 and 505 in Incropera and DeWitt [1990].

[4] The expected profile can be estimated from previous results listed in the literature (such as the results discussed by Thomas and Guven [1994] or from predictions with Ray Tracing techniques).

More meteorological data, date, time, and location inputs could be added to the HCE performance model to better represent actual field test data results. By adding wind direction, for example, an effective wind speed could be approximated by using the component of the wind vector that is normal to the receiver axis in the forced convection calculations. Also, knowing additional meteorological data will allow a calculation for a more accurate approximation of the effective sky temperature.[5] And with the date, time, and location inputs the solar incident angle could be calculated instead of input (see Section 5.2).

Other improvements could include additional logic to smooth the transition between the turbulent and laminar models and adding a manual input for the receiver length. Currently, if the laminar selection is chosen, the model switches to the laminar Nusselt number when the Reynolds number drops below 2300. This will cause a discontinuity in the HTF convection calculation. Additional logic could smooth this transition, similar to the logic that was used for the convection heat transfer from the absorber to the glass envelope. The receiver length is currently dependent on the test type and collector type (see Table 3.4). To manually enter a receiver length additional logic would need to be added along with a "user-defined" entry similar to the "user-defined" option for the absorber selective coating option in the two-dimensional design version of the code (see Section 3.2.1).

Additional model improvements could include temperature-dependent optical properties, changing the solar absorption terms to heat generation terms, and adding exergy analysis. Currently (see Section 2.1.6.1), the absorptance terms are independent of temperature, and the emissivities were determined at temperatures lower than the HCE will see during normal operation. Once additional testing is complete, improved temperature-dependent functions may be determined. If so, these updated properties can easily be added to the HCE performance models. As mentioned in Section 2, the solar absorption is actually a heat generation phenomenon. This is especially true for the glass envelope, since the heat absorption occurs throughout its volume. The model could be changed to incorporate this effect; however, the thermal conductance would also need to reflect this change. Finally, an internal or external procedure (written in a software code such as Dynamic-C) could be used to add exergy analysis to the HCE performance model. This would allow component exergy generations terms, and an overall second law efficiency to be output, to better indicate the availability for HCE performance improvement and to help prioritize design changes to improve trough performance.

## 3.    EES Codes

The HCE performance model has been coded into EES. The basic function of EES is to solve algebraic equations. EES is unique from other software because it automatically identifies all unknowns and groups the equations for the most efficient solution. Once a solution is found, the solution to all the unknowns can be viewed. This includes solutions to arrays. EES also supports user-defined procedures and functions, similar to FORTRAN, and provides built-in mathematical and thermal-physical property functions. Furthermore, EES supports user-generated property lookup tables and parametric tables. The lookup tables provide an easy means for adding user-defined thermal-physical properties, or any other data needed in the equations in the code. The parametric tables are similar to spreadsheets and are convenient for conducting parametric studies, such as heat losses as a function of HTF inlet temperature. EES also has a diagram window, which can be used for easy selection of input variables and can support simple drawings, such as a schematic of a thermodynamic flow cycle. EES can also solve differential and complex equations, and supports optimization, linear and nonlinear regression, uncertainty propagation, and generates user-defined plots. It can also be integrated with external functions and procedures written in a high-level language such as PASCAL, C, or FORTRAN. A complete EES user manual, provided by

---

[5] Duffie and Beckman [1991] list several references for relations to estimate an effective sky temperature based on different meteorological data.

F-Chart Software, can be downloaded from the Web site http://fchart.com/ [Klein 2002] for more detailed explanations of the capabilities of EES and detailed instructions.

Four versions of the EES code were written to solve the HCE performance model. Two include the one-dimensional energy balance model and two include the two-dimensional model. Each can be used to evaluate and refine optical properties and HCE design parameters. Each is tailored for a different task.

- The "Design Study" version is best suited for evaluating HCE design changes such as a proposed new selective coating or a new envelope material. It can also be used to evaluate the effects of damage to an HCE, like lost vacuum or missing glass envelope.

- The "AZTRAK Test Data " version was written specifically for evaluating the data from the AZTRAK test platform at SNL. This version is compatible with the AZTRAK and weather data output files and calculates the resulting heat loss and efficiency based on the input weather and HTF flow properties. In this version the energy absorbed in the glass envelope is included as part of the optical loss and not the heat loss. This enables comparisons with the heat loss as it is reported from the testing – the thermal energy leaving the absorber, not the glass envelope. The results can be used to evaluate the AZTRAK test data and to better explain the resulting heat losses and efficiencies.

- The "KJC Test-Loop Data" version can be used to evaluate the data from two rows of collectors (test-loop) at a SEGS plant located in Kramer Junction, California, and operated by KJCOC. This version, like the AZTRACK test data version, is compatible with the field test data and weather data outputs (type, units, etc.), and can be used to help understand the test data results.

- The "Two-Dimensional Design Study" version was written to evaluate the effects of the pressure drop and HTF temperature changes along the length of the HCE. This version is valuable for evaluating effects associated with receiver lengths, and predicting the outlet temperature and velocity based on a given set of inlet data.

These last three versions (AZTRAK Test Data version, KJC Test-Loop version, and Two-Dimensional Design Study version) can also be used to evaluate effects of design changes and HCE conditions with actual field criteria (wind speed, ambient temperatures, solar incident angles, solar insolation, flow rates, etc.). A brief description of each version of the codes is discussed below, and the two design study versions are provided in Appendices E and F.

## 3.1    One-Dimensional Heat Transfer EES Codes

The EES codes titled "One-Dimensional Design Study" and "AZTRAK Test Data" include only the one-dimensional heat transfer analysis. These codes can be used to evaluate the HCE efficiencies for short receivers (~< 500 m, see Section 4), or when the effects of receiver length are not needed, for instance, when evaluating relative changes that result from different selective coating properties. In the case of the AZTRAK test data, receiver lengths are limited by the size of the rotating platform, which is only about 10 m; therefore, HTF properties have little variation along the length of the receiver and a two-dimensional model makes little difference in comparison to the one-dimensional model.

### 3.1.1  One-Dimensional Design Study Version

The one-dimensional design study version of the EES program is useful for evaluating relative design and parameter effects on HCE performance (see Section 6). It can also be used to evaluate current or proposed

selective coatings by selecting or manually inputting the optical properties for the case and to evaluate the effects of damage to the HCEs, such as lost vacuum or missing glass envelope.

### 3.1.1.1 Lookup Tables

As stated in Section 3, EES supports user-generated lookup tables. The design study version, as well as the other versions, has lookup tables for various HTFs and for argon gas. The HTF tables include

- Therminol VP1
- Therminol 59
- Therminol 66
- Therminol XP
- Dowtherm Q

- Dowtherm RP
- Syltherm 800
- Xceltherm 600
- Water, salt (60% $NaNO_3$, 40% $KNO_3$)
- Hitec XL

Part of the Therminol VP1 lookup table is shown in Table 3.1. The properties include temperature ($^o$C), density (kg/m$^3$), vapor pressure (Pa), specific heat (J/kg-K), dynamic viscosity (kg/m-s), and thermal conductance (W/m-K). All the data in the HTF tables are based on laboratory tests conducted by the manufacturers and were taken at the HTF saturation pressure. Therefore, small variances in the properties can be expected from sample to sample and because of pressure effects. However, temperature has the strongest influence on the properties. If the program evaluates properties outside the recommended HTF temperature range, a warning message will appear. HTFs can easily be added by inserting a lookup table with the appropriate properties and making a few changes to the code.

Argon gas is included as a lookup table for evaluating its effects in the HCE annulus space between the absorber and the glass envelope (see Section 6.3). Pressurizing this space with argon has been proposed as an option to a vacuum or as a temporary fix if vacuum is lost. The properties in the argon table were compiled for a constant pressure of 100 kPa. The properties of the other two annulus gases (air and hydrogen) are already provided in the EES program as embedded thermal-physical property tables. For more information on the HTF fluids or argon data see the references in Appendix A.

**Table 3.1  Part of the Lookup Table for Therminol VP1**

|  | T [C] | $\rho$ [kg/m$^3$] | $P_v$ [kPa] | c [J/kg-K] | $\mu$ [kg/m-s] | k [W/m-K] |
|---|---|---|---|---|---|---|
| : | : | : | : | : | : | : |
| Run 17 | 172 | 938 | 9.97 | 1970 | 0.000486 | 0.118 |
| Run 18 | 182 | 929 | 13.8 | 2000 | 0.00045 | 0.1165 |
| Run 19 | 192 | 920 | 18.9 | 2030 | 0.000418 | 0.115 |
| Run 20 | 202 | 911 | 25.3 | 2050 | 0.000389 | 0.1135 |
| Run 21 | 212 | 902 | 33.5 | 2080 | 0.000364 | 0.1119 |
| Run 22 | 222 | 893 | 43.7 | 2110 | 0.000341 | 0.1103 |
| : | : | : | : | : | : | : |

### 3.1.1.2 Diagram Window

Figure 3.1 shows the diagram window used in the design study version of the EES HCE heat transfer code. The window enables the user to manually input data from pull-down menus and the keypad. The diagram window is divided into seven sections: Ambient Conditions, HCE and Collector Properties,

Optical Properties, Modeling Properties, Heat Transfer Fluid Properties, "User-Defined" Absorber Selective Coating Properties, and "User-Defined" Collector Type Properties.



**Figure 3.1  Diagram window from the Design Study version of the heat transfer code**

- The Ambient Conditions section includes direct normal incident solar irradiation, wind speed, ambient temperature, and solar incident angle. All these inputs can be typed in by right clicking the curser on the input boxes. None of the inputs are bounded; typing in an erroneous value will either cause the program to fail or produce erroneous results.

- The HCE and Collector Properties section has pull-down menus for selecting collector type, absorber material, absorber selective coating, gas in the annulus, and options for whether or not the glass envelope is intact. Clicking on the arrow next to the selection box and highlighting the desired choice selects the option. The collector type choices are LS-2, LS-3, and IST. The first two choices are standard collector types found in SEGS plants, and the IST collector type is a proposed smaller collector design. The LS-2 and LS-3 are second- and third-generation parabolic trough collectors built by Luz International Ltd. The IST is a parabolic trough collector built by Industrial Solar Technology. The optical properties and geometry for each collector type are written into the program and are discussed in Section 2.1.6.1. References for the optical properties are listed in Appendix B.

  The absorber material choices include three stainless steels: 304L, 316L, 321H, and one copper: B42 (see Section 2.1.2). The absorber selective coating has eight choices: Luz black chrome and Luz Cermet coatings, five Solel UVAC Cermet coatings, and a user-defined choice. Two of the five Solel

UVAC coatings, 0.07 and 0.10 @ 400$^{\circ}$C, are not found in the SEGS plants, but rather are coating types the manufacturer Solel has proposed. All the other optical properties are based on tests conducted by SNL (see Section 2.1.6.1). The Solel UVAC Cermets labeled "SNL test a" and "SNL test b" are from two separate test results from either end of a single HCE that was tested. The Solel UVAC Cermet labeled "SNL test avg" is the average of these two results. The last choice, user-defined, is used to evaluate coating properties input manually. The remaining input in the HCE and Collector Properties window is the annulus absolute pressure, which is typed in.

- The "Optical Properties" section has an input box for the trough solar weighted mirror reflectivity, and outputs for optical efficiency and optical loss. The reflectivity value is an estimated value of the mirror solar reflectance, and indicates mirror quality and cleanliness. The two outputs are provided for convenience when a user is trying to match a certain optical efficiency by adjusting the mirror reflectance.

- The "Modeling Properties" section includes pull-down windows for HTF flow type and an option for including a laminar flow model in the analysis. The flow type choices are either pipe flow or annulus flow. If the annulus pipe flow is chosen, a valid annulus diameter needs to be typed in the box provided. The annulus flow type is included because HCEs are sometimes tested with an inner pipe or plug to help simulate Reynolds numbers that are typically achieved in a SEGS plant (see Section 2.1.1.3). The option for laminar flow is included so losses associated with cooler HTF temperatures ($\sim< 100^{\circ}$C) can be evaluated. These temperatures could be seen during extended down times and during startups or testing.

- The "Heat Transfer Fluid Properties" section has an input box for the HTF flow rate and a pull-down menu for the HTF type. Again, there are no restrictions on the value that can be input for the HTF flow rate. Values outside normal operating ranges could result in erroneous outputs. However, warnings are embedded into the code that will print out if the flow rate results in Reynolds numbers below the minimum in which the equations are valid. The choices for the HTF type are the same as described in Section 3.1.1.1 for the lookup tables.

- The "'User-Defined' Absorber Selective Coating Properties" section contains input boxes for the coating optical properties and glass envelope transmittance. This section is valid only if the "User-Defined" selective coating option is chosen. If another selective coating option is chosen, optical properties written in the code are used (see Section 2.1.6.1).

### 3.1.1.3   Parametric Table

The parametric table for the one-dimensional design study version of EES is shown in Table 3.2. It acts as a spreadsheet. It contains user inputs and program outputs. For this case the input is the HTF temperature, $T_{1ave}$ ($^{\circ}$C), defined as the average bulk HTF temperature between the inlet and outlet of the receiver. The outputs include the HCE heat loss per receiver length, $q_{HeatLoss}$ (W/m); heat gain into the HTF fluid per receiver length, $q_{HeatGain}$ (W/m); and the collector efficiency, $\eta_{Col}$ (%). The efficiency is defined as the total HTF heat gain per receiver length divided by the direct normal solar insolation at the collector aperture per receiver length. If any changes are required, the parametric table can easily be modified. Changing the input variables might also require one or more variable guesses or bounds to be changed. In order for the program to converge, the variable guesses need to be "reasonably" close. Instructions on modifying the table and variable information can be found in the general EES user manual.

**Table 3.2  Parametric Table for the Design Study Version of the Heat Transfer Code**

| > <br> 1..7 | $T_{1ave}$ <br> [C] | $q_{HeatLoss}$ <br> [W/m] | $q_{HeatGain}$ <br> [W/m] | $\eta_{Col}$ <br> [%] |
|---|---|---|---|---|
| Run 1 | 100 | 11.03 | 3510 | 73.90 |
| Run 2 | 150 | 25.81 | 3495 | 73.59 |
| Run 3 | 200 | 49.83 | 3471 | 73.08 |
| Run 4 | 250 | 87.1 | 3434 | 72.30 |
| Run 5 | 300 | 142.8 | 3378 | 71.13 |
| Run 6 | 350 | 223.5 | 3298 | 69.43 |
| Run 7 | 400 | 337.3 | 3184 | 67.03 |

### 3.1.2  AZTRAK Test Data Version

This version of the EES program was created to help verify the model and to evaluate the data collected from testing HCEs and collectors on the AZTRAK rotating test platform at SNL (see Section 5.1). Information on the AZTRAK testing along with sample test results can be found in Dudley et al. [1994].

The AZTRAK Test Data version is very similar to the one-dimensional design study version. It is also based on the one-dimensional heat transfer model. However, the heat loss for this version of the code includes only the heat losses from the absorber and not from the glass envelope. This was done because of the way the heat loss was measured during the testing. The solar insolation absorption into the glass envelope is included as an optical loss. The lookup tables are all the same, and the diagram window is only slightly different. Furthermore, conversion statements were added to the code where appropriate, so output data from the testing could be input directly into the parametric table.

#### 3.1.2.1  Diagram Window

The diagram window for the AZTRAK test data version of the EES code is shown in Figure 3.2. All the input options shown are the same as discussed in the design study version. For this version, some of the inputs have been moved to the parametric table, the option for pipe flow has been removed, and the "User-Defined" selective coating is not included.



**Figure 3.2  Diagram window from the AZTRAK Test Data version of the heat transfer code**

### 3.1.2.2 Parametric Table

As shown as Table 3.3, the parametric table for the AZTRAK test data version of the EES program contains six inputs and four outputs. The input data are set up to match the data provided by the actual AZTRAK testing. The data include:

- Direct normal insolation, $I_b$ (W/m$^2$)
- Wind speed, $v_6$ (m/s)
- Ambient temperature, $T_6$ ($^o$C)
- Inlet bulk HTF temperature, $T_{in}$ ($^o$C)
- Outlet bulk HTF temperature, $T_{out}$ ($^o$C)
- HTF volumetric flow rate, $v_1$, (L/min)

The output data include:

- The difference between the average HTF and the ambient temperature, $T_{diffAir}$ ($^o$C)
- HCE heat loss per collector aperture area, $q_{heat, loss, col, area}$ (W/m$^2$)
- HTF heat gain, $q_{HeatGain}$ (W/m)
- Collector efficiency, $\eta_{Col}$ (%)

All necessary unit conversions are made in the code.

**Table 3.3 Parametric Table for the AZTRAK Test Data Version of the Heat Transfer Code**

| > 1..8 | $I_b$ [W/m$^2$] | $V_6$ [m/s] | $T_6$ [C] | $T_{in}$ [C] | $T_{out}$ [C] | $v_1$ [L/min] | $T_{diffAir}$ [C] | $q_{AbsorbertHeatLoss}$ [W/m$^2$] | $q_{HeatGain}$ [W/m] | $\eta_{Col}$ [%] |
|---|---|---|---|---|---|---|---|---|---|---|
| Run 1 | 933.7 | 2.6 | 21.2 | 102 | 124 | 47.7 | 91.9 | 5.616 | 3402 | 72.5 |
| Run 2 | 968.2 | 3.7 | 22.4 | 151 | 173 | 47.8 | 139.8 | 9.389 | 3510 | 72.1 |
| Run 3 | 982.3 | 2.5 | 24.3 | 197 | 219 | 49.1 | 184.2 | 15.18 | 3533 | 71.6 |
| Run 4 | 909.5 | 3.3 | 26.2 | 250 | 269 | 54.7 | 233.8 | 24.51 | 3218 | 70.4 |
| Run 5 | 937.9 | 1.0 | 28.8 | 297 | 316 | 55.5 | 278.6 | 37.86 | 3256 | 69.1 |
| Run 6 | 880.6 | 2.9 | 27.5 | 299 | 317 | 55.6 | 280.6 | 38.38 | 3042 | 68.7 |
| Run 7 | 20.9 | 2.6 | 29.5 | 379 | 398 | 56.8 | 359.3 | 76.71 | 2998 | 64.8 |
| Run 8 | 903.2 | 4.2 | 31.1 | 355 | 374 | 56.3 | 333.9 | 63.35 | 3000 | 66.1 |

### 3.2 Two-Dimensional Heat Transfer EES Codes

The length of a receiver in an operating field can reach hundreds or thousands of meters. For instance, the receivers on the KJC test loops are almost 800 m long, yet consist of only two rows of collectors. For long receiver lengths the change in flow rate (caused by the density change) and pressure drop can have an appreciable effect on the heat transfer model (see Section 4). Because of this, and to study the effects of receiver lengths, two versions of the EES heat transfer code include a two-dimensional heat transfer model: "Two-Dimensional Design Study" and "KJC Test-Loop Data."

### 3.2.1 Two-Dimensional Design Study Version

Like the One-Dimensional Design Study version, the two-dimensional version can be used to evaluate design and parameter changes. It can also be used to study property and temperature changes along the length of the receiver (see Section 6.12).

### 3.2.1.1 Diagram Window

The diagram window for the Two-Dimensional Design Study version is shown in Figure 3.3. It is very similar to the One-Dimensional Design Study version shown in Figure 3.1. For the two-dimensional case, an input for the number of receiver length segments has been added to the Modeling Properties section. Also, the flow type and the "User-Defined" collector type properties have been removed; however, both can be added if needed.



**Ambient Conditions**

Direct Normal Incident Solar Irradiation = 950 [W/m²]

Wind Speed = 0 [mph]

Ambient Temperature = 22 [C]

Solar Incident Angle From Aperture Normal (0-75) = 0 [degrees]

**HCE and Collector Properties**

Collector Type = LS-2

Absorber Material = 321H

Absorber Selective Coating = Solel UVAC Cermet (SNL test avg)

Gas in Annulus = Air

Annulus Absolute Pressure = 0.0001 [torr]

Glass Envelope Intact? Yes

**Optical Properties**

Solar Weighted Mirror Reflectivity = 0.9

Total Optical Efficiency = 0 [%]

Total Optical Loss / Receiver Length = 1185 [W/m]

**Modeling Properties**

Test Type (only used with LS-2 collector) = KJC Test Loop

Total Number of Discrete Segments (# of Nodes - 1) = 10

**Heat Transfer Fluid Properties**

Heat Transfer Fluid Flow Rate = 140 [gpm]

Heat Transfer Fluid = Therminol VP1

**"User-Defined" Absorber Selective Coating Properties**
(Only Valid if Absorber Selective Coating = "User-Defined")

Coating Absorptance = 0.98

Coating Emittance (@ 100 °C) = 0.04

Coating Emittance (@ 400 °C) = 0.1

Glass Envelope Transmittance = 0.97

**Figure 3.3  Diagram window from the Two-Dimensional Design Study version of the heat transfer code**

As shown in Section 4, the number of segments to use depends on the total length of the receiver. Too few segments result in larger errors in the calculations; too many results in excessive iteration times, with little gain in model accuracy. Also, adding more segments requires the initial guesses and bounds of the additional variables to be updated to the variable information window, which can become very time consuming. Reducing the number of segments from a previous run usually requires no modifications to the variable information window.

The current version of the two dimensional model dynamic window does not have an explicit input for receiver length. The receiver length used in the model will depend on both the collector type and test type inputs. Table 3.4 summarizes the receiver lengths used in the code. A possible future modification to the program could be to add a manual input for the receiver length.

**Table 3.4  Collector and Test Type Receiver Lengths**

| Collector Type | Test Type | Receiver Length (m) |
|---|---|---|
| LS-2 | SNL AZTRAK Platform | 8.12 |
| LS-2 | KJC Test-loop | 779.52 |
| LS-3 | N/A | 97.44 |
| IST | N/A | 2.16 |

### 3.2.1.2  Parametric Table

The parametric table for the two-dimensional model is shown as Table 3.5. In addition to the heat gain, heat loss, and efficiency as shown with the one-dimensional design study version, the table includes the parameters resulting from the flow effects: HTF outlet temperature, $T_{1outlet}$ ($^{o}$C); inlet and outlet velocities, $v_{1inlet}$ and $v_{1outlet}$ (m/s); and the pressure drop, $\Delta P$ (Pa). The table also includes the total losses per receiver length caused by optical effects, $q_{OptLoss}$ (W/m).

**Table 3.5  Parametric Table for the Two-Dimensional Design Study Version of the Heat Transfer Code**

| > 1..7 | $T_{1inlet}$ [C] | $T_{1outlet}$ [C] | $v_{1inlet}$ [m/s] | $v_{1outlet}$ [m/s] | $\Delta P$ [Pa] | $q_{HeatLoss}$ [W/m] | $q_{HeatGain}$ [W/m] | $\eta_{Col}$ [%] |
|---|---|---|---|---|---|---|---|---|
| Run 1 | 125 | 275.7 | 2.582 | 2.998 | 576151 | 56.50 | 3340 | 72.90 |
| Run 2 | 150 | 298.6 | 2.582 | 3.018 | 551632 | 73.42 | 3324 | 72.53 |
| Run 3 | 175 | 321.7 | 2.582 | 3.044 | 530224 | 94.12 | 3303 | 72.08 |
| Run 4 | 200 | 344.8 | 2.582 | 3.073 | 510399 | 119.20 | 3278 | 71.53 |
| Run 5 | 225 | 368.0 | 2.582 | 3.114 | 492940 | 149.40 | 3248 | 70.87 |
| Run 6 | 250 | 391.1 | 2.582 | 3.165 | 477001 | 185.40 | 3212 | 70.09 |
| Run 7 | 275 | 414.0 | 2.582 | 3.243 | 462750 | 227.80 | 3169 | 69.16 |

### 3.2.2  KJC Test-Loop Data Version

The KJC Test-Loop Data version of the HCE heat analysis software was created to verify the software model and to evaluate the KJC test-loop data. The test data can be copied directly from the KJCOC performance spreadsheets and pasted into the parametric tables. The code has been written to convert all inputs into the correct units before running the iterations.

### 3.2.2.1  Diagram Window

An example of the diagram window for the KJC Test-Loop Data version is shown in Figure 3.4. The main difference between this diagram window and that for the Two-Dimensional Design Study version is that some inputs were moved to the parametric table, and like the AZTRAK version, the "user-defined" selective coating optioned is not included. The inputs that were moved to the parametric table include all the ambient conditions and the HTF flow rate. The option to select the test type was also removed.

**HCE and Collector Properties**

Collector Type = **LS-2**

Absorber Material = **321H**

Absorber Selective Coating = **Solel UVAC Cermet (SNL test avg)**

Gas in Annulus = **Air**

Annulus Absolute Pressure = **0.0001** **[torr]**

Glass Envelope Intact? **Yes**

**Modeling Properties**

Total Number of Discrete Segments (# of Nodes -1) = **10**

**Heat Transfer Fluid Properties**

Heat Transfer Fluid = **Therminol VP1**

**Optical Properties**

Solar Weighted Mirror Reflectivity = **0.904**

**Figure 3.4  Diagram window from the KJC Test-Loop Data version of the heat transfer code**

### 3.2.2.2    Parametric Table

As shown in Table 3.6, the parametric table for the KJC Test-Loop Data version of the heat transfer code contains eight inputs and nine outputs. The inputs coincide with measured data from the KJC Test-Loop. The HTF temperatures, $T_{inF}$ and $T_{outF}$; HTF flow rate, $V_{1volg}$; and ambient conditions, $I_b$, $T_{6F}$, $V_{6mph}$ were all copied from the Excel spreadsheets created by KJCOC to evaluate the test-loop data. The time input is included to reference the data and is not used in any calculations. The solar incident angle, $\theta$, has to be calculated independently. The incident angles used to generate the data in this report were copied from an Excel HCE spreadsheet used to evaluate the KJCOC performance data [Price 2000]. All parameter units in the parametric table are converted to metric within the EES code.

The output data in the parametric table include:

- Outlet temperature, $T_{1outletF}$, ($^{o}F$)
- Outlet flow rate, $v_{1volg,outlet}$, (gpm)
- Pressure drop, $\Delta P$ (Pa)
- Heat loss through the HCE support brackets, $q_{cond,bracket}$ (W)
- Optical loss due to the solar incident angle, $q_{opt,loss,K}$ (W/m)
- Total optical loss, $q_{opt,loss}$, (W/m)
- Heat loss, $q_{HeatLoss}$, (W/m)
- Heat gain, $q_{HeatGain}$, (W/m)
- Collector efficiency, $\eta_{Col}$

All the unit length energy terms are based on the total receiver length. The optical loss caused by the solar incident angle is determined by reducing the solar insolation by the incident angle modifier given in Section 2.1.6.1. However, the total optical loss is determined by reducing the solar insolation by the effective optical efficiency, which includes the incident angle modifier term.

**Table 3.5 Parametric Table for the KJC Test-Loop Data Version of the Heat Transfer Code**

| >  1..288 | Time | $T_{inF}$ [F] | $T_{outF}$ [F] | $V_{1Volg}$ [gpm] | $I_b$ [W/m$^2$] | $T_{6F}$ [F] | $V_{6mph}$ [mph] | $\Theta$ [deg] | $T_{1outlet}$ [F] | .. |
|---|---|---|---|---|---|---|---|---|---|---|
| : | : | : | : | : | : | : | : | : | : | ... |
| Run190 | 1550 | 446 | 587 | 93.8 | 446.5 | 64.2 | 14.72 | 36.2 | 579.5 | ... |
| Run191 | 1555 | 443 | 563 | 93.4 | 785.2 | 64.1 | 13.16 | 35.5 | 677.8 | ... |
| Run192 | 1600 | 448 | 543 | 93.5 | 768.7 | 64.5 | 15.6 | 34.8 | 680.3 | ... |
| Run193 | 1605 | 454 | 518 | 93.7 | 757 | 64.8 | 15.22 | 34.1 | 684.5 | ... |
| Run194 | 1610 | 456 | 505 | 93.9 | 732.6 | 64.8 | 14.54 | 33.4 | 681 | ... |
| Run195 | 1615 | 452 | 490 | 93.8 | 699.6 | 64.7 | 12.95 | 32.7 | 670.5 | ... |
| Run196 | 1620 | 447 | 462 | 93.9 | 681.5 | 64.5 | 13.12 | 32.0 | 662 | ... |
| : | : | : | : | : | : | : | : | : | : | ... |

| ... | $v_{1outlet}$ [gpm] | $\Delta P$ [Pa] | $q_{cond,bracket}$ [W] | $q_{opt,loss,K}$ [W/m] | $q_{opt,loss}$ [W/m] | $q_{HeatLoss}$ [W/m] | $q_{HeatGain}$ [W/m] | $\eta_{Col}$ [%] |
|---|---|---|---|---|---|---|---|---|
| ... | : | : | : | : | : | : | : | : |
| ... | 102.2 | 229596 | 1078 | 25.27 | 109.3 | 500.6 | 966.5 | 50.0 |
| ... | 110.5 | 231911 | 1963 | 28 | 150.2 | 844.9 | 1674 | 51.8 |
| ... | 110.5 | 231283 | 1940 | 29.7 | 153.2 | 793.5 | 1615 | 52.3 |
| ... | 110.8 | 231057 | 1928 | 29.81 | 157 | 748.5 | 1567 | 52.8 |
| ... | 110.6 | 231403 | 1884 | 29.32 | 155.7 | 693.1 | 1494 | 53.3 |
| ... | 109.6 | 231264 | 1820 | 27.82 | 149.3 | 632.7 | 1405 | 53.9 |
| ... | 109.2 | 232594 | 1795 | 27.46 | 143.6 | 588 | 1349 | 54.6 |
| ... | : | : | : | : | : | : | : | : |

## 4. Comparison between the One- and Two-Dimensional Models

The one- and two-dimensional models both have advantages and disadvantages. The one-dimensional model is less complex; therefore, it is easier to modify, requires less iteration time, and has less trouble converging. The two-dimensional model consists of many arrays, requires longer iteration times, and can have problems converging, especially if all the array guess values are not within reasonable bounds and sequence. The code can also be more difficult to modify. However, it provides a higher degree of accuracy than the one-dimensional model when evaluating long receivers (> 700 m).

The two-dimensional model includes HTF pressure losses, HTF velocity changes, and receiver support bracket conduction losses (see Section 2.2). The two-dimensional model also captures some of the nonlinearity of the HTF temperature changes along the length of the receiver. As the receiver length increases, each effect becomes more significant and the error associated with using the one-dimensional model increases. Two questions are explored here:

- At what receiver length do the axial direction effects become significant?
- When should the two-dimensional model be used instead of the one-dimensional model?

The process used to compare the one- and two-dimensional models was to start with the KJCOC test-loop receiver length of 779.52 m (the KJC Test-Loop Data version of the EES Heat Transfer Code uses the two-dimensional model) and determine a step size that resulted in a "reasonable" level of accuracy for a "reasonable" convergence time. Then the two-dimensional model results (using the determined step size) were compared to results using the one-dimensional model. For an equal comparison, the average HTF temperature used in the one-dimensional model is the linear average between the inlet and outlet temperatures from the two-dimensional model.

Figures 4.1a and 4.1b show the inlet, outlet, and average temperatures used in the one- and two-dimensional model comparison. The two-dimensional model captures the nonlinearity that results from the heat losses; therefore, the HTF temperature through the length of the receiver will be nonlinear and will be slightly higher on average as determined by the two-dimensional model then the linear average used in the one-dimensional model. This will result in the one-dimensional model underestimating the heat losses and overestimating the heat gain. Furthermore, the two-dimensional model is actually a summation of discrete one-dimensional segments and not a continuous two-dimensional model; as the discrete segment lengths approach zero the discrete model will approach a continuous model.

Table 4.1 and Figure 4.2 show the results of the step size study. The "number of steps" in the first column in Table 4.1 is the number of discrete receiver segments modeled in the axial direction. The "step size" is the total receiver length (779.5 m) divided by the number of steps. In this case, the total receiver length of 779.5 m was chosen simply because it was the length of the KJCOC test-loop. Any arbitrary length could have been chosen. Actual receiver lengths can be many times greater then the test-loop length. The test-loop receiver length, however, is an appropriate length to help determine at what receiver length the axial direction effects become significant, ~ 80 m, according to Figure 4.2 where the heat loss first shows a drop as compared to smaller step sizes. The last column in Table 4.1 "time" is the time required for the EES program to reach convergence. Besides being dependent on the step size, the time is also dependent on how close the initial variable guesses are to the solution, and the speed of the microprocessor. The closer the initial guesses are to the solution, the shorter the iteration time. However, given the same guess values, the iteration time will always increase with decreasing step size (or increasing number of steps).

42
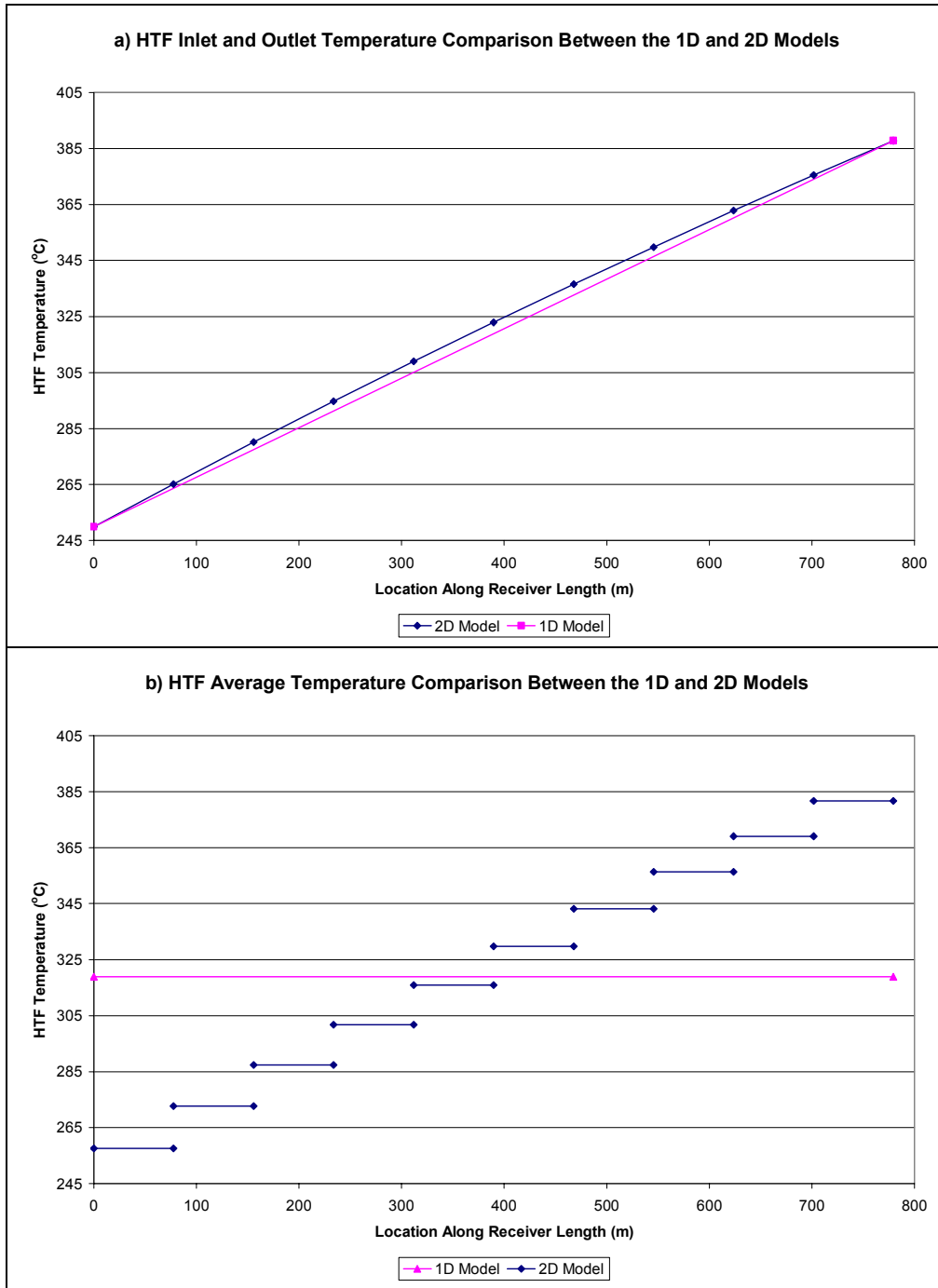
**Figure 4.1 a) HTF inlet and outlet and b) average HTF temperature comparisons between the one- and two-dimensional models.**

**Table 4.1  Iteration Time for Different Receiver Step Sizes**

| Number of Steps | Step Size* (m) | Time (s) |
|---|---|---|
| 100 | 7.795 | 91411.5 |
| 50 | 15.59 | 13200 |
| 20 | 38.98 | 11819 |
| 10 | 77.95 | 311 |
| 4 | 194.9 | 39 |
| 1 | 779.5 | 6 |
| * Total length of solar receiver = 779.5 m | | |
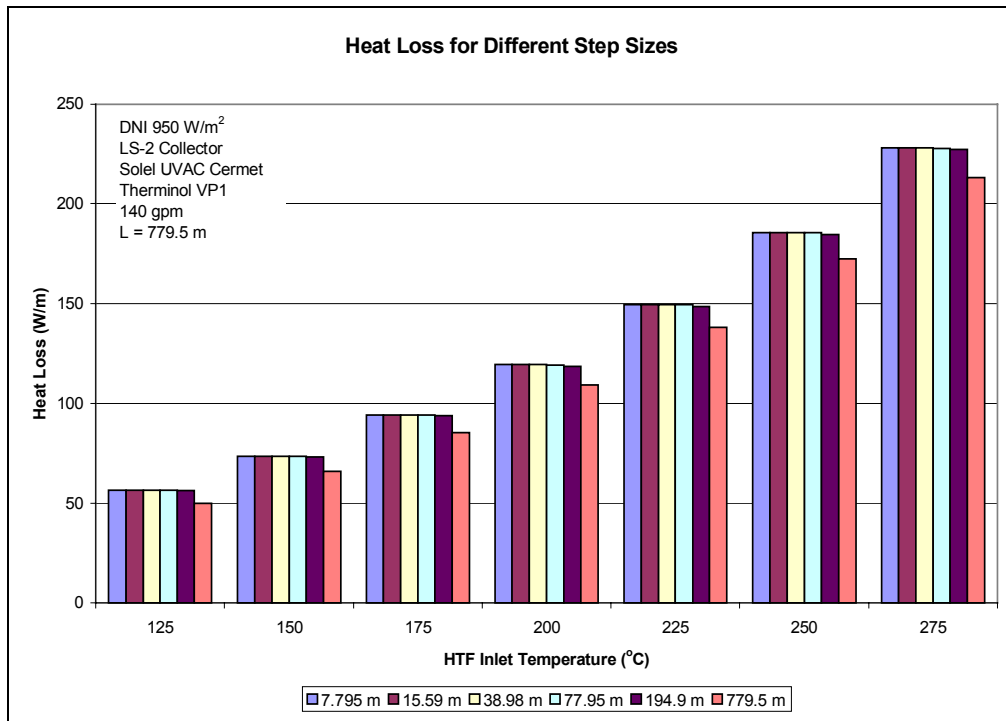


**Figure 4.2  Heat loss chart for different receiver length step sizes**

Figure 4.3 shows the heat gain and collector efficiency per receiver length and Figure 4.4 shows the heat loss per receiver length, for the one- and two-dimensional models. As expected, the one-dimensional model overpredicts heat gain and efficiency and underpredicts heat loss. Specifically, it gives heat gain and efficiency values that are approximately 0.5% different than the two-dimensional model, and heat loss values that are 5% to 10% different. The small differences between the one- and two-dimensional models for heat gain and efficiency values appear because the optical losses remain the same between the two models and the heat losses are relatively small compared to the optical losses (see Section 5.2). The charts also show that the higher the HTF temperature the larger the difference between the one- and two-dimensional models. These differences will continue to increase with receiver length, and receivers can be many times longer than those used here. Additional comparisons between the one- and two-dimensional models are shown in Figures 6.10, 6-16, and 6.17 in Sections 6.6, 6.9, and 6.10, respectively.
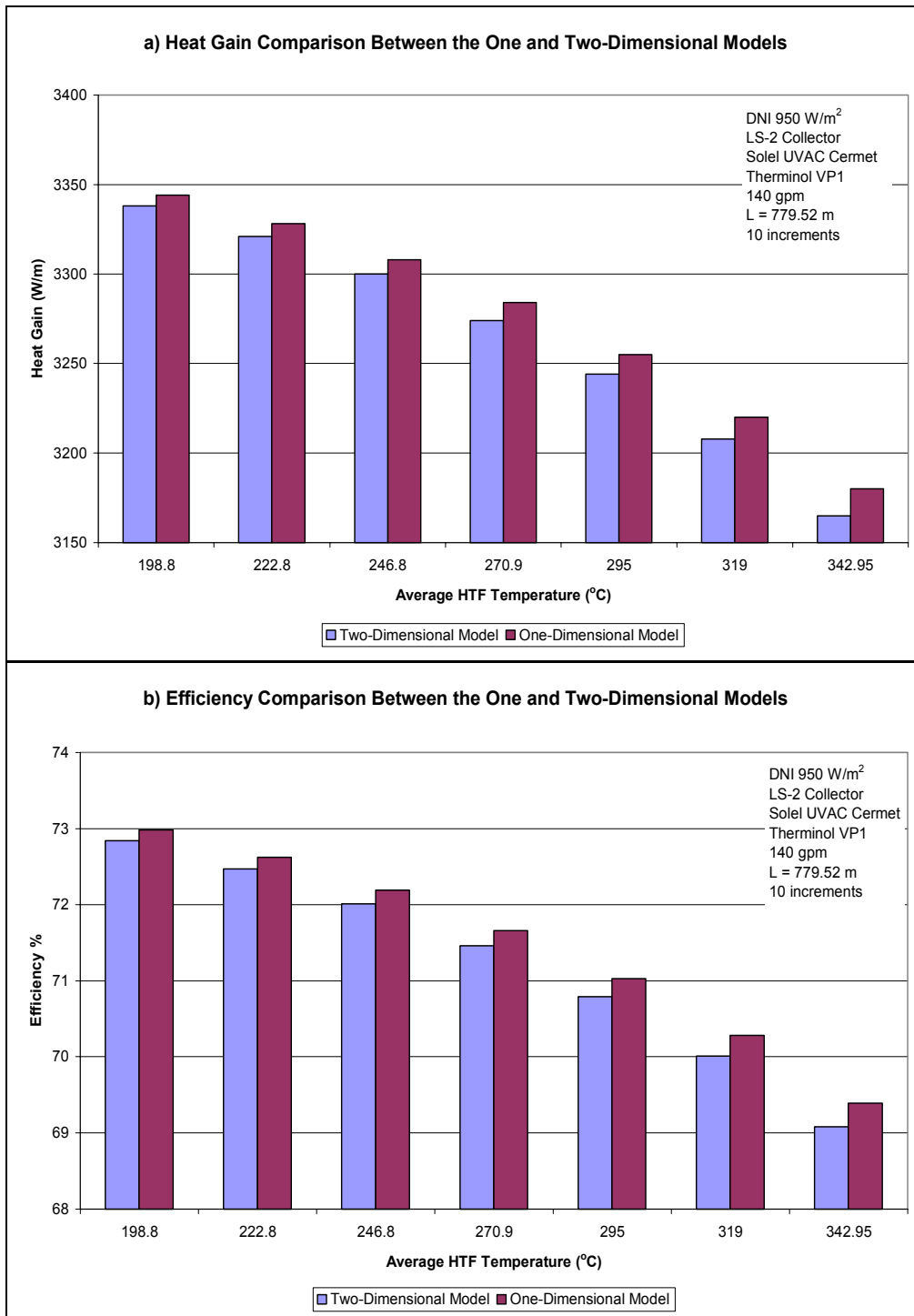
**Figure 4.3 a) Heat gain and b) efficiency charts comparing the one- and two-dimensional models for different HTF temperatures**
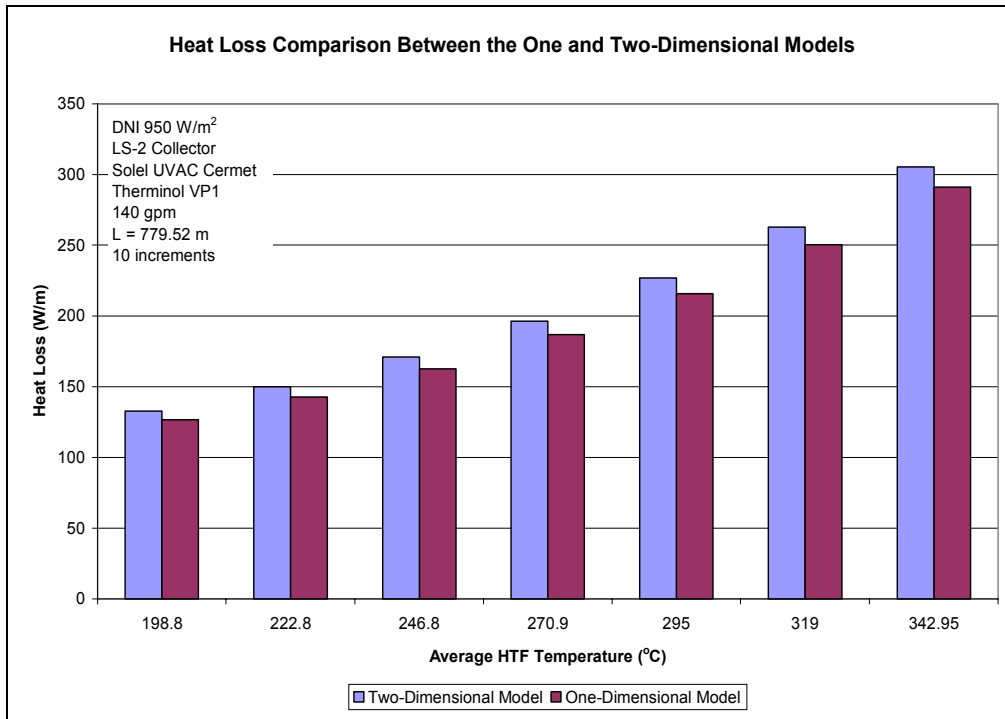
Figure 4.4 Heat loss chart comparing the one- and two-dimensional models for different HTF temperatures

## 5. Comparison with Experimental Data

To verify the accuracy of the heat transfer models, the EES heat transfer codes were compared with two sets of data from HCE field tests. One set was from tests conducted from June 1992 through January 1993 on the AZTRAK rotating test platform at SNL. The second set of data consists of three days of test data from a test-loop of collectors in a SEGS plant in Kramer Junction, California. A picture of the AZTRAK rotating test platform is shown in Figure 5.1. It consists of a rotating platform, a two-axis tracking control system, and all associated pumping equipment and instrumentation to test a segment of a trough collector and receiver. The trough shown consists of an LS-2 type collector segment with two Luz Cermet HCEs of 4.06 m each. All the data used in the comparisons and a detailed explanation of the AZTRAK rotating test platform tests are reported in Dudley et al. [1994].

The second set of data, from a test-loop of collectors in a SEGS plant (Figure 1.1), includes data for January 2, March 22, and June 21, 2001. The test-loop consists of two rows of collectors containing 16 LS-2 type SCAs in series each with 12 Luz Cermet selective coating HCEs at 4.06 m for a total receiver length of 779.52 m. The test-loop was instrumented to record HTF flow rates and HTF inlet and outlet temperatures. There was also instrumentation to record the direct normal solar irradiation, ambient temperature, and wind speed.

When using the same HTF input property data and meteorological data as those from the field tests, the EES heat transfer codes gave results that agreed well with the field test data.

Figure 5.1  AZTRAK rotating test platform at SNL. An LS-2 type collector module is shown installed on the platform.

## 5.1    Comparison with SNL AZTRAK Data

The eight charts in Figures 5.2 to 5.6 show the comparison between the EES AZTRAK Test Data version of the heat transfer model and the 1992 data from the AZTRAK rotating platform tests [Dudley, et al. 1994]. The AZTRAK test data included data for two different HCE selective coating types: Luz Cermet and Luz black chrome. For each coating, four test conditions were compared:

- On-sun and vacuum in the annulus
- On-sun and no vacuum in the annulus
- Off-sun and vacuum in the annulus
- Off-sun and no vacuum in the annulus

The no vacuum condition was created simply by drilling small holes into the HCE bellows (see Figure 1.4) allowing air to fill the annulus space. The AZTRAK off-sun tests were conducted after sunset with the collectors pointing toward the sky. Wind tests were conducted on the Luz black chrome HCE with the glass envelope removed; these data were compared with the EES program results.

To simulate the test conditions with the EES code, the input data from the tests were copied into the parametric tables and the solar weighted reflectivity was adjusted until the optical efficiency calculated with EES matched the field tests results. The reflectivity values used are shown in Table 5.1.

The one-dimensional heat transfer model compares well with the AZTRAK field test data. All trends are followed, and with a few exceptions, the data from the EES program are within the error bounds of the AZTRAK test data. However, the spread between data appears to increase with rising temperature for the Luz Cermet selective coating case. This could be due to either the changes in optical properties with temperature or to the possible sagging of the HCEs, causing a slight misalignment between HCE and collector. The optical properties used in the code are based on optical tests at lower temperatures. Therefore, the optical property equations given in Section 2.1.6.1 may be incorrect at elevated

temperatures for the Luz Cermet case – the Luz black chrome field test data show better agreement with the EES data. The HTF properties could also explain some of the differences. As the HTF manufacturers state in the information sheets, the thermophysical properties could vary slightly from batch to batch and could change over time, especially when exposed to thermal cycling (see Appendix A for references). Some of the extraneous points could also be due to typing or recording errors either in Dudley et al. [1994], actual test data recording, or in the EES parametric tables.

**Table 5.1  Mirror Reflectivity and Optical Efficiency for Each Test Type**

| Test Type | Solar Weighted Mirror Reflectivity | Total Optical Efficiency (%) |
|---|---|---|
| Luz Cermet, Vacuum | 0.9337 | 73.1 |
| Luz Cermet, Loss Vacuum | 0.9353 | 73.3 |
| Luz Black Chrome, Vacuum | 0.9289 | 74.1 |
| Luz Black Chrome, Loss Vacuum | 0.9221 | 73.3 |

For convenience, all figures from the AZTRAK data comparisons are listed in Table 5.2, along with general comments about the comparisons.

**Table 5.2  List of Figures and Comments for the AZTRAK Test Platform Data Comparison**

| Figure | Description | Comments |
|---|---|---|
| All | All | • Difference between the EES data and AZTRAK data for the Luz Cermet selective coating case tends to increase with increasing temperature.<br>• The Luz black chrome selective coating resulted in better agreement between the EES data and AZTRAK data than the Luz Cermet selective coating.<br>• EES data accurately depict all trends.<br>• With a few exceptions, the EES data agree with the AZTRAK data within the instrument error bounds. |
| 5.2 a) | Luz Cermet, efficiency for vacuum and loss vacuum cases | • Two EES data points lie outside the AZTRAK error bounds. |
| 5.2 b) | Luz Cermet, heat loss for vacuum and loss vacuum cases with solar | • Nine EES data points lie outside the AZTRAK error bounds.<br>• EES data seem to underpredict the heat loss.<br>• Shows the least agreement between the EES data and AZTRAK data. |
| 5.3 | Luz Cermet, heat loss for vacuum and loss vacuum cases without solar | • One EES data point lies outside the AZTRAK data error bounds. |
| 5.4 a) | Luz black chrome, efficiency for vacuum and loss vacuum cases with solar | • All EES data points are within the AZTRAK data error bounds. |
| 5.4 b) | Luz black chrome, heat loss for vacuum and loss vacuum cases with solar | • One EES data point lies outside the AZTRAK data error bounds. |
| 5.5 | Luz black chrome, heat loss for vacuum and loss vacuum cases without solar | • One EES data point lies outside the AZTRAK data error bounds. |
| 5.6 a) | Luz Cermet, efficiency trend with wind | • Model tends to overpredict losses with increasing wind speed. |
| 5.6 b) | Luz Cermet, heat loss trend with wind | |
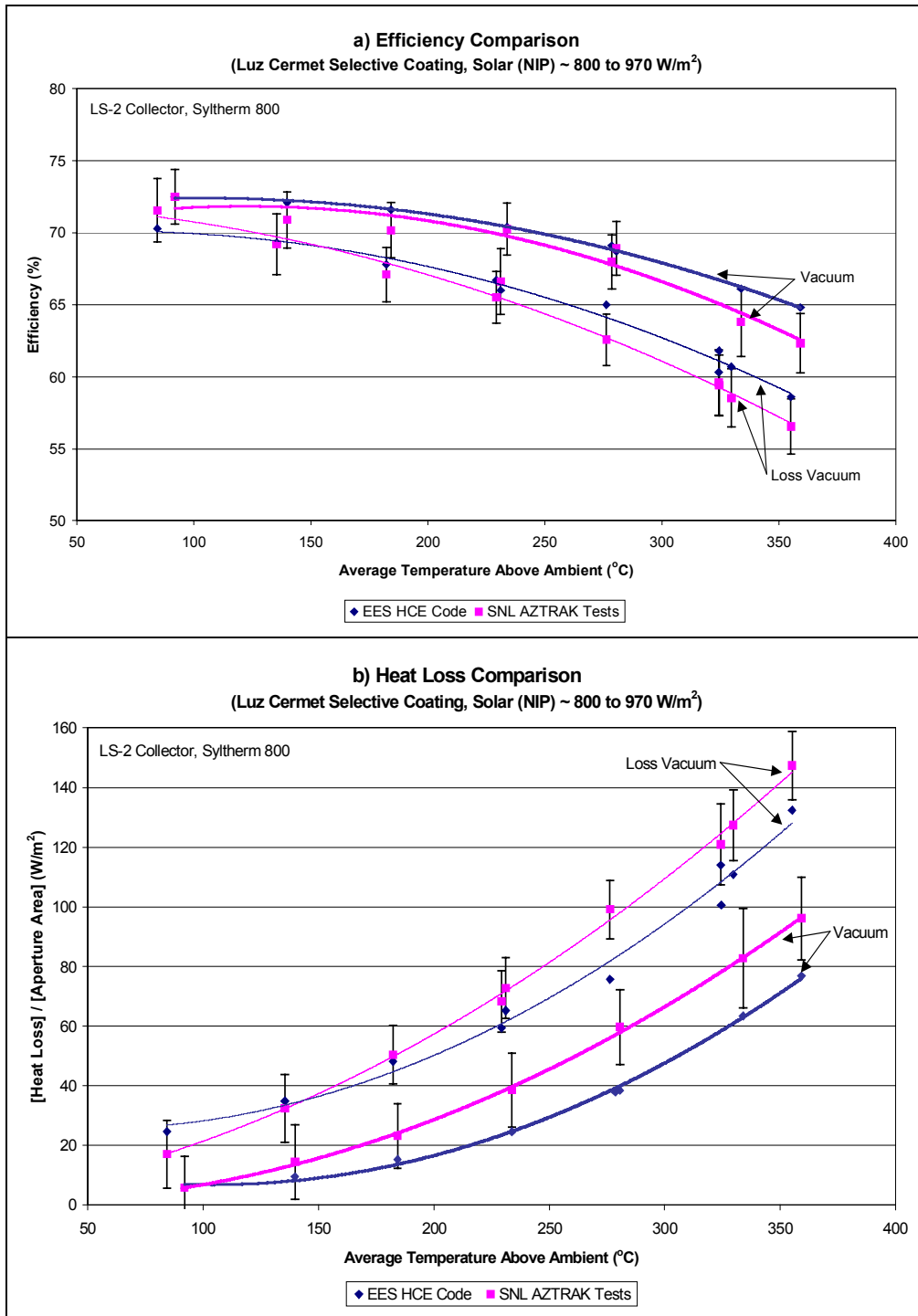
**Figure 5.2 a) Efficiency and b) heat loss charts comparing the EES HCE code and SNL AZTRAK test data for Luz Cermet selective coating**
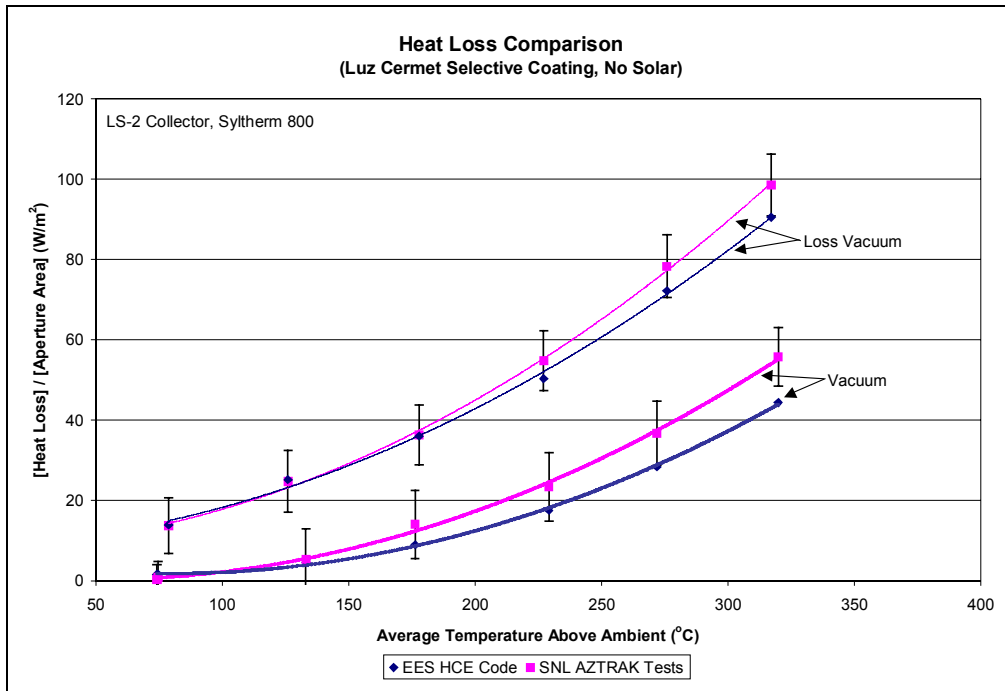
**Figure 5.3  Heat loss comparison chart between the EES HCE code and SNL AZTRAK test data for the off-sun case and Luz Cermet selective coating**

The heat transfer model overpredicts losses with wind (see Figure 5.6). This is expected, since in the program the wind direction is modeled as normal to the HCE axis, and the input wind speed is assumed to be the speed at the HCE height. In reality, many obstructions around the collectors and in general the wind won't be normal to the HCE axis. In addition, the wind speed anemometer is located well above the collector and any obstructions; therefore the wind speed recorded will be higher than the speed at the collector height. Figure 5.6 shows that the error associated with the wind loss can be as high as 30% for the missing glass envelope case; however, the wind has a smaller effect on the heat loss when the glass envelope is in place, especially with a vacuum between the absorber and glass envelope (see Section 6.4). Since the HCE model overpredicts wind related losses, reducing the wind effects in the EES codes on a future revision may be worthwhile.

There are many other explanations for the differences between the EES data and AZTRAK data. For instance, there could be other unaccounted optical effects during the testing, such as HCE and mirror alignment, aberration in mirrors, deflections in collector structure during tracking, and controller tracking errors. Furthermore, the solar flux along the receiver axial and circumferential directions is not uniform, because of some or all the effects just mentioned and collector geometry, yet the EES model assumes uniformity along both directions. Another difference between the test data and model data could be due to the vacuum level in the annulus and presence of hydrogen in the annulus. Both are explored more fully in Sections 6.3 and 6.5. Given all the possible sources of inaccuracies, the one-dimensional EES Heat Transfer Model does a good job modeling the HCE performance for a short segment of collector, such as the size that fits on the AZTRAK rotating test platform.
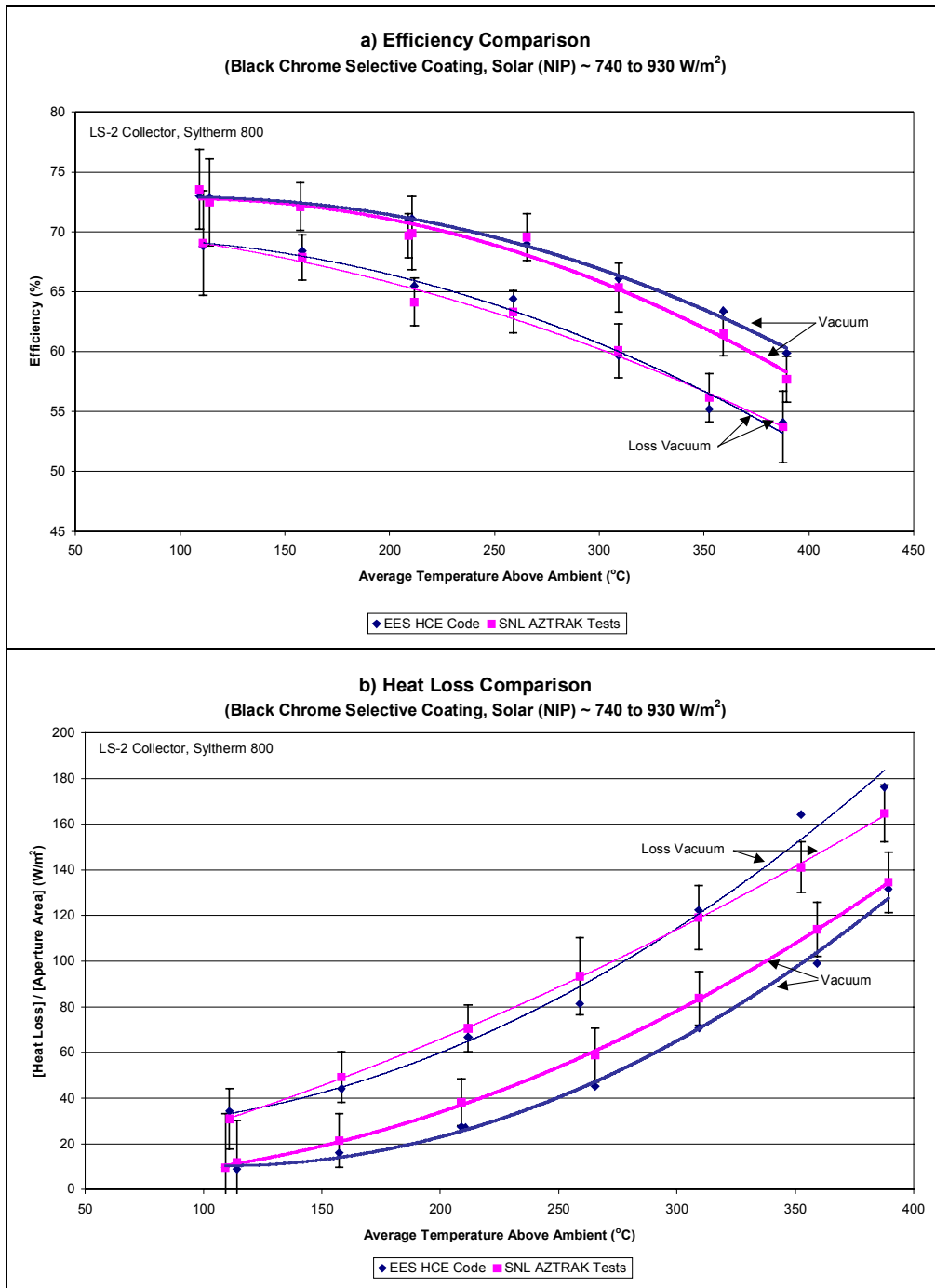
**Figure 5.4a) Efficiency and b) heat loss chart comparing the EES HCE code and SNL AZTRAK test data for Luz black chrome selective coating**
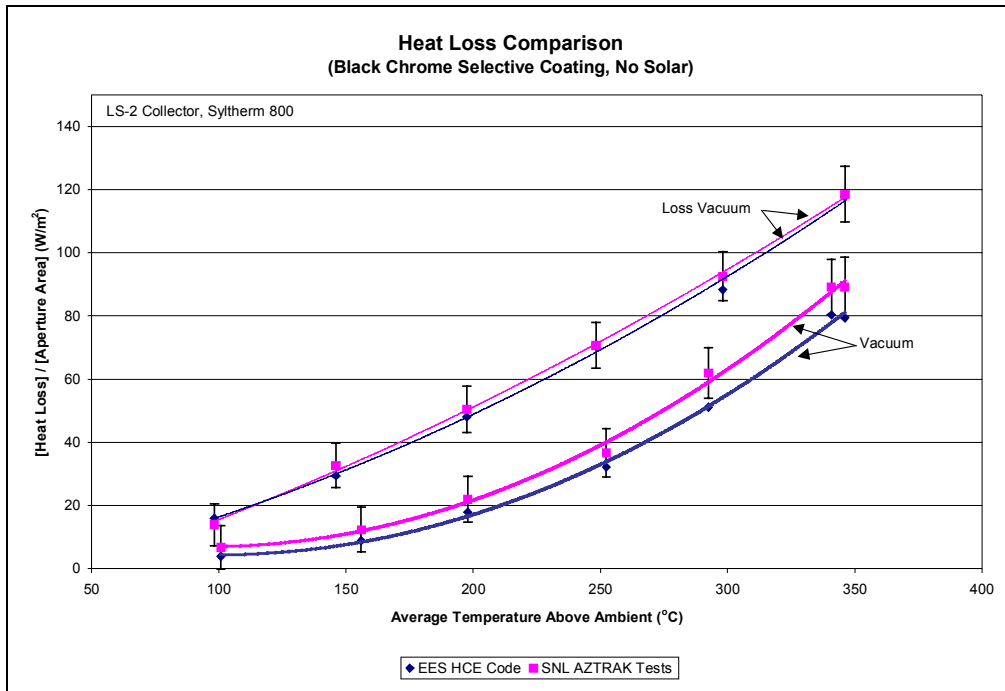
**Figure 5.5  Heat loss comparison chart between the EES HCE code and SNL AZTRAK test data for the off-sun case and Luz black chrome selective coating**
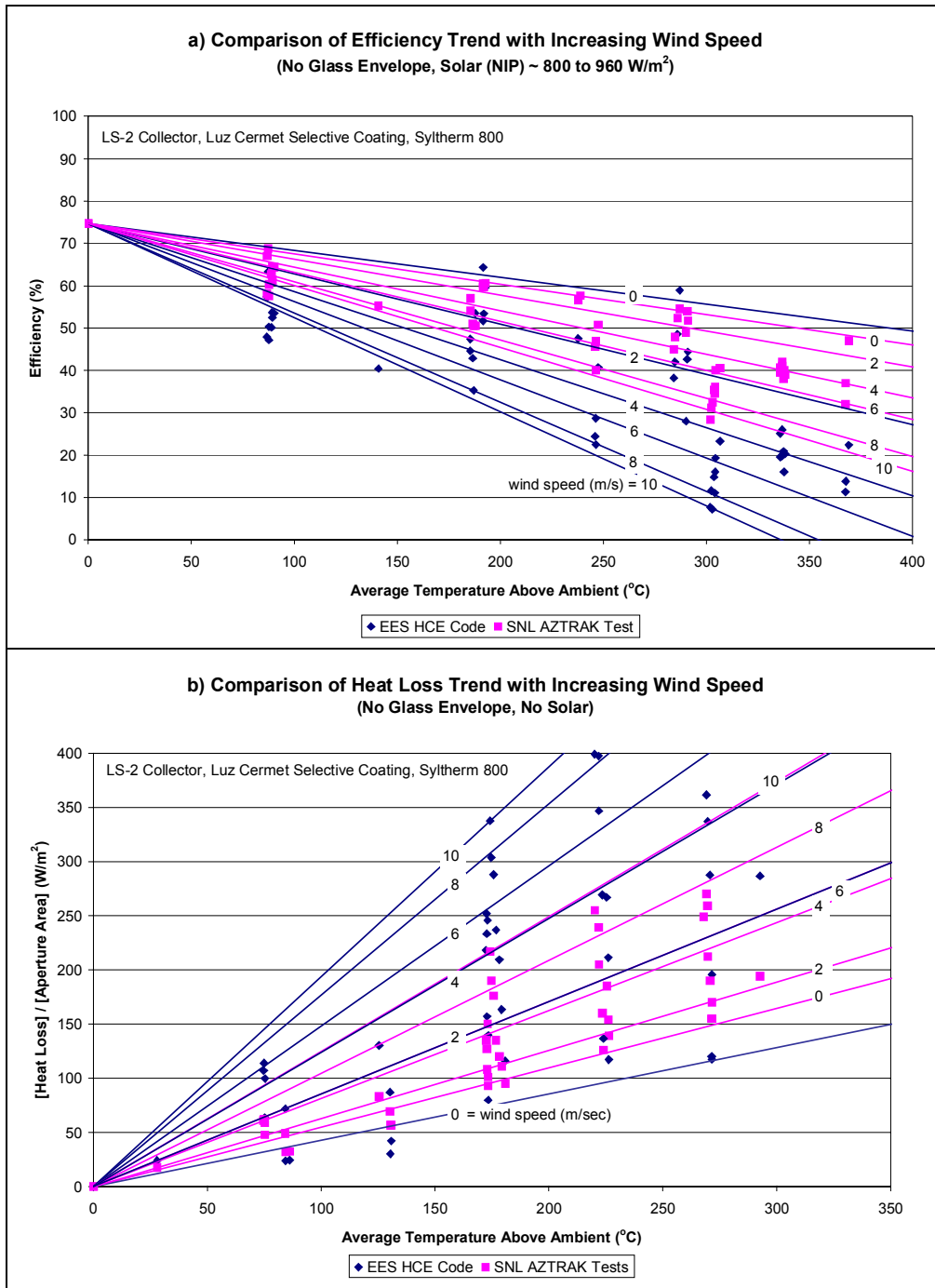
**Figure 5.6 a) Efficiency trend and b) heat loss trend charts comparing the EES HCE code and SNL AZTRAK test data for varying wind speeds and no glass envelope**

## 5.2    Comparison with KJC Test-Loop Data

Three days of data—a winter day, a spring day, and a summer day—were used to compare the KJC test-loop with the EES model. The test-loop comprised LS-2 type collectors with Luz Cermet HCEs. In the EES heat transfer model, all HCEs were assumed to be in good condition and under vacuum. The test-loop had a few bad HCEs, but the number was small compared to the total number in the test-loop. The

KJC Test-Loop Data version of the EES code consists of a two-dimensional model to account for the effects of the long receiver (pressure drop, thermal expansion of HTF, HCE support brackets).

The EES data compared well with the KJC test-loop data, as shown in Figures 5.7 through 5.9, where the heat gain and outlet temperatures were compared for each of the three days of data. Like the AZTRAK test data comparison, there are plenty of reasons to help explain differences between the model and test data. In addition to those already mentioned in Section 5.1, startup and shutdown transients, cloud transients, and sections of collectors taken off line will cause differences between the model and test data. However, these differences are fairly noticeable in the data – sunrise and sunset periods in all the figures, and Figure 5.9 around 12:30 p.m. Also, end losses and shading will contribute to the differences, since the KJCOC test-loops track on one axis. All the figures along with general comments are listed in Table 5.3.

**Table 5.3  List of Figures and Comments for the KJC Test-Loop Data Comparison**

| Figure | Description | Comments |
|--------|-------------|----------|
| All | All | Transients explain the larger differences between the EES data and KJC data during startups and shutdowns.<br><br>Except for the periods of transients, the EES data and KJC data showed good agreement. |
| 5.7 a) | 01-02-03, Heat gain comparison | Transients caused by clouds explain the scattering and increase in differences during late afternoon. |
| 5.7 b) | 01-02-03, Outlet temperature comparison | |
| 5.8 a) | 03-22-01, Heat gain comparison | Increase in difference around 9:30 is most likely due to a collector segment being taken off line. |
| 5.8 b) | 03-22-01, Outlet temperature comparison | Brief increase in outlet temperature around 11:30 a.m. is most likely due to a flow rate adjustment. |
| 5.9 a) | 06-21-01, Heat gain comparison | Increase in difference after 12:30 p.m. is most likely due to a collector segment being taken off line. |
| 5.9 b) | 06-21-01, Outlet temperature comparison | Transients caused by clouds explain the scattering and increase in differences during late afternoon. |

Because the SEGS troughs track in one axis only (east/west), the solar incident angle effect had to be included as an input. The incident angle, which is between the collector's projected area normal and the direct normal incident solar, was determined with another spreadsheet. Its effects are estimated in the model with an equation that was developed from testing at SNL (see Section 2.1.6.1).

In addition to the heat gain and outlet temperature comparisons, power loss components determined from the model were plotted and are shown in Figures 5.10 through 5.12. The losses include both heat and optical. Furthermore, the optical losses caused by the incident angle effect have been plotted separately. This demonstrates how the incident angle effect depends on the time of year – incident angle is smallest during the summer months. The plots also reveal that the optical losses are much larger than the heat losses. This means any error in the estimated optical losses could overshadow errors in the heat loss. Table 5.4 further illustrates this point by listing the actual calculated daily average values with percentages of the total losses. The plots also indicate that the heat losses are lower in the winter than the summer. This is because the plants typically operate at lower HTF temperatures during the winter (see Figure 5.13), when energy demand is lower. Also shown in the plots is the solar insolation to help indicate transient periods, such as sunrise, sunset, and cloudy conditions.
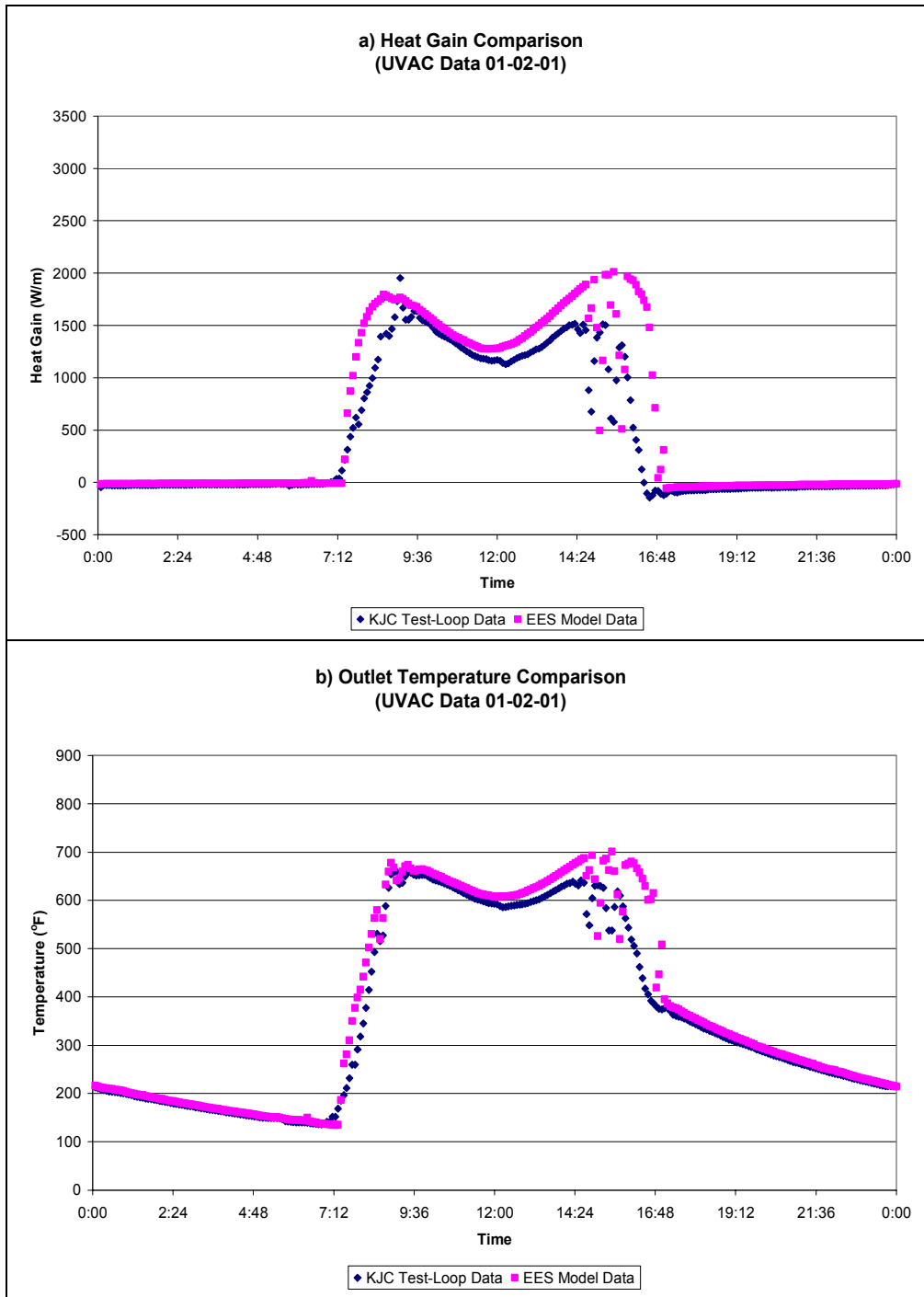
**Figure 5.7 a) Heat gain and b) outlet temperature charts comparing the EES HCE code and KJC test-loop data for 01-02-01**
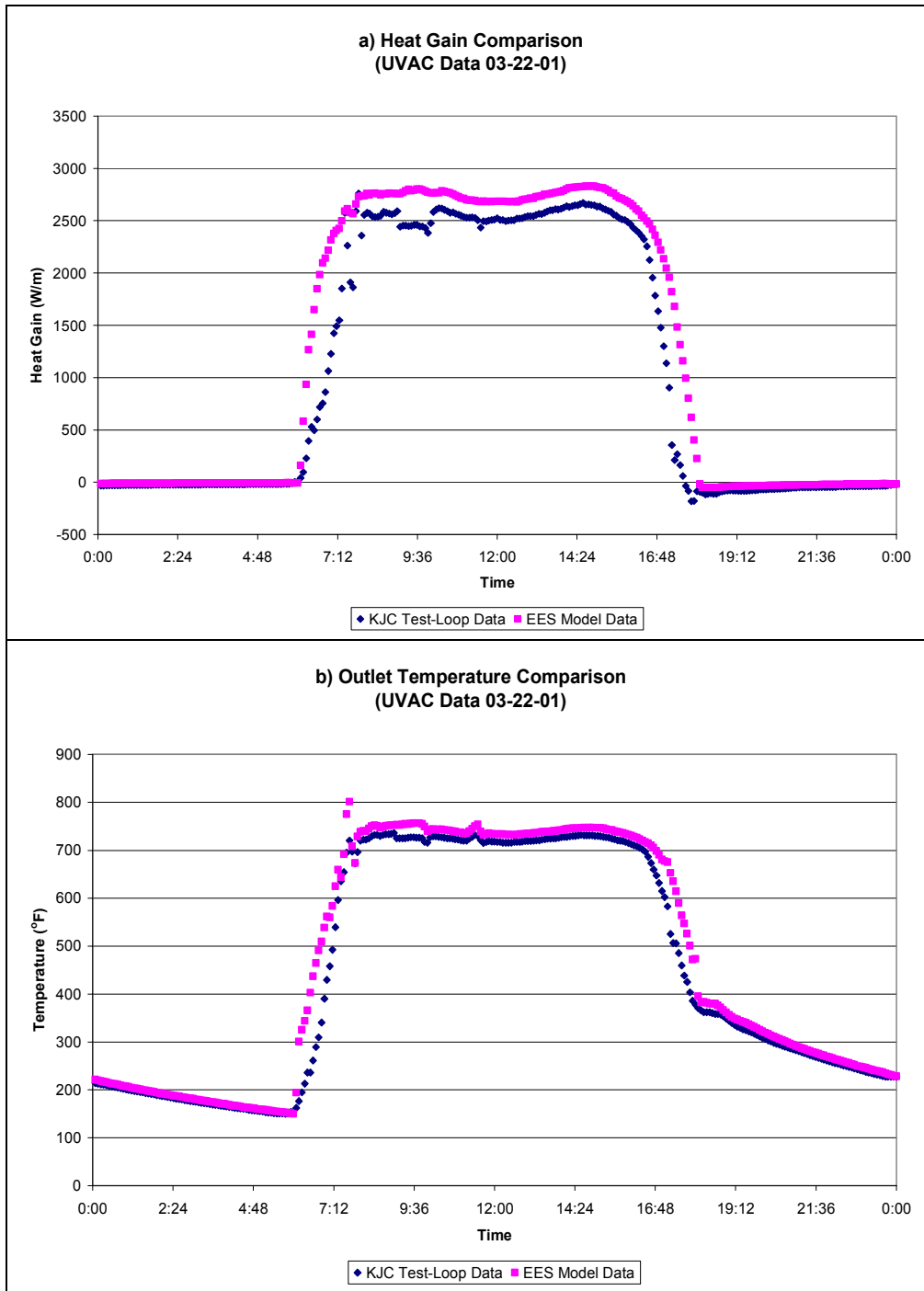
**Figure 5.8 a) Heat gain and b) outlet temperature charts comparing the EES HCE code and KJC test-loop data for 03-22-01**
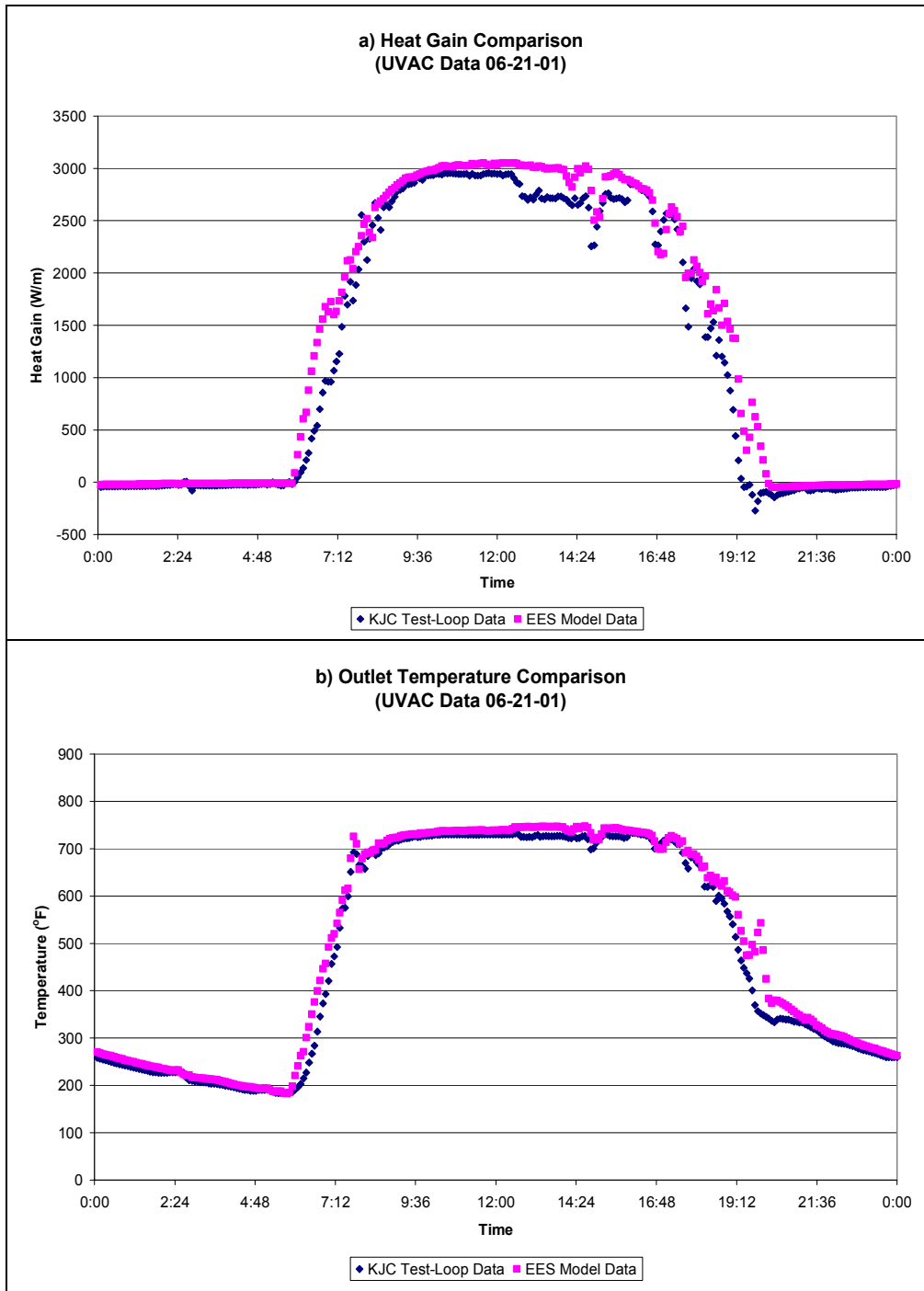
**Figure 5.9 a) Heat gain and b) outlet temperature charts comparing the EES HCE code and KJC test-loop data for 06-21-01**
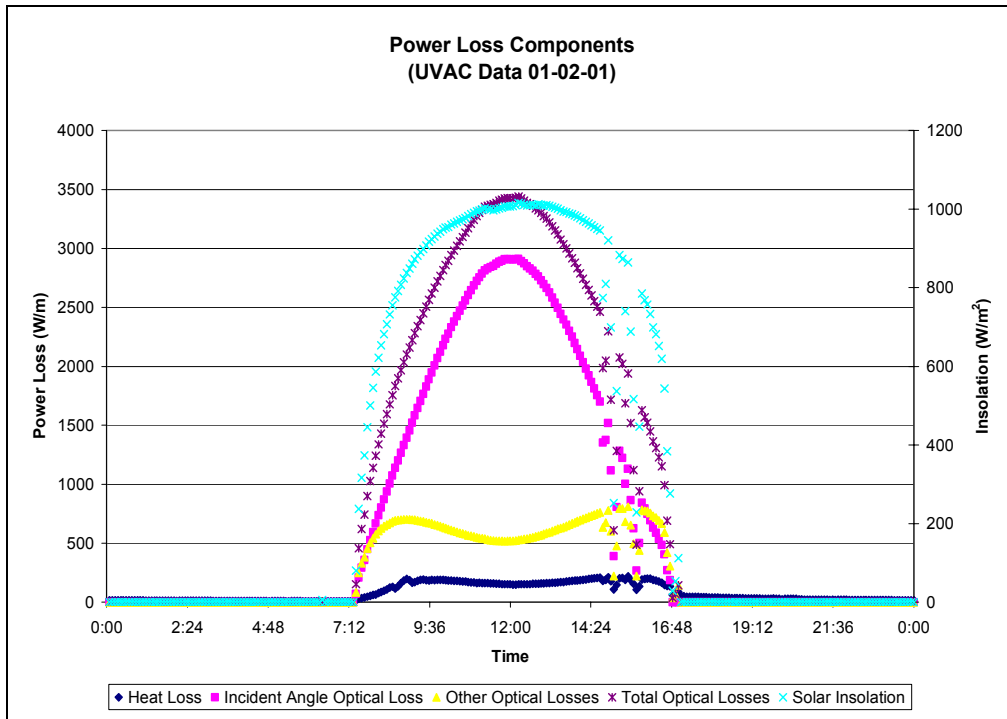
**Figure 5.10 Power loss components and solar insolation chart from the KJC test-loop data for 01-02-01**
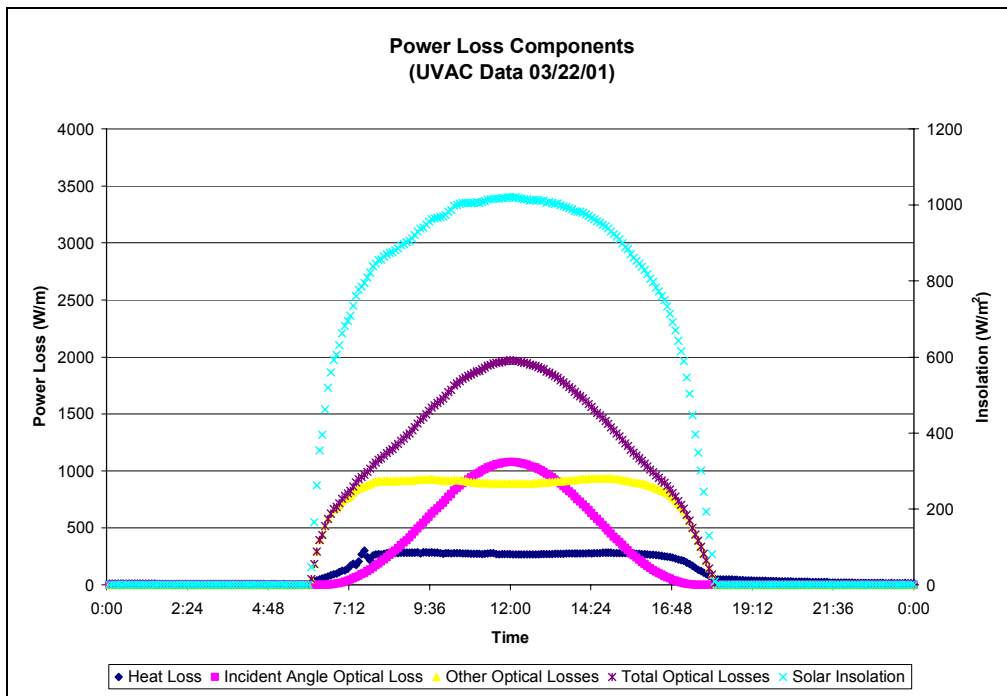


**Figure 5.11  Power loss components and solar insolation chart from the KJC test-loop data for 03-22-01**
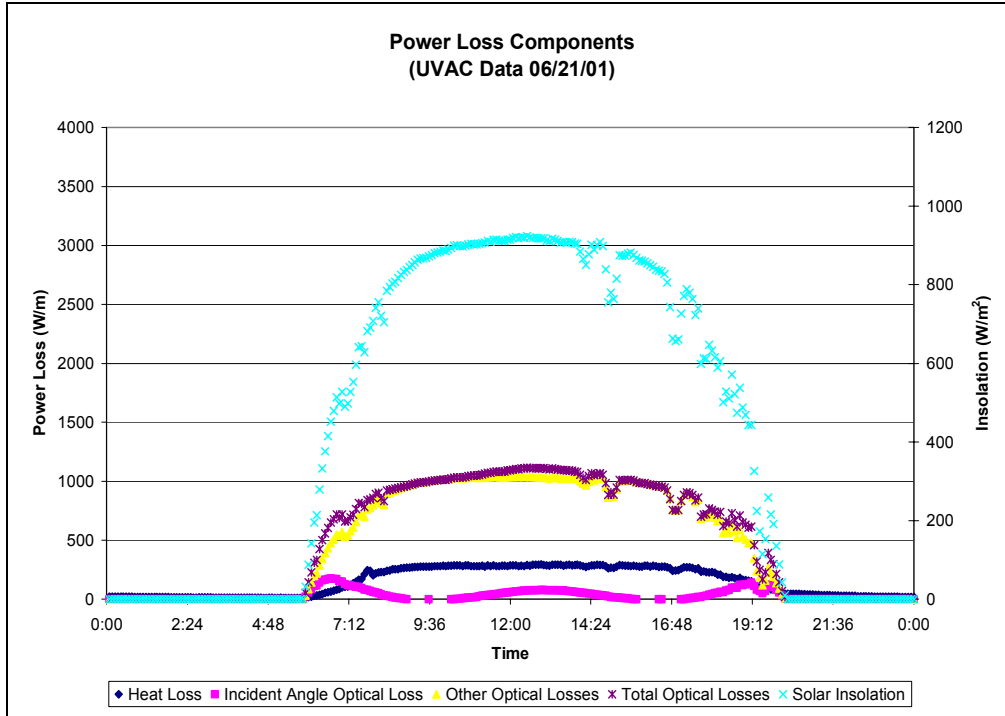
**Figure 5.12 Power loss components and solar insolation chart from the KJC test-loop data for 06-21-01**

**Table 5.4  Daily Average Losses per Receiver Length**

| Date | Heat Loss (W/m) | Optical Losses (W/m) | | Total Losses (W/m) |
|---|---|---|---|---|
| | | Incident Angle | Other | |
| 01-02-01 | 74 (7%) | 696 (69%) | 238 (24%) | 1008 |
| 03-22-01 | 130 (17%) | 241 (31%) | 409 (52%) | 780 |
| 06-21-01 | 113 (18%) | 29 (5%) | 484 (77%) | 657 |

The conductive losses through the HCE support brackets were evaluated with the KJC Test-Loop version of the code. Table 5.5 lists the results of this study. As shown, on average the brackets can contribute 1% to 1.5% of the total heat losses from the HCE. And the instantaneous heat loss through the brackets can be higher than 3%, depending on the operating and ambient conditions. This study assumes that all the brackets are similar in design to those pictured in Figures 2.3 and 2.4 and are not insulated from the HCE absorber.

**Table 5.5  Estimated Heat Loss Percentages Caused by HCE Support Brackets**

| Day | Percentage of Total Heat Loss | |
|---|---|---|
| | maximum | average |
| 01/02/01 | 3.2% | 1.3% |
| 03/22/01 | 2.8% | 0.9% |
| 06/21/01 | 2.5% | 1.5% |
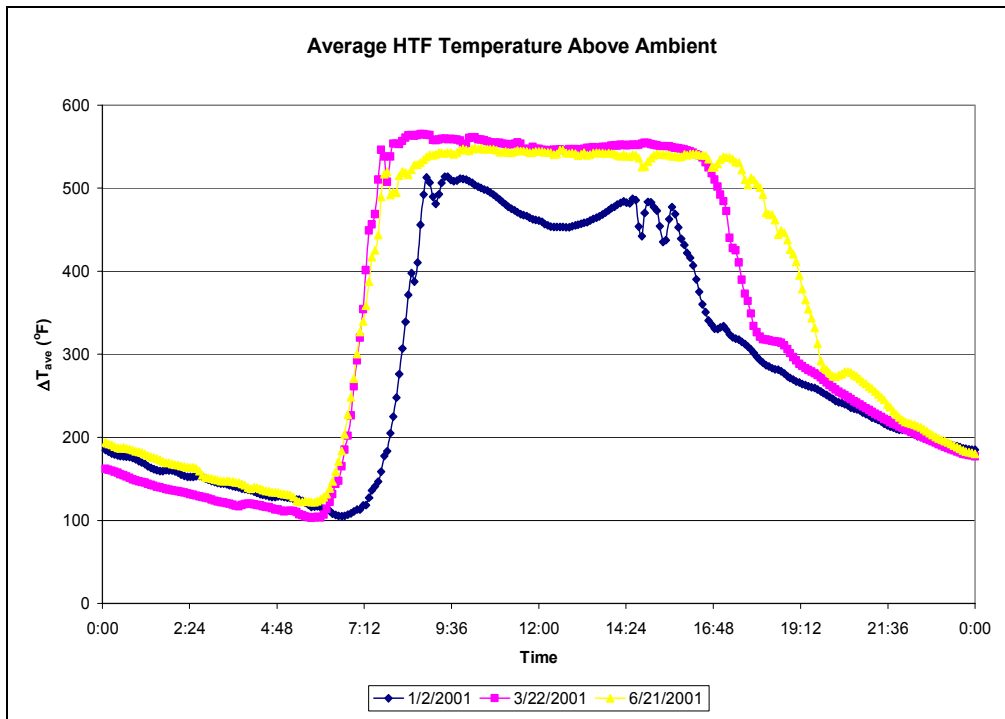
**Figure 5.13  Average HTF temperatures above ambient for each KJC test-loop data set**

## 6.    Design and Parameter Studies

Numerous examples of design and parameter studies using the HCE performance models implemented in EES are shown below. The examples demonstrate the utility of the software program and identify and prioritize some methods for improving collector and HCE performance. The HCE performance models do not include an optimization routine; but rather, using the EES software, simultaneously solve a set of equations that describe the energy balance between the HTF and surrounding ambient conditions, given a set of inputs (see Section 2). Thus, the results described below were compiled by rerunning the EES program for each change in a design or parameter variable and then copying the outputs to an EXCEL spreadsheet for comparisons.

Twelve design conditions and parameters were evaluated with the EES HCE performance codes. Table 6.1 summarizes the results. Charts showing the various comparisons are discussed in Sections 6.1–6.12.

**Table 6.1  HCE Design and Parameter Study Summary**

| Design Option or Parameter | Purpose of Evaluation | Results and Comments |
|---|---|---|
| Absorber Pipe Base Material (Section 6.1) | To determine influence of less expensive materials (316L, B42 copper, and carbon steel) on the HCE performance | • Negligible, yet material selection is also driven by material strength, corrosion properties, installation ease, coating application, and cost considerations. |
| Selective Coating (Section 6.2) | To compare the differences on HCE performance between all the absorber coatings that have been used or have been proposed | • Chronologically, the improvements in coatings have improved HCE performance.<br>• Solel's proposed UVAC Cermet with emittance of 0.07 @ 400$^o$C gives the best HCE performance.<br>• HCE performance would be sensitive to any variance in selective coating optical properties. |
| Annulus Gas Type (Section 6.3) | To evaluate the differences on HCE performance between vacuum, air, argon, and hydrogen in the HCE annulus | • Vacuum gives the best result.<br>• Filling the annulus with an inert gas is better than air.<br>• Hydrogen permeation can degrade HCE performance. |
| HCE Condition and Wind Speed (Section 6.4) | To evaluate the loss in HCE performance because of loss vacuum in annulus, or a broken glass envelope. | • A broken glass envelope on an HCE gives unacceptable performance results, especially with windy conditions.<br>• The wind has little influence on HCE performance when the annulus vacuum is intact, but does when the vacuum is lost. |
| Annulus Gas Type (Section 6.3) | To evaluate the differences on HCE performance between vacuum, air, argon, and hydrogen in the HCE annulus | • Vacuum gives the best result.<br>• Filling the annulus with an inert gas is better than air.<br>• Hydrogen permeation can degrade HCE performance. |
| Annulus Pressure (Section 6.5) | To determine sensitivity of HCE performance to the vacuum level inside the HCE annulus | • Vacuum levels less than 0.1 torr show negligible improvements from the 0.0001 torr level.<br>• HCE performance declines appreciably with pressures of 100 torr or greater in the annulus.<br>• If hydrogen in present, the HCE performance is even more sensitive to annulus pressure. |
| Mirror Reflectance (Section 6.6) | To determine sensitivity of trough performance to the mirror reflectance. | • The trough performance drops appreciably with solar weighted reflectivity less than 0.9.<br>• Keeping mirrors clean is very important to CSA performance. |
| Solar Incident Angle (Section 6.7) | Determine sensitivity of trough performance to solar incident angle. | • Trough performance is very sensitive to solar incident angle. |

Table 6.1 (cont.)

| Design Option or Parameter | Purpose of Evaluation | Results and Comments |
|---|---|---|
| Solar Insolation (Section 6.8) | Determine sensitivity of trough performance to solar insolation. | • Trough performance very sensitive to solar insolation.<br>• Factors such as atmospheric pollutants and particu- lates should be considered when choosing a solar site. |
| HTF Flow Rate (Section 6.9) | Determine sensitivity of trough performance to HTF flow rate. | • HCE performance has weak dependency to HTF flow rate. |
| HTF Type (Section 6.10) | To determine sensitivity of HCE performance to the type of heat transfer fluid | • Trough performance has weak dependency to HTF type.<br>• Operation of the HCE at higher temperatures decreases the HCE performance yet increases the power cycle efficiency. |
| Glass Envelope Diameter (Section 6.11) | Determine sensitivity of trough performance to glass envelope diameter. | • Appears to be an optimal diameter that minimizes the heat losses.<br>• Influence of diameter on heat loss is more sensitive when the annulus is not under vacuum.<br>• Clearance for absorber pipe bowing needs to be included. |
| Temperature and Heat Flux Variation along Receiver Length (Section 6.12) | Determine temperature and heat flux profiles along length of receiver. | • The temperatures along the length of the receiver increase in a slightly nonlinear fashion.<br>• The temperature differences between the HTF and absorber ($T_1$ and $T_2$), between the inner and outer absorber pipe surfaces ($T_2$ and $T_3$), and between the inner and outer glass-envelope surfaces ($T_4$ and $T_5$) all remain constant.<br>• The temperature difference between the absorber and glass-envelope ($T_3$ and $T_4$) changes in a slightly nonlinear fashion.<br>• Radiation heat transfer fluxes increase nonlinearly.<br>• Heat gain per receiver length decreases as the HTF temperature increases.<br>• Heat loss per receiver length increases as the HCE cross-sectional temperatures increase.<br>• Optical losses per unit receiver length remain constant. |

## 6.1 Absorber Pipe Base Material

Four different absorber pipe base materials were evaluated; three stainless steels: 321H, 316L, and 304L; and one copper: B42. The materials were chosen to determine the influences of less expensive materials on the HCE performance. All the stainless steels evaluated have been used in HCEs; the copper has not. As shown in Figure 6.1, the differences in efficiency and heat loss between the materials are negligible. However, other factors such as material strength, corrosion properties, installation ease, coating application, and costs weigh in to determine the selection of the absorber pipe base material.

The most recent HCE design uses 321H stainless steel as the absorber base material. It was selected because it is very strong and thought to reduce the problem of bending, and because it slows the hydrogen permeation rate.

Both 304L and 316L stainless steels were used in earlier HCE fabrications; however, HCE bowing problems led to the belief that these materials were not strong enough. Later, after the decision to use the more expensive 321H material was made, the bowing problem was discovered to be due to the temperature cycling during plant startups rather than a material strength issue. Originally, the cost difference between 316L and 321H was significant. Now that vendors are set up for the 321H polishing process, the cost difference may be less important, especially when ordered in large quantities. However, 316L remains a good candidate for HCEs, and further cost analysis may be warranted [Mahoney 2002; Cohen 2002].

Carbon steel is not included in the codes, but can be easily added; however, it has its own problems as an absorber pipe. For instance, carbon steel is very difficult to use with vacuum. If used in a vacuum, the steel would need to go through an expensive and timely process of removing out-gassing, which includes keeping the material in an oven at very high temperatures for days. The preparation process for applying selective coatings, including cleaning and polishing, is also lengthy and expensive. Furthermore, carbon steel may pose corrosion problems at the welded joints. In the past, carbon steel in SEGS plants has been used only for very specific applications; for instance, for the vacuum-insulated pipes in SEGS VIII headers [Mahoney 2002; Cohen 2002].

Copper pipe may cost less, but at current plant operating temperatures, it does not have proper strength and could lead to bowing and joint failure issues. However, if operating temperatures are reduced in future plants, copper piping may be worth re-evaluating as a means to reduce costs [Mahoney 2002; Cohen 2002].
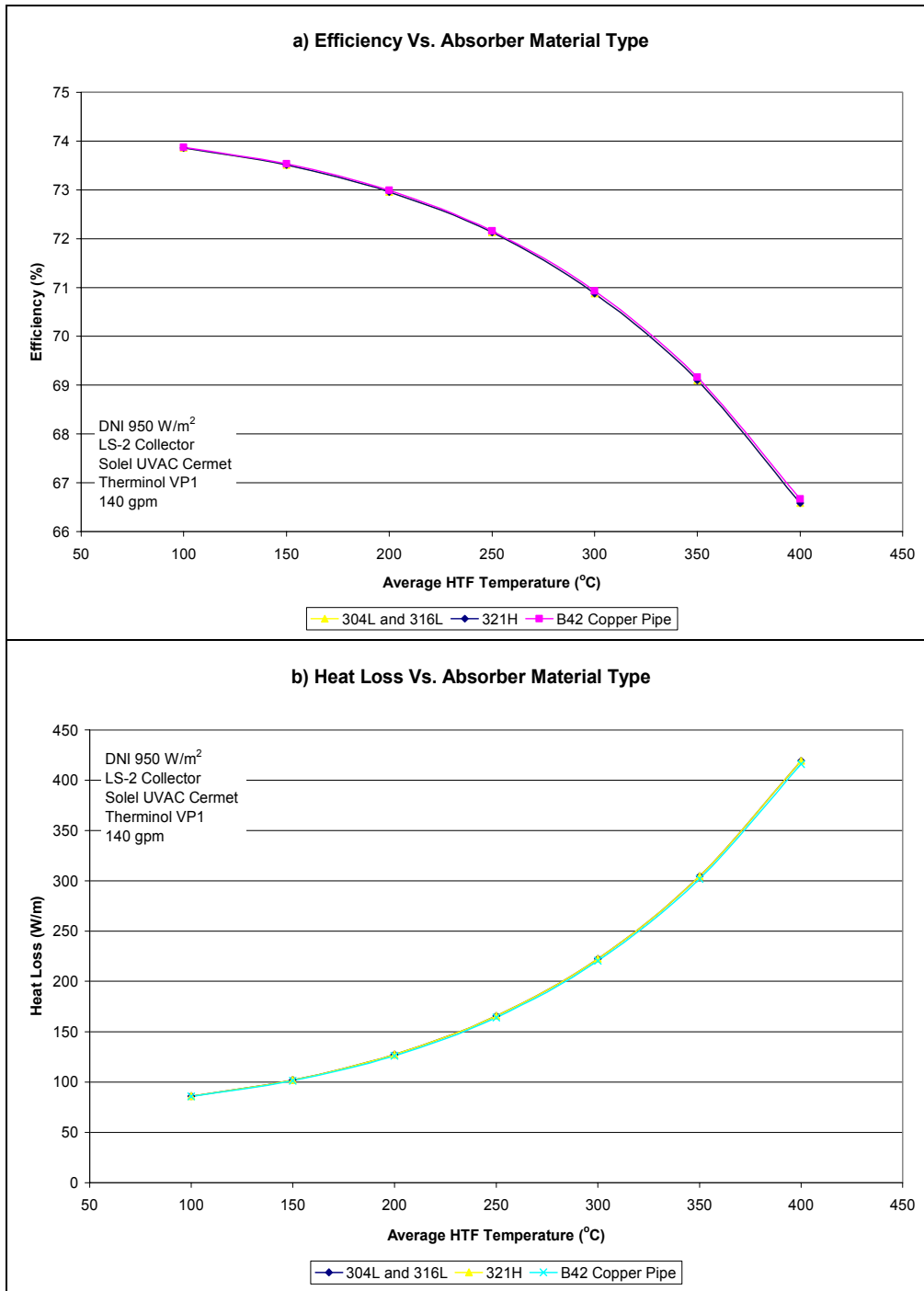
**Figure 6.1 a) Efficiency and b) heat loss charts comparing different HCE absorber pipe base material types**

## 6.2 Selective Coating

Six different selective coatings were evaluated to compare HCE performances for all the absorber coatings that have been used or proposed. The optical properties for the first four types, Luz black chrome, Luz Cermet, Solel UVAC Cermet (SNL test a), and Solel UVAC Cermet (SNL test b), were all

determined in testing at SNL. Two Solel UVAC Cermet coatings are included because the test results varied when testing either end of the same HCE [Mahoney 2002]. The last two coating types are theoretical, as proposed by Solel.

The results of the selective coating type comparisons are shown in Figures 6.2 and 6.3. The bar chart in Figure 6.2 compares the magnitudes of the heat gain, heat loss, and optical loss for each. The selective coating type has a strong influence on each energy rate component, since each coating has different emittance and absorptance values. Figure 6.3 shows the efficiency and heat loss as a function of HTF temperature. Again, the shapes of the curves reflect the different optical property functions for each selective coating type (see Section 2.1.6.1). As shown in Figure 6.3, the 0.07 @ 400°C proposed coating could increase the efficiency by as much as 8.5% (@ 400°C HTF temperature) over current coatings. The figures also illustrate that improvements to the selective coatings have significantly increased collector efficiency.

HCE performance is very sensitive to the optical properties of the selective coatings. Therefore, any manufacturing variances in coatings could result in significant energy losses. Further variance testing and manufacturing quality checks may thus be warranted.
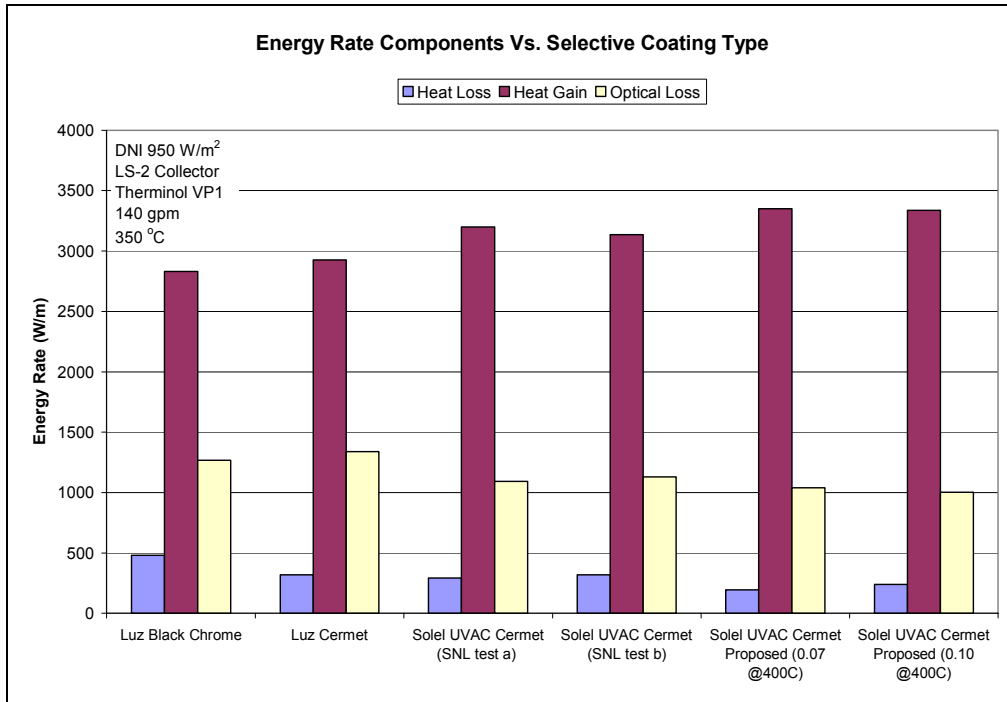


**Figure 6.2  Energy rate component chart for each selective coating type**
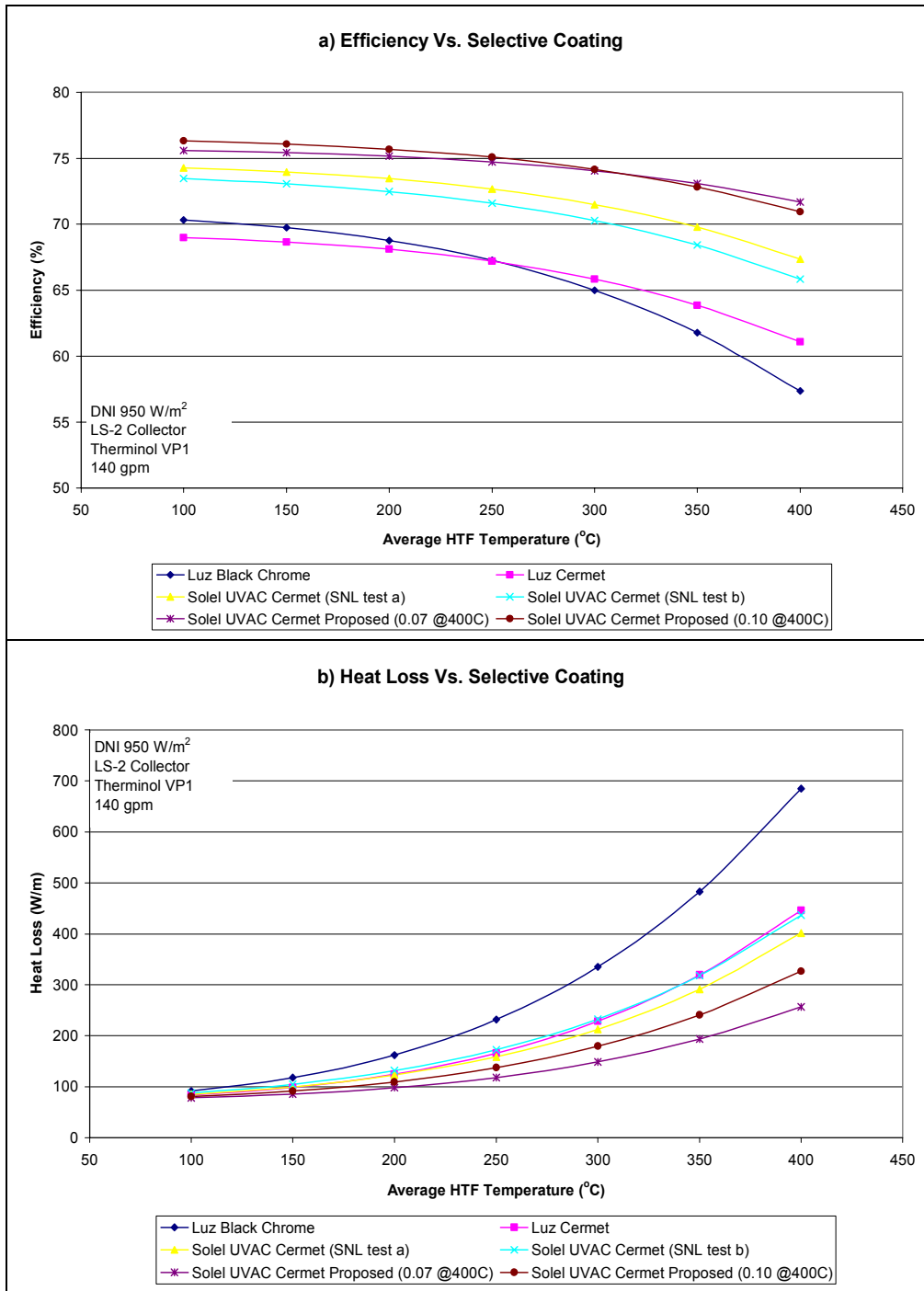
**Figure 6.3  a) Efficiency and b) heat loss charts comparing different HCE types**

## 6.3    Annulus Gas Type

Figure 6.4 shows the efficiency and heat loss comparison of vacuum, air, argon, and hydrogen in the annulus space between the absorber and glass envelope in the HCE. A vacuum in the annulus results in the best HCE performance. An inert gas with a low thermal conduction coefficient, such as argon, is the

next best option shown. However, it provides only a slight improvement over air (argon is ~2.5% gain over air at $400^{o}$C HTF temperature). Hydrogen decreases the HCE performance significantly.

Currently, the HCEs are manufactured with the annulus space under a vacuum of 0.0001 torr (various other annulus pressures were evaluated and are discussed in Section 6.5). The problem with a vacuum in the annulus space is maintaining it. Historically, this has been a problem in SEGS plants. The main cause of vacuum loss has been failure of the glass-to-metal seal, which has been modified recently with promising results. Another cause of vacuum loss is hydrogen permeation.

An inert gas, such as argon, has been considered as a possible alternative to a vacuum. Filling the annulus space with an inert gas instead of a vacuum could result in higher reliability and help mitigate the hydrogen permeation problem – further study is required to show whether this is true. Pumping an inert gas into the annulus space between the absorber and glass envelope could also be an alternative to replacing an HCE after the vacuum has been lost.

Hydrogen is included in the study because it naturally permeates into the annulus space from the HTF, and historically has resulted in lower HCE efficiencies. This potential for a drop in HCE performance caused by hydrogen permeation was discovered early on in the HCE development. In fact, more than $1 million has been spent on investigating the hydrogen permeation rate and on developing the getter bridge to absorb the gas [Cohen 2002]. At the permeation rates for the current HTF and absorber materials, the number of getters installed in an HCE have a lifetime of 30 years before they become saturated. However, some of the older HCEs installed in SEGS plants before the study was completed may have had too few getters installed to absorb the hydrogen properly [Mahoney 2002]. Furthermore, an attempt was made to implement a hydrogen removal (HR) device to provide a longer lifetime for the HCEs. Unfortunately, the HR device caused HCE glass envelope breakage, and therefore further development has been halted. As this study hints at, hydrogen may be one reason some SEGSs run at a lower than expected efficiency.

To indicate whether a vacuum has been lost, the current HCE design has a barium marker (getter) in the annulus, which turns white when exposed to oxygen. Unfortunately, the barium marker is not sensitive to hydrogen. If the hydrogen getter bridge does not remove the hydrogen sufficiently, a vacuum could be replaced by hydrogen without an indication. To date, this is not known to be a problem; however, it does raise the following questions:

- At what hydrogen concentration and annulus pressure does the HCE performance degrade?
- At what pressure and concentration is the getter bridge in equilibrium with the permeation rate (see Section 6.5).
- Is a different vacuum loss indicator, such as one based on temperature, needed?
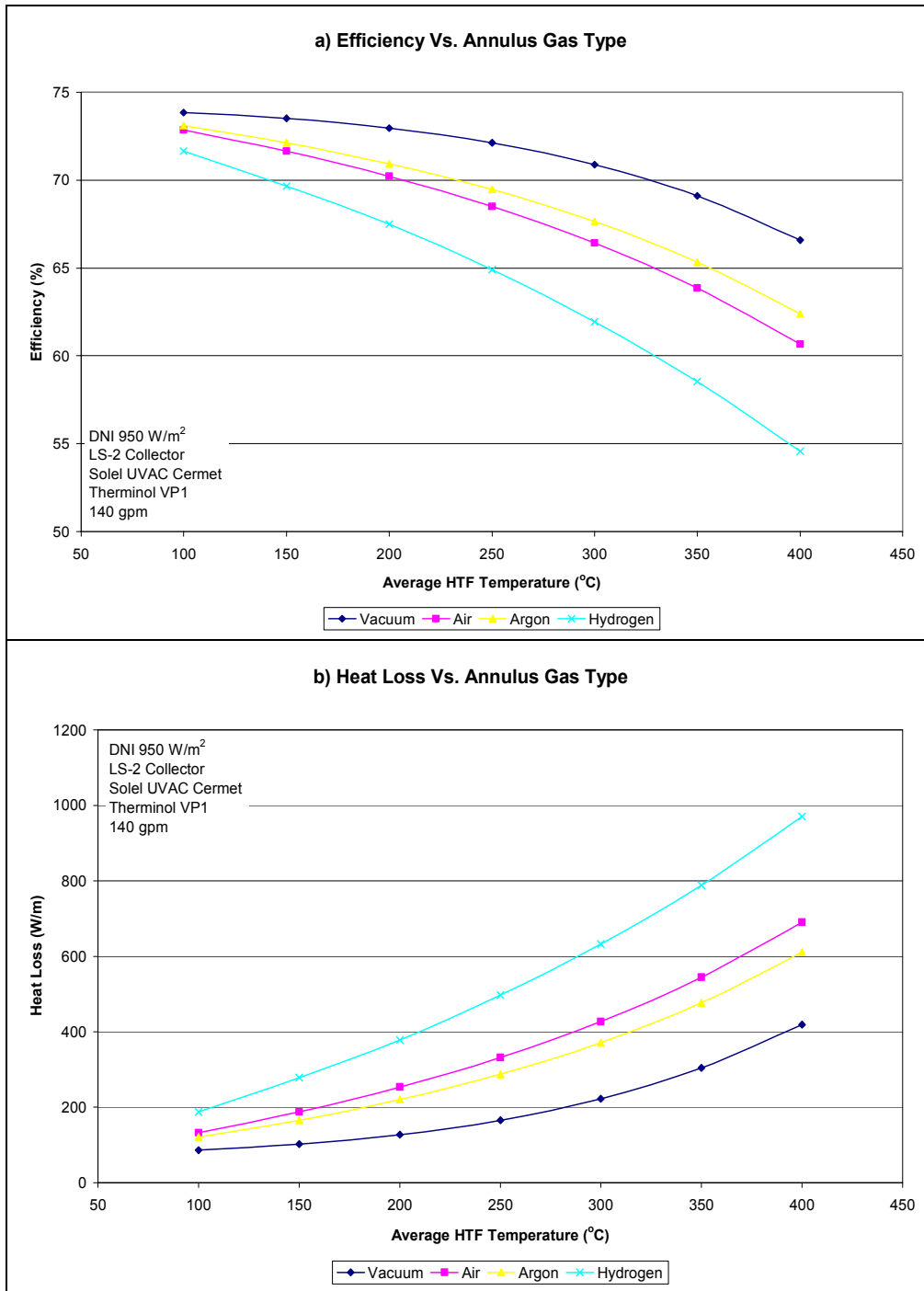
**Figure 6.4  a) Efficiency and b) heat loss charts comparing different annulus gas types**

## 6.4    HCE Condition and Wind Speed

The charts in Figure 6.5 compare three HCE conditions – vacuum, loss vacuum, and broken glass envelope – all at different wind speeds. All three conditions have been experienced in SEGS plants. With a vacuum in the annulus, the heat losses from the HCE are affected little by wind. Wind has more influence when the vacuum is lost. The model shows that the decrease can be as large as 12% over the

vacuum case (@ 400°C HTF temperature and 20 mph wind). If the glass envelope is broken, the HCE performance can drop by as much as 105% over the vacuum case (@ 400°C and 20 mph wind). However, this decrease is probably smaller than modeled, since the wind will most likely be obstructed and the wind direction will be something other than normal to the HCE (see Section 5.1).
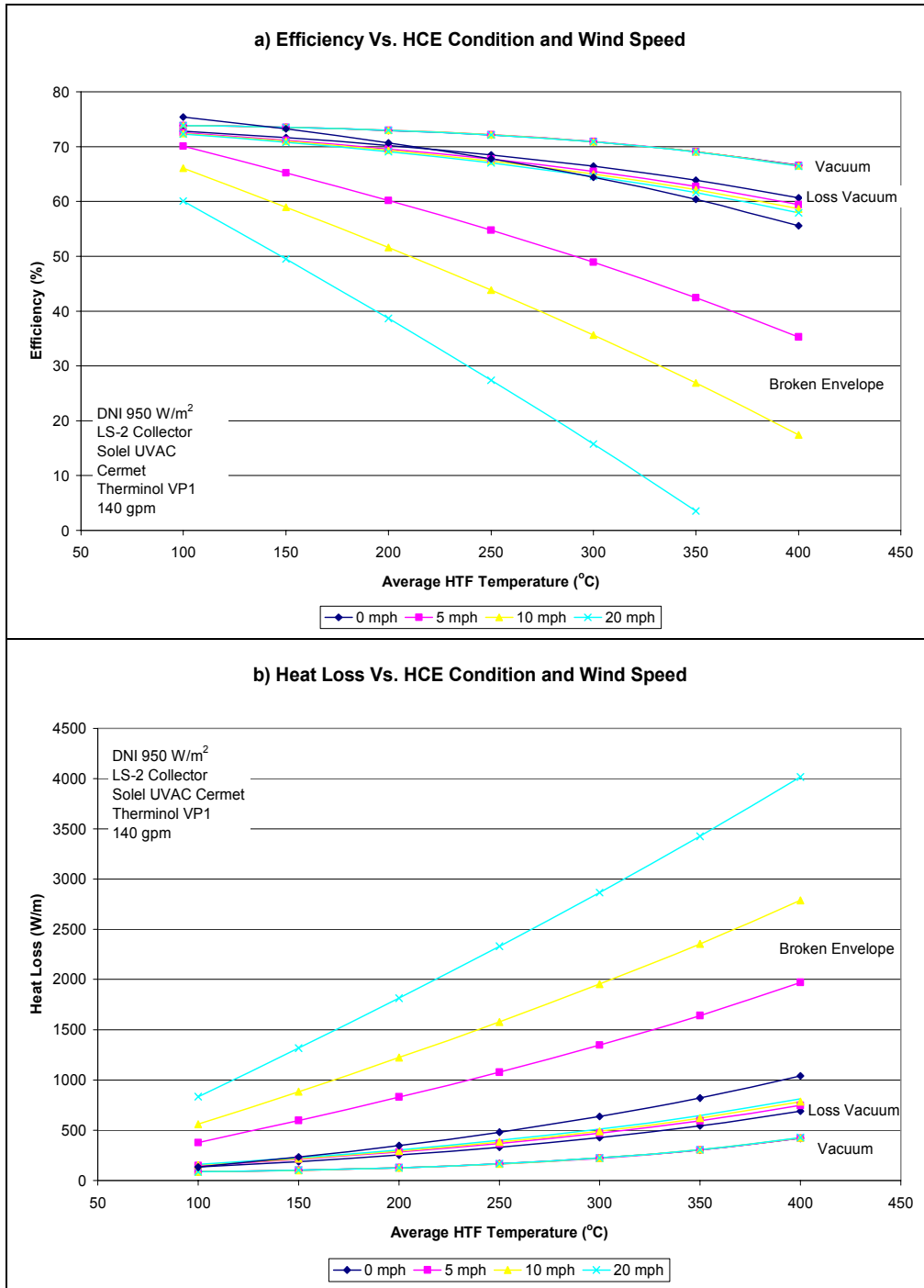


**Figure 6.5  a) Efficiency and b) heat loss charts comparing different HCE conditions as functions of wind speed**

69

## 6.5 Annulus Pressure

Figures 6.6–6.8 show the changes in HCE performance as a function of the pressure in the annulus space between the absorber and glass envelope. Both air and hydrogen as the annulus gases are shown in the charts. The question being explored with this study is: "At what pressure deviation from the 0.0001 torr (manufactured pressure) does heat losses become a problem?" As the charts show, annulus pressures between 0.0001 torr and 0.1 torr have slight influence on the HCE performance. Pressures above 0.1 torr, however, can significantly affect the HCE performance, especially if hydrogen has permeated into the annulus space. In fact, partial vacuums from 1 torr to 760 torr decrease performance from 1% to 8.5% for air (@ 400°C), and about triple those values for hydrogen.

**Heat Loss Vs. Annulus Pressure**

DNI 950 W/m$^2$
LS-2 Collector
Solel UVAC Cermet
Therminol VP1
140 gpm
350 °C

(Chart: Heat Loss (W/m) vs. Annulus Pressure (torr), with Air and Hydrogen curves)
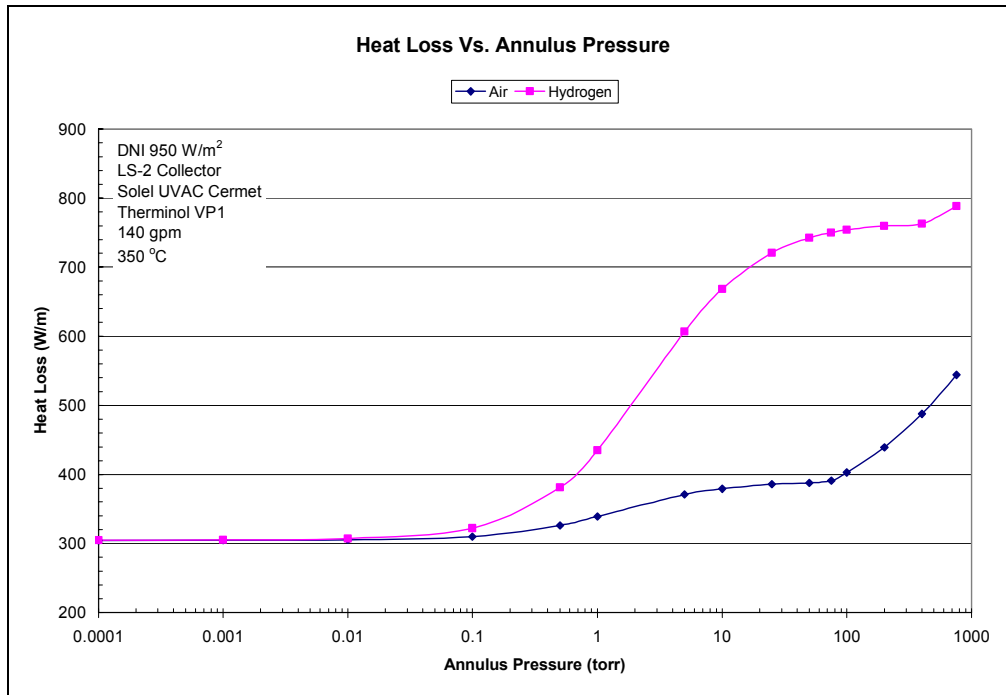
**Figure 6.6 Heat loss chart as a function of annulus pressure for air and hydrogen as the annulus gas**

From the evidence in the charts, if some HCEs installed in the SEGS plants are at partial vacuum, the energy losses could become significant. Since there is no vacuum measurement on the HCEs, numerous questions go unanswered:

- What are the actual pressures in the HCEs, both when they arrive from the manufacturer and after they've been installed over a period of time?
- How much annulus pressure variance is there from HCE to HCE?
- At what annulus pressure does the barium indicator trigger a lost vacuum?
- What is the annulus pressure when the hydrogen concentration is in equilibrium with the getter bridge?

Developing a means to measure the annulus pressures could help answer these questions. One such possible means may be to measure the outer glass envelope surface with an infrared camera and compare the results with the model predictions. Development of other means may be warranted.

70
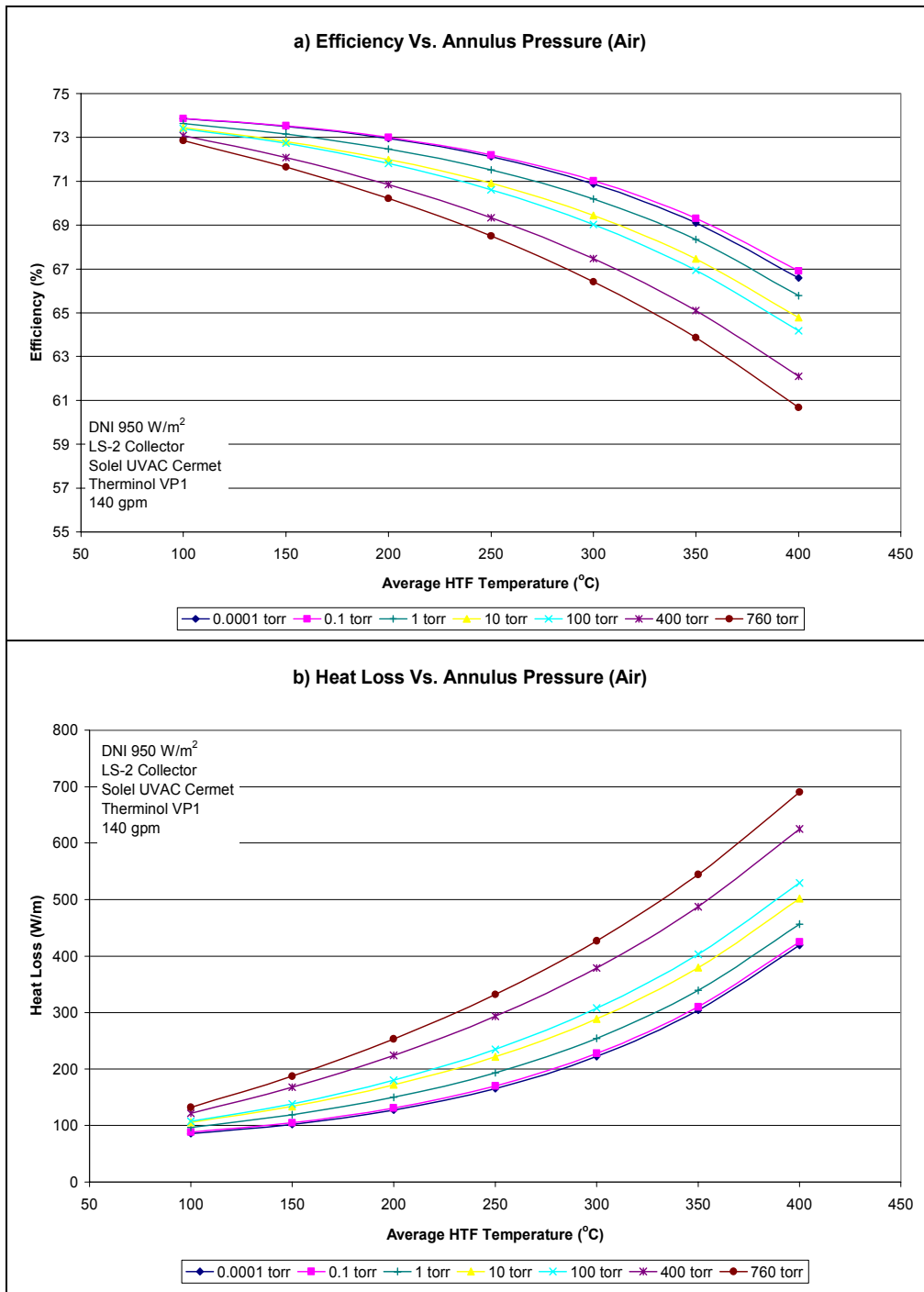
**Figure 6.7  a) Efficiency and b) heat loss charts for different annulus pressures and air as the annulus gas**
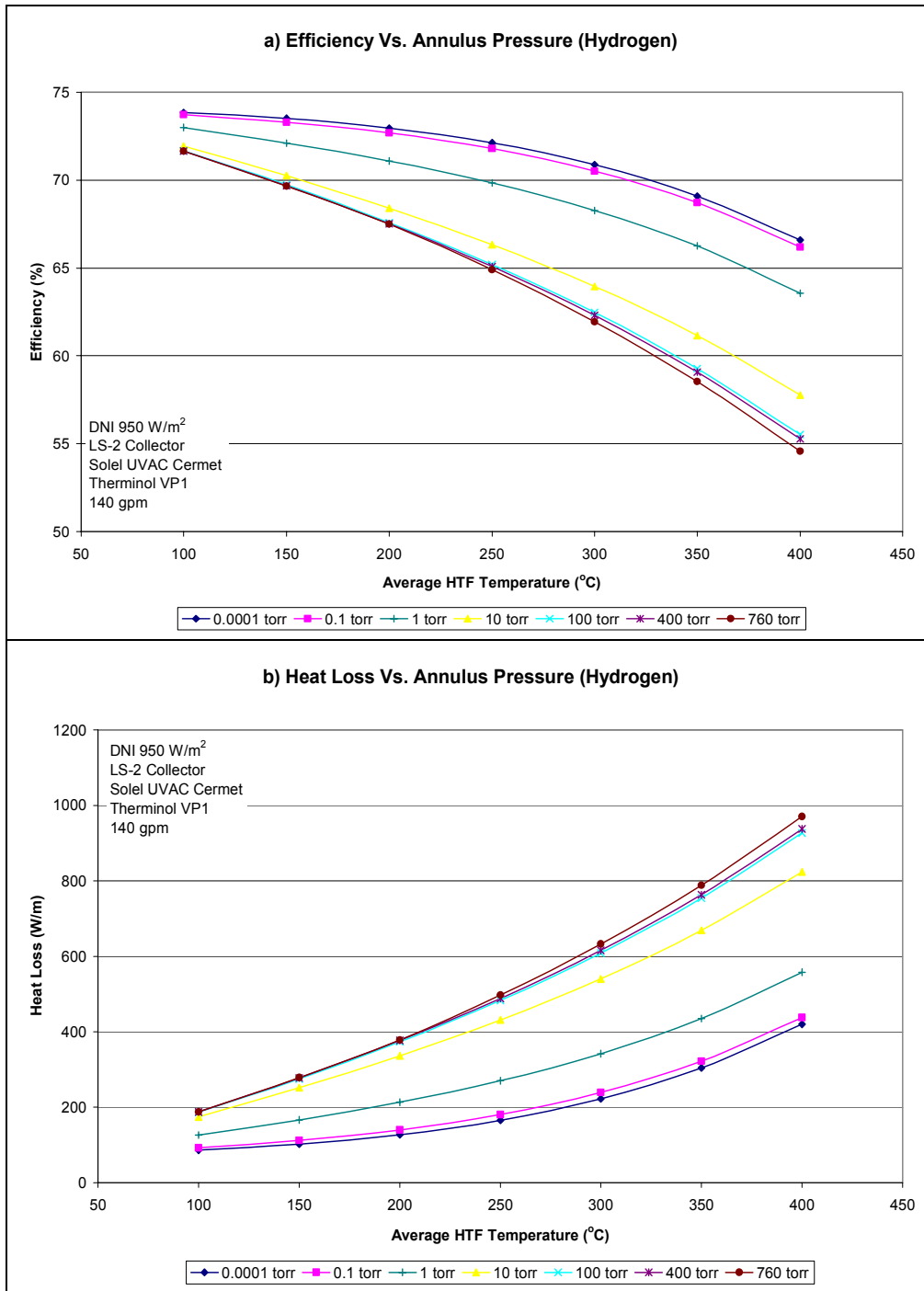
**Figure 6.8 a) Efficiency and b) heat loss charts for different annulus pressures and hydrogen as the annulus gas**

Being able to answer annulus pressure questions could lead to important HCE performance improvements. For instance, manufacturing quality control may need to be improved to tighten the annulus pressure variance from HCE to HCE. Also, perhaps the barium indicator does not turn white until the annulus pressure is close to atmospheric. If this is the case, a more precise vacuum indicator may be needed. Furthermore, actual HCE annulus pressure measurements could warrant a closer review of the

previous getter bridge studies, and thus an improvement on mitigating the hydrogen permeation into the annulus.

## 6.6  Mirror Reflectance

Mirror reflectance has a strong influence on collector efficiency (see Figures 6.9 and 6.10). For instance, at an HTF temperature of $400^{\circ}$C, a decrease of 0.15 in reflectance results in efficiency decrease of 24.5%. This indicates that any error in mirror reflectance could easily explain the differences between the model predictions and field data (see Section 5). For example, a 5% error in reflectance could explain a 7% decrease in efficiency (@ $400^{\circ}$C). This study also hints at the importance of keeping the trough mirrors and the glass envelopes on the HCEs clean.

Reflectance is currently measured with an instrument that measures a very small point on the mirror with each reading; therefore, the technician taking the measurements is trusted to take a large enough sampling to represent the true average reflectance of a collector, or an entire SEGS plant. Does this current reflectance measuring technique give a dependable value of average mirror reflectance? Or, Should a new instrument be developed that takes a reading over a larger surface area to better estimate the overall mirror reflectance and reduce error associated with the measurement statistical dependency?

Figure 6.9 shows that the HCE heat loss has only a slight dependence on mirror reflectance, whereas the heat gain and optical losses have a strong dependence. This is because the average HTF temperature and other parameters that influence the HCE heat loss directly were held constant during this study. This would not be completely true in an actual plant, where the HTF temperature would eventually drop with decreasing solar input. However, in actual operations small changes in the solar input would be compensated by changing the HTF flow rate, and thus maintaining the HTF temperature (and thus heat loss).

Both the one- and two-dimensional model results were plotted in Figure 6.10 to further illustrate the differences between the two models. The two-dimensional model captures some of the nonlinearity in the temperature profiles along the longitudinal direction of the HCE, and includes the energy losses associated with the HTF pressure drop and thermal expansion of the HTF. As the total receiver length increases, the difference between the one- and two-dimensional models would become more prominent.
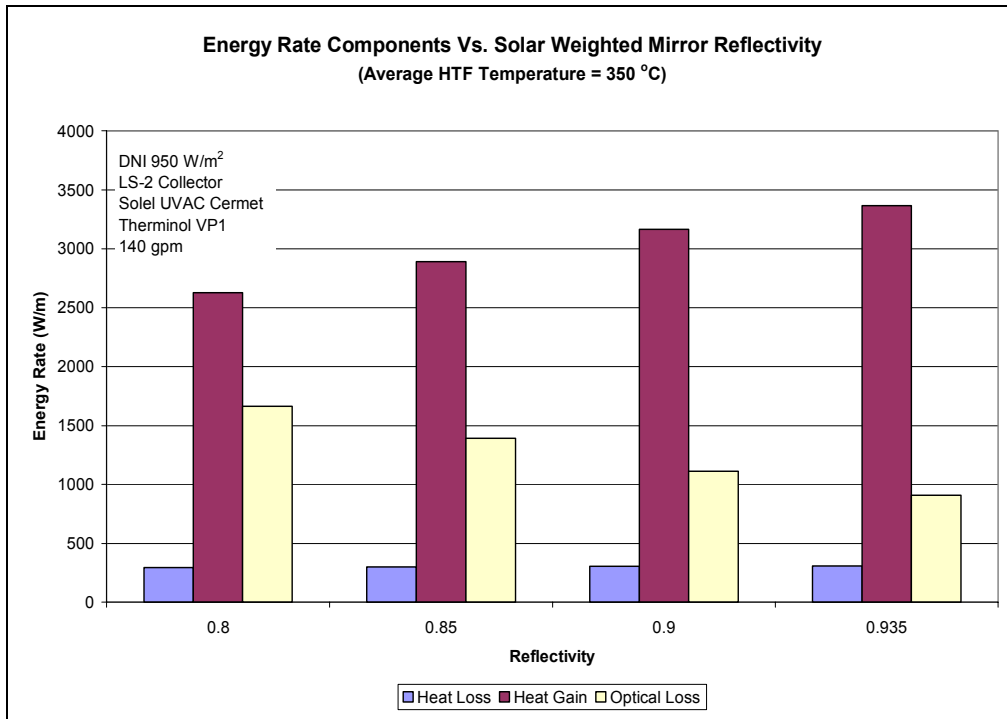
**Figure 6.9  Energy rate component chart for different solar weighted reflectivities**
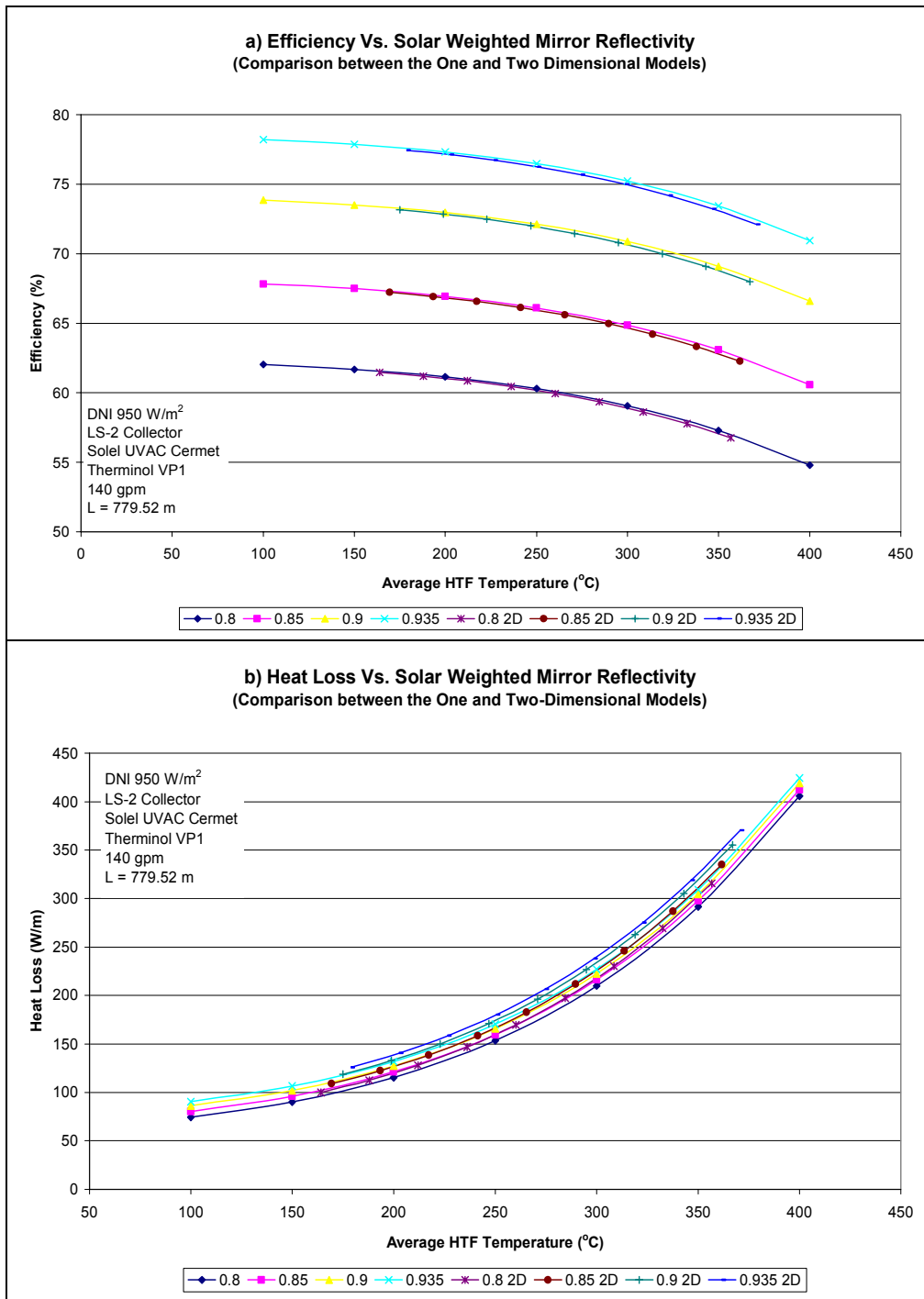
**Figure 6.10 a) Efficiency and b) heat loss charts comparing different solar weighted reflectivities. Both the one- and two-dimensional model results are included for comparison.**

## 6.7    Solar Incident Angle

The charts in Figures 6.11 and 6.12 show the sensitivity of HCE performance to solar incident angle. The HCE heat loss is affected only slightly in this study, since the average HTF temperature and other parameters directly affecting the heat loss are held constant. However, the solar incident angle has a large impact on the optical loss and heat gain. Specifically, with an incident angle of $30^o$ the performance is reduced by approximately 15% and at $60^o$ by approximately 65%.

**Energy Components Vs. Solar Incident Angle**
(Average HTF Temperature = 350 $^o$C)

DNI 950 W/m$^2$
LS-2 Collector
Solel UVAC Cermet
Therminol VP1
140 gpm

Energy Rate (W/m)

Heat Loss   Heat Gain   Optical Loss
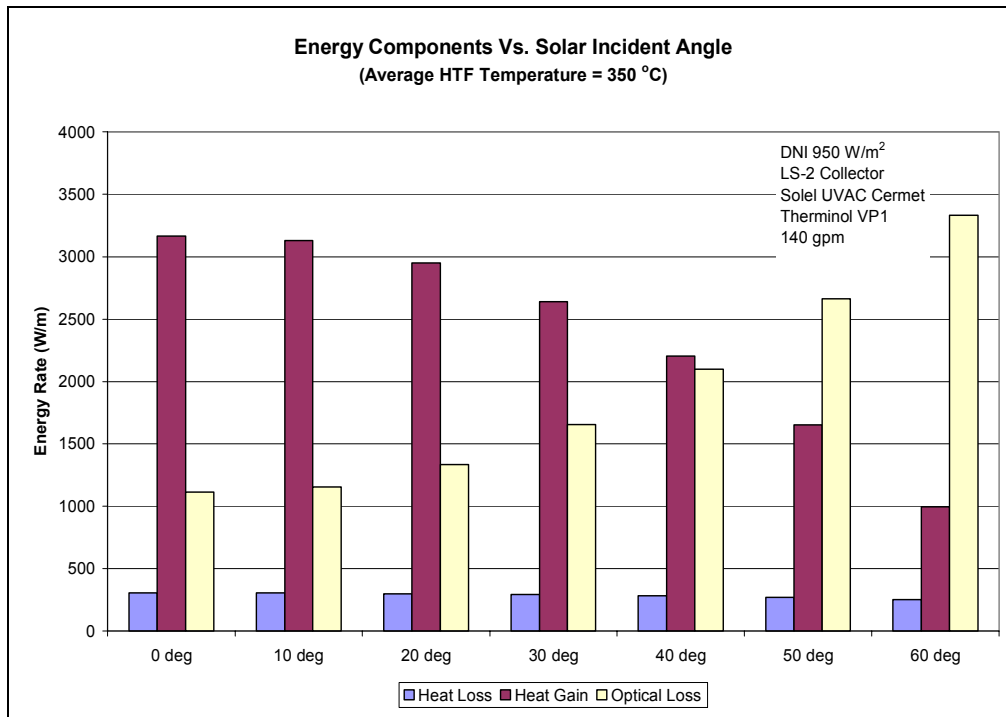
**Figure 6.11  Energy rate component chart as a function of different solar incident angles**

For a single-axis tracking system, like the SEGS plants in California, the solar incident angle depends on location and time of year. Figure 6.13 shows where the actual solar incident angles for a day in spring, summer, and winter. The largest incident angles occur during the winter months; the smallest angles occur during the summer.

Although previous studies have shown that equipment costs associated with tilting the collectors offset the money gained in additional energy, new studies may be worth evaluating now that the actual incident angle losses are better understood. Furthermore, other options to reduce the solar incident angle effects such as roughening the outer surface of the absorber [Duffie and Beckman 1991] or developing coatings that are less sensitive to incident angle may be beneficial.
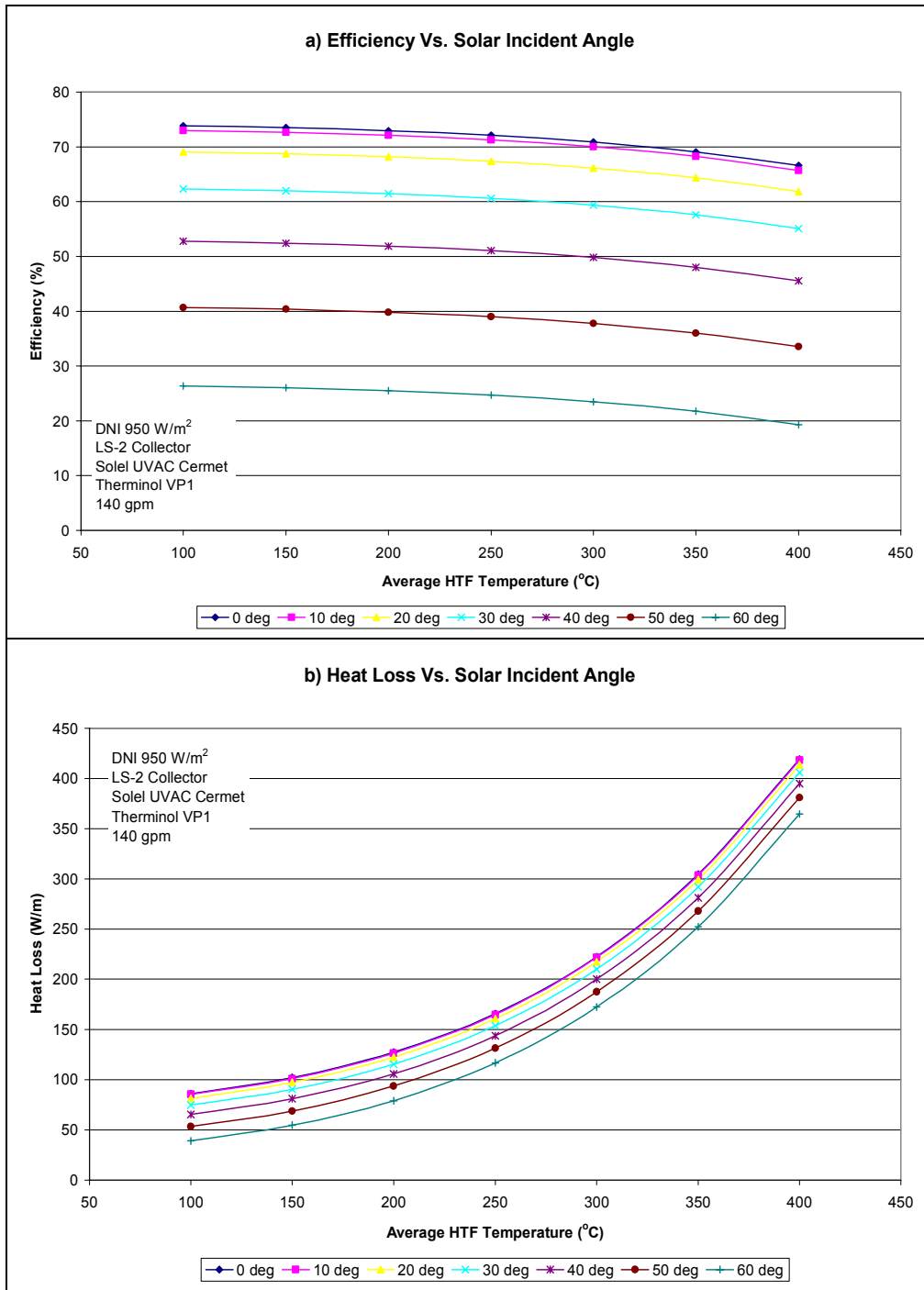
**Figure 6.12  a) Efficiency and b) heat loss charts comparing different solar incident angles**
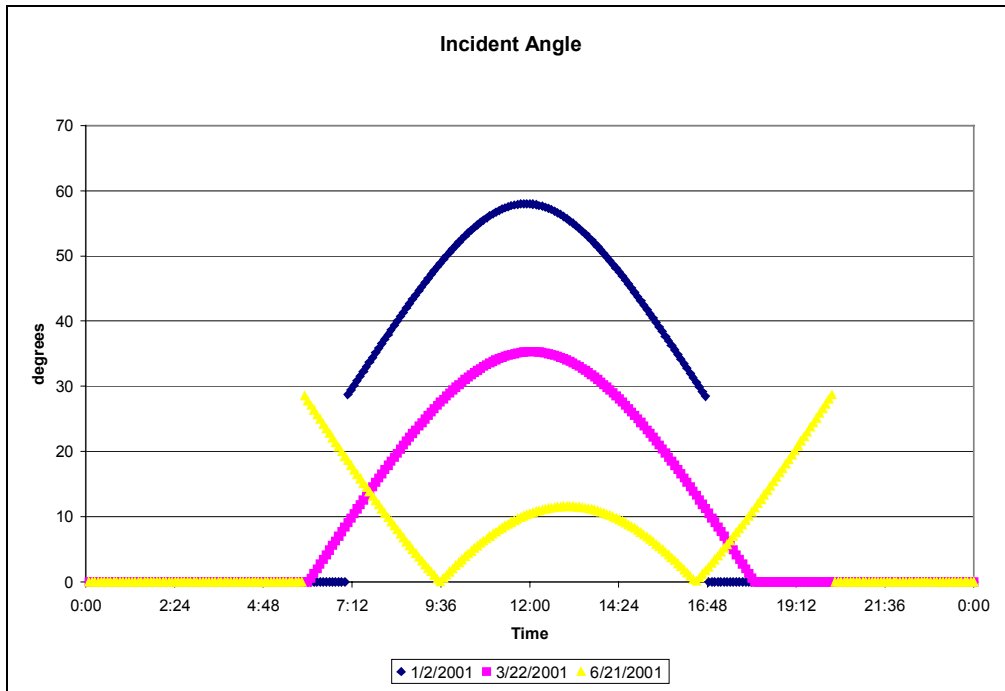
**Figure 6.13  Chart showing solar incident angles for three different times of year from actual data for a north-south oriented SEGS plant in Kramer Junction, California**

## 6.8    Solar Insolation

Figures 6.14 and 6.15 show the influence solar insolation has on HCE performance. Once again, the parameters with the strongest influence on HCE heat loss are held constant, so only the optical losses and heat gain increase significantly with increasing solar insolation. As shown, the HCE performance improves with increasing solar insolation. Therefore, besides clouds, sites with high pollutants and other particulates in the air – such as dust and sand – would have a negative impact on HCE performance. This study hints at the importance of choosing a SEGS plant site away from industrial areas with a lot of pollution, areas with high automotive traffic, or areas prone to frequent dust storms.
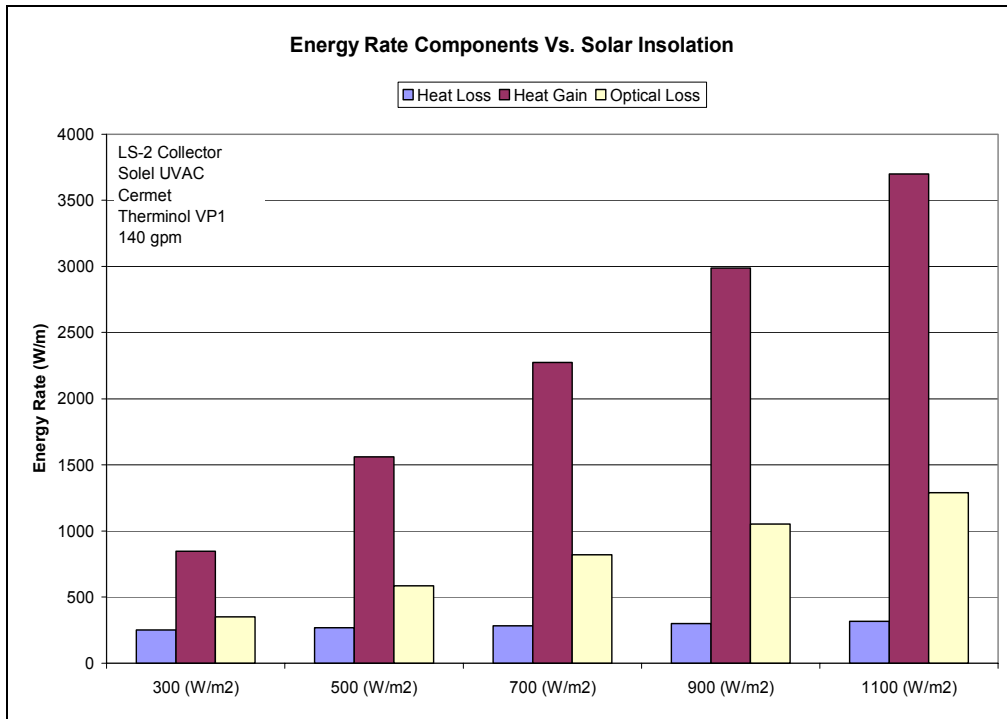
**Figure 6.14  Energy rate component chart for different solar insolation values**
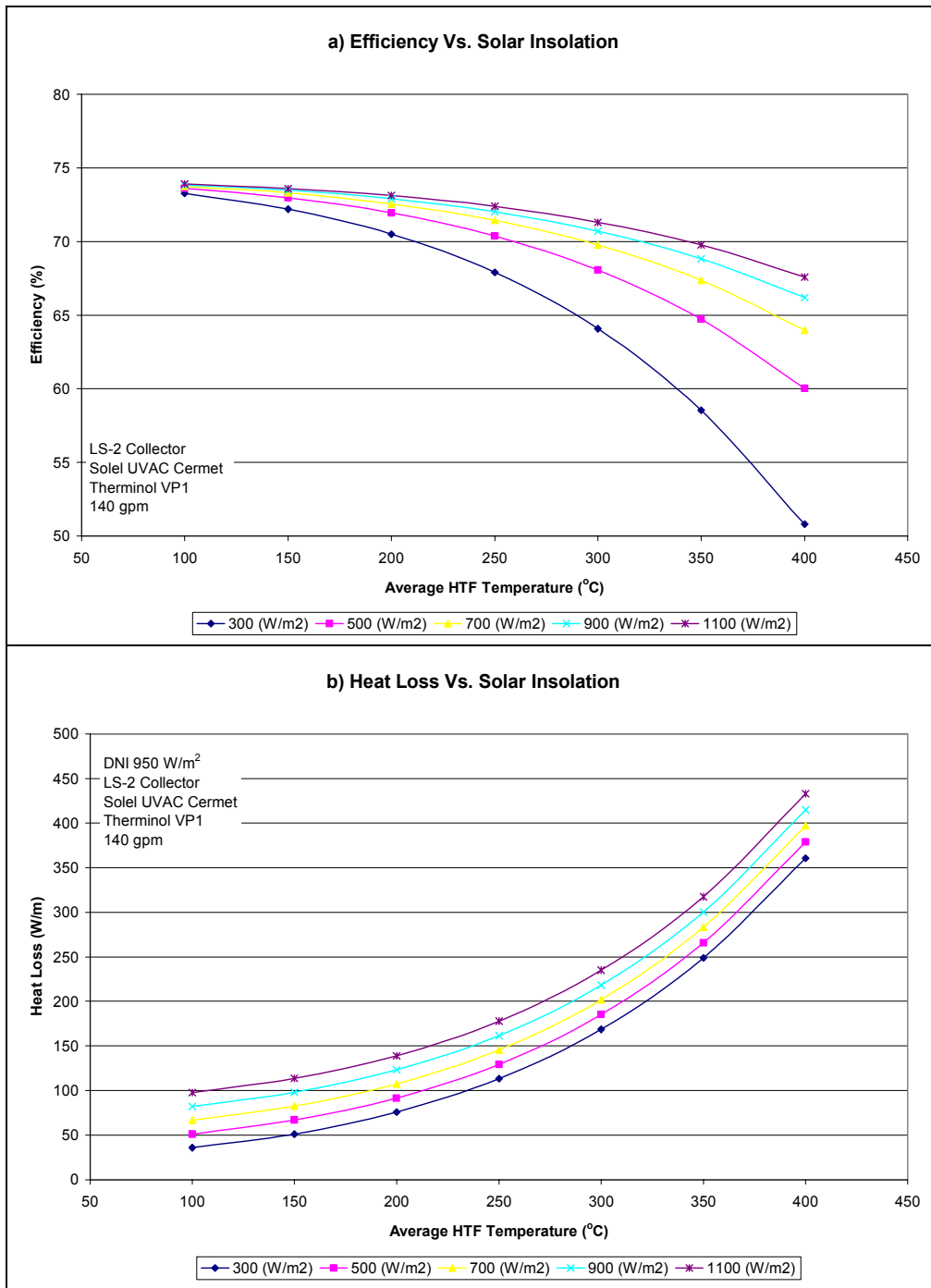
**Figure 6.15  a) Efficiency and b) heat loss charts for different solar insolation values**

## 6.9    HTF Flow Rate

Figure 6.16 shows that the HTF flow rate has little effect on HCE performance for the range of flow rates evaluated (100 gpm to 160 gpm). The figure includes the one- and two-dimensional model results. As expected, the two-dimensional model shows that the HCE performance depends more on the flow rate than the one-dimensional model. This is because the pressure loss and thermal expansion effects on the

HTF are included in the two-dimensional model. A more detailed study of the flow rate effects should include the power cycle side of the plant and losses through pumps and other equipment and piping. An exergy analysis would be more beneficial than an energy analysis for this type of study, since it would identify components that have the greatest influence on the HCE performance (and thus the most room for improvement).
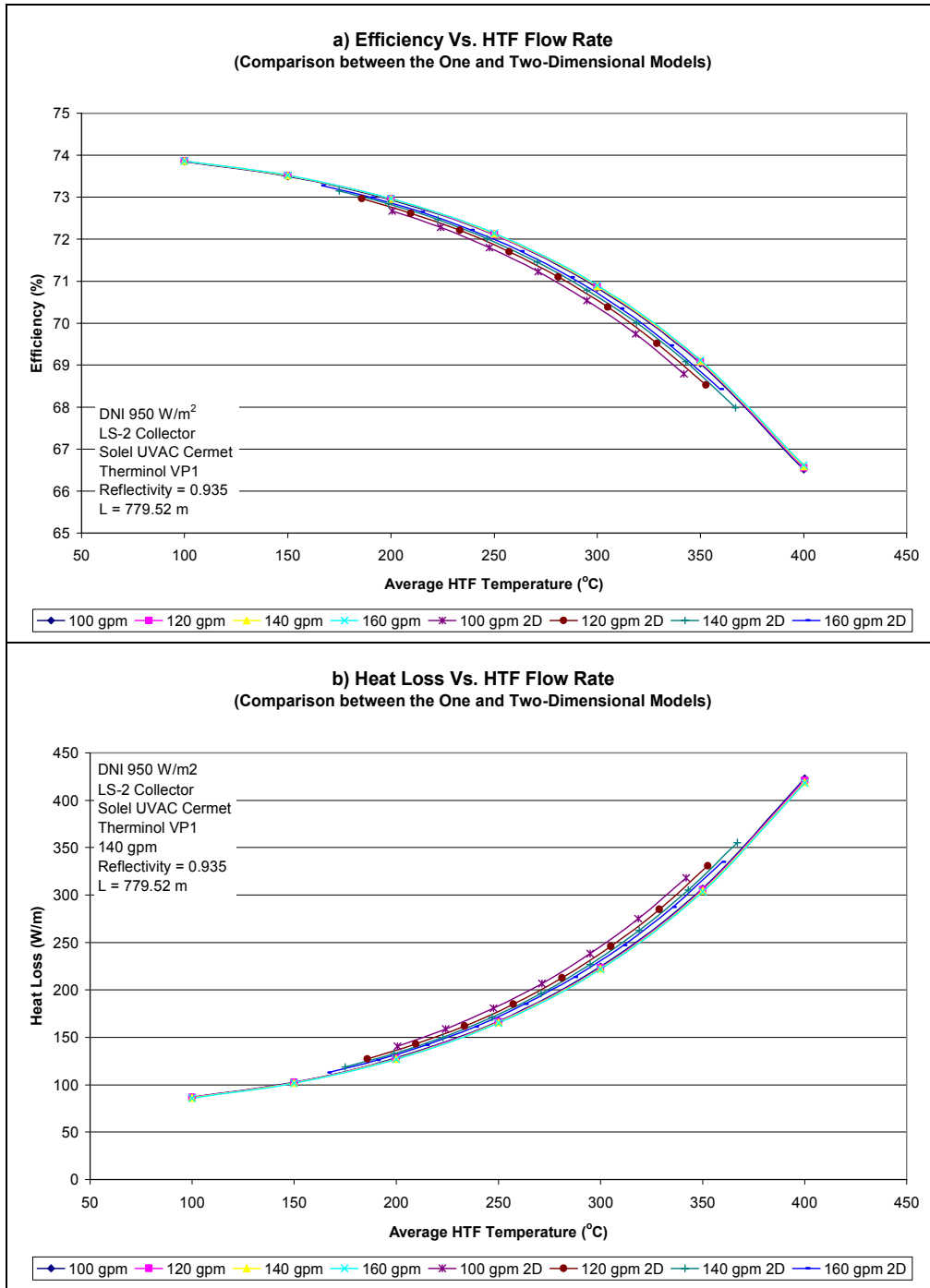


**Figure 6.16  a) Efficiency and b) heat loss charts comparing different flow rates and including both the one- and two-dimensional models**

## 6.10   HTF Type

The charts in Figure 6.17 reveal that the HTF type has little effect on HCE performance. However, each fluid type has a range of recommended operating temperatures, and efficiency drops with increasing HTF temperature. Thus, fluids that can operate at lower temperatures would improve HCE performance. Each HTF type has other advantages. For instance, HTF types like salts can be used as thermal storage media, but also could require additional heating during off-sun hours to prevent solidification in piping and equipment. Also, cost and availability could dictate which HTF to use. Since power cycle efficiencies increase as the working fluid temperature increases, a complete study would need to include both the solar and power cycle sides.
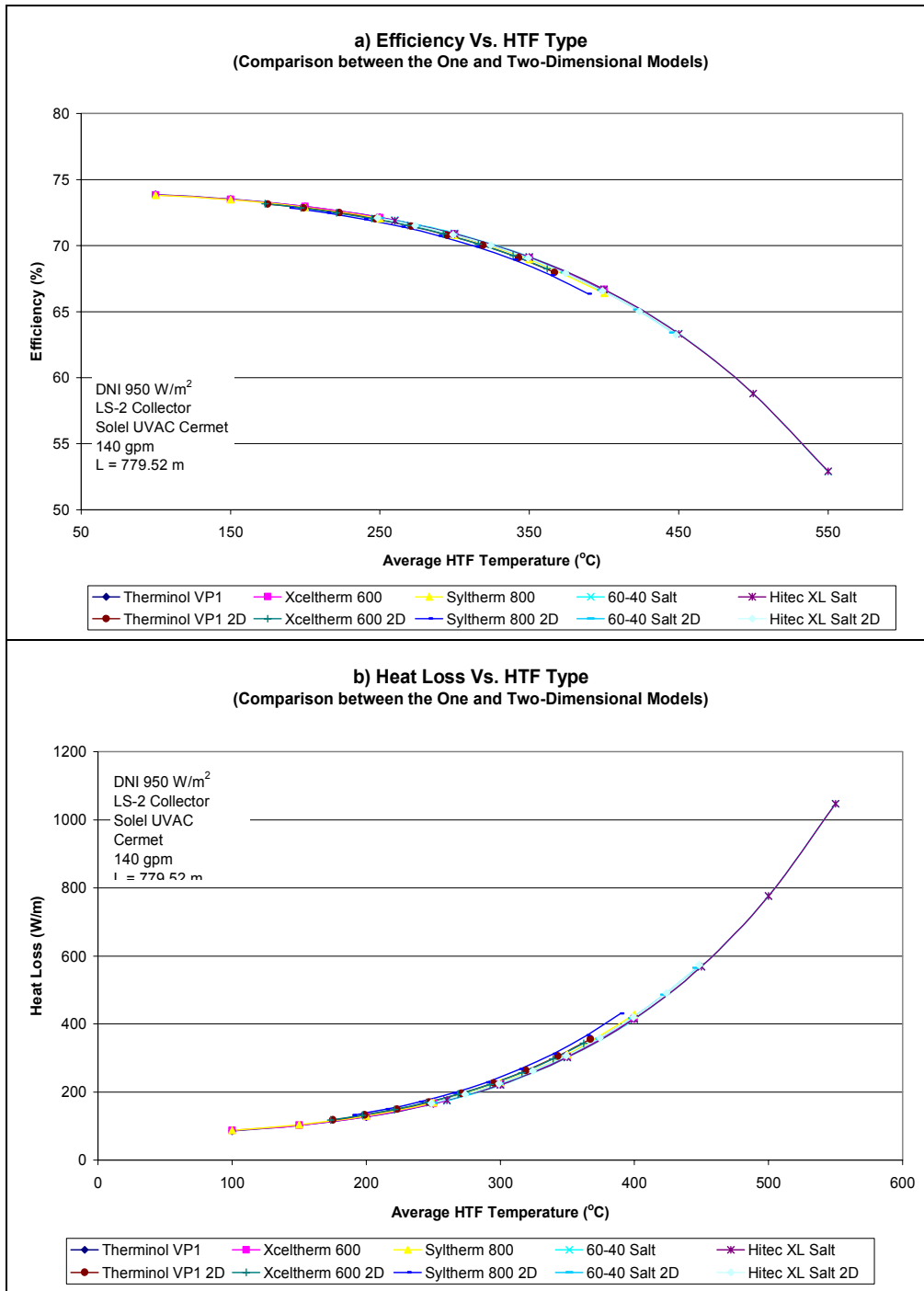
**Figure 6.17  a) Efficiency and b) heat loss charts comparing different HTF types and including both the one- and two-dimensional models**

## 6.11   Glass Envelope Outer Diameter

The charts in Figure 6.18 show that:

- The glass envelope diameter has an optimal size to minimize heat losses from the HCE.
- This effect is most sensitive when the annulus is not under vacuum.
- The optimization reflects the fact that as the diameter is increased, the annulus gap between the absorber and glass envelope increases, which decreases the heat transfer between the absorber and glass envelope, but increases the surface area for heat transfer to the environment.
- Decreasing the glass envelope diameter increases the heat transfer across the annulus gap, but decreases the surface area for heat transfer to the environment.

Another problem with a too-small annulus gap is that it could cause tolerance problems with the absorber pipe, since the absorber pipe will tend to bow slightly when heated. A more detailed glass envelope optimization study would need to include the thermal deflections of the absorber.
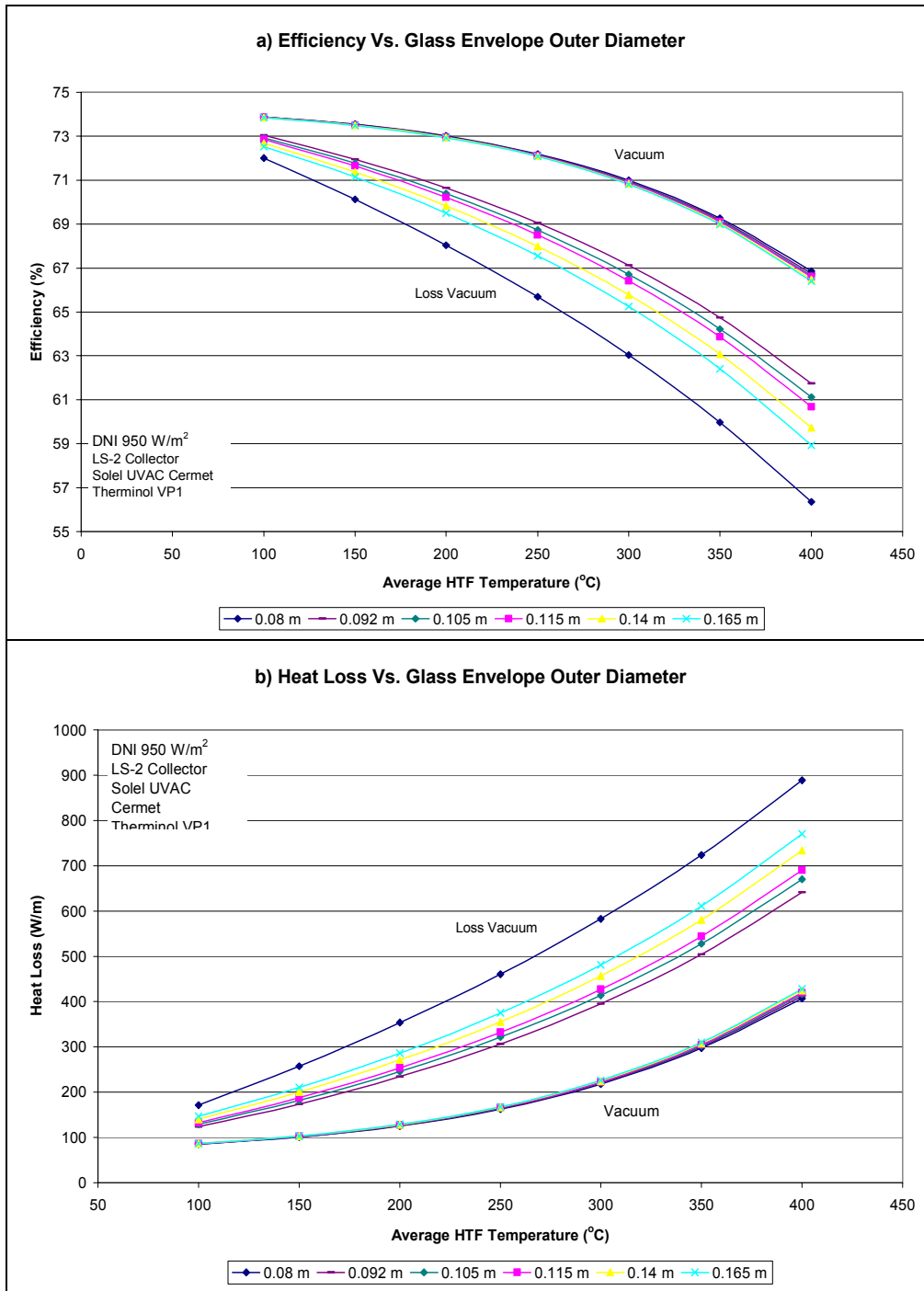
**Figure 6.18  a) Efficiency and b) heat loss charts comparing different glass envelope diameters**

## 6.12   Parameter Variation along Receiver Length

The chart in Figure 6.19 shows the temperature variations along the length of the solar receiver (total length of 779.5 m) for each temperature in the cross-section of an HCE (also see Figure 2.1), as modeled with the two-dimensional HCE performance model. As expected, the temperatures along the length of the receiver increase in a slightly nonlinear fashion because:

- The radiation heat transfer functions are nonlinear.
- Heat gain per receiver length decreases as the HTF temperature increases.
- The heat loss per receiver length increases as the HCE cross-sectional temperatures increase.

Also, the temperature differences between the HTF and absorber ($T_1$ and $T_2$), between the inner and outer absorber pipe surfaces ($T_2$ and $T_3$), and between the inner and outer glass-envelope surfaces ($T_4$ and $T_5$) all remain constant, since the heat transfer coefficients are constants (see Sections 2.1.1, 2.1.2, and 2.1.4). However, the temperature difference between the absorber and glass-envelope ($T_3$ and $T_4$) changes in a slightly nonlinear fashion because:

- The selective coating emissivity is a function of temperature (see Section 2.1.6.1).
- The radial heat transfer is nonlinear.
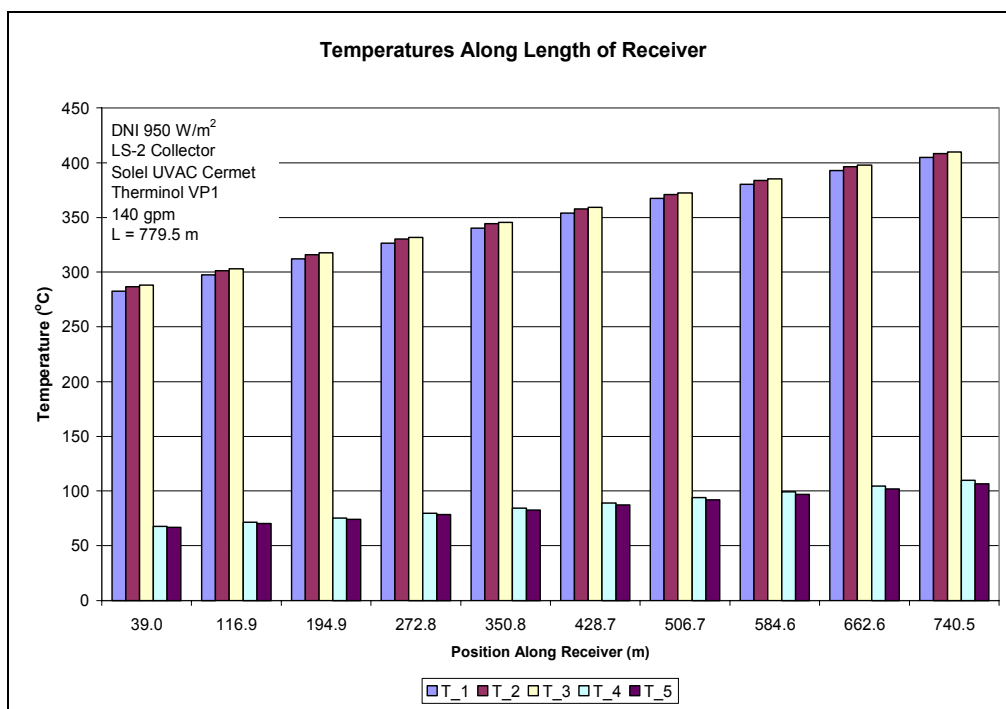


**Figure 6.19  HCE cross-section temperature chart at position along receiver length**

The heat loss, heat gain, and optical loss along the length of the receiver are shown in Figure 6.20. Both the heat loss and heat gain reflect the trends shown with the temperature variations in Figure 6.19. The optical loss, however, is constant; since all the optical properties in the effective optical efficiency terms are assumed to be independent of temperature (see Section 2.1.6.1).

**Energy Rate Components Along Receiver Length**
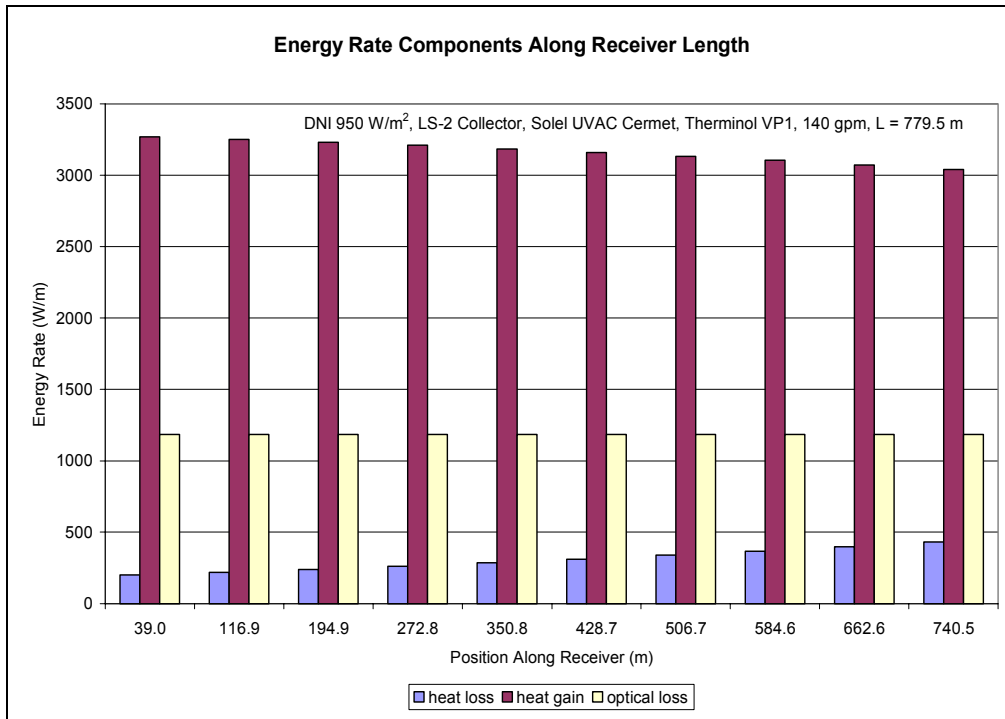


**Figure 6.20  Energy rate components chart as a function of position along receiver (total receiver length = 779.5 m)**

## 6.13   Recommendations

Table 6.2 lists recommendations based on the HCE design and parameter study. Many of the recommendations have already been mentioned throughout this report; however, where justified, further explanation is given.

Understanding the manufacturing tolerances and degradation rates of the optical properties and HCE annulus vacuum levels is important (see Sections 6.2, 6.3, and 6.5). The selective coating optical properties may vary over the length of the HCE and from HCE to HCE. The testing done shows this to be the case. Since the optical properties have a strong influence on HCE performance, further testing of the selective coating variation and testing to determine the optical property degradation is recommended. This testing should include determining variations throughout a SEGS plant, especially one that has been operating for many years.

Some HCEs in a SEGS plant are likely to have annulus pressures higher than the specified 0.0001 torr, because of manufacturing inconsistencies or hydrogen permeation (see Sections 6.3 and 6.5). If this is so, developing a means to measure the HCE annulus pressure on installed HCEs is important. One possible technique could be to measure the temperature of the outer glass envelope surface using an infrared camera and evaluating the data with the HCE performance model; however, this technique needs further evaluation.

The model tends to overpredict wind-induced heat losses (see Section 6.4). Reducing forced convection effects by one-half in the model may lead to better results, especially for the missing glass envelope case. However, more comparisons with field test data need to be done.

Solar incident angle has a strong influence on HCE performance (see Section 6.7). Tilting the troughs slightly (~ 5°) along the rotating axis, or possibly changing the absorber surface texture [Duffie 2000] or changing the selective coating properties to be less sensitive to solar incident angle could be cost effective. Conducting more incident angle tests on additional HCE types could also be beneficial. The HCE performance model could be used to give more insight to these investigations.

Section 6.10 discusses how the HTF type has little effect on the HCE performance for any one temperature; however, the trends indicate that the HCE performance decreases with increasing HTF temperature. This indicates that methods for decreasing the HTF temperature could be beneficial, especially if it could be done in such a way as not to decrease the power cycle efficiency. A possible solution might be to run the power cycle side with a fluid with a lower vapor pressure, such as ammonia or a hydrocarbon.

Finally, heat transfer enhancing mechanisms such as coiled spring inserts, twisted tape inserts, helical ribs, or roughening the inner absorber surface, may be worth evaluating. All these mechanisms would increase the convection surface area and enhance turbulent flow [Incropera and DeWitt 1990]. The current HCE performance model cannot be used to evaluate heat transfer enhancing devices without significant changes. However, an alternative to developing a more complex model may be to conduct field testing. For instance, measuring the radial temperature profile of the HTF and the temperature difference between the absorber inner surface and bulk HTF temperature, which would help determine what improvements, if any, a heat transfer enhancement device could make. If there is room for improvement, additional field testing of flow enhancement devices may continue to be less expensive than developing a more complex heat transfer analysis model. Of course any advantage to increasing the heat gain by an enhancement device would have to be balanced with the increase in pumping losses.

**Table 6.2  Recommendations from HCE Design and Parameter Study**

| Design Option or Parameter | Recommendations |
|---|---|
| Absorber Pipe Base Material (Section 6.1) | • Re-evaluate 316-L.<br>• Add carbon steel to study. |
| Selective Coating (Section 6.2) | • Re-evaluate optical properties at elevated temperatures.<br>• Update optical properties.<br>• Determine optical property variation.<br>• Evaluate optical property degradation.<br>• Determine the manufacturing variances. |
| Annulus Gas Type (Section 6.3) | • Add additional inert gasses to study (xenon, neon, etc.)<br>• Determine effect of inert gases to hydrogen permeation.<br>• Develop a better device for determining loss of vacuum (or partial vacuum).<br>• Determine hydrogen concentration level when in equilibrium with getter bridge and HTF permeation. |
| HCE Condition and Wind Speed (Section 6.4) | • Reduce wind effects by approximately one-half.<br>• Re-evaluate wind effects with different annulus pressures.<br>• Re-evaluate wind effects with hydrogen as the annulus gas. |
| Annulus Pressure (Section 6.5) | • Determine annulus pressure variations throughout a SEGS plant (thermal imaging techniques).<br>• Determine annulus pressure with hydrogen permeation.<br>• Determine what the manufacturing variances are. |
| Mirror Reflectance (Section 6.6) | • Develop improved reflectance measuring techniques.<br>• Measure true optical errors. |
| Solar Incident Angle (Section 6.7) | • Run a study simulating trough tilt angles on actual field test data.<br>• Evaluate changes to absorber outer surface on reducing incident angle effects (roughening surface, threads, different selective coating characteristics, etc.). |
| HTF Type (Section 6.10) | • Develop means to conduct HTF property testing in field.<br>• Evaluate combine cycle operation to reduce HTF temperature (HTF to ammonia or hydrocarbon as the power cycle fluid).<br>• Evaluate alternative working fluid to reduce HTF temperature (ammonia or hydrocarbon). |
| Glass Envelope Diameter (Section 6.11) | • Re-evaluate sizing now that HCE performance has been improved. |
| Temperature and Heat Flux Variation along Receiver Length (Section 6.12) | • Conduct an optimization study on length. |
| General | • Complete HCE testing with HTF heat transfer enhancing devices (coiled spring, twisted tape, twisted insert, roughened surface) |

## 7. Conclusion

This report described the development, validation, and use of an HCE performance software model implemented in EES. All equations, correlations, and parameters used in the model were discussed in detail. The model was implemented in EES in four different versions. Two were developed for HCE design and parameter studies, and two for evaluating field test data. Both one- and two-dimensional analyses were used in the codes. Discussions of each version of the codes included relevant EES diagram windows, parameter tables, and lookup tables. The model was then shown to be accurate by comparing with actual HCE field test data. Following this, the model versatility was demonstrated by conducting various design and parameter studies. This also demonstrated how the HCE performance model implemented in EES could be used as a development tool for improving the HCE performance. Several recommendations were drawn from the design and parameter study (see Table 6.2). Several suggestions for improving the HCE performance model were also discussed.

# APPENDIXES

# A. Lookup Table References

**Argon:**
Ahlberg, K., ed. (1985) *AGA Gas Handbook*. Stockholm, Sweden: Almqvist & Wiksell International.

**Hitec XL:**
Data from EXCEL spreadsheet provided by Mary Jane Hall of NREL and
Coastal Chemical Company. "HITEC Heat Transfer Salt." Sales Data Sheet. Pasadena, Texas.

**Nitrate Salt (60% NaNO$^3$, 40% KNO$^3$):**
Data from EXCEL spreadsheet provided by Mary Jane Hall of NREL and
Zavoico, A. B. (July 2001). *Solar Power Tower, Design Basis Document, Revision 0*. SAND2001-2100.
Work performed by Nextant, San Francisco, California, and SANDIA National Laboratories,
Albuquerque, New Mexico.

**Syltherm 800:**
"Syltherm 800, Silicon Heat Transfer Fluid." (November 2001). Form No. 176-01469-1101 AMS. The
Dow Chemical Company, http:// www.dowtherm.com.

**Therminol VP1:**
"Therminol, Heat Transfer Fluids, Computed Properties of Therminol VP-1 vs. Temperature (Liquid
Phase)." (2001). Solutia Inc., www.therminol.com.

**Therminol 59:**
"Therminol 59, Heat Transfer Fluid by Solutia." (2001). Technical Bulletin 7239271. Solutia Inc.,
www.therminol.com.

**Therminol 66:**
"Therminol 66, Heat Heat Transfer Fluid by Solutia." (2001). Technical Bulletin 7239146C. Solutia Inc.,
www.therminol.com.

**Therminol XP:**
"Therminol XP, Heat Heat Transfer Fluid by Solutia." (2001). Technical Bulletin 7239262. Solutia Inc.,
www.therminol.com.

**Dowtherm Q:**
"Dowtherm Q, Heat Transfer Fluid, Product Technical Data." (June 1997). The Dow Chemical
Company., www.dow.com/heattrans.

**Dowtherm RP:**
"Dowtherm RP, Heat Transfer Fluid, Product Technical Data." (November 1996). The Dow Chemical
Company., www.dow.com/heattrans.

**Xceltherm 600:**
"Exceltherm 600, Engineering Properties." (1998). Radco Industries, Inc., http://www.radcoind.com.

# B. Optical and Material Property References

**Luz Black Chrome (SNL test):**
Visual Basic Heat Transfer Code and based on test data from Rod Mahoney of SNL, 8/93.

**Luz Cermet (SNL test):**
Visual Basic Heat Transfer Code and based on test data from Rod Mahoney of SNL, 11/06/98.

**Solel UVAC Cermet (SNL test a), Solel UVAC Cermet (SNL test b), Solel UVAC Cermet (SNL test avg):**
Tests conducted by Rod Mahoney of SNL and presented in a Power Point presentation dated April 23, 2001, "HCE Issues; Cermet Preliminary Results Optical Properties & Construction Forum 2001."

**Solel UVAC Cermet (0.07 @ 400C), Solel UVAC Cermet (0.15 @ 400C):**
Table in
Price, H. (2002) *Concentrated Solar Power Use in Africa*. NREL/TP. Golden, Colorado: National Renewable Energy Laboratory.

**Glass Envelope (borosilicate glass):**
Estimated from Plots in
Touloukian, Y. S., D. P. DeWitt, eds. (1972). *Radiative Properties, Nonmetalic Solids.* Thermophysical Properties of Matter, Vol. 8, New York: Plenum Publishing.

**304L, 316L Stainless Steel:**
Linear best fit of data from tables in
Touloukian, Y. S., R. W. Powell; et al., eds. (1970). *Thermal Conductivity, Metallic Elements and Alloys.* Thermophysical Properties of Matter, Vol. 1, New York: Plenum Publishing.

**321H Stainless Steel:**
Linear best fit of data from tables in
Davis, J. R., ed. (2000). *Alloy Digest, Sourcebook, Stainless Steels*. Materials Park, Ohio: ASM International.
and
ASM Handbook Committee (1978). *Metals Handbook. Properties and Selection – Stainless Steels, Tool Materials, and Special Purpose Metals*, Vol. 3, Metals Park, Ohio: American Society for Metals.

**B42 Copper Pipe:**
ASM Handbook Committee (1978). *Metals Handbook. Properties and Selection – nonferrous alloys and pure metals*, Vol. 2, Metals Park, Ohio: American Society for Metals.

**Gas Molecular Diameters:**
Marshal, N., transl. (1976). *Gas Encylopedia*. New York: Elsevier.

# C. Heat Transfer Fluid Change in Enthalpy

An estimate for the change in enthalpy of a heat transfer fluid (HTF) flowing through a heat collection element (HCE) for a solar trough collector can be derived by starting with the state postulate that any two independent, intensive, thermodynamic properties are sufficient to establish the stable thermodynamic state of a pure, simple, compressible substance [Howell and Buckius 1987]. This postulate allows the differential change in enthalpy and entropy to be determined as functions of temperature and pressure,

$$dh(T,P) = \left(\frac{\partial h}{\partial T}\right)_P dT + \left(\frac{\partial h}{\partial P}\right)_T dP \qquad (C.1)$$

$$ds(T,P) = \left(\frac{\partial s}{\partial T}\right)_P dT + \left(\frac{\partial s}{\partial P}\right)_T dP \qquad (C.2)$$

Substituting equation C.2 into Gibb's equation $dh = Tds + vdP$ [Çengel and Boles 2002], gives

$$dh = T\left(\frac{\partial s}{\partial T}\right)_P dT + \left[v + T\left(\frac{\partial s}{\partial P}\right)_T\right]dP \qquad (C.3)$$

Equating the coefficients of $dT$ and $dP$ in Equations C.1 and C.3 and using the definition of specific heat at constant pressure $c_P \equiv \left(\frac{\partial h}{\partial T}\right)_P$ [Howell and Buckius 1987], gives

$$\left(\frac{\partial s}{\partial T}\right)_P = \frac{c_P}{T} \qquad (C.4a)$$

$$\left(\frac{\partial h}{\partial P}\right)_T = v + T\left(\frac{\partial s}{\partial P}\right)_T \qquad (C.4b)$$

Using the fourth Maxwell relation $\left(\frac{\partial s}{\partial P}\right)_T = -\left(\frac{\partial v}{\partial T}\right)_P$ [Çengel and Boles 2002], results in

$$\left(\frac{\partial h}{\partial P}\right)_T = v - T\left(\frac{\partial v}{\partial T}\right)_P \qquad (C.5)$$

Substituting all the above results into Equation C.1 and integrating determines the change in enthalpy

$$\Delta h(T,P) = \int c_P dT + \int \left[v - T\left(\frac{\partial v}{\partial T}\right)_P\right]dP \qquad (C.6)$$

Equation C.6 can be simplified if the specific heat and specific volumes are linear in the regions of interest and if the second term on the right is negligible compared to the first term. The specific heats for all the HTFs used in the HCE performance models are plotted in Figure C.1 and the specific volumes are

plotted in Figure C.2. The change in HTF temperature along the length of the receiver is approximately 15°C for each 80 m of length (recommended increment for a two-dimensional heat transfer model). As shown, both the specific heat and specific volume are nearly linear for all the HTF's over small temperature increments (< 25°C). Therefore, both specific heat and specific volume can be treated as constants at there average values for relatively small HTF temperature changes.
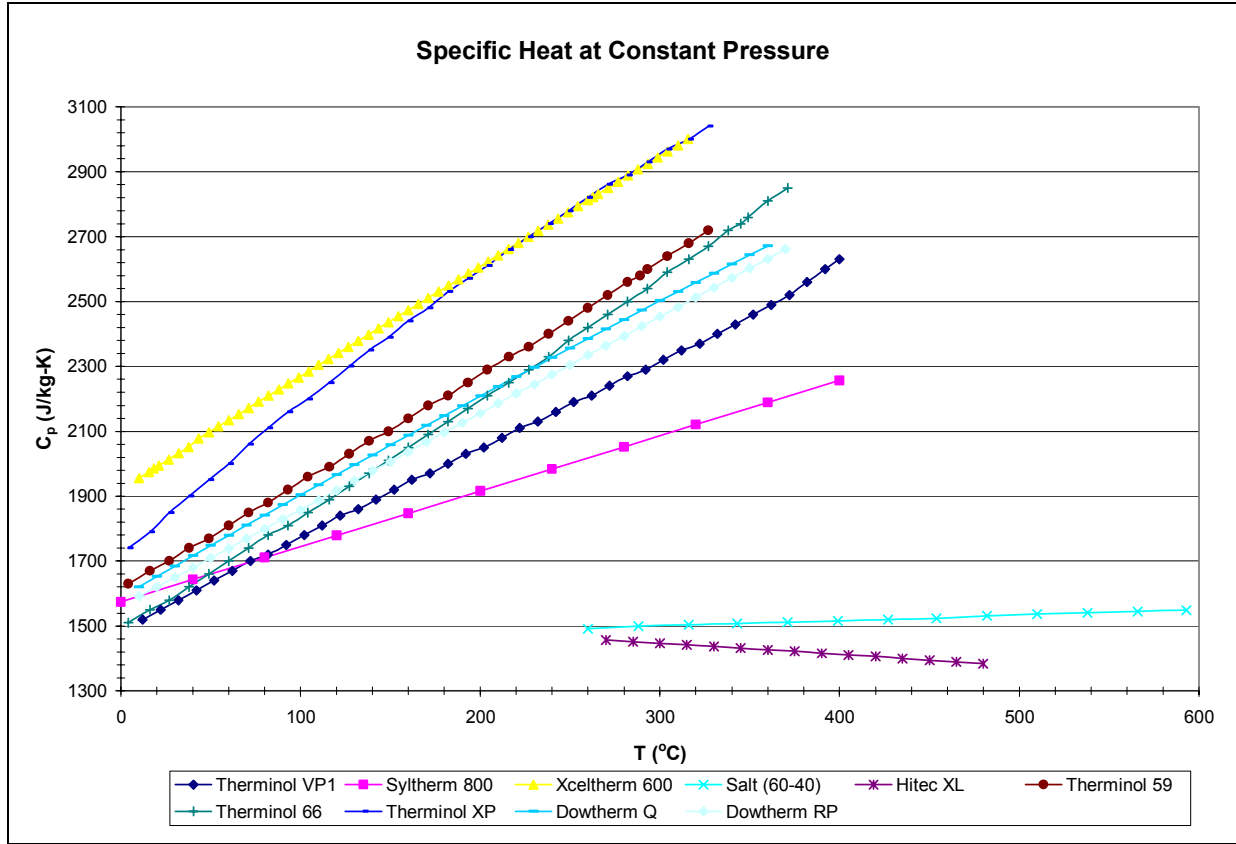


**Figure C.1  Specific heat at constant pressure for each HTF used in the HCE performance model**
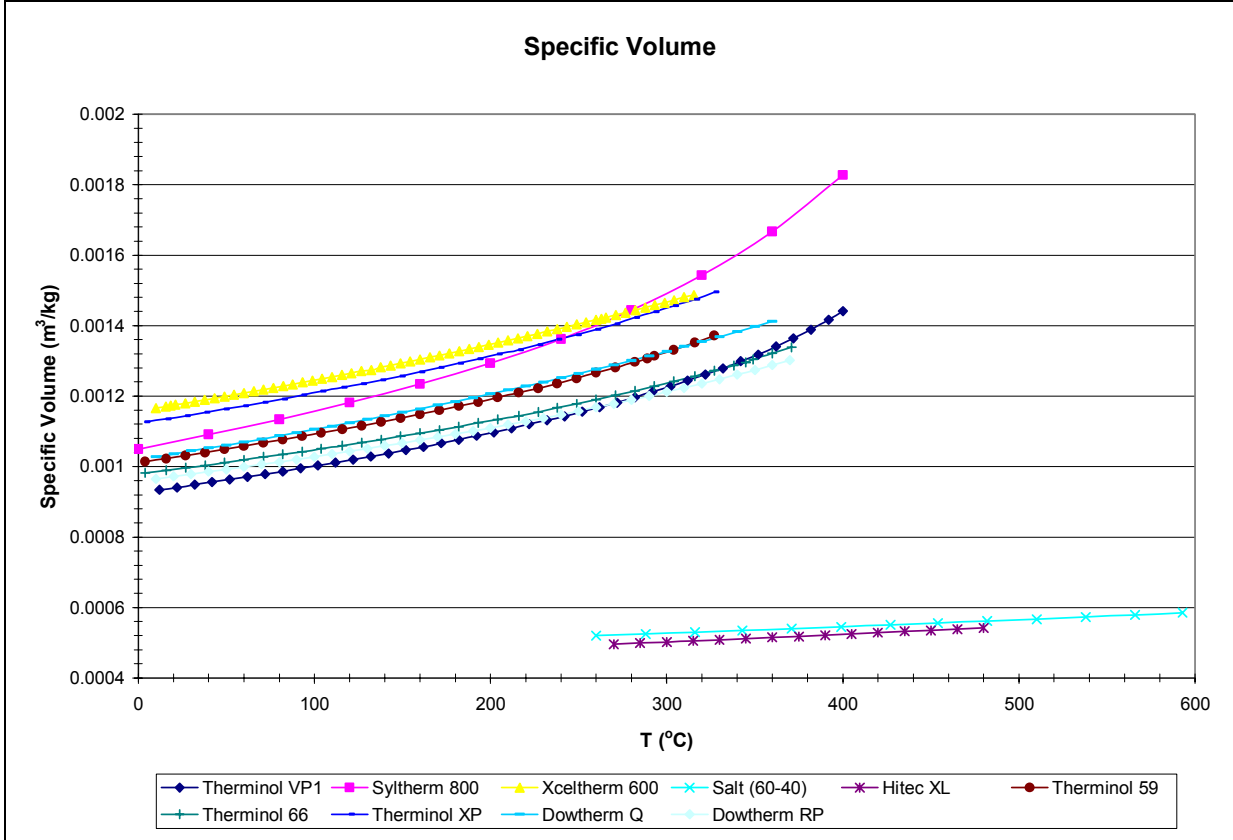
**Figure C.2  Specific volume for each HTF used in the HCE performance model**

An order of magnitude study can be used to determine whether the second term in Equation C.6 is negligible in comparison to the first term. To accomplish this, all the HTFs used in the HCE performance model have been listed in Table C.1, along with the orders of magnitude of the relevant terms. The temperature ranges shown in the second column have been included to show where the orders of magnitude change relative to temperature for each term. As shown in the table, the second term in Equation C.6 (last column) is consistently significantly smaller then the first term (third column), $10° <<$ $10^4$; therefore the second term in Equation C.6 can be neglected without introducing any significant error. The change in enthalpy then becomes

$$\Delta h \approx c_{p,ave}\Delta T \tag{C.7}$$

In most cases, for liquids the know specific heat will be $c_p$. However, if $c_v$ is the known value, it can be substituted for $c_p$ with little error, since the specific heats will differ only slightly for liquids.

**Table C.1  Orders of Magnitude of Change in Enthalpy Terms in Equation C.6 for Each HTF**

| HTF | Temperature Range | $(C_{p,ave})(\Delta T)$ [J/kg] | $v_{ave}$ [m³/kg] | $T_{ave}(\Delta v/\Delta T)$ [kg/m-s] | $(v_{ave} - T_{ave}(\Delta v/\Delta T))\Delta P$ [J/kg] |
|---|---|---|---|---|---|
| Therminol VP1 | Low | $10^4$ | $10^{-4}$ | $10^{-4}$ | $10^0$ |
| | Mid | $10^4$ | $10^{-3}$ | $10^{-4}$ | 0 |
| | High | $10^4$ | $10^{-3}$ | $10^{-3}$ | $10^0$ |
| Therminol 59 | Low | $10^4$ | $10^{-3}$ | $10^{-4}$ | $10^0$ |
| | Mid | $10^4$ | $10^{-3}$ | $10^{-4}$ | $10^0$ |
| | High | $10^4$ | $10^{-3}$ | $10^{-4}$ | $10^0$ |
| Therminol 66 | Low | $10^4$ | $10^{-4}$ | $10^{-4}$ | $10^0$ |
| | Mid | $10^4$ | $10^{-3}$ | $10^{-4}$ | $10^0$ |
| | High | $10^4$ | $10^{-3}$ | $10^{-3}$ | $10^0$ |
| Therminol XP | Low | $10^4$ | $10^{-3}$ | $10^{-4}$ | $10^0$ |
| | Mid | $10^4$ | $10^{-3}$ | $10^{-4}$ | $10^0$ |
| | High | $10^4$ | $10^{-3}$ | $10^{-3}$ | $10^0$ |
| Dowtherm Q | Low | $10^4$ | $10^{-3}$ | $10^{-4}$ | $10^0$ |
| | Mid | $10^4$ | $10^{-3}$ | $10^{-4}$ | $10^0$ |
| | High | $10^4$ | $10^{-3}$ | $10^{-4}$ | $10^0$ |
| Dowtherm RP | Low | $10^4$ | $10^{-4}$ | $10^{-4}$ | $10^0$ |
| | Mid | $10^4$ | $10^{-3}$ | $10^{-4}$ | $10^0$ |
| | High | $10^4$ | $10^{-3}$ | $10^{-4}$ | $10^0$ |
| Syltherm 800 | Low | $10^4$ | $10^{-3}$ | $10^{-4}$ | $10^0$ |
| | Mid | $10^4$ | $10^{-3}$ | $10^{-4}$ | 0 |
| | High | $10^4$ | $10^{-3}$ | $10^{-3}$ | $10^0$ |
| Salt 60-40 | Low | $10^4$ | $10^{-4}$ | $10^{-5}$ | $10^0$ |
| | Mid | $10^4$ | $10^{-4}$ | $10^{-4}$ | $10^0$ |
| | High | $10^4$ | $10^{-4}$ | $10^{-4}$ | $10^0$ |
| Hitec XL | Low | $10^4$ | $10^{-4}$ | $10^{-4}$ | $10^0$ |
| | Mid | $10^4$ | $10^{-4}$ | $10^{-4}$ | $10^0$ |
| | High | $10^4$ | $10^{-4}$ | $10^{-4}$ | $10^0$ |
| Xceltherm 600 | Low | $10^4$ | $10^{-3}$ | $10^{-4}$ | $10^0$ |
| | Mid | $10^4$ | $10^{-3}$ | $10^{-4}$ | $10^0$ |
| | High | $10^4$ | $10^{-3}$ | $10^{-4}$ | $10^0$ |

# D. Radiation Heat Transfer Zonal Analysis for the Glass Envelope

A radiation heat transfer analysis for the glass envelope is conducted below to evaluate the effects of the collector and temperature distribution on the radiation heat losses from the receiver. A generalized zone analysis approach is used in the analysis, and as shown in Figure D.1, the collector and HCE cross-section is separated into four zones. Zone 1 is the receiver half closest to the collector. Zone 2 is the receiver half furthest from the collector. Zone 3 is the collector. Zone 4 is the sky opposite the collector.
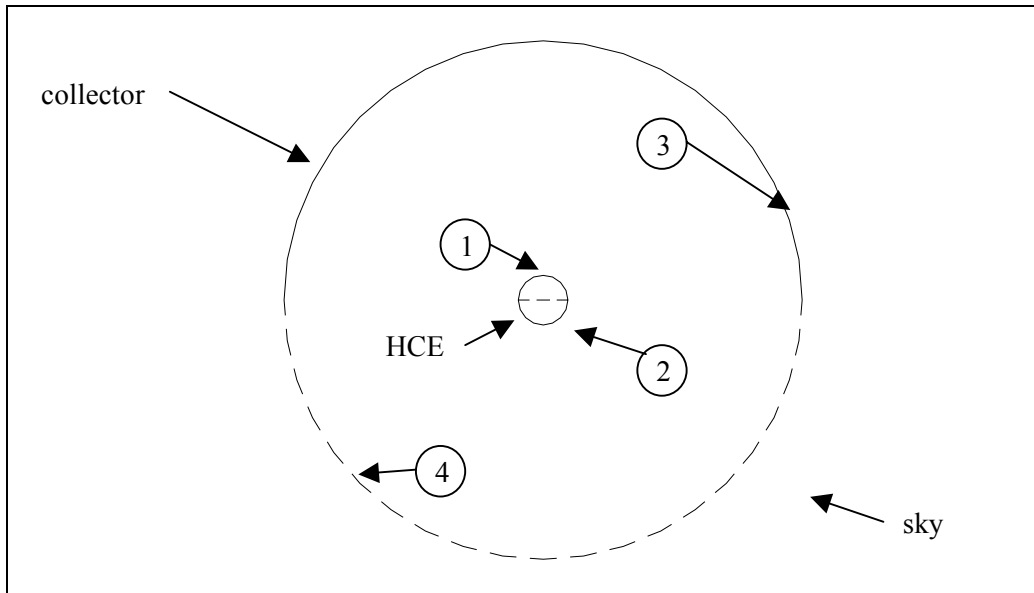


**Figure D.1   Zone definitions for the generalized zone analysis of the radiation heat loss from the receiver**

With the four zones defined in Figure D.1, four separate cases can be evaluated:

**Case 1** is with one uniform receiver temperature and no collector ($T_1 = T_2$, $T_3 = T_4 = T_{sky}$).
**Case 2** is with two uniform receiver temperatures and no collector ($T_1 \neq T_2$, $T_3 = T_4 = T_{sky}$).
**Case 3** is one uniform receiver temperature and collector present ($T_1 = T_2$, $T_3 = T_{ambient}$, $T_4 = T_{sky}$).
**Case 4** is two uniform receiver temperatures and collector present ($T_1 \neq T_2$, $T_3 = T_{ambient}$, $T_4 = T_{sky}$).

The collector temperature is set equal to ambient and the sky temperature is approximated as 8° less than ambient.

Similar to other generalized zone analysis for radiative exchange in an enclosure, the following assumptions were made for the analysis that follows [Ozisk 1973].

- Radiative properties are uniform and independent of direction and frequency.
- Surfaces are diffuse emitters and diffuse reflectors.
- Radiative-heat flux leaving the surface is uniform over the surface of each zone.
- Surfaces are opaque in the frequency of interest ($\alpha + \rho = 1$).
- Temperatures are uniform over each surface.

The first step in the analysis is to define the radiative geometric configuration factors (view factors). For an enclosure with four surfaces there will be 16 view factors. Four can be set to zero, since the receiver surface is convex.

$$F_{1-1} = 0 \tag{D.1a}$$
$$F_{1-2} = 0 \tag{D.1b}$$
$$F_{2-1} = 0 \tag{D.1c}$$
$$F_{2-2} = 0 \tag{D.1d}$$

From symmetry, five additional view factors can be eliminated.

$$F_{1-3} = F_{2-4} \tag{D.2a}$$
$$F_{2-3} = F_{1-4} \tag{D.2b}$$
$$F_{3-1} = F_{4-2} \tag{D.2c}$$
$$F_{3-2} = F_{4-1} \tag{D.2d}$$
$$F_{3-3} = F_{4-4} \tag{D.2e}$$

View factor algebra can be used to define two additional view factors, which will be needed in the analysis.

$$F_{3-(1+2)} = F_{3-1} + F_{3-2} \tag{D.3}$$
$$F_{4-(1+2)} = F_{4-1} + F_{4-2} \tag{D.4}$$

And now, taking advantage of reciprocity, another view factor relationship can be eliminated by symmetry.

$$F_{(1+2)-3} = F_{(1+2)-4} \tag{D.5}$$

Three additional view factors are defined by taking advantage of view factors catalogued in tables. From *A Catalog of Radiation Configuration Factors*, by Howell [1983]

$$F_{(1+2)-3} = \frac{1}{2} \tag{D.6}$$

$$F_{3-3} = 1 - \frac{2}{\pi}\left[\left(1 - \left(\frac{r_{(1+2)}}{r_3}\right)^2\right)^{\frac{1}{2}} + \frac{r_{(1+2)}}{r_3}\sin^{-1}\left(\frac{r_{(1+2)}}{r_3}\right)\right] \tag{D.7}$$

$$F_{3-4} = \frac{2}{\pi}\left[\left(1 - \left(\frac{r_{(1+2)}}{r_3}\right)^2\right)^{\frac{1}{2}} + \frac{r_{(1+2)}}{r_3}\sin^{-1}\left(\frac{r_{(1+2)}}{r_3}\right)\right] - \frac{r_{(1+2)}}{r_3} \tag{D.8}$$

Now, four more relationships are needed to define all the view factors. The first can be approximated with the help of Hottel's crossed-string method [Siegel and Howell 2002]. Figure D.2 shows the required line segments for this method.

$$F_{3-1} = \frac{(2L_1 + 2L_2)}{2A_3} \tag{D.9}$$

with,

$$L_1 = L_{ab} + L_{bc} \tag{D.10a}$$

$$L_{ab} = \sqrt{(L_{ae'})^2 + (L_{e'b})^2} \tag{D.10b}$$

$$L_{bc} = \frac{\pi r_1}{2} \tag{D.10c}$$

$$L_2 = L_{cd} \tag{D.10d}$$

$$L_{cd} = r_3 - r_1 \tag{D.10e}$$

And finally, from reciprocity the remaining three view factors can be found.

$$F_{3-(1+2)} = \frac{A_{(1+2)}}{A_3} F_{(1+2)-3} = \frac{r_{(1+2)}}{r_3/2} \frac{1}{2} = \frac{r_{(1+2)}}{r_3} \tag{D.11}$$

$$F_{1-3} = \frac{A_3}{A_1} F_{3-1} = \frac{r_3}{r_1} F_{3-1} \tag{D.12}$$

$$F_{2-3} = \frac{A_3}{A_2} F_{3-2} = \frac{r_3}{r_2} F_{3-2} \tag{D.13}$$
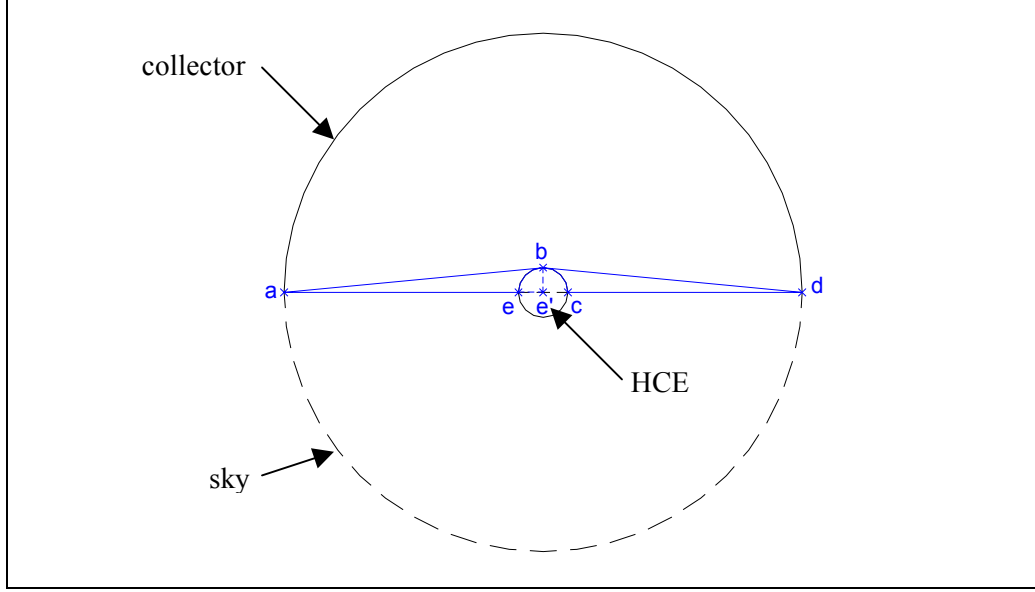
**Figure D.2 Line segments used for the string method approximation for view factors**

The radiosities and heat fluxes can be determined from the following basic relations for radiative heat exchange in enclosures [Ozisik 1977].

$$R_i = \varepsilon_i \sigma T_i^4 + \rho_i \sum_{j=1}^{4} R_j F_{i-j} \tag{D.14}$$

$$q_i'' = R_i - \sum_{j=1}^{4} R_j F_{i-j} \tag{D.15}$$

$$i = 1,2,3,4$$

Using Equation D.1 and treating the sky as a blackbody give the following radiosity equations.

$$R_1 = \varepsilon_1 \sigma T_1^4 + \rho_1 \left( R_3 F_{1-3} + R_4 F_{1-4} \right) \tag{D.16}$$

$$R_2 = \varepsilon_2 \sigma T_2^4 + \rho_2 \left( R_3 F_{2-3} + R_4 F_{2-4} \right) \tag{D.17}$$

$$R_3 = \varepsilon_3 \sigma T_3^4 + \rho_3 \left( R_1 F_{3-1} + R_2 F_{3-2} + R_3 F_{3-3} + R_4 F_{3-4} \right) \tag{D.18}$$

$$R_4 = \sigma T_4^4 \tag{D.19}$$

Solving for $R_3$ gives

$$R_3 = \frac{\varepsilon_3 \sigma T_3^4 + \sigma \rho_3 \left\{ \varepsilon_e \left( F_{3-1} T_1^4 + F_{3-2} T_2^4 \right) + T_4^4 \left[ \rho_e \left( F_{3-1} F_{1-4} + F_{3-2} F_{2-4} \right) + F_{3-4} \right] \right\}}{1 - \rho_3 \left[ \rho_e \left( F_{1-3} F_{3-1} + F_{3-2} F_{2-3} \right) + F_{3-3} \right]} \tag{D.20}$$

The heat flux leaving the glass envelope can be determined by eliminating the summations in Equations D.14 and D.15 and summing the heat fluxes from either side of the HCE.

$$q'_{(1+2)} = 2\pi r_1 \left(q''_1 + q''_2\right) \tag{D.21}$$

$$q''_1 = \frac{\varepsilon_1}{\rho_1}\left(\sigma T_1^4 - R_1\right) \tag{D.22}$$

$$q''_2 = \frac{\varepsilon_2}{\rho_2}\left(\sigma T_2^4 - R_2\right) \tag{D.23}$$

Assuming that the emissivity of the glass (pyrex) envelope and collector (low iron glass) is independent of temperature

$$\varepsilon_1 = \varepsilon_2 = \varepsilon_e = 0.86$$
$$\varepsilon_3 = 0.9$$

All the required information for solving the four cases is now available. Table D.1 shows an Excel spreadsheet used to solve the radiation heat transfer for each case. The results show that by assuming the collector has no effect and that the glass envelope temperature is uniform around the circumference, introduces an error in over predicting radiation heat transfer of 5%–10%. As shown in Figure D.3, this error is consistent regardless of the temperature difference between the front and back of the HCE – assuming the same average temperature around the circumference. Table D.1 also shows that neglecting the collector and modeling the glass envelope temperature as nonuniform would increase the radiation heat transfer by about 5%.

**Table D.1  Radiation Heat Transfer Zonal Analysis Parameters and Results**

| Test Criterion | Radiosities (W/m²) | | | Heat Fluxes (W/m) | | | % Diff |
|---|---|---|---|---|---|---|---|
| | $R_1$ | $R_2$ | $R_3$ | $q_1$ | $q_2$ | $q_{1+2}$ | |
| no collector, uniform envelope temperature | 785.70 | 785.70 | 385.49 | 72.3 | 72.3 | 144.6 | 0 |
| no collector, two uniform envelope temperatures | 1018.26 | 597.99 | 385.49 | 114.3 | 38.4 | 152.7 | 5.6 |
| collector, uniform envelope temperature | 785.70 | 785.70 | 428.33 | 64.6 | 64.6 | 129.1 | -10.7 |
| collector, two uniform envelope temperatures | 1018.26 | 597.99 | 428.72 | 106.5 | 30.6 | 137.1 | -5.2 |

| Inputs | | | View Factors | |
|---|---|---|---|---|
| Collector Type = | LS-2 | | $F_{1-3} =$ | 0.82212 |
| $D_{envelope}$ (m) = | 0.115 | | $F_{1-4} =$ | 0.17788 |
| $D_{collector}$ (m) = | 4.803 | | $F_{2-3} =$ | 0.17788 |
| $\varepsilon_{envelope} =$ | 0.86 | | $F_{2-4} =$ | 0.82212 |
| $\rho_{envelope} =$ | 0.14 | | $F_{3-1} =$ | 0.019685 |
| $\varepsilon_{collector} =$ | 0.9 | | $F_{3-2} =$ | 0.004259 |
| $\rho_{collector} =$ | 0.1 | | $F_{3-3} =$ | 0.363198 |
| $\Delta T$ (K) = | 50 | | $F_{3-4} =$ | 0.612859 |
| $T_{ave}$ (K) = | 350 | | | |
| $T_{ave,e1}$ (K) = | 375 | | | |
| $T_{ave,e2}$ (K) = | 325 | | | |
| $T_{amb}$ (K) = | 295.15 | | | |
| $T_{sky}$ (K) = | 287.15 | | | |
| $\sigma$ (W/m²-K⁴) = | 5.67E-08 | | | |
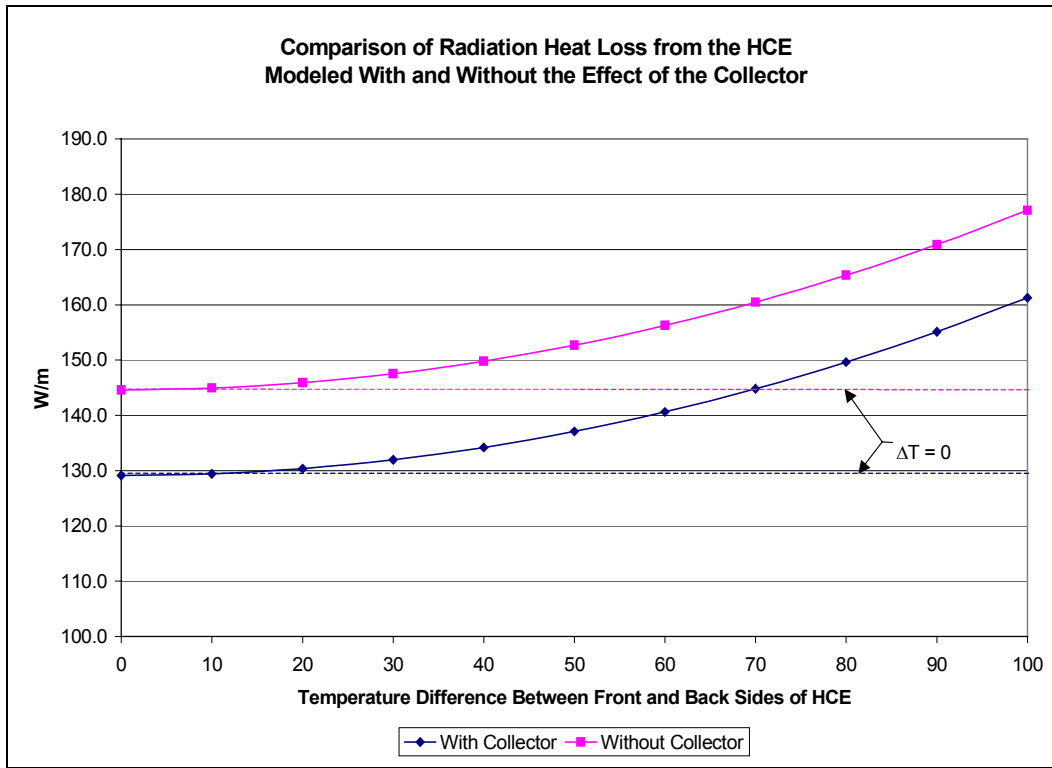
**Figure D.3  Radiation heat loss comparison chart showing difference between modeling the radiation loss with and without the collector effects**

# E. One-Dimensional Design Study Version of EES Code

(Tab settings have been shortened and numerous comment statements have been omitted to reduce length of following code.)

```
"*********************************************************************************************************
    PROCEDURE Pq_12conv :  Convective heat transfer rate from the HTF to the inside of the
receiver tube
*********************************************************************************************************"
PROCEDURE Pq_12conv(T_1ave, T_2, Fluid$: q_12conv)
$Common D_2, D_p, D_h, L, v_1, Flow_Type$, IncludeLaminar$

    " Warning Statements if HTF is evaluated out of recommended temperature ranges "
    If (Fluid$ = 'Syltherm 800') Then
        If (T_1ave < -40) or (400 < T_1ave) Then CALL WARNING('The result may not be accurate,
since Syltherm 800 fluid properties are out of recommended temperature range, -40 C < T < 400 C.
See Procedure Pq_12conv.T_1ave = XXXA1', T_1ave)
    EndIf
    If (Fluid$ = 'Therminol VP1') Then
        If (T_1ave < 12) or (400 < T_1ave) Then CALL WARNING('The result may not be accurate,
since Therminol VP1 fluid properties are out of recommended temperature range, 12 C < T < 400 C .
See Procedure Pq_12conv.T_1ave = XXXA1', T_1ave)
    EndIf
    If (Fluid$ = 'Xceltherm 600') Then
        If (T_1ave < -20) or (316 < T_1ave) Then CALL WARNING('The result may not be accurate,
since Xceltherm 600 fluid properties are out of recommended temperature range, -20 C < T < 316 C..
See Procedure Pq_12conv.T_1ave = XXXA1', T_1ave)
    EndIf
    If (Fluid$ = 'Therminol 59') Then
        If (T_1ave < -45) or (315 < T_1ave) Then CALL WARNING('The result may not be accurate,
since Therminol 59 fluid properties are out of recommended temperature range, -45 C < T < 315 C..
See Procedure Pq_12conv.T_1ave = XXXA1', T_1ave)
    EndIf
    If (Fluid$ = 'Therminol 66') Then
        If (T_1ave < 0) or (345 < T_1ave) Then CALL WARNING('The result may not be accurate,
since Therminol 66 fluid properties are out of recommended temperature range, 0 C < T < 345 C..
See Procedure Pq_12conv.T_1ave = XXXA1', T_1ave)
    EndIf
    If (Fluid$ = 'Therminol XP') Then
        If (T_1ave < -20) or (315 < T_1ave) Then CALL WARNING('The result may not be accurate,
since Therminol XP fluid properties are out of recommended temperature range, -20 C < T < 315 C..
See Procedure Pq_12conv.T_1ave = XXXA1', T_1ave)
    EndIf
    If (Fluid$ = 'Dowtherm Q') Then
        If (T_1ave < -35) or (330 < T_1ave) Then CALL WARNING('The result may not be accurate,
since Dowtherm Q fluid properties are out of recommended temperature range, -35 C < T < 330 C..
See Procedure Pq_12conv.T_1ave = XXXA1', T_1ave)
    EndIf
    If (Fluid$ = 'Dowtherm RP') Then
        If (T_1ave < -20) or (350 < T_1ave) Then CALL WARNING('The result may not be accurate,
since Dowtherm RP fluid properties are out of recommended temperature range, -20 C < T < 350 C..
See Procedure Pq_12conv.T_1ave = XXXA1', T_1ave)
    EndIf
    If (Fluid$ = 'Salt (60% NaNO3, 40% KNO3)') Then
```

If (T_1ave < 260) or (621 < T_1ave) Then CALL WARNING('The result may not be accurate, since Salt (60% NaNO3, 40% KNO3) fluid properties are out of recommended temperature range, 260 C < T < 621 C. See Procedure Pq_12conv.T_1ave = XXXA1', T_1ave)
    EndIf
If (Fluid$ = 'Hitec XL') Then
    If (T_1ave < 266) or (480 < T_1ave) Then CALL WARNING('The result may not be accurate, since Hitec XL fluid properties are out of recommended temperature range, 266 C < T < 480 C. See Procedure Pq_12conv.T_1ave = XXXA1', T_1ave)
    EndIf
If (Fluid$ = 'Water') Then
    If (T_1ave < 0) or (100 < T_1ave) Then CALL WARNING('The result may not be accurate, since Water fluid properties are out of recommended temperature range, 0 C < T < 100 C. See Procedure Pq_12conv.T_1ave = XXXA1', T_1ave)
    EndIf

    " Thermophysical properties for HTF "
    MU_1 := INTERPOLATE(Fluid$,'MU','T',T=T_1ave)  "[kg/m-s]"
    MU_2 := INTERPOLATE(Fluid$,'MU','T',T=T_2)  "[kg/m-s]"
    Cp_1 := INTERPOLATE(Fluid$,'Cp','T',T=T_1ave)  "[J/kg-K]"
    Cp_2 := INTERPOLATE(Fluid$,'Cp','T',T=T_2)  "[J/kg-K]"
    k_1 := INTERPOLATE(Fluid$,'k','T',T=T_1ave)  "[W/m-K]"
    k_2 := INTERPOLATE(Fluid$,'k','T',T=T_2)  "[W/m-K]"
    RHO_1 := INTERPOLATE(Fluid$,'RHO','T',T=T_1ave)  "[kg/m^3]"

    Re_D2 := (RHO_1 * D_h * v_1) / (MU_1)

    Pr_2 := (Cp_2 * MU_2) / k_2
    Pr_1 := (Cp_1 * MU_1) / k_1

    " Nusselt Number for laminar flow case if option to include laminar flow model is chosen "
    If (IncludeLaminar$ = 'Yes') and (Re_D2 <= 2300) Then
        If (Flow_Type$ = 'Annulus Flow') Then
            DRatio := D_p/D_2
            Nu#_D2 := INTERPOLATE(Nu#, 'Nu#_D2','Dp/D2', Dp/D2=DRatio)  "estimate for uniform heat flux case"
        Else
            Nu#_D2 := 4.36            "uniform heat flux"
        EndIf
    Else

        " Warning statements if turbulent/transitional flow Nusselt Number correlation is used out of recommended range "
        If (Pr_1 <= 0.5) or (2000 <= Pr_1) Then CALL WARNING('The result may not be accurate, since 0.5 < Pr_1 < 2000 does not hold. See PROCEDURE Pq_12conv. Pr_1 = XXXA1', Pr_1)
        If (Pr_2 <= 0.5) or (2000 <= Pr_2) Then CALL WARNING('The result may not be accurate, since 0.5 < Pr_2 < 2000 does not hold. See PROCEDURE Pq_12conv. Pr_2 = XXXA1', Pr_2)
        If ( Re_D2 <= (2300) ) or (5*10^6 <= Re_D2 ) Then CALL WARNING('The result may not be accurate, since 2300 < Re_D2 < (5 * 10^6) does not hold. See PROCEDURE Pq_12conv. Re_D2 = XXXA1', Re_D2)

        " Turbulent/transitional flow Nusselt Number correlation (modified Gnielinski correlation) "
        f := (1.82 * LOG10(Re_D2) - 1.64)^(-2)
        Nu#_D2 := (f / 8) * (Re_D2 - 1000) * Pr_1 / (1 + 12.7 * (f / 8)^(0.5) * (Pr_1^(0.6667) -1)) * (Pr_1 / Pr_2)^0.11
    EndIf

```
    h_1 := Nu#_D2 * k_1 / D_h   "[W/m^2-K]"
    q_12conv := h_1 * D_2 * PI  * (T_2 - T_1ave)   "[W/m]"

End


"*************************************************************************************************************
    FUNCTION fq_34conv :    Convective heat transfer rate between the absorber outer surface and
the glazing inner surface
*************************************************************************************************************"
FUNCTION fq_34conv(T_3, T_4)
$Common D_3, D_4, L, P_a, P_6, g, v_6, T_0, T_6, T_std, AnnulusGas$, GlazingIntact$

    P_a1 := P_a * CONVERT(torr, kPa)   "[kPa]"

    T_34 := (T_3 + T_4) / 2   "[C]"
    T_36 := (T_3 + T_6) / 2   "[C]"

    If (GlazingIntact$ = 'No') Then

        " Thermophysical Properties for air "
        Rho_3 := Density(AIR, T=T_3, P=P_6)   "[kg/m^3]"
        Rho_6 := Density(AIR, T=T_6, P=P_6)   "[kg/m^3]"

        If (v_6 <= 0.1) Then
            MU_36 := viscosity(AIR, T=T_36)   "[N-s/m^2]"
            Rho_36 := Density(AIR, T=T_36, P=P_6)   "[kg/m^3]"
            Cp_36 := CP(AIR, T=T_36)   "[kJ/kg-K]"
            k_36 := conductivity(AIR, T=T_36)   "[W/m-K]"
            NU_36 := MU_36 / Rho_36   "[m^2/s]"
            Alpha_36 := k_36 / (Cp_36 * Rho_36 * 1000)   "[m^2/s]"
            Beta_36 :=  1 / (T_36 + T_0)   "[1/K]"
            Ra_D3 := g * Beta_36 * ABS(T_3 - T_6) * (D_3)^3 / (Alpha_36 * NU_36)

            " Warning Statement if following Nusselt Number correlation is used out of recommended
range "
            If (Ra_D3 <= 10^(-5)) or (Ra_D3 >= 10^12) Then CALL WARNING('The result may not be
accurate, since 10^(-5) < Ra_D3 < 10^12 does not hold. See Function fq_34conv. Ra_D3 = XXXA1',
Ra_D3)

            " Churchill and Chu correlation for natural convection from a long isothermal horizontal
cylinder "
            Pr_36 := NU_36 / Alpha_36
            Nu#_bar := (0.60 + (0.387 * Ra_D3^(0.1667)) / (1 + (0.559 / Pr_36)^(0.5625))^(0.2963) )^2
            h_36 := Nu#_bar * k_36 / D_3   "[W/m^2-K]"
            fq_34conv := h_36 * PI * D_3 * (T_3 - T_6)   "[W/m]"

        Else

            " Thermophysical Properties for air "
            MU_3 := viscosity(AIR, T=T_3)   "[N-s/m^2]"
            MU_6 := viscosity(AIR, T=T_6)   "[N-s/m^2]"
            k_3 := conductivity(AIR, T=T_3)   "[W/m-K]"
            k_6 := conductivity(AIR, T=T_6)   "[W/m-K]"
            Cp_3 := CP(AIR, T=T_3)   "[kJ/kg-K]"
            Cp_6 := CP(AIR, T=T_6)   "[kJ/kg-K]"
```

```
        NU_6 := MU_6 / Rho_6  "[m^2/s]"
        NU_3 := MU_3 / Rho_3  "[m^2/s]"
        Alpha_3 := k_3 / (Cp_3 * Rho_3 * 1000)  "[m^2/s]"
        Alpha_6 := k_6 / (Cp_6 * Rho_6 * 1000)  "[m^2/s]"
        Re_D3 := v_6 * D_3 / NU_6
        Pr_3 := NU_3 / Alpha_3
        Pr_6 := NU_6 / Alpha_6

        " Warning Statements if following Nusselt Number correlation if used out of range "
        If (Re_D3 <= 1) or (Re_D3 >= 10^6) Then CALL WARNING('The result may not be
accurate, since 1 < Re_D3 < 10^6 does not hold. See Function fq_34conv. Re_D3 = XXXA1',
Re_D3)
        If (Pr_6 <= 0.7) or (Pr_6 >= 500) Then CALL WARNING('The result may not be accurate,
since 0.7 < Pr_6 < 500 does not hold. See Function fq_34conv. Pr_6 = XXXA1', Pr_6)

        " Coefficients for external forced convection Nusselt Number correlation (Zhukauskas's
correlation) "
        If (Pr_6 <= 10) Then
            n := 0.37
        Else
            n := 0.36
        EndIf

        If (Re_D3 < 40) Then
            C := 0.75
            m := 0.4
        Else

            If (40 <= Re_D3) and (Re_D3 < 10^3) Then
                C := 0.51
                m := 0.5
            Else
                If (10^3 <= Re_D3) and (Re_D3 < 2*10^5) Then
                    C := 0.26
                    m := 0.6
                Else
                    If (2*10^5 <= Re_D3) and (Re_D3 < 10^6) Then
                        C := 0.076
                        m := 0.7
                    EndIf
                EndIf
            EndIf
        EndIf

        " Zhukauskas's correlation for external forced convection flow normal to an isothermal
cylinder "
        Nu#_bar := C * (Re_D3)^m  * (Pr_6)^n * (Pr_6 / Pr_3)^(0.25)
        h_36 := Nu#_bar  *  k_6  /  D_3  "[W/m^2-K]"
        fq_34conv :=  h_36  *  D_3  *  PI  *  (T_3 - T_6)  "[W/m]"
    EndIf
  Else

    " Thermophysical Properties for gas in annulus space "
    If (AnnulusGas$ = 'Argon') Then
        MU_34 := INTERPOLATE('Argon', 'MU', 'T', T = (T_34 + T_0))  "[kg/m-s]"
        Cp_34 := INTERPOLATE('Argon', 'Cp', 'T', T = (T_34 + T_0))  "[kJ/kg-K]"
```

```
          Cv_34 := INTERPOLATE('Argon', 'Cv', 'T', T = (T_34 + T_0))  "[kJ/kg-K]"
          Rho_34 := P_a1 / (0.20813 * (T_34 + T_0))  "[kg/m^3]"
          k_34 := INTERPOLATE('Argon', 'k', 'T', T = (T_34 + T_0))  "[W/m-K]"
          k_std := INTERPOLATE('Argon', 'k', 'T', T = (T_std + T_0))  "[W/m-K]"
     Else
          MU_34 := VISCOSITY(AnnulusGas$, T=T_34)  "[kg/m-s]"
          Cp_34 := CP(AnnulusGas$, T=T_34)  "[kJ/kg-K]"
          Cv_34 := CV(AnnulusGas$, T=T_34)  "[kJ/kg-K]"
          k_34 := CONDUCTIVITY(AnnulusGas$, T=T_34)  "[W/m-K]"
          Rho_34 := DENSITY(AnnulusGas$, T=T_34, P=P_a1)  "[kg/m^3]"
          k_std := CONDUCTIVITY(AnnulusGas$, T=T_std)  "[W/m-K]"
     EndIf


     " Modified Raithby and Hollands correlation for natural convection in an annular space
between horizontal cylinders "
          Alpha_34 := k_34 /(Cp_34 * Rho_34 * 1000)  "[m^2/s]"
          NU_34 := MU_34 / Rho_34  "[m^2/s]"
          Beta_34 := 1 / (T_34 + T_0)  "[1/K]"
          Ra_D3 := g * Beta_34 * ABS(T_3 - T_4) * (D_3)^3 / (Alpha_34 * NU_34)
          Ra_D4 := g * Beta_34 * ABS(T_3 - T_4) * (D_4)^3 / (Alpha_34 * NU_34)
          Pr_34 := NU_34 / Alpha_34
          Natq_34conv := 2.425 * k_34 * (T_3 - T_4) / (1 + (D_3/ D_4)^(0.6))^(1.25) * (Pr_34 * Ra_D3 /
(0.861 + Pr_34))^(0.25)  "[W/m]"
          P := P_a * CONVERT(torr, mmHg)  "[mmHg]"
          C1 := 2.331*10^(-20)  "[mmHg-cm^3/K]"


     " Free-molecular heat transfer for an annular space between horizontal cylinders "
     If (AnnulusGas$ = 'Air') Then
          Delta := 3.53 * 10^(-8)  "[cm]"
     EndIf

     If (AnnulusGas$ = 'H2') Then
          Delta := 2.4 * 10^(-8)  "[cm]"
     EndIf

     If (AnnulusGas$ = 'Argon') Then
          Delta := 3.8*10^(-8)  "[cm]"
     EndIf

     Lambda := C1 * (T_34 + T_0) / (P * Delta^2)  "[cm]"
     Gamma := Cp_34 / Cv_34
     a := 1
     b := (2 - a) / a * (9 * Gamma - 5) / (2 * (Gamma + 1))
     h_34 := k_std / (D_3 / 2 * ln(D_4 / D_3) + b * Lambda * (D_3 / D_4 + 1))  "[W/m^2-K]"
     Kineticq_34conv  := D_3 * PI * h_34 * (T_3 - T_4)  "[W/m]"

     " Following compares free-molecular heat transfer with natural convection heat transfer and
uses the largest value for heat transfer in annulus "
     If (Kineticq_34conv > Natq_34conv) Then
          fq_34conv := Kineticq_34conv  "[W/m]"

          " Warning Statement if free-molecular heat transfer correlation is used out of range "
          If  (Ra_D4 < 10^7) Then CALL WARNING('The result may not be accurate, since (D_4 /
(D_4 - D_3))^4 < Ra_D4 < 10^7 does not hold. See Function fq_34conv. Ra_D4 = XXXA1', Ra_D4)

     Else
```

```
            fq_34conv := Natq_34conv  "[W/m]"
        EndIf
    EndIf

End


"*************************************************************************************************************
    FUNCTION fq_34rad : Radiation heat transfer rate between the absorber surface and glazing
inner surface
*************************************************************************************************************"
FUNCTION fq_34rad(T_3, T_4)
$COMMON D_3, D_4, L, T_7, T_0, sigma, EPSILON_3, EPSILON_4, GlazingIntact$

    If (GlazingIntact$ = 'No') Then
        fq_34rad :=EPSILON_3 * PI * D_3  * sigma * ((T_3 + T_0)^4 - (T_7 + T_0)^4)  "[W/m]"
    Else
        fq_34rad := PI * D_3 * sigma * ((T_3 + T_0)^4 - (T_4 + T_0)^4) / (1 / EPSILON_3 + D_3 / D_4
* ( 1 / EPSILON_4 - 1))  "[W/m]"
    EndIf

END


"*************************************************************************************************************
    FUNCTION fq_56conv :    Convective heat transfer rate between the glazing outer surface and the
ambient air
*************************************************************************************************************"
FUNCTION fq_56conv(T_5, T_6)
$Common D_5, L,  P_6, v_6, g, T_0, GlazingIntact$

    T_56 := (T_5 + T_6)/2  "[C]"

    " Thermophysical Properties for air "
    MU_5 := VISCOSITY(Air,T=T_5)  "[kg/m-s]"
    MU_6 := VISCOSITY(Air,T=T_6)  "[kg/m-s]"
    MU_56 := VISCOSITY(Air, T=T_56)  "[kg/m-s]"
    k_5 := CONDUCTIVITY(Air,T=T_5)  "[W/m-K]"
    k_6 := CONDUCTIVITY(Air,T=T_6)  "[W/m-K]"
    k_56 := CONDUCTIVITY(Air, T=T_56)  "[W/m-K]"
    Cp_5 := SPECHEAT(Air,T=T_5)  "[kJ/kg-K]"
    Cp_6 := SPECHEAT(Air,T=T_6)  "[kJ/kg-K]"
    Cp_56 := CP(AIR, T=T_56)  "[kJ/kg-K]"
    Rho_5 := DENSITY(Air,T=T_5, P=P_6)  "[kg/m^3]"
    Rho_6 := DENSITY(Air,T=T_6, P=P_6)  "[kg/m^3]"
    Rho_56 := DENSITY(Air, T=T_56, P=P_6)  "[kg/m^3]"

    " If the glass envelope is missing then the convection heat transfer from the glass envelope is
forced to zero by T_5 = T_6 "
    If (GlazingIntact$ = 'No') Then
        fq_56conv := (T_5 - T_6)  "[W/m]"
    Else
        If (v_6 <= 0.1) Then

            " Coefficients for Churchill and Chu natural convection correlation "
            NU_56 := MU_56 / Rho_56  "[m^2/s]"
```

Alpha_56 := k_56 / (Cp_56 * Rho_56 * 1000)  "[m^2/s]"
Beta_56 :=  1 / (T_56 + T_0)  "[1/K]"
Ra_D5 := g *Beta_56 * ABS(T_5 - T_6) * (D_5)^3 / (Alpha_56 * NU_56)

" Warning Statement if following Nusselt Number correlation is used out of range "
If (Ra_D5 <= 10^(-5)) or (Ra_D5 >= 10^12) Then CALL WARNING('The result may not be accurate, since 10^(-5) < Ra_D5 < 10^12 does not hold. See Function fq_56conv. Ra_D5 = XXXA1', Ra_D5)

" Churchill and Chu correlation for natural convection for a horizontal cylinder "
Pr_56 :=  NU_56 / Alpha_56
Nu#_bar := (0.60 + (0.387 * Ra_D5^(0.1667)) / (1 + (0.559 / Pr_56)^(0.5625))^(0.2963) )^2
h_6 := Nu#_bar * k_56 / D_5  "[W/m^2-K]"
fq_56conv := h_6 * PI * D_5 * (T_5 - T_6)  "[W/m]"

Else

" Coefficients for Zhukauskas's correlation "
Alpha_5 := k_5 / (Cp_5 * Rho_5 * 1000)  "[m^2/s]"
Alpha_6 := k_6 / (Cp_6 * Rho_6 * 1000)  "[m^2/s]"
NU_5 := MU_5 / Rho_5  "[m^2/s]"
NU_6 := MU_6 / Rho_6  "[m^2/s]"
Pr_5 := NU_5 / Alpha_5
Pr_6 := NU_6 / Alpha_6
Re_D5 := v_6 * D_5 * Rho_6 / MU_6

" Warning Statement if following Nusselt Number correlation is used out of range "
If (Pr_6 <= 0.7) or (Pr_6 >= 500) Then CALL WARNING('The result may not be accurate, since 0.7 < Pr_6 < 500 does not hold. See Function fq_56conv. Pr_6 = XXXA1', Pr_6)
If (Re_D5 <= 1) or (Re_D5 >= 10^6) Then CALL WARNING('The result may not be accurate, since 1 < Re_D5 < 10^6 does not hold. See Function fq_56conv. Re_D5 = XXXA1 ', Re_D5)

" Zhukauskas's correlation for forced convection over a long horizontal cylinder "
If (Pr_6 <= 10) Then
    n := 0.37
Else
    n := 0.36
EndIf

If (Re_D5 < 40) Then
    C := 0.75
    m := 0.4
Else
    If (40 <= Re_D5) and (Re_D5 < 10^3) Then
        C := 0.51
        m := 0.5
    Else
        If (10^3 <= Re_D5) and (Re_D5 < 2*10^5) Then
            C := 0.26
            m := 0.6
        Else
            If (2*10^5 <= Re_D5) and (Re_D5 < 10^6) Then
                C := 0.076
                m := 0.7
            EndIf

```
                EndIf
            EndIf
         EndIf

         Nu#_6 := C * Re_D5^m *  Pr_6^n  *(Pr_6/Pr_5)^0.25
         h_6 := Nu#_6 * k_6 / D_5  "[W/m^2-K]"
         fq_56conv := h_6 * PI * D_5 * (T_5 - T_6)  "[W/m]"
      EndIf
   EndIf
End
```

**********************************************************************************************************************
    FUNCTION fq_57rad : Radiation heat transfer rate between the glazing outer surface and the sky
**********************************************************************************************************************"
```
FUNCTION  fq_57rad(T_5, T_7)
$COMMON EPSILON_5, D_5, L, sigma, T_0, GlazingIntact$
```

   " If glass envelope is missing then radiation heat transfer from glass envelope is set to zero;
otherwise, radiative heat transfer for a small convex object in a large cavity "
```
   If (GlazingIntact$ = 'No') Then
      fq_57rad := 0  "[W/m]"
   Else
      fq_57rad  := EPSILON_5 * PI * D_5 * sigma * ((T_5 + T_0)^4 - (T_7 + T_0)^4)  "[W/m]"
   EndIf

END
```

**********************************************************************************************************************
    FUNCTION fq_5SolAbs :  Solar flux on glazing
**********************************************************************************************************************"
```
FUNCTION fq_5SolAbs(q_i)
$COMMON GlazingIntact$, Alpha_env, OptEff_env
```

   " If glass envelope is missing then solar absorption in glass envelope is set to zero; otherwise,
solar absorption is estimated with an optical efficiency term "
```
   If (GlazingIntact$ = 'No') Then
      fq_5SolAbs :=0  "[W/m]"
   Else
      fq_5SolAbs := q_i * OptEff_env * Alpha_env  "[W/m]"
   EndIf

END
```

**********************************************************************************************************************
    PROCEDURE Pq_45cond :  One dimensional energy equation about inside surface of glazing
**********************************************************************************************************************"
```
PROCEDURE Pq_45cond(q_34conv, q_34rad: q_45cond)
$COMMON GlazingIntact$
```

   " If glass envelope is missing then radial conduction through glass envelope is set to zero;
otherwise, the energy balance is used "
```
   If (GlazingIntact$ = 'No') Then
      q_45cond :=0  "[W/m]"
```

```
    Else
        q_45cond := q_34conv + q_34rad  "[W/m]"
    EndIf

END


"**********************************************************************************************************
    PROCEDURE Pq_56conv :  One dimensional energy equation about outside surface of glazing
**********************************************************************************************************"
PROCEDURE Pq_56conv(q_45cond, q_5SolAbs, q_57rad: q_56conv)
$COMMON GlazingIntact$

    " If the glass envelope is missing then the convective heat transfer from the envelope is set to
zero; otherwise, the energy balance is used "
    If (GlazingIntact$ = 'Yes') Then
        q_56conv := q_45cond + q_5SolAbs - q_57rad  "[W/m]"
    Else
        q_56conv := 0  "[W/m]"
    EndIf

END


"**********************************************************************************************************
    FUNCTION fA_cs : Inside cross sectional flow area of absorber
**********************************************************************************************************"
FUNCTION fA_cs(D_2, D_p)
$COMMON Flow_Type$

    " If 'SNL AZTRAK Platform' then the HTF flow area accounts for the inserted plug "
    If (Flow_Type$ = 'Annulus Flow') Then
        fA_cs := PI * (D_2 ^2 - D_p ^2) / 4     "[m^2]"
    Else
        fA_cs := PI * (D_2 ^2 / 4)  "[m^2]"
    EndIf

END


"**********************************************************************************************************
    FUNCTION fETA_Col :    Collector efficiency
**********************************************************************************************************"
FUNCTION fETA_Col(q_12conv, q_i)

    " If the solar insolation is zero or the efficiency is negative, then the collector efficiency is set to
zero "
    If (q_i =0) Then
        fETA_Col := 0
    Else
        If ((q_12conv/q_i)<=0.001) Then
            fETA_Col := 0
        Else
            fETA_Col :=q_12conv/q_i
        EndIf
    EndIf
```

END


```
"*********************************************************************************************************
    FUNCTION fk_23:  Absorber conductance
*********************************************************************************************************"
{ Based on linear fit of data from "Alloy Digest, Sourcebook, Stainless Steels"; ASM International,
2000.}

FUNCTION fk_23(T_2, T_3)
$COMMON AbsorberMaterial$

    T_23 := (T_2 + T_3) / 2  "[C]"

    If (AbsorberMaterial$ = '304L') or (AbsorberMaterial$ = '316L') Then
        fk_23 := 0.013 * T_23 + 15.2  "[W/m-K]"
    EndIf

    If (AbsorberMaterial$ = '321H') Then
        fk_23 := 0.0153 * T_23 + 14.775  "[W/m-K]"
    EndIf

    If (AbsorberMaterial$ = 'B42 Copper Pipe') Then
        fk_23 := 400  "[W/m-K]"
    EndIf

END


"*********************************************************************************************************
    PROCEDURE pSelectiveCoatingProperties: Selective Coating Emissivity and Absorptance
*********************************************************************************************************"
PROCEDURE pSelectiveCoatingProperties(T_3: EPSILON_3, Alpha_abs, TAU_envelope)
$COMMON SelectiveCoating$, T_0, TAU_envelope_UD, Alpha_abs_UD, EPSILON_3_100_UD,
EPSILON_3_400_UD

    " Calculates emissivity and determines optical properties for chosen selective coating type "
    If (SelectiveCoating$ = 'User-Defined') Then
        TAU_envelope := TAU_envelope_UD
        Alpha_abs := Alpha_abs_UD
        EPSILON_3 :=  EPSILON_3_100_UD - (EPSILON_3_400_UD - EPSILON_3_100_UD)/3 +
T_3 * (EPSILON_3_400_UD - EPSILON_3_100_UD)/300
    Endif

    If (SelectiveCoating$ = 'Black Chrome (SNL test)') Then
        TAU_envelope := 0.935
        Alpha_abs := 0.94
        EPSILON_3 := 0.0005333 * (T_3+T_0) - 0.0856
        If (EPSILON_3 < 0.11) Then
            EPSILON_3 := 0.11
        EndIf
    Endif

    If (SelectiveCoating$ = 'Luz Cermet (SNL test)') Then
        TAU_envelope := 0.935
```

```
        Alpha_abs := 0.92
        EPSILON_3 := 0.000327 * (T_3+T_0) - 0.065971
        If (EPSILON_3 < 0.05) Then
            EPSILON_3 := 0.05
        EndIf
    Endif

    If (SelectiveCoating$ = 'Solel UVAC Cermet (SNL test a)') Then
        TAU_envelope := 0.965
        Alpha_abs := 0.96
        EPSILON_3 := 2.249*10^(-7)*(T_3)^2 + 1.039*10^(-4)*T_3 + 5.599*10^(-2)
    EndIf

    If (SelectiveCoating$ = 'Solel UVAC Cermet (SNL test b)') Then
        TAU_envelope := 0.965
        Alpha_abs := 0.95
        EPSILON_3 := 1.565*10^(-7)*(T_3)^2 + 1.376*10^(-4)*T_3 + 6.966*10^(-2)
    EndIf

    If (SelectiveCoating$ = 'Solel UVAC Cermet (SNL test avg)') Then
        TAU_envelope := 0.965
        Alpha_abs := 0.955
        EPSILON_3 := 1.907*10^(-7)*(T_3)^2 + 1.208*10^(-4)*T_3 + 6.282*10^(-2)
    EndIf

    If (SelectiveCoating$ = 'Solel UVAC Cermet (0.10 @ 400C)') Then
        TAU_envelope := 0.97
        Alpha_abs := 0.98
        EPSILON_3 := 2.084*10^(-4)*T_3 + 1.663*10^(-2)
    EndIf

    If (SelectiveCoating$ = 'Solel UVAC Cermet (0.07 @ 400C)') Then
        TAU_envelope := 0.97
        Alpha_abs := 0.97
        EPSILON_3 := 1.666*10^(-4)*T_3 + 3.375*10^(-3)
    EndIf

END


"*********************************************************************************************************
    PROCEDURE pHCEdimensions:  HCE dimensions based on HCE type
*********************************************************************************************************"
PROCEDURE pHCEdimensions(CollectorType$: D_2, D_3, D_4,  D_5, W_aperture)
$COMMON  D_2_UD, D_3_UD, D_4_UD, D_5_UD, W_aperture_UD

    " The following determines the HCE dimensions depending on the HCE type chosen in the
Diagram Window "
    If (CollectorType$ = 'User-Defined') Then
        D_2 := D_2_UD  "[m]"
        D_3 := D_3_UD  "[m]"
        D_4 := D_4_UD  "[m]"
        D_5 := D_5_UD  "[m]"
        W_aperture := W_aperture_UD  "[m]"
    EndIf
```

```
If (CollectorType$ = 'LS-2') Then
    D_2 := 0.066  "[m]"
    D_3 := 0.070  "[m]"
    D_4 := 0.109  "[m]"
    D_5 := 0.115 "[m]"
    W_aperture := 4.8235  "[m]"
EndIf

If (CollectorType$ = 'LS-3') Then
    D_2 := 0.066  "[m]"
    D_3 := 0.070  "[m]"
    D_4 := 0.115  "[m]"
    D_5 := 0.121  "[m]"
    W_aperture := 5.59  "[m]"
EndIf

If (CollectorType$ = 'IST') Then
    D_2 := 0.066  "[m]"
    D_3 := 0.070  "[m]"
    D_4 := 0.075  "[m]"
    D_5 := 0.0702  "[m]"
    W_aperture := 3.053  "[m]"
EndIf

END


"***********************************************************************************************************
    PROCEDURE pOpticalEfficiency:    Optical Efficiencies based on HCE type
***********************************************************************************************************"
PROCEDURE pOpticalEfficiency(CollectorType$: OptEff_env, OptEff_abs)
$COMMON GlazingIntact$, K, Reflectivity, TAU_envelope, Shadowing_UD, TrackingError_UD,
GeomEffects_UD, Rho_mirror_clean_UD, Dirt_mirror_UD, Dirt_HCE_UD, Error_UD

    " The following determines the optical properties depending on the HCE type chosen in the
Diagram Window
    The properties should be modified as better data becomes available "
    If (CollectorType$ = 'User-Defined') Then
        Shadowing := Shadowing_UD
        TrackingError := TrackingError_UD
        GeomEffects := GeomEffects_UD
        Rho_mirror_clean := Rho_mirror_clean_UD
        Dirt_mirror := Dirt_mirror_UD
        Dirt_HCE := Dirt_HCE_UD
        Error := Error_UD
    EndIf

    If (CollectorType$ = 'LS-2') Then
        Shadowing := 0.974
        TrackingError := 0.994
        GeomEffects := 0.98
        Rho_mirror_clean := 0.935
        Dirt_mirror := Reflectivity/Rho_mirror_clean
        Dirt_HCE := (1+ Dirt_mirror)/2
        Error := 0.96
    EndIf
```

```
    If (CollectorType$ = 'LS-3') or (CollectorType$ = 'IST') Then
        Shadowing := 0.974
        TrackingError := 0.994
        GeomEffects := 0.98
        Rho_mirror_clean := 0.935
        Dirt_mirror := Reflectivity/Rho_mirror_clean
        Dirt_HCE := (1+ Dirt_mirror)/2
        Error := 0.96
    EndIf

    " following if statement prevents Dirt_mirror and Dirt_HCE from being larger then 1 if the input for
Reflectivity is larger then Rho_mirror_clean "
    If (Dirt_mirror > 1) Then
        Dirt_mirror := 1
        Dirt_HCE := 1
    EndIf

    If (GlazingIntact$ = 'No') Then
        OptEff_env := 0
        OptEff_abs := Shadowing * TrackingError * GeomEffects * Rho_mirror_clean * Dirt_mirror *
Error * K
    Else
        OptEff_env := Shadowing * TrackingError * GeomEffects * Rho_mirror_clean * Dirt_mirror *
Dirt_HCE * Error * K
        OptEff_abs := OptEff_env * TAU_Envelope
    Endif

END


"****************************************************************************************************************
    FUNCTION fD_h: Hydraulic diameter
****************************************************************************************************************"
FUNCTION fD_h(Flow_Type$)
$COMMON D_2, D_p

    " If 'SNL AZTRAK Platform' is chosen, then the inside absorber diameter accounts for the inserted
plug "
    If (Flow_Type$ = 'Annulus Flow') Then
        fD_h := D_2 - D_p  "[m]"
    Else
        fD_h := D_2  "[m]"
    EndIf

END


"****************************************************************************************************************
    FUNCTION fq_cond_bracket:    Heat loss estimate through HCE support bracket
****************************************************************************************************************"
FUNCTION fq_cond_bracket(T_3)
$COMMON  T_6, T_0, P_6, v_6, g

    " effective bracket perimeter for convection heat transfer"
    P_brac := 0.2032  "[m]"
```

" effective bracket diameter (2 x 1in) "
D_brac := 0.0508  "[m]"

" minimum bracket cross-sectional area for conduction heat transfer"
A_cs_brac := 0.00016129  "[m^2]"

" conduction coefficient for carbon steel at 600 K"
k_brac := 48  "[W/m-K]"

" effective bracket base temperature"
T_base := T_3 - 10  "[C]"

" estimate average bracket temperature "
T_brac := (T_base + T_6) / 3  "[C]"

" estimate film temperature for support bracket "
T_brac6 := (T_brac + T_6) /2  "[C]"

" convection coefficient with and without wind"
If (v_6 <= 0.1) Then

    MU_brac6 := viscosity(AIR, T=T_brac6)  "[N-s/m^2]"
    Rho_brac6 := Density(AIR, T=T_brac6, P=P_6)  "[kg/m^3]"
    Cp_brac6 := CP(AIR, T=T_brac6)  "[kJ/kg-K]"
    k_brac6 := conductivity(AIR, T=T_brac6)  "[W/m-K]"
    NU_brac6 := MU_brac6 / Rho_brac6  "[m^2/s]"
    Alpha_brac6 := k_brac6 / (Cp_brac6 * Rho_brac6 * 1000)  "[m^2/s]"
    Beta_brac6 :=  1 / (T_brac6 + T_0)  "[1/K]"
    Ra_Dbrac := g * Beta_brac6 * ABS(T_brac - T_6) * (D_brac)^3 / (Alpha_brac6 * NU_brac6)

    " Warning Statement if following Nusselt Number correlation is used out of recommended range "
    If (Ra_Dbrac <= 10^(-5)) or (Ra_Dbrac >= 10^12) Then CALL WARNING('The result may not be accurate, since 10^(-5) < Ra_Dbrac < 10^12 does not hold. See Function fq_cond_bracket. Ra_Dbrac = XXXA1', Ra_Dbrac)

    " Churchill and Chu correlation for natural convection from a long isothermal horizontal cylinder "
    Pr_brac6 := NU_brac6 / Alpha_brac6
    Nu#_bar := (0.60 + (0.387 * Ra_Dbrac^(0.1667)) / (1 + (0.559 / Pr_brac6)^(0.5625))^(0.2963) )^2
    h_brac6 := Nu#_bar * k_brac6 / D_brac  "[W/m^2-K]"

Else

    " Thermophysical Properties for air "
    MU_brac := viscosity(AIR, T=T_brac)  "[N-s/m^2]"
    MU_6 := viscosity(AIR, T=T_6)  "[N-s/m^2]"
    Rho_6 := Density(AIR, T=T_6, P=P_6)  "[kg/m^3]"
    Rho_brac := Density(AIR, T=T_brac, P=P_6)  "[kg/m^3]"
    k_brac := conductivity(AIR, T=T_brac)  "[W/m-K]"
    k_6 := conductivity(AIR, T=T_6)  "[W/m-K]"
    k_brac6 := conductivity(AIR, T=T_brac6)  "[W/m-K]"
    Cp_brac := CP(AIR, T=T_brac)  "[kJ/kg-K]"
    Cp_6 := CP(AIR, T=T_6)  "[kJ/kg-K]"

```
NU_6 := MU_6 / Rho_6  "[m^2/s]"
NU_brac := MU_brac / Rho_brac  "[m^2/s]"

Alpha_brac := k_brac / (Cp_brac * Rho_brac * 1000)  "[m^2/s]"
Alpha_6 := k_6 / (Cp_6 * Rho_6 * 1000)  "[m^2/s]"
Re_Dbrac := v_6 * D_brac / NU_6
Pr_brac := NU_brac / Alpha_brac
Pr_6 := NU_6 / Alpha_6

" Warning Statements if following Nusselt Correlation is used out of range "
If (Re_Dbrac <= 1) or (Re_Dbrac >= 10^6) Then CALL WARNING('The result may not be
accurate, since 1 < Re_Dbrac < 10^6 does not hold. See Function fq_cond_bracket. Re_Dbrac =
XXXA1', Re_Dbrac)
If (Pr_6 <= 0.7) or (Pr_6 >= 500) Then CALL WARNING('The result may not be accurate,
since 0.7 < Pr_6 < 500 does not hold. See Function fq_cond_bracket. Pr_6 = XXXA1', Pr_6)

" Coefficients for external forced convection Nusselt Number correlation (Zhukauskas's
correlation) "
If (Pr_6 <= 10) Then
    n := 0.37
Else
    n := 0.36
EndIf

If (Re_Dbrac < 40) Then
    C := 0.75
    m := 0.4
Else

    If (40 <= Re_Dbrac) and (Re_Dbrac< 10^3) Then
        C := 0.51
        m := 0.5
    Else
        If (10^3 <= Re_Dbrac) and (Re_Dbrac < 2*10^5) Then
            C := 0.26
            m := 0.6
        Else
            If (2*10^5 <= Re_Dbrac) and (Re_Dbrac < 10^6) Then
                C := 0.076
                m := 0.7
            EndIf
        EndIf
    EndIf
EndIf

" Zhukauskas's correlation for external forced convection flow normal to an isothermal cylinder
"
Nu#_bar := C * (Re_Dbrac)^m  * (Pr_6)^n * (Pr_6 / Pr_brac)^(0.25)
h_brac6 := Nu#_bar  *  k_brac6  /  D_brac  "[W/m^2-K]"

EndIf

" estimated conduction heat loss through HCE support brackets / HCE length "
fq_cond_bracket := SQRT(h_brac6 * P_brac * k_brac * A_cs_brac) * (T_base - T_6)/4.06  "[W/m]"

END
```

```
"**********************************************************************************************
     FUNCTION fq_HeatLoss: Heat loss definition
**********************************************************************************************"
FUNCTION fq_HeatLoss(q_34conv, q_34rad, q_56conv, q_57rad, q_cond_bracket)
$COMMON GlazingIntact$

    If (GlazingIntact$ = 'Yes') Then
        fq_HeatLoss := q_56conv + q_57rad + q_cond_bracket  "[W/m]"
    Else
        fq_HeatLoss := q_34conv + q_34rad + q_cond_bracket  "[W/m]"
    EndIf

END


"**********************************************************************************************
     Constants and conversions
**********************************************************************************************"
" Stefan-Boltzmann constant "
sigma = 5.67E-8  "[W/m^2-K^4]"

" Used to convert temperature from C to K "
T_0 = 273.15  "[C]"

" Gravitational constant "
g = 9.81  "[m/s^2]"

" Wind speed from MPH to m/s conversion "
v_6 = v_6mph * CONVERT(mph, m/s)  "[m/s]"


"**********************************************************************************************
     Optical properties
**********************************************************************************************"
Alpha_env = .02

" Calls procedure that determines optical properties "
CALL pSelectiveCoatingProperties(T_3: EPSILON_3, Alpha_abs, TAU_envelope)

" Calls procedure that determines effective optical efficiencies at the glass envelope and absorber "
CALL pOpticalEfficiency(CollectorType$: OptEff_env, OptEff_abs)

" Inner and outer glass envelope emissivities (Pyrex)"
EPSILON_4 = 0.86
EPSILON_5 = 0.86

" Incident angle modifier from test data for SEGS LS-2 receiver "
K = COS(THETA) + 0.000884 * THETA - 0.00005369 * (THETA)^2


"**********************************************************************************************
     Heat collector element size
**********************************************************************************************"
" Calls procedure for determining HCE dimensions based on 'CollectorType' "
CALL pHCEdimensions(CollectorType$: D_2, D_3, D_4, D_5,  W_aperture)
```

```
"***************************************************************************************************************
    Ambient conditions
***************************************************************************************************************"
" Effective sky temperature estimated as 8 C below ambient "
T_7 = T_6 - 8  "[C]"

" Converts ambient pressure from 0.83 atm to kPa, ambient pressure is treated as a constant "
P_6 = 0.83 * CONVERT(atm, kPa)  "[kPa]"

" Standard ambient air temperature "
T_std = 25  "[C]"

" Incoming solar radiation per aperture length "
q_i  = I_b *  W_aperture  "[W/m]"

"***************************************************************************************************************
    Temporary outputs and inputs
***************************************************************************************************************"
" Space used for any temporary outputs or inputs "

"***************************************************************************************************************
    Hydraulic diameter
***************************************************************************************************************"
"Calls function to calculate HTF hydraulic diameter "
D_h = fD_h(Flow_Type$)


"***************************************************************************************************************
    Heat transfer fluid flow rates
***************************************************************************************************************"
" Calls function to calculate HTF cross-section flow area "
A_cs = fA_cs(D_2, D_p)  "[m^2]"

" Converts HTF flow rate from gpm to m^3/s "
v_1volm = v_1volg* CONVERT(gpm, m^3/s)  "[m^3/s]"

" HTF velocity "
v_1 = v_1volm / (A_cs)  "[m/s]"


"***************************************************************************************************************
    q_12conv     Convective heat transfer rate between the heat transfer fluid and absorber
***************************************************************************************************************"
CALL Pq_12conv(T_1ave, T_2, Fluid$: q_12conv)


"***************************************************************************************************************
    q_23cond     Conduction heat transfer rate through the absorber
***************************************************************************************************************"

" Absorber conductance, temperature and material type dependent "
k_23 = fk_23(T_2, T_3)  "[W/m-K]"

q_23cond = 2 * PI  * k_23 * (T_3 - T_2) / LN(D_3 / D_2)  "[W/m]"
```

```
"***************************************************************************************************************
    q_34conv    Convective heat transfer rate between the absorber pipe and glazing
***************************************************************************************************************"
q_34conv =  fq_34conv(T_3, T_4)  "[W/m]"


"***************************************************************************************************************
    q_34rad   Radiation heat transfer rate between the absorber surface and glazing inner surface
***************************************************************************************************************"
q_34rad = fq_34rad(T_3, T_4)  "[W/m]"


"***************************************************************************************************************
    q_45cond    Conduction  heat transfer rate through the glazing
***************************************************************************************************************"
" glass envelope conductivity "
K_45 = 1.04  "[W/m-K]"

q_45cond = 2 * PI  * K_45 * (T_4 - T_5) / LN(D_5 / D_4)  "[W/m]"


"***************************************************************************************************************
    q_56conv    Convective heat transfer rate from the glazing to the atmosphere
***************************************************************************************************************"
q_56conv = fq_56conv(T_5, T_6)  "[W/m]"


"***************************************************************************************************************
    q_57rad   Radiation heat transfer rate between the glazing outer surface and the sky
***************************************************************************************************************"
q_57rad = fq_57rad(T_5, T_7)  "[W/m]"


"***************************************************************************************************************
    q_3SolAbs        Solar flux on absorber pipe
***************************************************************************************************************"
q_3SolAbs = q_i * OptEff_abs * Alpha_abs  "[W/m]"


"***************************************************************************************************************
    q_5SolAbs        Solar Flux on glazing Envelope
***************************************************************************************************************"
q_5SolAbs = fq_5SolAbs(q_i)  "[W/m]"


"***************************************************************************************************************
    q_cond_bracketHCE support bracket conductive losses
***************************************************************************************************************"
q_cond_bracket = fq_cond_bracket(T_3)  "[W/m]"


"***************************************************************************************************************
 One dimensional (Radial) model
***************************************************************************************************************"
CALL Pq_45cond(q_34conv, q_34rad: q_45cond)  "[W/m]"
```

CALL Pq_56conv(q_45cond, q_5SolAbs, q_57rad: q_56conv)  "[W/m]"


q_12conv = q_23cond  "[W/m]"
q_3SolAbs - q_23cond - q_34conv - q_34rad - q_cond_bracket = 0  "[W/m]"
q_HeatLoss = fq_HeatLoss(q_34conv, q_34rad, q_56conv, q_57rad, q_cond_bracket)  "[W/m]"
q_OptLoss = q_i * (1-ETA_EffectiveOptEff/100)  "[W/m]"
q_HeatGain = q_12conv  "[W/m]"


"************************************************************************************************************
    ETA_Col Collector efficiency
************************************************************************************************************"
ETA_Col = fETA_Col(q_12conv, q_i)*100  "[%]"
ETA_EffectiveOptEff = (OptEff_abs * Alpha_abs + OptEff_env * Alpha_env)*100  "[%]"

# F. Two-Dimensional Design Study Version of EES Code

(Tab settings have been shortened and numerous comment statements have been omitted to reduce length of following code.)

```
"*********************************************************************************************************
    PROCEDURE Pq_12conv : Convective heat transfer rate from the HTF to the inside of the
receiver tube
*********************************************************************************************************"
PROCEDURE Pq_12conv(T_1ave, v_1ave, T_2, Fluid$: q_12conv, Cp_1)
$Common D_h, D_2, L, TestType$

    " Warning Statements if HTF is evaluated out of recommended temperature ranges "
    If (Fluid$ = 'Syltherm 800') Then
        If (T_1ave < -40) or (400 < T_1ave) Then CALL WARNING('The result may not be accurate,
since Syltherm 800 fluid properties are out of recommended temperature range, -40 C < T < 400 C.
See Procedure Pq_12conv.T_1ave = XXXA1', T_1ave)
    EndIf
    If (Fluid$ = 'Therminol VP1') Then
        If (T_1ave < 12) or (400 < T_1ave) Then CALL WARNING('The result may not be accurate,
since Therminol VP1 fluid properties are out of recommended temperature range, 12 C < T < 400 C .
See Procedure Pq_12conv.T_1ave = XXXA1', T_1ave)
    EndIf
    If (Fluid$ = 'Xceltherm 600') Then
        If (T_1ave < -20) or (316 < T_1ave) Then CALL WARNING('The result may not be accurate,
since Xceltherm 600 fluid properties are out of recommended temperature range, -20 C < T < 316 C..
See Procedure Pq_12conv.T_1ave = XXXA1', T_1ave)
    EndIf
    If (Fluid$ = 'Therminol 59') Then
        If (T_1ave < -45) or (315 < T_1ave) Then CALL WARNING('The result may not be accurate,
since Therminol 59 fluid properties are out of recommended temperature range, -45 C < T < 315 C..
See Procedure Pq_12conv.T_1ave = XXXA1', T_1ave)
    EndIf
    If (Fluid$ = 'Therminol 66') Then
        If (T_1ave < 0) or (345 < T_1ave) Then CALL WARNING('The result may not be accurate,
since Therminol 66 fluid properties are out of recommended temperature range, 0 C < T < 345 C..
See Procedure Pq_12conv.T_1ave = XXXA1', T_1ave)
    EndIf
    If (Fluid$ = 'Therminol XP') Then
        If (T_1ave < -20) or (315 < T_1ave) Then CALL WARNING('The result may not be accurate,
since Therminol XP fluid properties are out of recommended temperature range, -20 C < T < 315 C..
See Procedure Pq_12conv.T_1ave = XXXA1', T_1ave)
    EndIf
    If (Fluid$ = 'Dowtherm Q') Then
        If (T_1ave < -35) or (330 < T_1ave) Then CALL WARNING('The result may not be accurate,
since Dowtherm Q fluid properties are out of recommended temperature range, -35 C < T < 330 C..
See Procedure Pq_12conv.T_1ave = XXXA1', T_1ave)
    EndIf
    If (Fluid$ = 'Dowtherm RP') Then
        If (T_1ave < -20) or (350 < T_1ave) Then CALL WARNING('The result may not be accurate,
since Dowtherm RP fluid properties are out of recommended temperature range, -20 C < T < 350 C..
See Procedure Pq_12conv.T_1ave = XXXA1', T_1ave)
    EndIf
    If (Fluid$ = 'Salt (60% NaNO3, 40% KNO3)') Then
```

If (T_1ave < 260) or (621 < T_1ave) Then CALL WARNING('The result may not be accurate, since Salt (60% NaNO3, 40% KNO3) fluid properties are out of recommended temperature range, 260 C < T < 621 C. See Procedure Pq_12conv.T_1ave = XXXA1', T_1ave)
    EndIf
If (Fluid$ = 'Hitec XL') Then
      If (T_1ave < 266) or (480 < T_1ave) Then CALL WARNING('The result may not be accurate, since Hitec XL fluid properties are out of recommended temperature range, 266 C < T < 480 C. See Procedure Pq_12conv.T_1ave = XXXA1', T_1ave)
    EndIf
If (Fluid$ = 'Water') Then
    If (T_1ave < 0) or (100 < T_1ave) Then CALL WARNING('The result may not be accurate, since Water fluid properties are out of recommended temperature range, 0 C < T < 100 C. See Procedure Pq_12conv.T_1ave = XXXA1', T_1ave)
    EndIf

   " Thermophysical properties for HTF "
   MU_1 := INTERPOLATE(Fluid$,'MU','T',T=T_1ave)  "[kg/m-s]"
   MU_2 := INTERPOLATE(Fluid$,'MU','T',T=T_2)  "[kg/m-s]"
   Cp_1 := INTERPOLATE(Fluid$,'Cp','T',T=T_1ave)  "[J/kg-K]"
   Cp_2 := INTERPOLATE(Fluid$,'Cp','T',T=T_2)  "[J/kg-K]"
   k_1 := INTERPOLATE(Fluid$,'k','T',T=T_1ave)  "[W/m-K]"
   k_2 := INTERPOLATE(Fluid$,'k','T',T=T_2)  "[W/m-K]"
   RHO_1 := INTERPOLATE(Fluid$,'RHO','T',T=T_1ave)  "[kg/m^3]"

   Re_D2 := ABS((RHO_1 * D_h * v_1ave) / (MU_1))

   Pr_2 := ABS(Cp_2 * MU_2 / k_2)
   Pr_1 := ABS(Cp_1 * MU_1 / k_1)

   " Warning statements if Nusselt Number correlation is used out of recommended range "
   If (Pr_1 <= 0.5) or (2000 <= Pr_1) Then CALL WARNING('The result may not be accurate, since 0.5 < Pr_1 < 2000 does not hold. See PROCEDURE Pq_12conv. Pr_1 = XXXA1', Pr_1)
     If (Pr_2 <= 0.5) or (2000 <= Pr_2) Then CALL WARNING('The result may not be accurate, since 0.5 < Pr_2 < 2000 does not hold. See PROCEDURE Pq_12conv. Pr_2 = XXXA1', Pr_2)
     If ( Re_D2 <= (2300) ) or (5*10^6 <= Re_D2 ) Then CALL WARNING('The result may not be accurate, since 2300 < Re_D2 < (5 * 10^6) does not hold. See PROCEDURE Pq_12conv. Re_D2 = XXXA1', Re_D2)

   " Turbulent/transitional flow Nusselt Number correlation (modified Gnielinski correlation) "
   f_2 := (1.82 * LOG10(Re_D2) - 1.64)^(-2)
   Nu#_D2 := (f_2 / 8) * (Re_D2 - 1000) * Pr_1 / (1 + 12.7 * (f_2/ 8)^(0.5) * (Pr_1^(0.6667) -1)) * (Pr_1 / Pr_2)^0.11

   h_1 := Nu#_D2 * k_1 / D_h  "[W/m^2-K]"
   q_12conv := h_1 * D_2 * PI  * (T_2 - T_1ave)  "[W/m]"

End


"*********************************************************************************************************
   FUNCTION fq_34conv :   Convective heat transfer rate between the absorber outer surface and the glazing inner surface
*********************************************************************************************************"
FUNCTION fq_34conv(T_3, T_4, AnnulusGas$)
$Common D_3, D_4, L, P_a, P_6, g, v_6, T_0, T_6, T_std, GlazingIntact$

P_a1 := P_a * CONVERT(torr, kPa)  "[kPa]"

T_36 := (T_3 + T_6) / 2  "[C]"

If (GlazingIntact$ = 'No') Then

    " Thermophysical Properties for air "
    Rho_3 := Density(AIR, T=T_3, P=P_6)  "[kg/m^3]"
    Rho_6 := Density(AIR, T=T_6, P=P_6)  "[kg/m^3]"

    If (v_6 <= 0.1) Then
        MU_36 := viscosity(AIR, T=T_36)  "[N-s/m^2]"
        Rho_36 := Density(AIR, T=T_36, P=P_6)  "[kg/m^3]"
        Cp_36 := CP(AIR, T=T_36)  "[kJ/kg-K]"
        k_36 := conductivity(AIR, T=T_36)  "[W/m-K]"
        NU_36 := MU_36 / Rho_36  "[m^2/s]"
        Alpha_36 := k_36 / (Cp_36 * Rho_36 * 1000)  "[m^2/s]"
        Beta_36 :=  1 / (T_36 + T_0)  "[1/K]"
        Ra_D3 := g * Beta_36 * ABS(T_3 - T_6) * (D_3)^3 / (Alpha_36 * NU_36)

        " Warning Statement if following Nusselt Number correlation is used out of recommended range "
        If (Ra_D3 <= 10^(-5)) or (Ra_D3 >= 10^12) Then CALL WARNING('The result may not be accurate, since 10^(-5) < Ra_D3 < 10^12 does not hold. See Function fq_34conv. Ra_D3 = XXXA1', Ra_D3)

        " Churchill and Chu correlation for natural convection from a long isothermal horizontal cylinder "
        Pr_36 := NU_36 / Alpha_36
        Nu#_bar := (0.60 + (0.387 * Ra_D3^(0.1667)) / (1 + (0.559 / Pr_36)^(0.5625))^(0.2963) )^2
        h_36 := Nu#_bar * k_36 / D_3  "[W/m^2-K]"
        fq_34conv := h_36 * PI * D_3 * (T_3 - T_6)  "[W/m]"

    Else

        " Thermophysical Properties for air "
        MU_3 := viscosity(AIR, T=T_3)  "[N-s/m^2]"
        MU_6 := viscosity(AIR, T=T_6)  "[N-s/m^2]"
        k_3 := conductivity(AIR, T=T_3)  "[W/m-K]"
        k_6 := conductivity(AIR, T=T_6)  "[W/m-K]"
        k_36 := conductivity(AIR, T=T_36)  "[W/m-K]"
        Cp_3 := CP(AIR, T=T_3)  "[kJ/kg-K]"
        Cp_6 := CP(AIR, T=T_6)  "[kJ/kg-K]"
        NU_6 := MU_6 / Rho_6  "[m^2/s]"
        NU_3 := MU_3 / Rho_3  "[m^2/s]"

        Alpha_3 := k_3 / (Cp_3 * Rho_3 * 1000)  "[m^2/s]"
        Alpha_6 := k_6 / (Cp_6 * Rho_6 * 1000)  "[m^2/s]"
        Re_D3 := v_6 * D_3 / NU_6
        Pr_3 := NU_3 / Alpha_3
        Pr_6 := NU_6 / Alpha_6

        " Warning Statements if following Nusselt Correlation is used out of range "
        If (Re_D3 <= 1) or (Re_D3 >= 10^6) Then CALL WARNING('The result may not be accurate, since 1 < Re_D3 < 10^6 does not hold. See Function fq_34conv. Re_D3 = XXXA1', Re_D3)

If (Pr_6 <= 0.7) or (Pr_6 >= 500) Then CALL WARNING('The result may not be accurate, since 0.7 < Pr_6 < 500 does not hold. See Function fq_34conv. Pr_6 = XXXA1', Pr_6)

" Coefficients for external forced convection Nusselt Number correlation (Zhukauskas's correlation) "
    If (Pr_6 <= 10) Then
      n := 0.37
    Else
      n := 0.36
    EndIf

    If (Re_D3 < 40) Then
      C := 0.75
      m := 0.4
    Else

      If (40 <= Re_D3) and (Re_D3 < 10^3) Then
        C := 0.51
        m := 0.5
      Else
        If (10^3 <= Re_D3) and (Re_D3 < 2*10^5) Then
          C := 0.26
          m := 0.6
        Else
          If (2*10^5 <= Re_D3) and (Re_D3 < 10^6) Then
            C := 0.076
            m := 0.7
          EndIf
        EndIf
      EndIf
    EndIf

" Zhukauskas's correlation for external forced convection flow normal to an isothermal cylinder "
    Nu#_bar := C * (Re_D3)^m  * (Pr_6)^n * (Pr_6 / Pr_3)^(0.25)
    h_36 := Nu#_bar  *  k_36  /  D_3  "[W/m^2-K]"
    fq_34conv :=  h_36  *  D_3  *  PI  *  (T_3 - T_6)  "[W/m]"
  EndIf
Else

  T_34 := (T_3 + T_4) / 2  "[C]"

" Thermophysical Properties for gas in annulus space "
If (AnnulusGas$ = 'Argon') Then

  MU_34 := INTERPOLATE('Argon', 'MU', 'T', T = (T_34 + T_0))  "[kg/m-s]"
  Cp_34 := INTERPOLATE('Argon', 'Cp', 'T', T = (T_34 + T_0))  "[kJ/kg-K]"
  Cv_34 := INTERPOLATE('Argon', 'Cv', 'T', T = (T_34 + T_0))  "[kJ/kg-K]"
  Rho_34 := P_a1 / (0.20813 * (T_34 + T_0))  "[kg/m^3]"
  k_34 := INTERPOLATE('Argon', 'k', 'T', T = (T_34 + T_0))  "[W/m-K]"
  k_std := INTERPOLATE('Argon', 'k', 'T', T = (T_std + T_0))  "[W/m-K]"
Else
  MU_34 := VISCOSITY(AnnulusGas$, T=T_34)  "[kg/m-s]"
  Cp_34 := CP(AnnulusGas$, T=T_34)  "[kJ/kg-K]"
  Cv_34 := CV(AnnulusGas$, T=T_34)  "[kJ/kg-K]"
  k_34 := CONDUCTIVITY(AnnulusGas$, T=T_34)  "[W/m-K]"

```
        Rho_34 := DENSITY(AnnulusGas$, T=T_34, P=P_a1)  "[kg/m^3]"
        k_std := CONDUCTIVITY(AnnulusGas$, T=T_std)  "[W/m-K]"
    EndIf


    " Modified Raithby and Hollands correlation for natural convection in an annular space
between horizontal cylinders "
    Alpha_34 := k_34 /(Cp_34 * Rho_34 * 1000)  "[m^2/s]"
    NU_34 := MU_34 / Rho_34  "[m^2/s]"
    Beta_34 := 1 / (T_34 + T_0)  "[1/K]"
    Ra_D3 := g * Beta_34 * ABS(T_3 - T_4) * (D_3)^3 / (Alpha_34 * NU_34)
    Ra_D4 := g * Beta_34 * ABS(T_3 - T_4) * (D_4)^3 / (Alpha_34 * NU_34)
    Pr_34 := NU_34 / Alpha_34
    Natq_34conv := 2.425 * k_34 * (T_3 - T_4)  * (Pr_34 * Ra_D3 / (0.861 + Pr_34))^(0.25) / (1 +
(D_3/ D_4)^(0.6))^(1.25)  "[W/m]"


    " Free-molecular heat transfer for an annular space between horizontal cylinders "
    P := P_a * CONVERT(torr, mmHg)  "[mmHg]"
    C1 := 2.331*10^(-20)  "[mmHg-cm^3/K]"


    If (AnnulusGas$ = 'Air') Then
        Delta := 3.53 * 10^(-8)  "[cm]"
    EndIf


    If (AnnulusGas$ = 'H2') Then
        Delta := 2.4 * 10^(-8)  "[cm]"
    EndIf


    If (AnnulusGas$ = 'Argon') Then
        Delta := 3.8*10^(-8)  "[cm]"
    EndIf


    Lambda := C1 * (T_34 + T_0) / (P * Delta^2)  "[cm]"
    Gamma := Cp_34 / Cv_34
    a := 1
    b := (2 - a) * (9 * Gamma - 5) / (2 * a * (Gamma + 1))
    h_34 := k_std / (D_3 / 2 * ln(D_4 / D_3) + b * Lambda * (D_3 / D_4 + 1))  "[W/m^2-K]"
    Kineticq_34conv  := D_3 * PI * h_34 * (T_3 - T_4)  "[W/m]"


    " Following compares free molecular heat transfer with natural convection heat transfer and
uses the largest value for heat transfer in annulus "
    If (Kineticq_34conv > Natq_34conv) Then
        fq_34conv := Kineticq_34conv  "[W/m]"


        " Warning statement if free molecular correlation is used our of range"
        If  (Ra_D4 < 10^7) Then CALL WARNING('The result may not be accurate, since (D_4 /
(D_4 - D_3))^4 < Ra_D4 < 10^7 does not hold. See Function fq_34conv. Ra_D4 = XXXA1', Ra_D4)


    Else
        fq_34conv := Natq_34conv  "[W/m]"
    EndIf
  EndIf


End



"*********************************************************************************************************
```

\*\*\*\*\*\*\*\*\*\*\*\*\*\*\*\*\*\*\*\*\*\*\*\*\*\*\*\*\*\*\*\*\*\*\*\*\*\*\*\*\*\*\*\*\*\*\*\*\*\*\*\*\*\*\*\*\*\*\*\*\*\*\*\*\*\*\*\*\*\*\*\*\*\*\*\*\*\*\*\*\*\*\*\*\*\*\*\*\*\*\*\*\*\*\*\*\*\*\*\*\*\*\*\*\*\*\*\*"

FUNCTION fq_34rad(T_3, T_4, i)
$COMMON D_3, D_4, L, T_7, T_0, sigma, EPSILON_3[1..imax], EPSILON_4, GlazingIntact$

    If (GlazingIntact$ = 'No') Then
        fq_34rad :=EPSILON_3[i] * PI * D_3  * sigma * ((T_3 + T_0)^4 - (T_7 + T_0)^4)  "[W/m]"
    Else
        fq_34rad := PI * D_3 * sigma * ((T_3 + T_0)^4 - (T_4 + T_0)^4) / (1 / EPSILON_3[i] + D_3 / D_4 * ( 1 / EPSILON_4 - 1))  "[W/m]"
    EndIf

END


"\*\*\*\*\*\*\*\*\*\*\*\*\*\*\*\*\*\*\*\*\*\*\*\*\*\*\*\*\*\*\*\*\*\*\*\*\*\*\*\*\*\*\*\*\*\*\*\*\*\*\*\*\*\*\*\*\*\*\*\*\*\*\*\*\*\*\*\*\*\*\*\*\*\*\*\*\*\*\*\*\*\*\*\*\*\*\*\*\*\*\*\*\*\*\*\*\*\*\*\*\*\*
    FUNCTION fq_56conv :    Convective heat transfer rate between the glazing outer surface and the ambient air
\*\*\*\*\*\*\*\*\*\*\*\*\*\*\*\*\*\*\*\*\*\*\*\*\*\*\*\*\*\*\*\*\*\*\*\*\*\*\*\*\*\*\*\*\*\*\*\*\*\*\*\*\*\*\*\*\*\*\*\*\*\*\*\*\*\*\*\*\*\*\*\*\*\*\*\*\*\*\*\*\*\*\*\*\*\*\*\*\*\*\*\*\*\*\*\*\*\*\*\*\*\*\*\*\*\*\*\*"

FUNCTION fq_56conv(T_5, T_6)
$Common D_5, L,  P_6, v_6, g, T_0, GlazingIntact$

    T_56 := (T_5 + T_6) / 2  "[C]"

    " Thermophysical Properties for air "
    MU_5 := VISCOSITY(Air,T=T_5)  "[kg/m-s]"
    MU_6 := VISCOSITY(Air,T=T_6)  "[kg/m-s]"
    MU_56 := VISCOSITY(Air, T=T_56)  "[kg/m-s]"
    k_5 := CONDUCTIVITY(Air,T=T_5)  "[W/m-K]"
    k_6 := CONDUCTIVITY(Air,T=T_6)  "[W/m-K]"
    k_56 := CONDUCTIVITY(Air, T=T_56)  "[W/m-K]"
    Cp_5 := SPECHEAT(Air,T=T_5)  "[kJ/kg-K]"
    Cp_6 := SPECHEAT(Air,T=T_6)  "[kJ/kg-K]"
    Cp_56 := CP(AIR, T=T_56)  "[kJ/kg-K]"
    Rho_5 := DENSITY(Air,T=T_5, P=P_6)  "[kg/m^3]"
    Rho_6 := DENSITY(Air,T=T_6, P=P_6)  "[kg/m^3]"
    Rho_56 := DENSITY(Air, T=T_56, P=P_6)  "[kg/m^3]"

    " If the glass envelope is missing then the convection heat transfer from the glass envelope is forced to zero by T_5 = T_6 "
    If (GlazingIntact$ = 'No') Then
        fq_56conv := (T_5 - T_6)  "[W/m]"
    Else
        If (v_6 <= 0.1) Then

            " Coefficients for Churchill and Chu natural convection correlation "
            NU_56 := MU_56 / Rho_56  "[m^2/s]"
            Alpha_56 := k_56 / (Cp_56 * Rho_56 * 1000)  "[m^2/s]"
            Beta_56 :=  1 / (T_56 + T_0)  "[1/K]"
            Ra_D5 := g *Beta_56 * ABS(T_5 - T_6) * (D_5)^3 / (Alpha_56 * NU_56)

            " Warning Statement if following Nusselt Number correlation is used out of range "
            If (Ra_D5 <= 10^(-5)) or (Ra_D5 >= 10^12) Then CALL WARNING('The result may not be accurate, since 10^(-5) < Ra_D5 < 10^12 does not hold. See Function fq_56conv. Ra_D5 = XXXA1', Ra_D5)

" Churchill and Chu correlation for natural convection for a horizontal cylinder "
Pr_56 := NU_56 / Alpha_56
Nu#_bar := (0.60 + (0.387 * Ra_D5^(0.1667)) / (1 + (0.559 / Pr_56)^(0.5625))^(0.2963) )^2
h_6 := Nu#_bar * k_56 / D_5  "[W/m^2-K]"
fq_56conv := h_6 * PI * D_5 * (T_5 - T_6)  "[W/m]"

    Else

        " Coefficients for Zhukauskas's correlation "
        Alpha_5 := k_5 / (Cp_5 * Rho_5 * 1000)  "[m^2/s]"
        Alpha_6 := k_6 / (Cp_6 * Rho_6 * 1000)  "[m^2/s]"
        NU_5 := MU_5 / Rho_5  "[m^2/s]"
        NU_6 := MU_6 / Rho_6  "[m^2/s]"
        Pr_5 := NU_5 / Alpha_5
        Pr_6 := NU_6 / Alpha_6
        Re_D5 := v_6 * D_5 * Rho_6 / MU_6

        " Warning Statement if following Nusselt Number coorelation is used out of range "
        If (Pr_6 <= 0.7) or (Pr_6 >= 500) Then CALL WARNING('The result may not be accurate,
since 0.7 < Pr_6 < 500 does not hold. See Function fq_56conv. Pr_6 = XXXA1', Pr_6)
        If (Re_D5 <= 1) or (Re_D5 >= 10^6) Then CALL WARNING('The result may not be
accurate, since 1 < Re_D5 < 10^6 does not hold. See Function fq_56conv. Re_D5 = XXXA1 ',
Re_D5)

        " Zhukauskas's correlation for forced convection over a long horizontal cylinder "
        If (Pr_6 <= 10) Then
            n := 0.37
        Else
            n := 0.36
        EndIf

        If (Re_D5 < 40) Then
            C := 0.75
            m := 0.4
        Else
            If (40 <= Re_D5) and (Re_D5 < 10^3) Then
                C := 0.51
                m := 0.5
            Else
                If (10^3 <= Re_D5) and (Re_D5 < 2*10^5) Then
                    C := 0.26
                    m := 0.6
                Else
                    If (2*10^5 <= Re_D5) and (Re_D5 < 10^6) Then
                        C := 0.076
                        m := 0.7
                    EndIf
                EndIf
            EndIf
        EndIf

        Nu#_6 := C * Re_D5^m *  Pr_6^n  *(Pr_6/Pr_5)^0.25
        h_6 := Nu#_6 * k_6 / D_5  "[W/m^2-K]"
        fq_56conv := h_6 * PI * D_5 * (T_5 - T_6)  "[W/m]"
    EndIf

```
      EndIf
End


"*************************************************************************************************
    FUNCTION fq_57rad : Radiation heat transfer rate between the glazing outer surface and the sky
"*************************************************************************************************"
FUNCTION  fq_57rad(T_5, T_7)
$COMMON EPSILON_5, D_5, L, sigma, T_0, GlazingIntact$

   " If glass envelope is missing then radiation heat transfer from glass envelope is set to zero;
otherwise, radiative heat transfer for a small convex object in a large cavity "
   If (GlazingIntact$ = 'No') Then
      fq_57rad := 0  "[W/m]"
   Else
      fq_57rad  := EPSILON_5 * PI * D_5 * sigma * ((T_5 + T_0)^4 - (T_7 + T_0)^4)  "[W/m]"
   EndIf

END


"*************************************************************************************************
    FUNCTION fq_5SolAbs :  Solar flux on glazing
"*************************************************************************************************"
FUNCTION fq_5SolAbs(q_i)
$COMMON Alpha_env, OptEff_env, GlazingIntact$

   " If glass envelope is missing then solar absorption in glass envelope is set to zero; otherwise,
solar absorption is estimated with an optical efficiency term "
   If (GlazingIntact$ = 'No') Then
      fq_5SolAbs :=0  "[W/m]"
   Else
      fq_5SolAbs := q_i * OptEff_env * Alpha_env  "[W/m]"
   EndIf

END


"*************************************************************************************************
    PROCEDURE Pq_45cond :  One dimensional energy equation about inside surface of glazing
"*************************************************************************************************"
PROCEDURE Pq_45cond(q_34conv, q_34rad: q_45cond)
$COMMON GlazingIntact$

   " If glass envelope is missing then radial conduction through glass envelope is set to zero;
otherwise, the energy balance is used "
   If (GlazingIntact$ = 'No') Then
      q_45cond :=0  "[W/m]"
   Else
      q_45cond := q_34conv+ q_34rad  "[W/m]"
   EndIf

END


"*************************************************************************************************
```

130

**********************************************************************************************************"
PROCEDURE Pq_56conv(q_45cond, q_5SolAbs, q_57rad: q_56conv)
$COMMON GlazingIntact$

   " If the glass envelope is missing then the convective heat transfer from the envelope is set to
zero; otherwise, the energy balance is used "
   If (GlazingIntact$ = 'No') Then
      q_56conv := 0  "[W/m]"
   Else
      q_56conv := q_45cond+ q_5SolAbs - q_57rad  "[W/m]"
   EndIf

END


"**********************************************************************************************************
   FUNCTION fA_cs : Inside cross sectional flow area of absorber
**********************************************************************************************************"
FUNCTION fA_cs(D_2, D_p)
$COMMON TestType$

   " If 'SNL AZTRAK Platform'  then the HTF flow area accounts for the inserted plug "
   If (TestType$ = 'SNL AZTRAK Platform') Then
      fA_cs := PI * (D_2 ^2 - D_p ^2) / 4  "[m^2]"
   Else
      fA_cs := PI * (D_2 ^2 / 4)  "[m^2]"
   EndIf

END


"**********************************************************************************************************
   FUNCTION fETA_Col :    Collector efficiency
**********************************************************************************************************"
FUNCTION fETA_Col(q_12conv, q_i)

   " If heat is leaving the HTF, then the collector efficiency is set to zero "
   If ((q_12conv/q_i) <= 0.001) Then
      fETA_Col := 0
   Else
      fETA_Col := q_12conv/q_i
   EndIf

END


"**********************************************************************************************************
   FUNCTION fk_23:  Absorber conductance
**********************************************************************************************************"
{ Based on linear fit of data from "Alloy Digest, Sourcebook, Stainless Steels"; ASM International,
2000.}

FUNCTION fk_23(T_2, T_3)
$COMMON AbsorberMaterial$

```
    T_23 := (T_2  + T_3)/2  "[C]"


    If (AbsorberMaterial$ = '304L') or (AbsorberMaterial$ = '316L') Then
        fk_23 := 0.013 * T_23 + 15.2  "[W/m-K]"
    EndIf


    If (AbsorberMaterial$ = '321H') Then
        fk_23 := 0.0153 * T_23 + 14.775  "[W/m-K]"
    EndIf


    If (AbsorberMaterial$ = 'B42 Copper Pipe') Then
        fk_23 := 400  "[W/m-K]"
    EndIf


END


"********************************************************************************************************
    PROCEDURE pSelectiveCoatingProperties: Selective Coating Emissivity and Absorptance
********************************************************************************************************"
PROCEDURE pSelectiveCoatingProperties(imax, T_3[1..imax]: EPSILON_3[1..imax], Alpha_abs,
TAU_envelope)
$COMMON  T_0, TAU_envelope_UD, Alpha_abs_UD, EPSILON_3_100_UD, EPSILON_3_400_UD,
SelectiveCoating$

    " Do-Loop to calculate emissivity for all the HCE increments, and to return optical properties for
chosen selective coating type  "
    j := 0
    repeat
    j := j+1

    If (SelectiveCoating$ = 'User-Defined') Then
        TAU_envelope := TAU_envelope_UD
        Alpha_abs := Alpha_abs_UD
        EPSILON_3[j] :=  EPSILON_3_100_UD - (EPSILON_3_400_UD - EPSILON_3_100_UD)/3 +
T_3[j] * (EPSILON_3_400_UD - EPSILON_3_100_UD)/300
    Endif

    If (SelectiveCoating$ = 'Black Chrome (SNL test)') Then
        TAU_envelope := 0.935
        Alpha_abs := 0.94
        EPSILON_3[j] := 0.0005333 * (T_3[j]+T_0) - 0.0856
        If (EPSILON_3[j] < 0.11) Then
            EPSILON_3[j] := 0.11
        EndIf
    Endif

    If (SelectiveCoating$ = 'Luz Cermet (SNL test)') Then
        TAU_envelope := 0.935
        Alpha_abs := 0.92
        EPSILON_3[j] := 0.000327 * (T_3[j]+T_0) - 0.065971
        If (EPSILON_3[j] < 0.05) Then
            EPSILON_3[j] := 0.05
        EndIf
    Endif
```

```
If (SelectiveCoating$ = 'Solel UVAC Cermet (SNL test a)') Then
    TAU_envelope := 0.965
    Alpha_abs := 0.96
    EPSILON_3[j] := 2.249*10^(-7)*(T_3[j])^2 + 1.039*10^(-4)*T_3[j] + 5.599*10^(-2)
EndIf

If (SelectiveCoating$ = 'Solel UVAC Cermet (SNL test b)') Then
    TAU_envelope := 0.965
    Alpha_abs := 0.95
    EPSILON_3[j] := 1.565*10^(-7)*(T_3[j])^2 + 1.376*10^(-4)*T_3[j] + 6.966*10^(-2)
EndIf

If (SelectiveCoating$ = 'Solel UVAC Cermet (SNL test avg)') Then
    TAU_envelope := 0.965
    Alpha_abs := 0.955
    EPSILON_3[j] := 1.907*10^(-7)*(T_3[j])^2 + 1.208*10^(-4)*T_3[j] + 6.282*10^(-2)
EndIf

If (SelectiveCoating$ = 'Solel UVAC Cermet (0.10 @ 400C)') Then
    TAU_envelope := 0.97
    Alpha_abs := 0.98
    EPSILON_3[j] := 2.084*10^(-4)*T_3[j] + 1.663*10^(-2)
EndIf

If (SelectiveCoating$ = 'Solel UVAC Cermet (0.07 @ 400C)') Then
    TAU_envelope := 0.97
    Alpha_abs := 0.97
    EPSILON_3[j] := 1.666*10^(-4)*T_3[j] + 3.375*10^(-3)
EndIf

until (j>=(imax))

END


"********************************************************************************************************
    PROCEDURE pHCEdimensions:  HCE dimensions based on HCE type
********************************************************************************************************"
PROCEDURE pHCEdimensions(HCEtype$: D_4,  D_5, A_aperture, L_aperture, L_HCE,
Number_HCE)
$COMMON TestType$

If (HCEtype$ = 'LS-2') Then
    D_5 := 0.115  "[m]"
    D_4 := 0.109  "[m]"
    L_HCE := 4.06  "[m]"

    If (TestType$ = 'SNL AZTRAK Platform') Then
        A_aperture := 39  "[m^2]"
        Number_HCE := 2
        L_aperture := Number_HCE * L_HCE  "[m]"
    Else
        If (TestType$ = 'KJC Test Loop') Then
            A_aperture := 235 * 16  "[m^2]"
            Number_HCE := 12 * 16
            L_aperture := L_HCE *  Number_HCE  "[m]"
```

```
            Endif
        Endif
    EndIf

    If (HCEtype$ = 'LS-3') Then
        D_4 := 0.115  "[m]"
        D_5 := 0.121  "[m]"
        L_HCE := 4.06  "[m]"
        A_aperture := 545  "[m^2]"
        Number_HCE := 24
        L_aperture := L_HCE * Number_HCE  "[m]"
    EndIf

    If (HCEtype$ = 'IST') Then
        D_4 := 0.075  "[m]"
        D_5 := 0.0702  "[m]"
        A_aperture := 13.19  "[m^2]"
        L_HCE := 2.16  "[m]"
        Number_HCE := 1
        L_aperture := L_HCE * Number_HCE  "[m]"
    EndIf

END


"***************************************************************************************************************
    PROCEDURE pOpticalEfficiency:    Optical Efficiencies based on HCE type
***************************************************************************************************************"
PROCEDURE pOpticalEfficiency(HCEtype$: OptEff_env, OptEff_abs)
$COMMON Alpha_abs, Alpha_env, K, Reflectivity, TAU_envelope, GlazingIntact$

    " All the following optical properties should be modified as updated values are determined "
    If (HCEtype$ = 'LS-2') Then
        Shadowing := 0.974
        TrackingError := 0.994
        GeomEffects := 0.98
        Rho_mirror_clean := 0.935
        Dirt_mirror := Reflectivity/Rho_mirror_clean
        Dirt_HCE := (1+ Dirt_mirror)/2
        Error := 0.96
    EndIf

    If (HCEtype$ = 'LS-3') or (HCEtype$ = 'IST') Then
        Shadowing := 0.974
        TrackingError := 0.994
        GeomEffects := 0.98
        Rho_mirror_clean := 0.935
        Dirt_mirror := Reflectivity/Rho_mirror_clean
        Dirt_HCE := (1+ Dirt_mirror)/2
        Error := 0.96
    EndIf

    " following if statement prevents Dirt_mirror and Dirt_HCE from being larger then 1 if the input for
Reflectivity is larger then Rho_mirror_clean "
    If (Dirt_mirror > 1) Then
        Dirt_mirror := 1
```

```
        Dirt_HCE := 1
    EndIf

    If (GlazingIntact$ = 'No') Then
        OptEff_env := 0
        OptEff_abs := Shadowing * TrackingError * GeomEffects * Rho_mirror_clean * Dirt_mirror *
Error * K
    Else
        OptEff_env := Shadowing * TrackingError * GeomEffects * Rho_mirror_clean * Dirt_mirror *
Dirt_HCE * Error * K
        OptEff_abs := OptEff_env * TAU_Envelope
    Endif

END
```

```
"*************************************************************************************************
    FUNCTION fD_h:   Hydraulic diameter
*************************************************************************************************"
FUNCTION fD_h(TestType$)
$COMMON D_2, D_p

    " If 'SNL AZTRAK Platform' is chosen, then the inside absorber diameter accounts for the inserted
plug "
    If (TestType$ = 'SNL AZTRAK Platform') Then
        fD_h := D_2 - D_p  "[m]"
    Else
        fD_h := D_2  "[m]"
    EndIf

END
```

```
"*************************************************************************************************
    FUNCTION fq_cond_bracket:     Heat loss estimate through HCE support bracket
*************************************************************************************************"
FUNCTION fq_cond_bracket(T_3, i)
$COMMON L_HCE, Number_HCE, L_aperture, T_6, T_0, P_6, v_6, DELTAL, imax, g

    " effective bracket perimeter for convection heat transfer"
    P_brac := 0.2032  "[m]"

    " effective bracket diameter (2 x 1in) "
    D_brac := 0.0508  "[m]"

    " minimum bracket cross-sectional area for conduction heat transfer"
    A_cs_brac := 0.00016129  "[m^2]"

    " conduction coefficient for carbon steel at 600 K"
    k_brac := 48  "[W/m-K]"

    " effective bracket base temperature"
    T_base := T_3 - 10  "[C]"

    " estimate average bracket temperature "
    T_brac := (T_base + T_6) / 3  "[C]"
```

135

" estimate film temperature for support bracket "
T_brac6 := (T_brac + T_6) /2  "[C]"

" convection coefficient with and without wind"
If (v_6 <= 0.1) Then

    MU_brac6 := viscosity(AIR, T=T_brac6)  "[N-s/m^2]"
    Rho_brac6 := Density(AIR, T=T_brac6, P=P_6)  "[kg/m^3]"
    Cp_brac6 := CP(AIR, T=T_brac6)  "[kJ/kg-K]"
    k_brac6 := conductivity(AIR, T=T_brac6)  "[W/m-K]"
    NU_brac6 := MU_brac6 / Rho_brac6  "[m^2/s]"
    Alpha_brac6 := k_brac6 / (Cp_brac6 * Rho_brac6 * 1000)  "[m^2/s]"
    Beta_brac6 :=  1 / (T_brac6 + T_0)  "[1/K]"
    Ra_Dbrac := g * Beta_brac6 * ABS(T_brac - T_6) * (D_brac)^3 / (Alpha_brac6 * NU_brac6)

    " Warning Statement if following Nusselt Number correlation is used out of recommended
range "
    If (Ra_Dbrac <= 10^(-5)) or (Ra_Dbrac >= 10^12) Then CALL WARNING('The result may not
be accurate, since 10^(-5) < Ra_Dbrac < 10^12 does not hold. See Function fq_cond_bracket.
Ra_Dbrac = XXXA1', Ra_Dbrac)

    " Churchill and Chu correlation for natural convection from a long isothermal horizontal cylinder
"
    Pr_brac6 := NU_brac6 / Alpha_brac6
    Nu#_bar := (0.60 + (0.387 * Ra_Dbrac^(0.1667)) / (1 + (0.559 / Pr_brac6)^(0.5625))^(0.2963)
)^2
    h_brac6 := Nu#_bar * k_brac6 / D_brac  "[W/m^2-K]"

  Else

    " Thermophysical Properties for air "
    MU_brac := viscosity(AIR, T=T_brac)  "[N-s/m^2]"
    MU_6 := viscosity(AIR, T=T_6)  "[N-s/m^2]"
    Rho_6 := Density(AIR, T=T_6, P=P_6)  "[kg/m^3]"
    Rho_brac := Density(AIR, T=T_brac, P=P_6)  "[kg/m^3]"
    k_brac := conductivity(AIR, T=T_brac)  "[W/m-K]"
    k_6 := conductivity(AIR, T=T_6)  "[W/m-K]"
    k_brac6 := conductivity(AIR, T=T_brac6)  "[W/m-K]"
    Cp_brac := CP(AIR, T=T_brac)  "[kJ/kg-K]"
    Cp_6 := CP(AIR, T=T_6)  "[kJ/kg-K]"
    NU_6 := MU_6 / Rho_6  "[m^2/s]"
    NU_brac := MU_brac / Rho_brac  "[m^2/s]"

    Alpha_brac := k_brac / (Cp_brac * Rho_brac * 1000)  "[m^2/s]"
    Alpha_6 := k_6 / (Cp_6 * Rho_6 * 1000)  "[m^2/s]"
    Re_Dbrac := v_6 * D_brac / NU_6
    Pr_brac := NU_brac / Alpha_brac
    Pr_6 := NU_6 / Alpha_6

    " Warning Statements if following Nusselt Correlation is used out of range "
    If (Re_Dbrac <= 1) or (Re_Dbrac >= 10^6) Then CALL WARNING('The result may not be
accurate, since 1 < Re_Dbrac < 10^6 does not hold. See Function fq_cond_bracket. Re_Dbrac =
XXXA1', Re_Dbrac)
    If (Pr_6 <= 0.7) or (Pr_6 >= 500) Then CALL WARNING('The result may not be accurate,
since 0.7 < Pr_6 < 500 does not hold. See Function fq_cond_bracket. Pr_6 = XXXA1', Pr_6)

```
    If (Pr_6 <= 10) Then
        n := 0.37
    Else
        n := 0.36
    EndIf

    If (Re_Dbrac < 40) Then
        C := 0.75
        m := 0.4
    Else

        If (40 <= Re_Dbrac) and (Re_Dbrac< 10^3) Then
            C := 0.51
            m := 0.5
        Else
            If (10^3 <= Re_Dbrac) and (Re_Dbrac < 2*10^5) Then
                C := 0.26
                m := 0.6
            Else
                If (2*10^5 <= Re_Dbrac) and (Re_Dbrac < 10^6) Then
                    C := 0.076
                    m := 0.7
                EndIf
            EndIf
        EndIf
    EndIf

    " Zhukauskas's correlation for external forced convection flow normal to an isothermal cylinder
"
    Nu#_bar := C * (Re_Dbrac)^m  * (Pr_6)^n * (Pr_6 / Pr_brac)^(0.25)
    h_brac6 := Nu#_bar  *  k_brac6  /  D_brac  "[W/m^2-K]"

EndIf

" number of HCE support brackets for each HCE segment "
If (DELTAL <= L_HCE) Then

    index_1 := ROUND(i * DELTAL / L_HCE)
    index_2 := index_1 * L_HCE

    If (((i - 1) * DELTAL) <= index_2) AND (index_2 <= (i * DELTAL)) Then
        n := 1
    Else
        n := 0
    EndIf

Else

    n := ROUND(DELTAL / L_HCE)

EndIf

If (i = 1) OR (i = imax) Then
    n := n + 1
```

EndIf

    fq_cond_bracket := n * SQRT(h_brac6 * P_brac * k_brac * A_cs_brac) * (T_base - T_6)  "[W]"

END

FUNCTION fHeatLoss(q_34rad, q_34conv, q_56conv, q_57rad)
$COMMON GlazingIntact$

    If (GlazingIntact$ = 'No') Then
        fHeatLoss := q_34conv + q_34rad  "[W/m]"
    Else
        fHeatLoss := q_56conv + q_57rad  "[W/m]"
    EndIf

END

"Stefan-Boltzmann constant"
sigma = 5.67E-8  "[W/m^2-K^4]"

" Used to convert temperature from C to K "
T_0 = 273.15  "[C]"

" Gravitational constant "
g = 9.81  "[m/s^2]"

" Wind speed conversion "
v_6 = v_6mph * CONVERT(mph, m/s)  "[m/s]"

" Glass envelope conductance "
K_45 = 1.04  "[W/m-K]"

" Absorber pipe inside surface equivalent roughness factor "
e = 1.5E-6  "[m]"

" Glass envelope absorbtivity "
Alpha_env = .02

" Calls procedure that determines optical properties "
CALL pSelectiveCoatingProperties(imax, T_3[1..imax]: EPSILON_3[1..imax], Alpha_abs, TAU_envelope)

" Calls procedure that determines optical efficiencies at the glass envelope and absorber "
CALL pOpticalEfficiency(HCEtype$: OptEff_env, OptEff_abs)

" Inner and outer glass envelope surface emissivities (pyrex)"
EPSILON_4 = 0.86
EPSILON_5 = 0.86


" Incident angle modifier from test data for SEGS LS-2 Receiver "
K = COS(THETA) + 0.000884 * THETA - 0.00005369 * (THETA)^2


"*******************************************************************************************************
    Heat collector element size
*******************************************************************************************************"
" 'SNL AZTRAK Tracker' plug diameter"
D_p = 0.0508  "[m]"

" Inner and outer absorber pipe diameters "
D_2 = 0.066  "[m]"
D_3 = 0.070  "[m]"

" Calls procedure for determining HCE dimensions based on 'HCE Type'"
CALL pHCEdimensions(HCEtype$: D_4, D_5, A_aperture, L_aperture, L_HCE, Number_HCE)


"*******************************************************************************************************
    Ambient conditions
*******************************************************************************************************"
" Effective sky temperature estimated as 8 C below ambient "
T_7 = T_6 - 8  "[C]"

" Converts ambient pressure from 0.83 atm to kPa, ambient pressure is treated as a constant "
P_6 = 0.83 * CONVERT(atm, kPa)  "[kPa]"

" Standard ambient air temperature "
T_std = 25  "[C]"

" Incoming solar irradiance per aperture length "
q_i  = I_b *  A_aperture / L_aperture  "[W/m]"


"*******************************************************************************************************
    Indexes
*******************************************************************************************************"
" Iteration stepsize along aperture length "
DELTAL = (L_aperture)/(imax)  "[m]"


"*******************************************************************************************************
    Hydraulic diameter
*******************************************************************************************************"
" Calls function to calculate HTF hydraulic diameter "
D_h = fD_h(TestType$)


"*******************************************************************************************************
    Heat transfer fluid flow rates
*******************************************************************************************************"
" Calls function to calculate HTF cross-section flow area"

```
A_cs = fA_cs(D_2, D_p)  "[m^2]"

" Converts HTF flow rate from gpm to m^3/s "
v_1volm = v_1volg* CONVERT(gpm, m^3/s)  "[m^3/s]"

" Calculates HTF velocity "
v_1inlet = v_1volm / (A_cs)  "[m/s]"

" Mass flow rate (conserved) "
m_dot = v_1inlet * RHO_1inlet * A_cs  "[kg/s]"
RHO_1inlet = INTERPOLATE(Fluid$,'RHO','T',T=T_1inlet)  "[kg/m^3]"

"*********************************************************************************************************
*********************************************************************************************************
*********************************************************************************************************
    Do-loops for temperatures along aperture length
*********************************************************************************************************
*********************************************************************************************************
*********************************************************************************************************"
" Do-Loop to set the inlet temperature and velocity of each increment to the previous increment's
outlet temperature and velocity"
T_1in[1] = T_1inlet  "[C]"
v_1in[1] = v_1inlet  "[m/s]"

Duplicate i = 1, (imax-1)
T_1in[i+1] = T_1out[i]  "[C]"
v_1in[i+1] = v_1out[i]  "[m/s]"
End


" Do-Loop to conduct an energy balance on each increment that determines outlet temperature, heat
loss, and efficiency "
Duplicate i = 1,imax


v_1ave[i] = (v_1in[i] + v_1out[i])/2  "[m/s]"

" HTF Densities "
RHO_1out[i] = INTERPOLATE(Fluid$,'RHO','T',T=T_1out[i])  "[kg/m^3]"
RHO_1ave[i] = INTERPOLATE(Fluid$,'RHO','T',T=T_1ave[i])  "[kg/m^3]"
MU_1ave[i] = INTERPOLATE(Fluid$,'MU','T',T=T_1ave[i])  "[kg/m-s]"

Re_D2ave[i] = RHO_1ave[i] * v_1ave[i] * D_2 / MU_1ave[i]

" friction factor, f, relation "
1 / SQRT(f[i]) = -2.0 * LOG10( e / (D_2 * 3.7) + 2.51 / (Re_D2ave[i] * SQRT(f[i])))

"*********************************************************************************************************
    HTF velocities
*********************************************************************************************************"
" Outlet velocity of each increment "
v_1out[i] = m_dot / (RHO_1out[i] * A_cs)  "[m/s]"


"*********************************************************************************************************
```

***************************************************************************************************"

q_cond_bracket[i] = fq_cond_bracket(T_3[i], i)  "[W]"


"***************************************************************************************************

**HTF temperatures**
***************************************************************************************************"
" Outlet HTF temperature for each increment "
HeatLoss[i] = fHeatLoss(q_34rad[i], q_34conv[i], q_56conv[i], q_57rad[i])  "[W/m]"
T_1out[i] = ((q_5SolAbs + q_3SolAbs  - HeatLoss[i] )* DELTAL - q_cond_bracket[i])  / (m_dot *
Cp_1ave[i]) + ((v_1in[i])^2 - (v_1out[i])^2)/2 / Cp_1ave[i] + T_1in[i]  "[C]"

" Average HTF temperature for each increment "
T_1ave[i] = (T_1in[i] + T_1out[i])/2  "[C]"

DELTAP[i] = ( f[i] * (DELTAL / D_2) * (m_dot/A_cs)^2 ) /(2*RHO_1ave[i])  "[Pa]"


"***************************************************************************************************

**q_12conv[i]   Convective heat transfer rate between the heat transfer fluid and absorber**
***************************************************************************************************"
CALL Pq_12conv(T_1ave[i], v_1ave[i], T_2[i], Fluid$: q_12conv[i], Cp_1ave[i])


"***************************************************************************************************

**q_23cond[i]   Conduction heat transfer rate through the absorber**
***************************************************************************************************"
" Absorber conductance, temperature and material type dependent "
k_23[i] = fk_23(T_2[i], T_3[i])  "[W/m-K]"

q_23cond[i] = 2 * PI  * k_23[i] * (T_3[i] - T_2[i]) / LN(D_3 / D_2)  "[W/m]"


"***************************************************************************************************

**q_34conv[i]   Convective heat transfer rate between the absorber pipe and glazing**
***************************************************************************************************"
q_34conv[i] =  fq_34conv(T_3[i], T_4[i], AnnulusGas$)  "[W/m]"


"***************************************************************************************************

**q_34rad[i]     Radiation heat transfer rate between the absorber surface and glazing inner surface**
***************************************************************************************************"
q_34rad[i] = fq_34rad(T_3[i], T_4[i], i)  "[W/m]"


"***************************************************************************************************

**q_45cond[i]   Conduction heat transfer rate through the glass envelope**
***************************************************************************************************"
q_45cond[i] = 2 * PI  * K_45 * (T_4[i] - T_5[i]) / LN(D_5 / D_4)  "[W/m]"


"***************************************************************************************************

**q_56conv[i]   Convective heat transfer rate from the glazing to the atmosphere**
***************************************************************************************************"
q_56conv[i] = fq_56conv(T_5[i], T_6)  "[W/m]"

"********************************************************************************************
    q_57rad[i]     Radiation heat transfer rate between the glazing outer surface and the sky
********************************************************************************************"

q_57rad[i] = fq_57rad(T_5[i], T_7)  "[W/m]"


"********************************************************************************************
 One dimensional (Radial) model
********************************************************************************************"

CALL Pq_45cond(q_34conv[i], q_34rad[i]: q_45cond[i])  "[W/m]"
CALL Pq_56conv(q_45cond[i], q_5SolAbs, q_57rad[i]: q_56conv[i])  "[W/m]"

q_12conv[i] = q_23cond[i]  "[W/m]"
q_3SolAbs - q_23cond[i] - q_34conv[i] - q_34rad[i] - q_cond_bracket[i] / DELTAL = 0  "[W/m]"


End

"********************************************************************************************
********************************************************************************************
********************************************************************************************"


" Outlet temperature set equal to the final increment outlet temperature "
T_1outlet = T_1out[imax]  "[C]"

v_1outlet = v_1out[imax]  "[m/s]"

DELTAP_total = SUM(DELTAP[j], j=1, imax)  "[Pa]"


"********************************************************************************************
    Average HTF Temperature
********************************************************************************************"

T_ave = AVERAGE(T_1ave[1..imax])  "[C]"


"********************************************************************************************
    Effective optical efficiency and optical loss
********************************************************************************************"

EffectOptEff = (OptEff_abs * Alpha_abs + OptEff_env * Alpha_env)
Eta_EffectOptEff = EffectOptEff * 100  "[%]"
q_OptLoss = q_i * (1-EffectOptEff)  "[W/m]"


"********************************************************************************************
    ETA_Col Collector efficiency
********************************************************************************************"

" Total HTF convection heat gain equals summation of heat gain for each increment "
q_heat_gain = SUM((q_12conv[j] * DELTAL ), j=1,imax) / L_aperture  "[W/m]"
ETA_Col = fETA_Col(q_heat_gain, q_i) * 100  "[%]"


"********************************************************************************************
    q_3SolAbs        Solar flux on absorber pipe

```
***********************************************************************************************************"
q_3SolAbs = q_i * OptEff_abs * Alpha_abs  "[W/m]"


"*********************************************************************************************************
    q_5SolAbs        Solar Flux on glazing Envelope
***********************************************************************************************************"
q_5SolAbs = fq_5SolAbs(q_i)  "[W/m]"


"*********************************************************************************************************
    HCE heat losses
***********************************************************************************************************"
q_cond_bracket_total = SUM(q_cond_bracket[j], j=1, imax)  "[W]"
q_cond_bracket_L = q_cond_bracket_total / L_aperture  "[W/m]"
q_HeatLoss_ApertureLength = SUM((HeatLoss[j] * DELTAL), j=1, imax) / L_aperture +
q_cond_bracket_L  "[W/m]"
q_HeatLoss_HCEarea = q_HeatLoss_ApertureLength/(PI*D_5)  "[W/m^2]"
q_HeatLoss_ColArea = (q_HeatLoss_ApertureLength * L_aperture)/A_aperture  "[W/m^2]"
```

# REFERENCES

ASM Handbook Committee (1978). *Metals Handbook. Properties and Selection – Nonferrous Alloys and Pure Metals*, Vol. 2, Metals Park, OH: American Society for Metals.

Bejan, A. (1995). *Convection Heat Transfer, Second Edition*. New York, NY: John Wiley & Sons.

Bejan, A. (1988). *Advance Engineering Thermodynamics*. New York, NY: John Wiley & Sons.

Çengel, Y. A., Boles, M. A. (2002) *Thermodynamics an Engineering Approach, Fourth Edition*. New York, NY: McGraw-Hill.

Cohen, G. E. (29 July 2002). E-mail memorandum. Duke Solar Energy, Raleigh, NC.

Cohen, G. E.; Kearney, D. W.; Kolb, G. J. (June 1999) *Final Report on the Operation and Maintenance Improvement Program for Concentrating Solar Power Plants*. SAND99-1290. Albuquerque, NM: Sandia National Laboratories.

Davis, J. R., ed. (2000). *Alloy Digest, Sourcebook, Stainless Steels*. Materials Park, OH: ASM International.

Duke Solar Energy (November 20, 2001). *Subtask 1.2 Final Report, A Non-Imaging Secondary Reflector for Parabolic Trough Concentrators*. NREL Subcontract No. NAA-1-30441-06. Golden, CO: National Renewable Energy Laboratory.

Dudley, V. E.; Kolb, G. J.; Mahoney, A. R.; et al. (December 1994). *Test Results: SEGS LS-2 Solar Collector*. SAND94-1884. Albuquerque, NM: SANDIA National Laboratories.

Duffie, J. A.; Beckman, W. A. (1991). *Solar Engineering of Thermal Processes, Second Edition*. New York, NY: John Wiley and Sons.

KJC Operating Company (December 1993). *Final Report on HCE Heat Transfer Analysis Code*. SANDIA Contract No. AB-0227. Albuquerque, NM: Sandia National Laboratories.

Gnielinski, V. (April 1976). "New Equations for Heat and Mass Transfer in Turbulent Pipe and Channel Flow." *International Chemical Engineering* (16:2); pp. 359–363.

Howell, J. R. (1982). *A Catalog of Radiation Configuration Factors*. New York, NY: McGraw-Hill.

Howell, J. R.; Buckius, R. O. (1987). *Fundamentals of Engineering Thermodynamics*. New York, NY: McGraw-Hill.

Incropera, F.; DeWitt, D. (1990). *Fundamentals of Heat and Mass Transfer, Third Edition*. New York, NY: John Wiley and Sons.

Klein, S. A. (2002). *Engineering Equation Solver (EES) for Microsoft Windows Operating System: Commercial and Professional Versions*. Madison, WI: F-Chart Software. (available on the Web at http://www.fchart.com.)

Mahoney, R. (September 2002). Phone conversation. Sandia National Laboratories, Albuquerque, NM.

Marshal, N., transl. (1976). *Gas Encyclopedia*. New York, NY: Elsevier.

Munson, B. R.; Young, D. F., Okiishi, T. H. (1990). *Fundamentals of Fluid Mechanics.* New York, NY: John Wiley and Sons.

Ozisik, M. N. (1977). *Basic Heat Transfer.* New York, NY: McGraw-Hill Book Company.

Ozisik, M. N. (1973). *Radiative Transfer and Interactions with Conduction and Convection.* New York, NY: John Wiley and Sons.

Price, H. (1997). *Guidelines for Reporting Parabolic Trough Solar Electric System Performance.* NREL/CP-550-22729. Golden, CO: National Renewable Energy Laboratory.

Price, H. (2000). "UVAC Test HCE Heat Loss Model" Excel Spreadsheet. Golden, CO: National Renewable Energy Laboratory.

Price, H. (2001) *Concentrated Solar Power Use in Africa*. NREL/TP. Golden, CO: National Renewable Energy Laboratory.

Price, H.; Lupfert, E.; Kearney, D.; Zarza, E.; Cohen, G.; Gee, R.; (May 2002). "Advances in Parabolic Trough Solar Power Technology." *Journal of Solar Energy Engineering* (Vol. 124); pp. 109–125.

Ratzel, A.; Hickox, C.; Gartling, D. (February 1979). "Techniques for Reducing Thermal Conduction and Natural Convection Heat Losses in Annular Receiver Geometries." *Journal of Heat Transfer* (101:1); pp. 108–113.

Siegel, R., Howell, J. (2002) *Thermal Radiation Heat Transfer, Fourth Edition*. New York, NY: Taylor & Francis.

Solel Solar Systems Ltd. Web page – http://www.solel.com.

Thomas, A.; Guven, H. M. (1993). "Parabolic Trough Concentrators – Design, Construction and Evaluation." *Energy Conversion Management* (34:5); pp. 401–416.

Thomas, A.; Guven, H. M. (1994). "Effect of Optical Errors on Flux Distribution Around the Absorber Tube of a Parabolic Trough Concentrator" *Energy Conversion Management* (35:7); pp. 401–416.

Touloukian, Y. S.; DeWitt, D. P., eds. (1972). *Radiative Properties, Nonmetalic Solids.* Thermophysical Properties of Matter, Vol. 8, New York, NY: Plenum Publishing.

# REPORT DOCUMENTATION PAGE

| 1. AGENCY USE ONLY (Leave blank) | 2. REPORT DATE<br>October 2003 | 3. REPORT TYPE AND DATES COVERED<br>Technical report |
|---|---|---|

**4. TITLE AND SUBTITLE**
Heat Transfer Analysis and Modeling of a Parabolic Trough Solar Receiver Implemented in Engineering Equation Solver

**5. FUNDING NUMBERS**
CP032000

**6. AUTHOR(S)**
R. Forristall

**7. PERFORMING ORGANIZATION NAME(S) AND ADDRESS(ES)**
National Renewable Energy Laboratory
1617 Cole Blvd.
Golden, CO 80401-3393

**8. PERFORMING ORGANIZATION REPORT NUMBER**
NREL/TP-550-34169

**9. SPONSORING/MONITORING AGENCY NAME(S) AND ADDRESS(ES)**

**10. SPONSORING/MONITORING AGENCY REPORT NUMBER**

**11. SUPPLEMENTARY NOTES**

**12a. DISTRIBUTION/AVAILABILITY STATEMENT**
National Technical Information Service
U.S. Department of Commerce
5285 Port Royal Road
Springfield, VA 22161

**12b. DISTRIBUTION CODE**

**13. ABSTRACT** *(Maximum 200 words)*
This report describes the development, validation, and use of a heat transfer model implemented in Engineering Equation Solver. The model determines the performance of a parabolic trough solar collector's linear receiver, also called a heat collector element. All heat transfer and thermodynamic equations, optical properties, and parameters used in the model are discussed. The modeling assumptions and limitations are also discussed, along with recommendations for model improvement.

**14. SUBJECT TERMS**
heat transfer; engineering equation solver; parabolic trough; solar collector; heat collector element

**15. NUMBER OF PAGES**

**16. PRICE CODE**

| 17. SECURITY CLASSIFICATION OF REPORT<br>Unclassified | 18. SECURITY CLASSIFICATION OF THIS PAGE<br>Unclassified | 19. SECURITY CLASSIFICATION OF ABSTRACT<br>Unclassified | 20. LIMITATION OF ABSTRACT<br>UL |
|---|---|---|---|